NASA Technical Memorandum 74055

A PRELIMINARY STUDY OF THE PERFORMANCE AND CHARACTERISTICS OF A SUPERSONIC EXECUTIVE AIRCRAFT

VINCENT R. MASCITTI

SEPTEMBER 1977

National Aeronautics and Space Administration

Langley Research Center
Hampton, Virginia 23665

TABLE OF CONTENTS

FORWARD	i
SUMMARY	1
INTRODUCTION	2
SYMBOLS	3
CONFIGURATION CONSTRAINTS	7
CONFIGURATIONS STUDIED	8
MASS PROPERTIES	11
STABILITY AND CONTROL	18
PROPULSION	21
LOW-SPEED AERODYNAMICS	28
SUBSONIC/TRANSONIC AERODYNAMICS	36
SUPERSONIC AERODYNAMICS	38
MISSION ANALYSIS	47
TAKEOFF PERFORMANCE	50
NOISE PREDICTION	53
CONCLUDING REMARKS	59
REFERENCES	60

A PRELIMINARY STUDY OF THE PERFORMANCE AND CHARACTERISTICS OF A SUPERSONIC EXECUTIVE AIRCRAFT

Vincent R. Mascitti
NASA Langley Research Center

SUMMARY

A preliminary design study has been conducted to determine the impact of advanced supersonic technologies on the performance and characteristics of a supersonic executive aircraft. Four configurations with different engine locations and wing/body blending were studied with an advanced non-afterburning turbojet engine. One configuration incorporated an advanced General Electric variable cycle engine and two-dimensional inlet with internal ducting. A M 2.2 design Douglas scaled arrow-wing was used throughout this study with Learjet 35 accommodations (eight passengers).

All four configurations with turbojet engines meet the performance goals of 5926 km (3200 n. mi.) range, 1981 meters (6500 feet) takeoff field length, and 77 meters per second (150 knot) approach speed. The noise levels of turbojet configurations studied are excessive. However, a turbojet with mechanical suppressor was not studied. The variable cycle engine configuration is deficient in range by 555 km (300 n. mi.) but nearly meets subsonic noise rules (FAR 36 1977 edition), if coannular noise relief is assumed. All configurations are in the 33566 to 36287 kg (74,000 to 80,000 lbm) takeoff gross weight class when incorporating current titanium manufacturing technology.

A preferred configuration was not chosen for this study. While the performance results on the various configurations are encouraging, it is felt that significant performance improvement can be established with more effort. However, some uncertainties exist mainly in the prediction of aerodynamic characteristics, which can be resolved only by wind tunnel tests through the Mach number range. Further detailed system integration studies to the depth described in this status report should await the completion of planned experimental programs.

INTRODUCTION

Continuing growth in the general aviation industry may require at some future date the need for a small supersonic cruise business jet. Expanding international markets for corporations and diplomatic missions for government executives could create a demand for the convenience and availability that a long range supersonic jet would provide.

In the mid-late 1960's, preliminary designs, reference 1 and 2, were studied showing that transatlantic ranges could be achieved by Mach 2.0-2.7 aircraft carrying 8-12 passengers, with gross weights in the 33566 to 36287 kg (60,000 to 80,000 lbm) class. The studies included variable sweep or delta-wing technology with afterburning turbojet or turbofan engines typical of first generation SST technology. Noise characteristics were not reported. During this time the U.S. was engaged in the SST national competition and much of the detailed information on SST configurations was either classified by the U.S. Government or company proprietary. In 1971, Boeing conducted an unpublished study of a 10-passenger delta-wing aircraft, which resulted in 4778 km (2580 n. mi.) range, 46947 kg (103,500 lbm) gross weight with a takeoff field length of 1615 meters (5300 feet).

Soon after the cancellation of the U.S. SST program in 1971, NASA initiated a research program (SCAR) in supersonic cruise technology. In the past five years, NASA and the industry, reference 3, have identified solutions to the performance, economic, and environmental problems associated with first generation SST's. For example, arrow-wing or blended delta-wing configurations provide transpacific range 8500 km (4600 n. mi.). Aircraft employing variable cycle engines with coannular noise relief or low bypass ratio turbojet engines with advanced mechanical suppressors would meet the 108 EPNdB noise constraints (FAR 1969 edition). Advanced titanium technology such as superplastic forming diffusion bonding would provide substantial cost and weights savings compared to the methods available in 1971. In addition, an extensive experimental program was conducted by NASA and Douglas, reference 4, on a M 2.2 design in the transonic and supersonic speed range. The results of this experimental program were important to the current study as will be discussed in the next section.

With a great deal of information available in the open literature, preliminary design studies of a supersonic business jet were initiated in 1976 conducted by NASA Langley Research Center and Vought Corporation, Hampton Technical Center. The objective of this study was to determine the impact of advanced SCAR technologies on the performance and characteristics of a supersonic executive jet (SSXJET) and to identify technical problem areas. During the course of this study, four configurations (Mach 2.2 designs) were studied which incorporated a NASA generated advanced dry turbojet engine and a fifth configuration using a General Electric variable cycle engine. Special emphasis was placed upon the evaluation of terminal area noise characteristics and takeoff performance.

No attempt was made to determine the optimum cruise Mach number for a SSXJET class aircraft since that would require an extensive data base and a complete market and economic study, which was beyond the scope of the present effort. Rather, the Mach 2.2 design constraint was chosen due to the availability of high-speed wind tunnel data and models, and a low-speed experimental data base which will be established in the coming year.

SYMBOLS

AR, A	aspect ratio
A_{TOTAL}	total wetted area
A_{WET}	component wetted area
b	wing span
C_D	drag coefficient
C_{D_g}	drag coefficient in ground effect
$\Delta C_{D_{GEAR}}$	landing gear drag increments
$C_{D_{MIN}}$	minimum drag coefficient
$C_{D_{NET}}$	net drag coefficient
$C_{D_{TEST}}$	drag coefficient from test
$C_{D_{WAVE}}$	wave drag coefficient
$C_{D_{0\%}}$, $C_{D_{100\%}}$	zero and full suction drag coefficients
$\Delta C_{D_{PROPULSION}}$	propulsion drag increment
ΔC_D	zero-lift drag increment
C_L	lift coefficient, $\frac{Lift}{q\ S_{ref}}$
C_{L_α}	lift-curve slope per degree
C_{L_g}	lift coefficient in ground effect

$C_{L_{NET}}$	net lift coefficient
$C_{L_{TEST}}$	lift coefficient from test
ΔC_L	lift coefficient at minimum drag point on polar relative to $C_l = 0$.
C_M	pitching moment coefficient, $\frac{\text{pitching moment}}{q\, S_{ref}\, \bar{c}_{ref}}$
C.G.	center of gravity
C_μ, $C_{\mu_{REF}}$	flap knee blowing coefficient
$\bar{c}_{REF}$	reference mean aerodynamic chord
DEG	degree
ft	feet
h	altitude
h_o	wing height for ground effect calculations
i_t	horizontal tail incidence angle measured
K_A	atmospheric factor
K_L	lift parameter = $\frac{\beta w}{\gamma P_h M^2 \ell^2}$
K_S	shape factor
ℓ	fuselage length
L/D	lift-to-drag ratio
$(L/D)_{MAX}$	maximum lift-to-drag ratio
L_1, L_2, L_3	designate leading-edge devices and deflections
l_t	tail length
M_∞, M	freestream Mach number

m	meter
MIN DEM	minimum demonstrated
NX	number of Mach cutting planes in wave drag analysis
N$_\theta$	number of aircraft roll angles used in wave drag analysis
P_g	sea level pressure
P_h	pressure at altitude
ΔP	sonic boom overpressure
PSP	polar shape parameter
q	dynamic pressure
rad	radian
S_{REF}	wing reference area
S_{ht}	exposed, projected horizontal tail area
sec	second
t/c	wing thickness ratio
t_1, t_2, t_3, t_4	designate model trailing-edge flaps and deflections
T_1, T_2, T_3	designate SSXJET concepts trailing-edge flaps and deflections
$\bar{v}$	horizontal tail volume coefficient, $\frac{S_{ht}\, l_t}{S_{ref}\, \bar{c}_{ref}}$
W	aircraft weight
x	longitudinal coordinate
x/c	chordwise fraction
X_n, Y_n, Z_n	nacelle coordinates

Y	spanwise coordinate
$Y/b/2$	semispan fraction
α	angle of attack of the wing reference plane
α_o	angle of attack for zero lift
α_{WRP}	wing reference plane angle of attack
β	Mach number parameter = $\sqrt{M^2-1}$
γ	ratio of specific heats, = 1.4
δ_e	elevator deflection measured from tail chord plane
δ_{FLAP}	flap deflection angle
θ	aircraft roll angle for wave drag analysis
$\ddot{\theta}$	pitching acceleration
μ	Mach angle
σ_D, σ_i, σ_L	ground effect parameters

CONFIGURATION CONSTRAINTS

In formulating the study of a supersonic executive aircraft one must consider the credibility of the data base to be employed. The Mach 2.7 design base established by NASA, Boeing, and Lockheed during the past national supersonic transport program was considered for this study, and indeed much of the NASA data and the technology developed from the SCAT 15F arrow-wing concept has been used indirectly. However, it was felt that Mach 2.7 was on the high side for a supersonic executive jet since it requires more sophisticated variable geometry engines, inlet and nozzles that would provide low to moderate operating costs for supersonic transport but larger component development costs. Since the economics of a SSXJET could be dominated more by initial cost considerations rather than operating costs, a lower Mach number data base was sought.

An important experimental program (Ref.4) was recently completed for a Mach 2.2 transport design. A jointly sponsored NASA/Douglas wind tunnel test program was conducted at the NASA Ames Research Center at transonic and supersonic speeds. Results of these tests verified a high level of aerodynamic efficiency for the Douglas design wing (trimmed $L/D_{max} = 9.1$) when incorporated with a transport fuselage carrying 273 passengers. These encouraging high speed results has led to the generation of a new NASA experimental program at low-speeds, wherein a 9.14 meter (30 ft) model of the Douglas concept will be tested in the NASA Langley full scale tunnel. The model is currently under construction and is scheduled for testing early in 1978. This model is designed to be of multi-purpose to facilitate fuselage, nacelle and empennage changes that will be required to test a SSXJET configuration. Because of past and anticipated experimental data, the Douglas design wing was chosen for this study. The scaled geometry, shown in Figure 1, has been held constant throughout the study for all configurations. This arrow-wing planform offers several advantages over a delta wing planform similar to that used on the Anglo-French Concorde and USSR TU-144. The planform of the wing essentially determines the drag-due-to-lift as well as the wave drag characteristics of the wing. Drag-due-to-lift is significantly reduced when the leading edge is swept well behind the design Mach line and the trailing-edge notch ratio is maximized. Also, because the leading-edge is swept at 1.24 Rad. (71^{o}), a subsonic leading-edge radius can be used to improve low-speed lift and stability requirements. By clipping the wing tip from a pointed arrow the structural span is decreased and eliminates that portion of the wing where experiment has indicated a breakdown of the theoretically predicted flow. Unsweeping the wing tip in the region of high local upwash, in this case to .99 Rad. (57^{o}), improves the subsonic efficiency and pitching moment characteristics with little detriment to the supersonic wave drag. To further minimize drag, the camber and twist distribution has been optimized for the Mach 2.2 cruise condition to minimize drag-due-to-lift. Wing thickness ratio varies from 2.2 percent at the root to 3.0 percent outboard of the trailing edge break.

The passenger compartment (eight passengers/two crew) is similar to the Learjet 35 shown in Figure 2. While this is not necessarily the optimum payload for a supersonic executive jet, it does represent the minimum passenger size considered feasible for this class of long range supersonic aircraft.

The material chosen for this study is titanium. 6AL-4V titanium alloys at Mach 2.2 temperatures are much more structurally efficient than the best aluminum alloys, when used for strength design parts for 70,000 hours design life. Improved manufacturing processes such as superplastic forming and diffusion bonding and the resulting innovative structural concepts could potentially provide part costs approaching those of aluminum, (Ref. 3).

Performance Goals and Ground Rules

The range goal for this study was 5926 km (3200 n. mi.) which corresponds to a New York to Paris flight. The prohibition of civil supersonic flight overland underscores the requirement for at least transatlantic range. However, many important city pairs such as Los Angeles to Honolulu at 4074 km (2200 n. mi.) could be serviced by this aircraft at reduced gross weight, lower takeoff power settings, and, consequently, reduced noise levels. The enroute mission and reserve legs used for performance evaluation are shown in Figure 3.

The takeoff field length goal was established at 1981 meters (6500 ft) maximum in order that the aircraft could access a larger number of airfields. Approach speed was constrained to 150 knots corresponding to nearly Learjet values.

No noise goals were established initially since noise regulations do not currently exist for civil supersonic aircraft. Also the simultaneous goals of 1981 meters (6500 ft) takeoff field length, (high thrust/weight) and larger highly swept wing (low wing loading) would drive the design to relatively low noise levels in any event. Noise was, therefore, a "fall out" of the performance evaluation.

With the above configuration constraints and ground rules defined, the problem was reduced to determining the minimum takeoff gross weight that will satisfy the design mission requirements.

CONFIGURATION STUDIED

The selection of configurations for this study was based on a parametric evaluation of engine type, location, and inlet considerations for a twin engine executive class transport airplane. All versions utilize the scaled wing planform geometry of the Douglas Mach 2.2 transport concept. Passengers, crew, baggage requirements, landing flare angle, takeoff rotation angle, and pilot vision envelope were maintained constant for all study concepts. Two engine concepts were used, a non-afterburning advanced turbojet engine with a mixed compression inlet and a variable cycle turbofan GE21/J11-B10 engine supplied by the General Electric Company. Both engines were scaled to the required thrust level and the corresponding engine weight for each configuration studied.

Four basic configurations were evaluated; a clean wing version with aft fuselage mounted nacelles (SSXJET) a similar concept with the nacelles mounted under the wing (SSXJET I), a blended wing/body version with aft fuselage nacelles (SSXJET II) and an aft fuselage integrated engine installation with under wing 2-dimensional inlets (SSXJET III).

SSXJET

With the wing geometry and passenger compartment fixed, the fuselage geometry and wing location are arranged to provide minimum wave drag at Mach 2.2 and to satisfy aircraft balance requirements. For the initial configuration development a parametric analysis was conducted for a range of airplane gross weights and thrust-to-weight ratios with a nominal wing loading of 3830 N/m^2 (80 psf). From this analysis a selected airplane was subjected to passenger, subsystems, and fuel volume verification.

It was discovered that in order to stay within a reasonable aircraft length and equivalent body fineness ratio, the airplane becomes fuel volume limited. This means that when payload and subsystems volumes are accommodated all remaining wing and fuselage volume is used for fuel containment and structure. Figure 4 shows the volume utilization for the wing and fuselage. This configuration has a wing area of 89.65 m^2 (965 ft^2), a fuselage length of 31.39 m (103 ft), and a wing span of 12.83 m (42 ft). The general arrangement and inboard profile of this configuration is shown in figures 5 and 6. Two nacelles are mounted on the aft fuselage in a location to provide ground clearance during landing flare and takeoff rotation. The aircraft accessary gear box is located in the aft fuselage between the engines and is driven by both engines. Because of concern with the takeoff field length requirement, this arrangement results in a clean wing freeing the entire wing trailing-edge for mechanical flaps. The empennage is a "T" tail arrangement with a variable incidence horizontal stabilizer and geared elevator. Main landing gear is a two strut arrangement with two wheels per strut and retracts inboard in the fuselage. Nose landing gear is dual wheeled and retracts forward of the crew compartment. The passenger compartment is nominally 1.727 meters (5.667 ft) in diameter and accommodates eight passengers. Baggage space is provided directly aft of the passenger compartment. Flight crew spacing is similar to the Learjet 35 with .192 Rad. (11^o) pilot vision angle over the nose. Windshield slope was selected to be slightly greater than the Mach angle at the M2.2 cruise condition. Fuel tanks and aircraft subsystems are located to satisfy required center of gravity location throughout the flight envelope.

The aft fuselage nacelle placement raises questions with regard to adverse local flow variations, which may vary with angle of attack, high local Mach numbers at the inlet face, and inlet distortion characteristics leading to engine unstart at supersonic speeds. High speed flow field measurements are required to address this problem area.

SSXJET I

This configuration is similar to the SSXJET except that the nacelles are located under the wing. The general arrangement and inboard profile are shown in Figures 7 and 8, respectively. This engine placement eliminates the local flow concerns mentioned above, since the wing acts to keep the flow aligned with the inlet through the angle of attack range and reduces the flow velocity to less than free stream values. Lower local Mach numbers result in smaller inlet size and increased pressure recovery, although no credit for this advantage was taken in this study. Spanwise and chordwise nacelle location was selected based on minimum wave drag and structural support considerations discussed in more detail in subsequent sections of this report. Wing and empennage areas and geometry remain the same as the previous configuration. The wing was relocated, however, to satisfy balance requirements and the fuselage cross section area was modified to minimize wave drag at the cruise condition. The "T" tail was retained to reduce the engine exhaust impingement on the horizontal stabilizer. Because of the thin wing, engine driven accessories are located in the fuselage and are driven by quill shaft from the engine to a right angle gear box in the fuselage.

SSXJET II

For this concept wing/body blending was employed. The advantage of wing/body blending coupled with a "wrap around" structure, is low supersonic wave drag by potentially reducing the maximum cross section area and providing more efficient use of aircraft volume. Figures 9 and 10 show the general arrangement and inboard profile, respectively. Wing and empennage areas and geometry remained the same as SSXJET along with nacelle location on the aft fuselage. The wing was positioned higher on the fuselage to facilitate the blending. As previously mentioned, the study aircraft are fuel volume limited for the same fuselage length. Therefore, area added in the wing/body fillet must be removed from the fuselage so that the M 2.2 area distribution would remain basically the same. Because of the "wrap around" structural requirements for this concept, usable fuel volume is slightly reduced relative to SSXJET and SSXJET I, since the airplane is volumetrically efficient. In an attempt to further reduce the cross section area of the crew compartment and its effect on supersonic wave drag, a derivative version of this configuration was developed. This concept, designated SSXJET II T, placed the pilot and co-pilot in a tandem arrangement with the pilot in the forward position. Figures 11 and 12 depict the general arrangement and inboard profile. Although a slight improvement in drag was achieved, one major disadvantage in this concept is evident. Due to the tandem arrangement and canopy requirements, access to the crew compartment is limited to external entrance and egress, therefore, isolating the crew from the passenger compartment.

SSXJET III

Each of the previously discussed concepts used the advanced turbojet engine and were sized to satisfy payload/range and takeoff field length requirements set forth in the ground rules. Takeoff noise calculations for these configurations resulted in high noise levels for this class of aircraft as discussed in the noise section. In light of these results, the SSXJET III configuration was developed in an attempt to satisfy noise constraints. Figures 13 and 14 are the general arrangement and inboard profile, respectively. The engine used is the variable cycle GE12/J11-B10 engine scaled to the required thrust level. All regualr performance characteristics were provided by General Electric together with scaling curves for weight and geometry. Installed thrust-to-weight ratio was increased from .37 to .51. This installed thrust permits takeoff at derated throttle settings resulting in lower exhaust gas velocity and, consequently, reduced noise levels both with and without coannular suppressive effects. Two dimensional inlets are located under the wing with the engines positioned in the aft fuselage. Again wing geometry was retained but the area was increased to 105 m^2 (1130 ft^2) to improve low speed characteristics and compensate for the reduction in trailing-edge flap area due to the underwing inlet. Fuselage length was increased .81 meters (2.67 ft) to 32.21 meters (105.67 ft) to compensate for the fuel loss due to engine ducting. Overall equivalent body fineness ratio was maintained as the previous concepts. A disadvantage of this two dimensional inlet arrangement is possibly boattail and base drag penalties not accounted for in this study.

Configuration Assessment

As previously mentioned, each of these configurations are fuel volume limited. In order to stay within the wing geometry constraints, no modifications or changes were investigated. A more detailed study would be required to assess the penalties of wing thickness changes and fuselage integration to provide additional fuel volume. Also, no attempt was made to determine if the thin wing provides sufficient thickness for control surface actuators and other subsystem requirements.

MASS PROPERTIES

The objective of the mass properties analysis is to evaluate candidate structural designs and establish, as realistically as possible, the minimum design gross weight at which a particular configuration can perform the desired mission goal.

In this study, the design mission goal was to achieve a configuration having the mission capability of carrying a payload consisting of eight passengers, their baggage, and a crew of two; a range of 5926 km (3200 n. mi.) at Mach 2.2 cruise speed.

Five configurations of supersonic executive jet transport (SSXJET) series aircraft were evaluated. These are: basic SSXJET, SSXJET I, SSXJET II, SSXJET II Tandem, and SSXJET III.

Methods and Criteria

One of the prime requisites for attaining valid design evaluations during early conceptual development of an aircraft system, is availability of accurate weight and balance data. Obtaining precise mass data would require a detailed structural weight analysis beyond the scope of this study. However, it is possible, after establishing a sound reference base, to produce first level mass data with reasonably adequate confidence levels. These data, while not highly detailed, do reveal trends and serve to isolate, identify, and assess impacts resulting from incorporation of variations in design or technology.

For this study a Vought Hampton developed computerized mass property estimating program, ESBULL, was used in the evaluation of the SSXJET series aircraft. This program is statistically based with empirical modifications. It was designed to generate mass properties for multi-engined commercial transports and was used in previous SCAR studies, references 6 and 12. The weight prediction portion has been correlated with data from Boeing, Lockheed and Douglas methods. A sample of the wing prediction performance for the program versus reported weights is presented in Figure 15. This plot contains several large subsonic transports and one small executive transport to correlate with a small scale aircraft. It also includes the data points for three large supersonic transports from the three companies. A comparison of the Vought Hampton generated weight data compared to data obtained from Boeing, Lockheed, and Douglas is presented in Table I(a) and I(b) for metric units and engineering units respectively.

The configuration selection, sizing, and mass analysis are based on the following mission requirement criteria:

- Payload - 8 passengers with baggage
- Range - nominally, 5926 km (3200 n. mi.)
- Design Cruise Speed - Mach 2.2
- fuel - Conventional Fossil (JP) fuel

The structural mass analysis is based on an all titanium primary structure. Design features and construction techniques for major components are:

- o Wing and Aerodynamic Surfaces - Stresskin titanium skin/core sandwich panels.
- o Fuselage - Titanium skin/stringer/frame construction.
- o Landing Gear - Two strut main gear and single strut nose gear structure of high strength steel alloy.
- o Engine - Single spool, non-afterburning advanced turbojet with variable geometry turbine and exhaust nozzle for all except SSXJET III, which has the GE21/J11-B10 double bypass engine.

The sizing and configuration selection synthesis for SSXJET was performed by generating a matrix of candidate aircraft with an array of Design Gross Weights (DGW) ranging from 31751 to 40823 kg (70,000 to 90,000 lbm) with sea level, standard day, uninstalled thrust-to-weight ratios (t/w) varying from .35 to .55. The resulting data from this program were subjected to mission performance evaluations. The candidate aircraft with the best match of DGW, and thrust-to-weight ratio meeting range and overall aerodynamic performance was selected.

Weights

Variations in mass characteristics due to configuration differences are discussed on an individual basis using basic SSXJET for comparison. Each configuration is described briefly in order to identify salient design features which effect mass characteristics.

The design mass characteristics and the group weights of the selected configurations are summarized in Tables II and III, respectively.

Basic SSXJET

As described in Configuration Studies portion of this report, the basic SSXJET is an arrow-wing, eight passenger airplane with two aft fuselage mounted dry turbojets. SSXJET has a maximum design takeoff gross weight of 35720.4 kg (73750 lbm).

SSXJET I

The major difference between basic SSXJET and SSXJET I is the engine location. On SSXJET I the engines (same engine as on SSXJET) are mounted beneath the wing, whereas on the basic SSXJET the engines are mounted on the aft fuselage.

This configuration change results in lower structural weights for both wing and fuselage for SSXJET I. The wing structural weight decreased because the engine pods contributed additional wing bending relief. Fuselage weight was decreased because removal of engines from the fuselage reduced aft fuselage structural loads. The combined effect of decreases in structural weight and recycling resulted in a design gross weight of 34926.6 kg (77000 lbm) for the SSXJET I. This is approximately 807.4 kg (1780 lbm) less than the basic SSXJET.

SSXJET II and II Tandem

The SSXJET II versions are nearly identical to the Basic SSXJET in overall configuration geometry, but differ in structural design. Both SSXJET II versions are blended wing/body concepts, which also differ from one another.

One version, designated SSXJET II Tandem, has a tandem cockpit arrangement where the pilots are seated one behind the other, similar to certain jet fight/trainer aircraft. The other version, designated SSXJET II, has a conventional side-by-side cockpit arrangement, characteristic of transport aircraft.

The blended wing/body concepts exhibit lower weights than the Basic SSXJET. The major difference occurs in the wing structural weight and is attributable to three factors: (1) blended wing/body design concepts result in relatively deep wing-root sections, resulting in high thickness to chord ratios and reduced wing weight; (2) reduction in the design gross weight (DGW) resulting from the decrease in fuel capacity 1270 kg (2800 lbm) less than Basic SSXJET (3) the downward cascading effect on DGW during recycling for sizing.

The combined effect of these factors, which translates into deeper, more efficient wing-root structure, lower wing loadings, and smaller engines (the wing area and t/w were held constant) resulted in a design gross weight of 33565.9 kg (74000 lbm) for the SSXJET II. This is approximately 2154.6 kg (4750 lbm) less than that of the Basic SSXJET. Weight differences between the SSXJET II versions due to forebody shape variations are too subtle for detection by the first level statistical methods. Therefore, only one set of weight values is shown to represent both the SSXJET II and SSXJET II Tandem concepts.

SSXJET III

Three distinct configuration changes distinguish the SSXJET III from the Basic SSXJET. These changes are: (1) increased wing area from 89.65 to 104.89 m^2 (965 to 1130 ft^2); (2) GE21/J11-B10 double bypass engines in lieu of scaled advanced dry turbojets; and (3) two-dimensional air intake and long-duct air induction in lieu of axisymmetric short-duct nacelle system.

These configuration changes result in a higher net structural weight for SSXJET III. Although wing area increased, wing structural weight decreased because of two reasons: (1) additional wing structural bending relief was gained from a 28 percent increase in wing fuel, and (2) wing loading was reduced from 3878 to 3352 N/m^2 (81 to 70 lbs/ft^2). Propulsion group weight increased due to installation of the more complex GE21/J11-B10 double bypass engines which are both larger and heavier than the scaled dry turbojets. The most significant weight increase occurs in the nacelle group. By design and configuration, the two-dimensional air intakes are located beneath the wing about mid-body, while the engines are located at the extreme aft fuselage. The result is that the air induction ducts leading from the inlets to the engine are unusually long and therefore heavy. The combined effects of all changes results in a design gross takeoff weight of 36081 kg (79545 lbm) for SSXJET III, which is 360.6 kg (795 lbm) greater than that of the Basic SSXJET.

Balance

Mass balance characteristics are a major parameter influencing design, configuration development, and flying qualities of all aircraft. Because of the broad operational requirements of supersonic aircraft, (flight at subsonic, transonic and supersonic speeds), the trim and stability requirements are more extensive than those for subsonic applications.

In order to attain the desired longitudinal stability characteristics and flying qualities in the design of fixed wing aircraft, it is desirable to position the wing in such a manner that the aircraft center of gravity is located as close to the aerodynamic center-of-lift as possible. Under flight conditions, the locations of the aerodynamic center migrates as a function of Mach number while the location of the airplane C.G. remains fixed. In subsonic applications the variation between the two centers is small, but in supersonic operation the aerodynamic center-of-lift migrates aft as the Mach number increases causing the longitudinal stability to increase to undesirable levels. On conventional subsonic aircraft, this unbalance of forces acting through the two centers can be trimmed (reduced) by deflection of control surfaces such as elevators, trim tabs, canards, or all-moving tail-planes. Deflection of surfaces for purposes of trimming creates trim drag, which if very large, is highly undesirable for a long range aircraft. These drag penalties effect supersonic aircraft performance to a greater degree than that of subsonic aircraft and a more efficient way of achieving aerodynamic trimming must be employed.

The arrow-wing geometry developed by NASA after extensive wind tunnel testing, employs wing camber and twist. The gentle camber slopes used in place of large control surface deflections reduce trim drag significantly. The amount of reduction achieved in this manner, by twist and camber alone, is still not sufficient if the C.G. were to remain in the same location for both subsonic and supersonic flight since some fairly high static margins would still need to be trimmed.

A fuel management system (fuel transfer system) is chosen as a means to augment the benefits of wing twist and camber. By using this system to pump fuel into aft tanks, as the Mach number increases, the C.G. can be moved aft to coincide with the aftward migration of the aerodynamic center and minimize trim unbalance. A system of this type, utilizing fuel as a form of useful ballast, is used by such current supersonic transports as the "Concorde" and Tupolev 144, and military aircraft such as the B-1, SR71, and YF12. This system is in operational use and is a proven method of achieving C.G. control.

In each of the SSXJET configurations, the wing is located in a manner which tailors the balance characteristics to provide the center of gravity limits required for stability and control as specified in the Stability and Control section.

The balance characteristics of each configuration are tailored so that both the aft C.G. location desirable for rotation/flare characteristics at takeoff and landing, and the more forward C.G. location providing minimum drag at cruise are attainable.

Combinations of fuel tank sequencing were investigated to determine the most forward and aft center of gravity excursions and define limit boundaries. The attainable C.G. excursion envelope with the desired cruise C.G. path providing minimum drag during a typical mission for each configuration are presented in Figures 16, 17, 18, and 19. All of the points along the desired flight path lie within the limit boundaries and are attainable by proper fuel management.

All the preceding comments apply in general to all of the configurations but a few comments are necessary to point out some differences between each of the configurations.

Basic SSXJET

Wing apex located at F.S. 226.8, aft fuselage mounted engines.

SSXJET I

Wing relocated with apex at F.S. 206.5 to compensate for engines being relocated from aft fuselage to beneath wing mounted position.

SSXJET II and II Tandem

Wing apex located at F.S. 226.8, same as on Basic SSXJET, balance characteristics vary only slightly between versions due to minor differences in mass distribution.

SSXJET III

Due to configuration and engine changes, wing apex is located at F.S. 220. SSXJET III marginally satisfies C.G. limits required by stability and Control.

Inertia

The inertia characteristics of an aircraft, which are closely related to the balance characteristics by being a function of the mass distribution, are equally important in determining aircraft configuration and flying qualities. The magnitude and type of inertia forces and accelerations which must be overcome and controllable by the aerodynamic control surfaces during flight maneuvering determines the size of the control surfaces. Response rate, a measure of flying quality which is the rate at which the aircraft undergoes a change in altitude and direction about its axes within a given time period, is also governed by the magnitude of the inertial forces and in turn affects size and capacity of the flight control systems.

SSXJET configurations do not differ greatly in configuration geometry from executive/business jets currently in operation. Several subsonic jets have aft fuselage mounted engines. As explained in the balance section, the supersonic aircraft configuration is more sensitive to balance and inertia considerations. The fineness ratio and area distribution required for Mach 2.2 cruise speed requires a long fuselage. Mounting of the engines on the aft fuselage at the extremity of the airframe results in a type of "dumbbell" distribution, with large discrete masses located far from the aircraft C.G. resulting in higher pitch and yaw inertias. Differences in inertias and principal axes, which are due to variations in geometry and mass occur among the configurations. Using Basic SSXJET for comparison, some of the more pronounced differences may be explained by reviewing each configuration individually.

SSXJET I

Inertia values differ from basic SSXJET due to redistribution of mass resulting from relocating engines from aft fuselage mounted to underwing position. The roll inertia from SSXJET I is higher than Basic SSXJET because the engine pods are farther outboard at the underwing location. However, pitch and yaw inertias are lower because moving engines closer to aircraft C.G. reduced the typical "dumbbell" distribution characteristic resulting from locating large discrete masses at the extremities of the airframe.

SSXJET II and II Tandem

Inertia values differ only slightly from Basic SSXJET due to reduced weight and minor variations in mass distribution.

SSXJET III

Inertias increase over Basic SSXJET due to increases in gross weight and overall dimensions, and the resulting redistribution of mass. The roll and yaw inertias are higher as a result of increased wing span and a greater amount of fuel located in the wings. Heavier engines located at the aft extreme fuselage, and dimensional increases in wing span and overall length contribute to increases in pitch and yaw inertias.

The inertia data for takeoff and normal landing conditions are summarized in Table IV.

Summary

The use of stresskin in the weight estimation was deemed a conservative approach because of the existance of other advanced materials and construction techniques which promise equal or lighter weights. Of the alternate materials and techniques under consideration, one in particular, seems extremely promising. This is a new and innovative patented process, developed by Rockwell International, which combines superplastic forming and diffusion bonding into a single process (Reference 34). This process, known as SPF/DB, capitalizes on a unique property of titianium which permits very large tensile elongations under proper conditions of temperature and strain rate. Diffusion bonding is the joining of titanium under pressure at elevated temperatures without melting or use of bonding agents. Through a natural phenomenon superplastic forming and diffusion bonding can be accomplished under identical parametric conditions. This is the basis for the SPF/DB process. This process holds greater promise because it reduces component manufacturing costs by decreasing part count and labor, and results in weight savings due to inherent structural efficiency. It is estimated that a 10 percent reduction in airframe structural weight of the Basic SEXJET could be attainable through application of the advanced technology SPF/DB process.

STABILITY AND CONTROL

The horizontal and vertical tails of the SSXJET were originally sized by using tail volume coefficients based on the previously studied AST series of supersonic aircraft (Reference 6). This section presents the analysis which was done in order to confirm the validity of the original estimate of horizontal tail size and to determine the operating center-of-gravity limits.

The horizontal tails of supersonic cruise configurations have traditionally been sized by the takeoff and approach control requirements. A similar procedure has been used for this study. The aerodynamic data used is based on wind tunnel data with theoretical corrections applied in order to account for

differences between the tested configuration and the SSXJET. The horizontal tail was assumed to be all movable with a geared elevator. A flap deflection of 30 degrees for both takeoff and approach was used for the stability and control analysis in order to be compatible with the takeoff noise characteristics presented in this study.

Criteria

The analysis was based on the following criteria:

Takeoff

- Takeoff center-of-gravity range of 0.544 m (21.6 inches) which is equivalent to 0.060 $\bar{c}_{ref}$.
- Takeoff forward center-of-gravity limit determined at the position for neutral stability with the landing gear located such that nose wheel lift-off can be achieved at a speed of 162 kts.

Approach

- Approach speed defined at a lift coefficient of 0.6 for a flap deflection of 30 degrees.
- Minimum demonstrated speed defined at a 0.5 g incremental maneuver from trim at the approach speed.
- Aft center-of-gravity limit based on the ability to provide a nose-down pitching acceleration of 0.24 rad/sec^2 at the minimum demonstrated speed and the maximum landing weight.

Analysis and Results

The basic data for this analysis were obtained from reference 4. Lift and pitching moment increments due to leading and trailing edge flap deflections were obtained from reference 10 and corrected for flap area by the method of reference 12. Using the data for tail-on and tail-off runs from reference 10, a zero incidence tail contribution to lift and pitching moment was obtained as a function of angle of attack. The horizontal tail control power data were constructed by using the data of reference 6 for a geared elevator type horizontal tail with areas of 4.18 m^2 (45 ft^2) and 6.04 m^2 (65 ft^2). The data indicated that this type horizontal tail with a tail incidence of $\pm$20 degrees and an elevator incidence of $\pm$25 degrees deflection would give maximum control effectiveness. The resulting low-speed lift and pitching moment data are shown in Figure 20 for a flap deflection of 30 degrees and maximum control deflections.

The takeoff center of gravity limits were estimated on the basis of the stability and control criteria noted previously, the takeoff gross weight and pitch moment of inertia, takeoff $C_{L_{MAX}}$ in ground effect for takeoff and out of ground effect for climb out. The approach center of gravity limits were based on the approach stability and control criteria at the normal landing weight. Applying the approach criteria of trimming a nose-up pitching acceleration of 0.24 rad/sec at the minimum demonstrated speed results in an aft center of gravity limit of 0.5350 $\bar{c}_{REF}$ for a horizontal tail with an area of 6.04 m^2 (65 ft^2) and 0.4846 $\bar{c}_{REF}$ for 4.18 m^2 (45 ft^2). The landing forward center of gravity limits were determined by establishing the maximum nose-up trim capability at the minimum demonstrated speed. These forward limits were 0.3384 $\bar{c}_{REF}$ for the 6.04 m^2 (65 ft^2) tail and 0.3805 $\bar{c}_{REF}$ for the 4.18 m^2 (45 ft^2) tail. The neutral stability center of gravity locations were determined to be 0.4695 $\bar{c}_{REF}$ and 0.4320 $\bar{c}_{REF}$ for the 6.04 m^2 (65 ft^2) and 4.18 m^2 (45 ft^2) horizontal tails, respectively. These computed center of gravity locations are plotted in Figure 21 as a function of horizontal tail volume coefficient. Using the criteria that the takeoff forward center of gravity location is 0.549 m^2 (21.6 inches) ahead of the aft center of gravity limit and is at the position for neutral stability, a horizontal tail volume coefficient of 0.1128 or area of 5.76 m^2 (62 ft^2) is required. The corresponding limits are 0.5216 $\bar{c}_{REF}$ for the aft center of gravity, 0.4615 $\bar{c}_{REF}$ for the takeoff forward center of gravity, and 0.3440 $\bar{c}_{REF}$ for the approach forward center of gravity. This aft limit is more forward than the aft limits characteristic of the AST configurations because of the increased pitch rate requirement during approach for the lighter SSXJET.

The SSXJET is statically unstable over the greater portion of its center of gravity range and the data indicates that the basic airframe would have considerable pitch-up tendencies. Therefore, a hardened stability augmentation system (HSAS) would be required to stabilize the aircraft and achieve acceptable handling qualities. The term "hardened" means that the stability augmentation system has sufficient redundancy to preclude loss of the system. These systems, although not used very frequently in the past, are being used on military aircraft and may soon be common on commercial aircraft.

The stability and trim curves were developed for a projected, exposed horizontal tail area of 5.76 m^2 (62 ft^2) and are presented in Figures 22 and 23. From Figure 22 it can be seen that there is adequate control to produce a nose down pitching acceleration of 0.24 rad/sec at the aft center of gravity limit. The approach forward center of gravity limit has been changed to 0.3611 $\bar{c}_{REF}$ in order to be able to trim the aircraft during approach at a 6 degree angle of attack. This was considered to be the maximum angle of attack for which adequate visibility over the nose could be achieved. From Figure 23, it can be seen that adequate control exists to trim in the takeoff and climb out configuration.

Summary

A horizontal tail with an area of 5.76 m^2 (62 ft^2) would provide the SSXJET configuration with sufficient control during takeoff, climb-out and approach. This compares favorably with the 6.04 m^2 (65 ft^2) area originally estimated. The center-of-gravity range for this configuration is from 36.11 to 52.16 percent of the reference mean aerodynamic chord. The data indicate that the SSXJET configuration would have pitch up tendencies and would require a hardened stability augmentation system in order to have acceptable handling qualities.

PROPULSION

To conduct airplane performance and acoustic studies, engine performance data sufficient to encompass the airplane flight envelope must be provided. Listed below is the minimum engine performance data required to properly conduct airplane performance analysis:

1. Mission performance - gross thrust, ram drag, and fuel flow at various altitudes and Mach numbers.

   A. For climb performance - data points for two different altitudes at each maximum cruise power levels.

   B. For cruise performance - data points for five Mach numbers and altitudes at maximum and four-part power-cruise settings.

2. Takeoff, landing, and acoustic performance - net engine thrust, exhaust gas flow rate, exhaust gas jet velocity, exhaust gas exit area, and exhaust gas exit temperature. These data must be provided for all combinations of three altitudes, three Mach numbers, at takeoff power and four-part power settings.

Engine performance data requirements are shown graphically in Figure 24. In this figure the engine data requirement is superimposed on a plot of the Mach-altitude climb schedule used in the SSXJET airplane studies.

Installed engine performance data for an advanced NASA turbojet engine, as described above, was provided for each SSXJET configuration studied. Engine performance data provided by the General Electric Company for the GE21/J11-B10 engine was used in the study of the SSXJET III airplane. The data reported in this document, however, are advanced turbojet engine performance used on the SSXJET configuration at a standard +8°C day and GE21/J11-B10 engine performance at standard day conditions for missions analysis and for both engines at standard +10°C conditions for takeoff, landing, and acoustic analysis. No data were available for the GE21/J11-B10 engine at standard +8°C conditions.

NASA Turbojet Discription

The advanced turbojet cycle employed in the SSXJET studies is one which was generated at the NASA Langley Research Center, as an improvement over the GE4/J5P engine which was designed for the United States Supersonic Transport porgram.

Turbojet engines are the most fuel efficient engines available for supersonic cruise conditions, however, are less efficient at subsonic cruise conditions and more noisy than turbofan engines at takeoff. It would be desirable, therefore, to have an engine which operates like a turbofan at takeoff and subsonic cruise condition; for example, a variable cycle engine.

However an attractive turbojet cycle can be conceived using a variable geometry turbine, and thus approach the variable cycle capability. The turbojet cycle used in this study is discussed in some detail in reference 5.

Basically, the variable geometry turbine turbojet permits the engine to operate at the design compressor pressure ratio and efficiency at a reduced turbine inlet temperature (reduced power setting) by adjusting the turbine inlet area. With the engine operating at these conditions, at part power, the engine operating efficiency is higher than it would be if the turbine inlet geometry were fixed. This results in a lower fuel consumption at part-power operating conditions encountered during subsonic cruise.

Another feature of the variable geometry turbine turbojet is that while operating at part power, the engine airflow is higher than with a fixed turbine turbojet. This is a desirable feature for jet noise reduction. Jet noise production is simply related to the engine exhaust gas velocity. Engine thrust is also related to both the exhaust gas velocity and flow rate. Thus, when the gas flow rate is increased at the same thrust level, the exhaust gas velocity is reduced with a resulting reduction in jet noise.

This engine cycle has been used in several supersonic transport design studies, one of which is reference 6.

A scaled version of this advanced turbojet engine has been used in the SSXJET studies and has the following sea level static standard day design charcteristics:

Overall compression ratio = 15:1

Turbine inlet temperature = 1700^{o}K (3060^{o}R)

Corrected engine inlet airflow = 72 kg/sec (158.7 lbm/sec)

Uninstalled gross thrust = 73000 N (16410 lbf)

Bare engine mass (weight) = 881 kg (1942 lbm)

This bare engine mass includes the gas generator, nozzle, and thrust reverser.

A sketch of this engine is shown on Figure 25.

The selected engine is not necessarily the optimum engine for a Mach 2.2 cruise SSXJET airplane. As shown in reference 5, it may be possible to select an engine with better performance by choosing one with a higher overall compressor pressure ratio. To determine the optimum engine for a particular airplane mission would require a complete evaluation of the entire desired airplane flight envelope for each available engine installation. Such an engine/airplane optimization was not accomplished in this study. Optimization, however, should be undertaken in future studies.

A nacelle to house the engine was configured as shown in Figure 26. The results of an unpublished study which evaluated the wave drag characteristics of various shape nacelles indicated that the configuration selected would have the minimum wave drag.

The cylindrical nozzle exit would also result in no boattail drag. In order to have a cylindrical nozzle exterior and still have a converging diverging fully expanded nozzle, an ejector nozzle was utilized. An ejector nozzle is one which induces a secondary flow into the nozzle. The secondary flow not only cools the nozzle walls but fills the void between the nozzle walls and exhaust gas stream, thus, minimizing nozzle losses. The large flight envelope of the SSXJET airplane is such that it is not possible to maintain a cylindrical nozzle exit at all flight conditions. An ejector nozzle does, however, minimize the nozzle boattail angle at those flight conditions where a nozzle boattail is necessary.

The inlet used is a scaled version of the NASA Ames developed "P" inlet of reference 7. This is an axisymmetric inlet with a translating spike. The translating spike is provided to match the required engine airflow at all flight operating conditions with minimum losses.

The maximum diameter of the nacelle was determined by the fully expanded nozzle exit diameter at the design cruise conditions of:

Mach number = 2.2

Altitude = 18288 m (60000 ft)

Atmosphere = Standard day

Other nacelle dimensions are based on the AST-100 nacelle and the GE4 engine of reference 6.

As the SSXJET studies progressed, the size and configuration of the airplane changed resulting in different size engine requirements. Different engine and

nacelle sizes were determined by means of the scaling data shown in Figure 27 from reference 9.

Installed performance of the engine was generated with the aid of the computer program of reference 9. The computer program generates engine performance by means of a cycle match procedure. It employs the GE4/J5P compressor map in a non-dimensional form, fixed combustor efficiency, and a fixed turbine polytropic efficiency. The design point calculation fixes the compressor design point, dimensionalizes the compressor and establishes the matching turbine flow function. The turbine flow function remains fixed and an engine operating point is determined by flow matching the compressor and turbine at a given turbine inlet temperature and engine rotor speed.

Installation effects of the inlet, nozzle, thrust reverser, service air bleed of 0.454 kg/sec (1 lbm/sec), and 149 kw (200 HP) power extraction are included in the calculation of installed engine performance.

Drags due to inlet spillage, bypass, nozzle boattail, and air conditioning are accounted for by applying a drag increment to the airplane drag polars. The combined drag increment for spillage, bypass, and nozzle boattail were estimated by scaling the propulsion drag increment from reference 6 based on reference wing area and engine airflow. The total drag increment is shown on Figure 28.

The installed performance data for the advanced turbojet at standard +8°C atmospheric conditions is presented on Figures 29 throught 31. Superimposed on Figure 31 are the beginning and end cruise operating points. Data for takeoff, landing, and noise studies at standard +10°C atmospheric conditions is provided on Figures 32 through 35.

Design sea level static thrust and airplane thrust to weight ratios at various conditions are tabulated below for the engine and the SSXJET airplane at a design gross weight of 35720 kg (78750 lbm).

Conditions	Thrust	Thrust/Weight
Uninstalled standard day	72995 N (61410 lbf)	.4168
Installed standard day	67577 N (15192 lbf)	.3858
Installed standard +8°C day	64677 N (14540 lbf)	.3693
Installed standard +10°C day	64000 N (14388 lbf)	.3654

General Electric Variable Cycle Engine Description

The GE21/J11-B10 engine is a double bypass variable cycle turbofan engine based on technology available in 1985. Double bypass variable cycle describes the function of the engine which, for takeoff and low-speed operation increases the bypass airflow to provide better low-speed performance both acoustically and thermodynamically. For high-speed performance, the bypass air is reduced to provide performance approaching that of a turbojet engine.

An additional feature of this engine is that the bypass airflow, which in other turbofan engines would be the outer stream, in this engine is diverted so that it exhausts through the nozzle plug and becomes the inner stream. This is done to gain the effects of coannular sound suppression (reference 8).

Geometric and engine performance data for the GE21/J11-B10 engine were provided by the General Electric Company. This engine is designed for a cruise Mach number of 2.2 at an altitude of 18288 m (60000 ft) for standard atmospheric conditions with the following design characteristics:

Bypass ratio = 0.35

Overall pressure ratio = 17.3

Maximum afterburning temperature = 1355°K (2439°R)

Corrected engine inlet airflow = 317.5/349.3 kg/sec (700/770 lbm/sec)

Engine mass (weight)

Gas generator, afterburner, annular

Nozzle and suppressor 5343 kg (11780 lbm)

Afterburner system 118 kg (260 lbm)

A sketch of the GE21/J11-B10 engine scaled to the SSXJET III size is shown on Figure 36.

The engine as provided by GE is much too large for the SSXJET III airplane; therefore, it was scaled to the required uninstalled thrust of 96526 N (21700 lbf) at sea level static standard day conditions. Scaling was accomplished by means of the scale factors suggested by GE as shown below:

Weight

$$Wt_2 = Wt_1 \left(\frac{Wa_2}{Wa_1}\right)^{1.1} = Wt_1 \left(\frac{Fn_2}{Fn_1}\right)^{1.1}$$

Diameter

$$D_2 = D_1 \left(\frac{Wa_2}{Wa_1}\right)^{.5} = D_1 \left(\frac{Fn_2}{Fn_1}\right)^{.5}$$

Length

$$L_2 = L_1 \left(\frac{Wa_2}{Wa_1}\right)^{.5} = L_1 \left(\frac{Fn_2}{Fn_1}\right)^{.5}$$

Where

Wt = Engine mass (weight)

D = Diameter

L = Length

Wa = Engine airflow

Fn = Net engine thrust

Subscript 1 = GE21/J11-B10 parameter

Subscript 2 = Desired engine parameter

Mass (weight) of the scaled engine is 1828 kg (4029 lbm) and includes the gas generator, afterburner, and annular nozzle with a built in thrust reverser.

In general, scaling an engine more than 25 percent either up or down is inadvisable. The above scaling factors provided by GE, however, are considered sufficiently accurate for the purpose of this study.

The performance data supplied includes the installation effects of inlet, nozzle, thrust reverser, afterbody drag, service airbleed of 0.454 kg/sec (1 lbm/sec) and 149 kg (200 HP) power extraction. The inlet performance included in the installed engine performance by GE was that of the Douglas Aircraft Company's axisymmetric external compression inlet. A sketch of the Douglas inlet is shown in Figure 37. Performance characteristics of this inlet, including propulsion drag, are shown on Figure 38. As with the turbojet engine, the propulsion drag as shown on Figure 38 was applied as an increment to airplane drag polars rather than charging it as a penalty to the engine performance.

The external compression inlet was not used on the SSXJET III, instead a two-dimensional inlet was sized to the scaled capture area of 0.814 m^2 (8.766 square feet) of the Douglas inlet and fitted to the SSXJET III airplane. The installed engine performance was not altered because of this change in inlet since it was assumed that a two-dimensional inlet could be designed to produce the same performance characteristics.

Engine performance as provided by GE was insufficient to perform mission, takeoff, landing, or noise studies. The data supplied is shown in block form on Figure 39.

It was necessary, therefore, to expand on the data supplied to provide enough data points to conduct the above studies. The supplied data was expanded by first correcting it for altitude, Mach number, and atmospheric conditions, then by adjusting the corrected data points for small changes in altitude and/or Mach number. The data as enriched by Vought Hampton for mission, takeoff, landing, and acoustic analysis is shown in block form on Figure 40. Engine performance data used in the SSXJET III mission studies is shown for standard atmospheric conditions in Figures 41 through 43.

Engine performance data for takeoff, landing, and noise studies were expanded (see Figure 40) to cover an altitude range from 0 to 1219 m (4000 ft) and a Mach number range from 0.0 to 0.4 based on the following assumptions:

1. The performance varies linearly with altitude at all Mach numbers.
2. The slope of the altitude variation is the same for all power settings at all Mach numbers and was determined by the full power data points supplied.
3. The performance varies linearly with Mach number at all altitudes.
4. The slope of the Mach number variation is the same as that determined for the GE21/J11-B10 engine at corresponding power settings of 50, 48, and 46, and the same as the slope of power setting 46, for all power settings below 46.

Graphs of the takeoff performance of the GE21/J11-B10 engine are provided on Figures 44 through 51 for standard +10°C atmospheric conditions.

The GE21/J11-B10 engine when installed in the SSXJET III airplane results in an aircraft design gross weight of 36076 kg (79545 lbm). Tabulated below for the SSXJET III at various conditions are the design sea level static thrust and airplane thrust-to-weight ratios.

Conditions	Thrust	Thrust/Weight
Uninstalled standard day	96526 N (21700 lbf)	.5456
Installed standard day	90228 N (20284 lbf)	.5099
Installed standard +8°C day	86416 N (19427 lbf)	.4885
Installed standard +10°C day	86060 N (19347 lbf)	.4864

Summary

From the results of these studies it can be concluded that the engine designs provided are adequate to meet the requirements of a feasible supersonic executive jet airplane. During the course of this study, no attempt was made to optimize the engine or inlet or airplane or in combination; therefore, the following are recommended:

- Conduct a detail design study of a variable cycle turbofan and/or a variable turbojet to achieve the best compromise between takeoff noise supersonic cruise, and supersonic cruise performance.
- Conduct detail design engine inlet integration studies to provide the required engine airflow with minimum losses.
- Conduct airplane/engine optimization studies to determine the best engine cycle/airplane configuration to meet the requirements of the mission and takeoff noise.

LOW-SPEED AERODYNAMIC CHARACTERISTICS

The untrimmed low-speed aerodynamic characteristics for the SSXJET and SSXJET I configurations have been estimated for trailing-edge flap deflections of 0^{o}, 5^{o}, 20^{o}, and 30^{o}. The lack of experimental data for the SSXJET series wing in the high-lift configuration has necessitated the use of analytical, experimental and empirical methods and data. This approach includes the use of a vortex lattice method for definition of the clean-wing lift curve and empirical estimates of landing gear and nacelle-fuselage interference drag increments. Additional data required for the analysis has been obtained from wind tunnel tests of a supersonic cruise concept. These data represent the culmination of an extensive research program employing the SCAT 15-F configuration as developed and tested at the NASA Langley Research Center. The purpose of this section is to discuss the techniques employed in the analysis and to present the results obtained. Although no detailed analyses have been performed for the SSXJET II and SSXJET III, low-speed characteristics for these configurations may be estimated through suitable extension of the SSXJET and SSXJET I results as noted.

High-Lift System Definition

The high-lift system applied to the SSXJET wing is illustrated in Figure 52a. The leading-edge devices L_1 and L_2 and the trailing-edge flaps T_1, T_2, and T_3 are all independent plain flaps with the areas indicated in the figure. Note that full-span trailing-edge flaps are defined for the SSXJET as the nacelles are located on the aft fuselage. The trailing-edge flaps are used in the normal sense to provide additional lift during takeoff and approach, and flap T_3 may also be used for roll control as required. The leading-edge device L_1 is used primarily for suppression of the vortex shed from the wing apex. This vortex suppression results in significant improvements in the longitudinal stability characteristics. Similarly, flap L_2 delays flow separation on the outboard wing panel and further retards the onset of pitchup due to tip stall. Deflection of these leading-edge devices does not eliminate pitchup, but it is delayed to angles of attack well beyond the normal operating envelope.

Insofar as the SSXJET I high-lift system is concerned, the primary effect of relocating the nacelles to the underwing position is the reduction in area for flaps T_1 and T_2 as shown in Figure 52b. Leading-edge devices L_1 and L_2, as well as trailing-edge flap T_3 are unchanged by the nacelle relocation. Total trailing-edge flap area for the SSXJET I is approximately 25 percent less than that for the SSXJET. The overall aerodynamic effect of this flap area reduction is, of course, of primary interest in the following analysis.

Data Base

The SSXJET is a derivative of the Douglas Mach 2.2 AST concept (reference 4). No low-speed wind tunnel data for the Douglas concept is available, however, and thus the choice of suitable data on which to base the analysis becomes the

fundamental concern. A survey of recent AST low-speed wind tunnel tests has indicated that the data of reference 10 would provide the most reasonable data base. A photograph of the model used in these tests in the Langley full-scale tunnel is shown in Figure 53. The configuration has an arrow-wing planform with an inboard sweep of 74°, a midspan of 70.5°, and an outboard sweep of 60°. Both leading-edge and trailing-edge flaps are included for lift augmentation and pitchup control. The wing twist and camber have been optimized for 1_g cruise at Mach 2.7, and the fuselage area ruling results in minimum configuration wave drag at cruise The model configuration included either two upper surface mounted nacelles or four underwing nacelles, a drooped nose for improved pilot visibility during takeoff and landing, vertical wing fins for improved directional stability during cruise, and an empennage. Of particular interest are the full span trailing-edge flaps tested in conjuction with upper surface mounted engines and the increased flap effectiveness obtained by blowing at the flap knee. The primary data base for the SSXJET analysis is thus defined as follows:

Full Scale Tunnel Test 369 (NASA TM X-72792)

Run	$t_1 = t_2 = t_3$	C_μ
320	0°	0.
331	20°	.025
352	30°	.025

where C_μ is the flap blowing coefficient based on the wing gross area.

All of these runs have:

- o two upper surface mounted engines (power off)
- o full span trailing-edge flaps
- o tail off
- o $L_{1,2} = 30°$ (apex leading-edge flaps)
- o $L_6 = 45°$ (tip panel leading-edge flap)
- o $t_4 = 5°$ (tip panel trailing-edge flap)

Other data have been used where required for specific lift or drag increments not directly obtainable from the above. Such departures are noted as required in the following text. Also note that "T" refers to SSXJET trailing-edge flaps while "t" corresponds to test model flaps.

Lift Development-SSXJET

The initial step in the development of the SSXJET lift curves involved defining a clean configuration lift curve to which the various lift increments due to flaps could be added. This baseline lift curve for the SSXJET has been developed using the vortex lattice method described in reference 11. Data input to this program included definition of the twisted and cambered SSXJET wing, the fuselage planform, and the horizontal tail at zero incidence. The horizontal tail is assumed fixed at zero incidence throughout this analysis.

Development of the lift increments due to trailing-edge flap deflection required that the lift data from runs 331 and 352 described above be corrected to eliminate the direct lift developed by the flap knee blowing. The net lift on the model is

$$C_{L_{NET}} = C_{L_{TEST}} - C_{\mu_{REF}} \sin (\alpha_{WRP} + \delta_{FLAP}) \qquad (1)$$

where $C_{\mu_{REF}}$ is blowing coefficient based on the wing reference area.

The lift increments due to model flap deflections of 20^o and 30^o (relative to 0^o) are then directly obtained for a series of angles of attack.

The flap lift increment correction technique described in reference 12 has been used to estimate the effect on lift of flap geometry differences between flaps t_1, t_2, and t_3 for the Test 369 model and flaps T_1 and T_2 for the SSXJET. These geometry differences have been found to have a relatively small effect on the flap lift.

Flap T_3 on the SSXJET corresponds to flap t_4 on the Test 369 model. Insofar as no data are available from Test 369 for t_4 deflections, data from reference 13 was selected for determination of the desired increment ($T_3 = 0^o$ to 5^o). The average value of this lift increment has been found to be .0040. This result has been corrected for flap geometry differences between the SCAT 15-F model reported in reference 13 and the SSXJET using the method of reference 12.

The effect of the SSXJET leading-edge device L_1 is to spoil the vortex lift generated by the wing apex. Insofar as the vortex lattice method used to develop the baseline SSXJET lift does not account for this additional vortex lift, the baseline lift may be assumed to reflect a deflection of 30^o for L_1. The lift contribution related to a 45^o deflection of L_2 becomes significant only for angles of attack beyond twenty degrees and thus has been assumed negligible herein.

Overall lift curves for the SSXJET have been developed using the baseline lift curve with its implicity L_1 and L_2 effects and the flap lift increments described above. The results of this analysis are shown in Figure 54. Note that the following configuration components are fixed:

$$L_1 = 30^o \quad L_2 = 45^o \quad T_3 = 5^o$$

$$i_t = 0^o \text{ (fixed)}$$

Also note that only out of ground effect lift curves are shown insofar as current takeoff analysis routines internally computes ground effects using the method of reference 12. SSXJET characteristics in ground effect are presented later in this section.

SSXJET I

Overall lift curves have been derived for the SSXJET I using the same assumptions, data base, and vortex lattice method which have been described above for the SSXJET. The reduction in area for flaps T_1 and T_2 has required application of the flap correction factor described in reference 4. This correction has indicated that approximately 60 percent of the flap lift increments derived for the SSXJET from the Test 369 data could be applied to the SSXJET I.

Nacelle-wing interference results in increased overall lift for the SSXJET I. Data from reference 13 have been used to estimate this interference lift increment as follows: Lift curves with nacelles on and off have been examined to determine an average lift increment for the SCAT 15-F with four underwing nacelles. This increment has subsequently been corrected to account for both the reduction to two nacelles and the ratios of nacelle inlet area to wing reference area for both the reference 13 model and the SSXJET I. This technique has resulted in a SSXJET I wing-nacelle interference lift coefficient of .0110.

Analysis of the leading-edge devices L_1 and L_2 and the trailing-edge flap T_3 parallels exactly the method above for the SSXJET.

The results of the SSXJET I lift analysis are shown in Figure 55. Note again that $L_1 = 30^o$, $L_2 = 45^o$, $T_3 = 5^o$, and that the horizontal tail is fixed at zero incidence.

Drag Development - SSXJET

The total drag for the SSXJET is assumed to consist of pressure drag, skin friction, interference drag, air conditioning and propulsion bleed drag, drag due to lift, and, where appropriate, landing gear drag. The development of these various drag items has necessarily involved the use of analytical, experimental, and empirical data as described below.

Skin friction and pressure drag have been estimated using the DATCOM method described in Section 4 of reference 14. Turbulent flow over a smooth, flat plate has been assumed. The pressure drag contribution is considerably less than the friction drag being proportional to $(t/c)^4$ where t/c is the wing thickness ratio.

Wing-body interference is accounted for directly in the computation of the skin friction and pressure drag items when using the method of reference 14. Nacelle-fuselage-empennage interference has been estimated using unpublished data for the Boeing 727 aircraft which has a nacelle enpennage arrangement very similar to that of the SSXJET. No other interference drag items have been considered.

Air conditioning and propulsion bleed drag increments have been derived using data from reference 12. These previous data have been corrected to account for the SSXJET engine airflow, a reduction from four engines to two, and the wing reference area change to the SSXJET value of 89.65 m^2 (965 ft^2).

Semi-empirical estimates of the landing gear drag have been made using data from reference 15. The nose gear consists of two wheels mounted on a single strut while the main gear involves two wheels mounted on each of two struts.

The overall zero-lift drag build up for the SSXJET is summarized in Table V. These data are applicable to the takeoff, approach, and landing segments of the flight envelope.

The drag contributions of the SSXJET leading-edge devices L_1 and L_2 have been incorporated as a shift in the minimum drag point. Data from runs 230 and 233 of the Test 369 data base (reference 10) directly provide the drag increment developed by the apex flaps when deployed to 30^o deflection. This increment has been corrected for the ratio of leading-edge flap area to wing gross area. This estimated drag shift due to L_1 at 30^o is .00194. The increment for L_2 deflected 45^o has been similarly derived using data from reference 16. The result for L_1 is .00435. Analysis of data from reference 13 for flap t_4 indicated that a 5^o deflection of SSXJET flap T_3 would have a negligible effect on the drag.

Determination of drag due to lift for the SSXJET utilizes the same primary data base noted above for the lift analysis. As in the lift analysis, the direct thrust effects due to flap blowing must first be removed:

$$C_{D_{NET}} = C_{D_{TEST}} + C_{\mu_{REF}} \cos (\alpha_{WRP} + \delta_{FLAP}) \tag{2}$$

These corrected data have been used to calculate polar shape parameter (PSP) values for the Test 369 model as follows:

$$PSP = \frac{C_{D_{0\%}} - \left(C_D - C_{D_{MIN}}\right)}{C_{D_{0\%}} - C_{D_{100\%}}} \tag{3}$$

The 0 percent suction lines for the Test 369 model are determined from the equation:

$$C_{D_{0\%}} = (C_L - \Delta C_L) \tan (\alpha_{WRP} - \alpha_0) \tag{4}$$

while the 100 percent values are given by:

$$C_{D_{100\%}} = (C_L - \Delta C_L)^2 / \pi AR \tag{5}$$

where AR is the wing aspect ratio based on the wing reference area. In these equations C_L is the total thrust corrected lift coefficient, ΔC_L is the lift coefficient at the minimum drag point, α_{WRP} is the angle of attack of the wing reference plane, and α_0 is the angle of attack for zero lift. $(C_D - C_{D_{MIN}})$ must be determined from the thrust corrected drag data where C_D is the total drag

coefficient and $C_{D_{MIN}}$ is the minimum drag. The drag polars to be developed for the SSXJET will thus reflect the "suction" levels developed by the Test 369 model and will be constructed about the minimum drag point.

The results of these calculations are presented in Figure 56. Polar Shape Parameter values for the case $t_1 = t_2 = t_3 = 5^o$ were estimated by linearly interpolating the PSP values at 0^o and 20^o.

The PSP values determined above have been assumed to be directly applicable to the SSXJET. No corrections for leading-edge Reynolds number have been applied to these PSP values. Although the direct lift and thrust effects due to flap blowing have been extracted from the Test 369 force coefficients, it has been assumed that the additional induced circulation due to blowing results in sufficiently improved leading-edge performance to justify omission of the leading-edge Reynolds number correction. Thus it becomes possible to compute the desired $(C_D - C_{D_{MIN}})$ values:

$$C_D - C_{D_{MIN}} = C_{D_{0\%}} - PSP\ (C_{D_{0\%}} - C_{D_{100\%}}) \qquad (6)$$

where $C_{D_{0\%}}$ and $C_{D_{100\%}}$ must be calculated for the SSXJET using the lift curves from Figure 53 and the aspect ratio AR = 1.84. The ΔC_L values required for these calculations are not directly available for the SSXJET, and thus the values determined from Test 369 have been assumed. This choice of ΔC_L values also implicitly accounts for the polar vertical shift due to deflection of L_1, L_2, and T_3 insofar as the corresponding model components for Test 369 were similary deployed.

The required lift coefficients for the polar definition have been obtained by adding to the $C_L - \Delta C_L$ values from Figure 54 the increments in ΔC_L associated with the various flap deflections. The ΔC_L value for $T_1 = T_2 = 5^o$ has been estimated by linearly interpolating the 0^o and 20^o flap data.

Total drag coefficients have been derived by adding the zero-lift drag increments previously discussed to the $C_D - C_{D_{MIN}}$ values determined from equation (6). Also included are the shifts in minimum drag due to L_1, L_2, and T_3 as well as the increments due to flap deflections from Test 369. The estimated landing gear drag has also been included for the $T_1 = T_2 = 20^o$ and 30^o cases.

These drag polars for the SSXJET are presented in Figure 57. Note again that no ground effects are included and that the horizontal tail is fixed at zero incidence. The lift-to-drag ratio values obtained from these polars are shown in Figure 58.

SSXJET I

Skin friction, pressure drag, air-conditioning and propulsion bleed drag, and landing gear drag values for the SSXJET I have been estimated as described above for the SSXJET, and, with the exception of the wing-nacelle interference, the values of these zero-lift drag items correspond to those of the SSXJET. As previously noted in the lift development above, data from reference 13 have been used to estimate the nacelle-wing interference for the SSXJET I. Nacelle on and off data from reference 13 have been used to derive the nacelle drag for the SCAT 15-F with four underwing nacelles. An estimate of the nacelle friction drag has been subtracted from this increment to obtain the interference drag. This result has subsequently been corrected to account for the reduction from four to two nacelles and the ratios of nacelle inlet area to wing reference area. The resultant wing-nacelle interference drag coefficient for the SSXJET I is .00275. This relatively high interference increment results because the SSXJET I nacelles are large compared to the wing. Table VI summarizes the complete zero-lift drag build-up for the SSXJET I.

Drag values for leading-edge devices L_1 and L_2 as well as trailing-edge flap T_3 corresponds to the values previously estimated for the SSXJET. Drag-due-to-lift for the SSXJET I has been determined using the polar shape parameter (PSP) technique and data base discussed above. To account for the effects of the nacelle flap cutout, the following technique has been applied: Additional PSP values have been determined from runs 233, 239, and 251 of Test 369 (reference 10). These runs provide data for the test model configured with four underwing nacelles and two trailing-edge flap cutouts. All other configuration components correspond to those described above for the SSXJET. These data have been corrected for flap blowing direct lift and thrust effects and the PSP values determined for trailing-edge flap angles of 0^{o}, 20^{o}, and 30^{o}. The SSXJET I PSP values presented in Figure 59 have been computed by averaging these two sets of Test 369 PSP values. This approach is intended to provide a reasonable estimate of the PSP values for the SSXJET I with its single flap cutout while maintaining consistency in the data base.

The SSXJET I drag polars have been constructed from the various drag items discussed above. Flap lift and drag increments used in the polar development are the geometry corrected values. The wing-nacelle interference lift and drag have been applied as shifts in the minimum drag point. These SSXJET I drag polars are presented in Figure 60 where the landing gear drag has been included for the 20-degree and 30-degree flap cases. The L/D curves derived from these polars are shown in Figure 61.

The analyses outlined above suffer from a lack of low-speed wind tunnel data for the Douglas wing on which the SSXJET concepts are based. It is felt, however, that the results presented represent a reasonable estimate of the low-speed aerodynamic performance of the aircraft. The analyses of the SSXJET I, in particular, represents a consistent extension of the SSXJET results and should provide a clear indication of the differences in the low speed characteristics of the two concepts.

SSXJET Characteristics In Ground Effect

As previously noted, current takeoff analysis routines internally compute ground effects on lift and drag and thus the out of ground coefficients presented above have been used directly in the takeoff analysis. The untrimmed in ground effect coefficients developed in the takeoff analysis are summarized below along with the basic approach employed. The development of these ground effect equations has been fully documented in reference 12.

The ratio of in ground lift coefficient to the out of ground value has been shown in reference 12 to be:

$$\sigma_L = \frac{C_{L_g}}{C_L} = 1 + \frac{1}{\frac{1}{2} + 32\left(\frac{h}{b}_o\right)^2 \frac{(6+A)^4}{(36+A)^2} + 4\frac{h}{b}_o \frac{(6+A)^2}{(36+A)} \left[1 + 32\left(\frac{h}{b}_o\right)^2 \frac{(6+A)^4}{(36+A)^2}\right]^{1/2}} \tag{7}$$

where h_o is the wing height above ground, b is the wing span, and A is the wing aspect ratio. At points away from the ground the drag may be expreseed as:

$$C_D = C_{D_{MIN}} + (C_L - C_{L_M})(\alpha - \alpha_o) \tag{8}$$

where $C_{D_{MIN}}$ is the minimum drag point, C_{L_M} is the corresponding lift coefficient, α is the angle of attack, and α_o is the angle of attack for zero lift. The drag in ground effect may be calculated from the expression:

$$C_{D_g} = C_{D_{MIN}} + \sigma_L \sigma_i (C_D - C_{D_{MIN}}) + (\alpha - \alpha_o) C_L (\sigma_L - 1) \tag{9}$$

where σ_i is given by:

$$\sigma_i = 1 - \frac{1}{1 + 32\left(\frac{h_o}{b}\right)^2 + 4\left(\frac{h_o}{b}\right)\left[1 + 32\left(\frac{h_o}{b}\right)^2\right]^{1/2}} \tag{10}$$

A drag factor is then computed using equation (8) and (9) as

$$\sigma_D = \frac{C_{D_g}}{C_D}$$

and applied to the out of ground drag coefficient values.

These equations have been included directly in the takeoff analysis routines to automatically compute ground effects throughout the takeoff profile. Typical results for the SSXJET configuration are presented in Figure 62. Also indicated in the figures are points corresponding to operating conditions during the ground run, at lift-off, and at the 10.7 m (35 ft.) obstacle point. The SSXJET wing span is approximately 12.8 m (42 ft.) and for h_o/b values of unity or greater, the ground effect is insignificant.

Extension to SSXJET II and SSXJET III Concepts

Although no detailed analyses of the low-speed aerodynamics for the SSXJET II and SSXJET III concepts have been made, reasonable lift and drag estimates may be made through suitable extensions of the analyses presented above.

The SSXJET II concepts are similar to the SSXJET discussed above except for the wing-body blending and forebody shaping. These differences are assumed to have a small effect on the low-speed aerodynamics and thus the SSXJET data are applicable to the SSXJET II aircraft.

Drag estimates for the SSXJET III have been made by correcting for the differences in zero-lift drag between the SSXJET I and SSXJET III. Both skin friction and propulsion bleed drag corrections have been made resulting in a net drag increase of six counts (.0006) for the SSXJET III relative to the SSXJET I. Differences in lift and drag-due-to-lift have been assumed negligible.

Summary

Low-speed aerodynamic characteristics for the SSXJET and SSXJET I concepts have been developed using a combination of analytical, experimental, and empirical methods and data. These studies represent a consistent approach to the development of the low-speed aerodynamic characteristics of the configurations and should clearly point to the differences between the two concepts in the high-lift configuration. More detailed analyses will require low-speed wind tunnel data for the Douglas AST wing on which the SSXJET series aircraft are based.

SUBSONIC/TRANSONIC AERODYNAMICS

The subsonic/transonic aerodynamic characteristics of the SSXJET configuration have been estimated through suitable corrections to available wind tunnel data for the Douglas Mach 2.2 AST concept (reference 4) on which the SSXJET is based. The study covers the Mach number range from 0.5 to 0.95 at lift coefficients from -0.04 to 0.28. The purpose of this section is to discuss the methods employed in the development of the SSXJET drag polars and to note the application of the results to subsequent configurations in the SSXJET series.

Data Base

The wind tunnel data used for this analysis consisted of preliminary data packages which have subsequently been published as reference 4. These original data were fairly limited in both data range and configuration build-up, thus necessitating a considerable amount of component drag prediction. Usable data consisted of polars for the wing-body at Mach numbers of 0.5, 0.7, 0.9, and 0.95 for a lift coefficient range of 0. to 0.28.

Polar Development

Extrapolation of the test polars was performed by fairing a smooth curve to reach the desired range of lift coefficients from -0.4 to 0.28 which provided the induced drag variation with lift for the wing-body. An additional induced drag increment equal to ten percent of $C_L \pi^2 / AR$ was added to account for lift effects of the nacelles and horizontal tail. This increment is based on unpublished data for the Boeing 727 aircraft and has been corrected to account for differences between the configurations and represents a conservative estimate of the nacelle and horizontal tail effects.

Skin friction corrections and interference drag values were computed using the method of reference 18. This method assumes fully turbulent flow over a smooth, insulated flat plate and makes suitable corrections for supervelocity effects, pressure drag, interference effects, excrescences, and surface roughness.

The propulsion bleed and air conditioning drag increments for the SSXJET were obtained from reference 12 and corrected to account for the engine size change and reduction from four to two engines. These drag increments are illustrated in Figure 63.

Zero trim drag has been assumed throughout the analysis.

Results

The resulting subsonic/transonic drag polars for the SSXJET are summarized in Figure 64. Note that for clarity the curves have been shifted to the right as indicated by the scale in the lower left corner of the figure.

Extension to Subsequent Concepts

The drag values derived above for the SSXJET have been assumed applicable to all subsequent concepts except for the SSXJET III. In this latter case, corrections have been made to account for the differences in skin friction drag associated with the increased wing size and inlet/nacelle arrangement. The

propulsion bleed drag has also been modified to reflect the GE21/J11-B10 engines included in this concept. For the Mach number range under consideration, these engines require a constant propulsion bleed increment of .00063 instead of the values previously presented in Figure 63. No air conditioning drag penalty is required for this engine. Resulting drag polars for the SSXJET III are presented in Figure 65.

Summary

SSXJET drag polars for the Mach number range 0.5 to 0.95 have been derived through suitable correction of available wind tunnel data. No detailed analyses for subsequent configurations have been conducted except for the SSXJET III. The SSXJET polars derived herein are assumed applicable to the SSXJET I and SSXJET II concepts while the necessary corrections for the SSXJET III have been developed.

SUPERSONIC AERODYNAMICS

Lack of appropriate experimental data for the supersonic Mach number range required by the SSXJET series aircraft has resulted in application of several analytical techniques for the calculation of configuration lift and drag characteristics for Mach numbers 1.1 to 2.2. These methods (references 18-21) have been used extensively for supersonic aerodynamic studies, and numerous correlations with wind tunnel data have established the validity of the approach (see references 19 and 22-24). The purpose of this section is to describe the methods of analysis employed, to present further correlations of the theoretical estimates with wind tunnel data for the Douglas Mach 2.2 AST concept on which the SSXJET series is based, to discuss the analyses of the various SEXJET concepts, and to assess the accuracy of the various analytical methods employed.

Supersonic operation of the SSXJET series aircraft over populated areas hinges on the level of sonic boom overpressure generated by the configurations. The relatively lower cruise Mach number and lower weights as well as the high cruise altitude might result in overpressure levels sufficiently low to allow transcontinental flight. An analysis has been conducted to assess the expected overpressure levels for the SSXJET series aircraft. Only "first cut" estimates of the overpressure levels have been made and no detailed analyses have been performed.

Analysis Methods

The supersonic aerodynamic characteristics of the various SSXJET concepts have been estimated using a series of computer programs available at the NASA/Langley Research Center. A brief description of these programs is given below, and detailed information may be found in the references.

Skin friction.- Configuration skin friction coefficients have been determined using the Sommer and Short T' method described in reference 18.

The aircraft is separated into its various components as shown in Figure 66 and the individual wetted areas and reference lengths determined. Components such as the wing which may exhibit large variations in reference length are further subdivided into strips as shown. Skin friction coefficients are then computed assuming a fully turbulent boundary layer over a smooth, adiabatic-wall flat plate with transition at the leading edge of each configuration component. The program accepts as input component wetted areas and reference lengths, and computes the skin friction drag coefficients for a given Mach number-altitude combination or for specified wind tunnel conditions.

Zero-lift wave drag.- The far-field wave drag program uses the supersonic area rule concept to compute the zero-lift wave drag of an arbitrary configuration. As described in reference 19, the program establishes a series of equivalent bodies of revolution by passing planes inclined at the Mach angle M through the configuration for several different aircraft roll angles θ. This procedure for developing the equivalent body area distribution is illustrated in Figure 67. The wave drag of each equivalent body is determined from the von Karman slender body theory which relates the wave drag to the freestream conditions and the equivalent smooth body area distribution. The discrete equivalent body wave drag values are then integrated to obtain the configuration overall wave drag.

Also included in the wave drag program are a series of routines for optimization of the configuration wave drag through suitable area ruling of the fuselage. Arbitrary restraint points may be specified at fuselage stations where minimum area conditions already exist. The program locates these points on the average equivalent body area distribution for the complete configuration and then solves for the fuselage shape giving minimum configuration wave drag while simultaneously satisfying the specified restraint conditions.

Wing analysis.- The wing lifting characteristics and drag due to lift have been computed using the method described in reference 22. Based on linearized supersonic wing theory, the method breaks an arbitrary planform wing into a mosaic of "Mach-box" rectilinear elements which are assumed to lie approximately in the horizontal plane as shown in Figure 68a. This sketch is illustrative only in that in actual practice many more grid elements would be used. These grid elements are then employed to numerically evaluate the linear theory integral equation which relates the lifting pressure at a given field point to the wing surface shape in the region of influence of that field point. The overall force coefficients for the camber surface at its input incidence are obtained by integrating the computed pressure distribution over the wing surface. This solution is combined using a superposition technique with a flat-wing solution per unit angle of attack. The nacelle-wing interference effects are computed as described below and incorporated into the wing drag polar.

Nacelle interference effects.- Nacelle-wing interference effects have been determined using the method outlines in reference 21. The program uses modified linearized theory to compute the loads imposed on a warped wing surface by nacelles located either above or below the wing. A typical nacelle-wing arrangement is shown in Figure 68b where the shaded areas represent the interference regions. A fundamental restriction of the program requires that the region of interference from the nacelle not extend forward of the wing leading edge or outward of the wing tip. In such cases, the disturbance field can spill over onto the upper (or lower) wing surface so that the field point pressure is influenced by both the camber surface and the nacelle. The interference loads cannot be determined using this method when these conditions exist. This difficulty has been overcome through recent unpublsihed NASA/LRC modifications to the basic method described above. This revised technique generates and uses an upwash field in conjunction with a wing camber surface force analysis scheme to compute the interference loads. This revised method is applicable to the lower supersonic Mach numbers at which the original approach could not be used.

Validation Of Analysis Methods

The analytical approach to the SSXJET analyses presented herein was originally chosen because of a lack of supersonic experimental data for the Douglas AST concept on which the SSXJET series is based. Such data has recently been published, however, and thus it is possible to further validate the SSXJET analysis methods through correlation of analytical and experimental results for the Douglas transport model. Both wing-body and wing-body-nacelle cases have been chosen and are discussed below.

Model description.- The wind tunnel model analyzed is a .015 scale representation of the Douglas Mach 2.2 AST concept and is fully detailed in reference 4. A photograph of the model in the 9 x 7 tunnel at the NASA/Ames Research Center is shown in Figure 69. The particular components involved in the analysis are defined as follows:

B_1 - Fuselage for the McDonnell-Douglas D-3230-2.2-5E supersonic cruise aircraft configuration. The model fuselage is accurately scaled forward of the full scale station 2450 inches and is distorted aft of that to accommodate the sting.

W_2 - Baseline wing for the Douglas concept with the camber surface optimized with a pitching moment constraint designed to give minimum drag due to lift for the trimmed configuration.

The wing-body ($B_1W_2X_2 + T_{b1}{}^{6.4}$) and wing-body-nacelle ($B_1W_2X_2N_2d_{1C}d_{1D} + T_{b1}{}^{6.4}$) configurations are subjects of the present investigation.

Analysis and results.- The analytical methods previously described have been used to estimate the model aerodynamic characteristics for Mach numbers of 1.6, 1.8, 2.0, and 2.2. Lift analysis has been conducted for the twisted and cambered wing alone with a constant lift displacement added equal to the nacelle normal force load on the wing as calculated using the nacelle interference program. The total drag is assumed to consist of skin friction, wave drag, and drag due to lift. Note again that nacelle effects on the wing drag due to lift are included directly in the method, and that no roughness has been included.

Lifting characteristics for the Douglas model are summarized in Figure 70. The agreement between theory and experiment is very good although the lift is slightly underestimated. This disagreement is probably due in part to the lifting and interference effects of the fuselage which have not been included in the analysis.

Drag polar correlations are presented in Figures 71 and 72 for the wing-body and wing-body-nacelle configurations, respectively. The agreement between theory and the tunnel data for the minimum drag point is good as is the total drag at the lower positive lift coefficients. At the higher lift coefficients, however, the predicted drag-due-to-lift factor results in relatively significant differences between the measured and predicted drag data for most Mach numbers. This fact is reflected in the L/D curves presented in Figure 73 which indicate excellent agreement with the data for lift coefficients in the usual range of interest (0. to .10), but which disagree near the $(L/D)_{MAX}$ point. The variation of $(L/D)_{MAX}$ with Mach number is shown in Figure 74. The predicted $(L/D)_{MAX}$ values agree fairly well with the measured values although the slope of the theoretical data for the wing-body case is incorrect. It should be noted that these results are for a configuration which is slender in the classical sense and for which the linear theory is well suited. The SSXJET configurations are all less slender and thus some degradation in the accuracy of the predictions is to be expected.

The methods presented above provide reasonably accurate estimates of the aerodynamic characteristics of the major components of this slender transport model for the Mach number-lift coefficient values of usual interest. Good estimates of the configuration supersonic performance may be obtained quickly and with very reasonable expenditure of computer effort using these methods.

Configuration Analysis

Five variations of the SSXJET concept have been consistently analyzed from the supersonic aerodynamic standpoint. In all cases the analytical techniques previously described have been used for development of the lift and drag characteristics. Inclusion of additional drag components are noted as required.

SSXJET.- The overall lifting characteristics of the SSXJET are summarized in Figure 75. Both lift-curve slope and lift-angle of attack data are presented. The lifting efficiency of the wing as expressed by the lift-curve slope decreases by approximately one-third as the Mach number is increased from 1.1 to 2.2. Typical operating conditions at Mach numbers of 1.2, 1.8, and 2.2 (start cruise) are also indicated in the figure.

Preliminary design considerations for the SSXJET dictated a fuselage length of 31.89 m (103 feet) with a series of minimum area stations in both the cockpit and passenger compartment as shown in Figure 76. These minimum area points were restrained in the wave drag optimization routines and two iterations performed to define a fuselage giving minimum configuration wave drag at Mach 2.2. The resulting fuselage area distributions are shown in Figure 76 along with the arbitrary initial shape. The final fuselage shape results in a configuration wave drag coefficient which is converged to within approximately one drag count of the succeeding iteration. Note also that the minimum area requirements have been fully satisfied. This optimum fuselage has been employed in the wave drag analysis of the SSXJET. A typical Mach 2.2 equivalent area distribution plot developed in conjunction with the analysis is shown in Figure 77. Both the total area and the contribution of the various configuration components are shown. The computed SSXJET wave drag characteristics are presented in Figure 78 as a function of Mach number. The cruise wave drag coefficient is .00467. Note that, although the configuration has been optimized for Mach 2.20, the SSXJET geometry as seen by the area rule and linear theory results in a relative minimum near Mach 1.80. The increase in wave drag at the design point probably indicates violation of the "smooth" slender body and linearized theory assumptions which are fundamental to the wave drag method. Further comments regarding uncertainties in the wave drag analysis may be found later and in the discussion of the SSXJET II concept.

Another interesting aspect of the wave drag analysis using the far-field program concerns convergence of the solution at a given Mach number. Both the number of aircraft roll angles ($N\theta$) at which the discrete equivalent body wave drag values are computed and the number of Mach cutting planes used in the area developments must be specified when the analysis is conducted. The dependence of the solution on the value of $N\theta$ has been found to be relatively insignificant for values of $N\theta$ = 16 or more. As shown in Figure 79, however, the number of cutting planes specified can introduce additional uncertainties into the analysis. As the number of cutting planes is increased to the program limit of NX = 100, the wave drag continues to increase. A converged solution is not obtained, however, and it becomes necessary to adopt the approach indicated in the lower portion of the figure. Here the computed wave drag coefficients have been plotted versus the inverse of the number of cutting planes employed. The curve is then extrapolated as shown to obtain the solution for NX becoming very large. This procedure should be followed for all pertinent Mach numbers to obtain the theoretically converged results. This convergence study was conducted subsequent to the studies of the various SSXJET configurations which were analyzed with NX = 50. The results for the SSXJET indicate a wave drag uncertainty at Mach 2.2 of approximately .0004 which amounts to less than 3 percent of the total SSXJET drag at cruise.

A configuration wetted area summary is presented in Table VII while the variation of skin friction drag with Mach number is shown in Figure 78. Note that the friction drag coefficient increases .00035 during constant lift coefficient cruise as the altitude increases.

A roughness drag penalty has been estimated using data previously developed in reference 12. The ratio of roughness drag to skin friction drag has been assumed to vary linearly between the values given in reference 12 at Mach

numbers of 1.2 and 2.7. These interpolated ratios of roughness to friction drag have been used in conjunction with the skin friction values discussed above to estimate the SSXJET roughness drag at the required Mach numbers. The results are presented in Figure 78.

Camber drag as computed by the wing analysis program is also presented in Figure 78.

Drag increments due to propulsion bleed and air conditioning have been estimated using data from reference 12. These previous data have been corrected to account for the SSXJET engine airflow, a reduction from the four engines to two, and the reference area change to 89.65 m^2 (965 ft^2). Note that in this analysis the airflow ratio correction has been applied to the air conditioning drag increment to obtain a more realistic estimate of the penalty. Figure 80 presents the results of this analysis.

The Douglas wing (W_2 of reference 4) which has been incorporated into the SSXJET concept has been designed to be self-trimming at Mach 2.2 for a center-of-gravity location at 53 percent of the mean chord and at a lift coefficient of 0.10. Insofar as these conditions approximate those for the SSXJET during cruise, the horizontal tail has been assumed to be oriented to the local flow such that zero-lift is maintained on the tail with the wing at zero pitching moment. This assumption has been applied to all supersonic Mach numbers, and thus no drag-due-to-lift penalty associated with the horizontal tail has been assessed. However, this assumption is good over a limited Mach number range and requires more study. Note that skin friction, roughness, and wave drag increments due to the tail have been included.

Selected drag polars developed through the analysis above are represented in Figure 81. Typical operating conditions at these Mach numbers are also indicated in the figure. The $(L/D)_{MAX}$ variation with Mach number is shown in Figure 82 where at the cruise Mach number, the $(L/D)_{MAX}$ potential decreases from 7.05 at start cruise to 6.93 at end cruise. As noted, the actual start cruise L/D is considerably lower than the maximum achievable performance. This disparity occurs because the wing size is dictated by considerations of landing and takeoff performance which results in an effectively oversized wing at cruise. The aircraft thus cruises at a C_L less than that required for $(L/D)_{MAX}$. Detailed resizing of wing and engine could provide substantial performance improvements.

SSXJET I.- The SSXJET I configuration has been derived from the SSXJET analyzed above by moving the nacelles to an underwing location. With the exception of the nacelle interference load computations, the methods used to determine the SSXJET I characteristics parallel those previously described.

A sensitivity study has been conducted to determine the effect of nacelle underwing location on the high-speed performance. As shown in Figure 83, six cases have been considered. The first three are for constant semispan location with varying chordwise positions while the remaining cases vary the semispan location at constant longitudinal coordinate. In all cases, the nacelle vertical location has been slightly adjusted to maintain the nacelle maximum diameter tangent to the wing trailing edge. Data defining these cases are summarized below:

Case	Y/b/2	X/c, %
1	.30	51.
2	.30	60.
3	.30	69.
4.	.40	61.
5	.50	47.
6	.20	74.

Results of this analysis are presented in Figure 84. Although Cases 1 and 2 could be eliminated from consideration due to their inferior $(L/D)_{MAX}$ performance, the choice of nacelle location from an aerodynamic viewpoint is not obvious. Since the Mach 2.2 $(L/D)_{MAX}$ values are nearly equal, the aerodynamic performance at the below cruise Mach numbers becomes the primary concern. Inboard relocation of the nacelles results in improved $(L/D)_{MAX}$ performance for lower Mach numbers, but this trend does not continue throughout the Mach number range of interest. Since the $(L/D)_{MAX}$ curves cross each other at various points the configuration does not appear to be overly sensitive to nacelle location and thus other parameters such as trailing-edge flap geometry or wing structural weight can be considered in the choice of nacelle location without serious degradations in the high-speed aerodynamic performance. Range assessments for these various cases have indicated less than a 3 percent spread in the results, and thus Case 1 has been selected as the SSXJET I baseline nacelle location. The reader should be cautioned that the large difference between L/D operating and L/D_{MAX} was important to this result. Opportunity exists to significantly improve the cruise wing-engine match which would alter the optimum engine location. Although its aerodynamic performance is somewhat inferior to other cases, this nacelle location offers a reasonable compromise for both aerodynamic and structural constraints. The lift and drag characteristics for this configuration are summarized in Figure 85 for selected Mach numbers.

Typical operating points for the selected SSXJET I configuration have been indicated in both Figures 84 and 85. A wetted area summary has been included in Table VII.

SSXJET II.- The SSXJET II is a blended wing-body concept configured for either side-by-side or tandem cockpit seating. Exact numerical models of these two concepts have been prepared and used in the analyses.

Significant difficulty was encountered in the wave drag analysis of the side-by-side cockpit version of the SSXJET II. As shown in Figure 86, the predicted wave drag variation with Mach number for the exact digital geometry definition exhibits rather erratic behavior for Mach numbers above 1.6. Modifying the fuselage geometry to an equivalent circle representation further aggravates the problem. The difficulty here is related to the rate of area growth in the forebody as well as the magnitude of the local body slopes. The basic assumptions to the linear theory employed in the wave drag method are violated and the resulting drag values are probably not accurate.

Relaxing the forebody camber for the side-by-side-cockpit concept results in a more realistic wave drag curve as shown, and these values have been included in the polar development.

The problems discussed above were not encountered for the SSXJET II with the tandem cockpit arrangement. The more slender forebody shape included for this pilot arrangement has resulted in area distributions more conducive to analysis using the slender body theory. The wave drag variation with Mach number for this configuration is also included in Figure 86.

These have drag problems have been encountered primarily in the analysis of the SSXJET II side-by-side concept although all of the configurations analyzed show indications of possible theory violations at the higher Mach numbers. These uncertainties in the wave drag analysis are significant in some cases (i.e., the SSXJET II), and point to the necessity of both fully understanding the limitations of the analysis methods and the need for supersonic test data to verify the analysis methods and provide the baseline drag levels of the configurations.

Wetted area data for both SSXJET II concepts are included in Table VII. The manner in which the wing-fuselage blending has been numerically modeled requires that the wing and fuselage wetted areas be added if a comparison of wetted areas is to be made with the other configurations.

Overall lift, drag, and lift-to-drag ratio performance for the two SSXJET II concepts are summarized in Figures 87 and 88. Note that the lifting characteristics of the two configurations are assumed to be the same. Typical operating points are also indicated in the figures.

SSXJET III.- The SSXJET III concept has increased wing area and fuselage length relative to the concepts discussed above and employs a two-dimensional inlet system located beneath the wing (see configuration assessment for rationale). This inlet system has been modeled as an equivalent area circular nacelle located at an "average" vertical position. No attempt has been made to account for the camber associated with the "S" shape of the actual inlet. It is felt that this representation provides reasonably correct distributions of both area and volume for the drag analysis.

Drag values have been estimated using the methods previously discussed although the use of the GE21/J11-B10 engine results in a revised total additive propulsion drag as shown in Figure 89. Also, note that an additional drag increment to account for such miscellaneous items as inlet-fuselage interference, locally separated flow, the small fuselage ventral, etc. has been calculated as 5 percent of the skin friction drag.

Wetted areas for the SSXJET III are included in Table VII while the lift and drag characteristics are summarized in Figures 90 and 91. Typical operating points are as indicated.

The begin cruise $(L/D)_{MAX}$ of 7.0 compares favorably with similar results for the other configurations presented above. As with the other configurations,

however, the actual start cruise L/D is considerably below the maximum performance level.

"First Cut" Sonic Boom Estimation for the SSXJET

The "first cut" prediction method of reference 25 has been used to compute the sonic boom overpressures generated by the SSXJET concept for Mach numbers 1.2 through cruise. This prediction technique is illustrated in Figure 92 which has been taken from reference 25. Weights at altitude typical of the SSXJET have been used along with the Mach number-altitude schedule common to all of the SSXJET series aircraft. An "average" shape factor has been used for the SSXJET as indicated in Figure 92.

Results of this analysis are presented in Figure 93. The relatively high weight and low altitude at the lower supersonic Mach numbers result in overpressure levels on the order of 86.2 N/m^2 (1.8 lbs/ft^2). This level steadily decreases and is about 52.7 N/m^2 (1.1 lbs/ft^2) at start cruise. An end cruise value of about 38.3 N/m^2 (0.8 lbs/ft^2) is indicated. As pointed out in reference 26, sonic boom overpressures on the order of 47.9 N/m^2 (1.0 lb/ft^2) probably represent the maximum boom level which would be acceptable to the general public. It should be noted that the values computed for the SSXJET represent the peak overpressure and do not address the associated lateral decay and cutoff distance associated with the sonic boom. This analysis for the SSXJET indicates that the potential for overland flight exists for aircraft of this class, but further optimization and boom minimization (through nose blunting, for example) of the configurations will be required.

Summary

Supersonic lift and drag characteristics for the various SSXJET configurations have been derived using a series of analytical techniques. The validity of the approach has been demonstrated through correlation of theory and experiment for the .015 scale Douglas AST configuration on which the SSXJET series is based. Analyses of the various SSXJET concepts has indicated some uncertainties in the computed wave drag values due to the lower fineness ratios of these configurations. In some cases it appears that the slender body theory fundamental to the wave drag analysis has been violated and the uncertainties are large. Resolution of these problems will require high-speed wind tunnel data for configurations more similar in fineness ratio to the SSXJET series than is the Douglas transport.

Sonic boom analysis for the SSXJET has indicated supersonic cruise overpressures on the order of 47.9 N/m^2 (1.0 lb/ft^2). Although no detailed analyses of the pressure signature shapes and magnitudes have been conducted for the various SSXJET concepts, it is felt that the results presented for the SSXJET provide a reasonable estimate of the overpressure levels to be expected. Further optimization of the configuration for sonic boom minimization could result in a vehicle with boom levels acceptable for overland flight.

MISSION ANALYSIS

The object of Mission Analysis is to evaluate the mission performance characteristics of a particular aircraft configuration and determine whether it attains, exceeds, or falls short of the design mission goals. Since the overall design objective is to optimize an aircraft configuration, to bring together the proper combination of aerodynamics, airframe, and power plant configured to the minimum size that will achieve, but not exceed the mission goal, mission evaluation plays a significant role in the sizing and configuration selection process during aircraft design.

The design mission goal for the SSXJET aircraft was defined as a range of 5926 km (3200 n. mi.) at a cruise speed of Mach 2.2 with a payload of 726 kg (1600 lbm) representing eight passengers with baggage.

Methods and Criteria

A NASA developed Long-Range-Cruise Mission program (unpublished) was used in the mission performance evaluations. Aerodynamic, propulsion, and weight data required as input for the mission program were developed. The input furnished by aerodynamics consists of drag coefficients and lift coefficients for each of a series of Mach numbers. The power plant input consists of an engine data package which contains gross thrust, fuel flow, and ram drag data at climb and cruise power for various altitudes and Mach numbers. Design gross weight (DGW), operating weight (OW), and payload are the mass property data required. Detailed information regarding these data can be found in each of the respective sections. After the aerodynamic, propulsion, weight, and fuel data have been established for use as input, an unpublished NASA/LaRC mission program is used to perform the mission analysis based on the following input data and criteria.

Input

- o Aircraft gross weight
- o Aircraft operating weight
- o Payload
- o Aerodynamic drag polars
- o Engine performance

Criteria:

Under the mission criteria established for this study, the design mission goal for the SSXJET aircraft is defined as follows: aircraft must have the capability of flying 5926 km (3200 n. mi.) at a cruise speed of Mach 2.2

while carrying a payload 726 kg (1600 lbm) consisting of eight passengers and their baggage and have sufficient fuel allowances to provide the following off-nominal operation capabilities.

- o 482 km (260 n. mi.) to alternate airport to be flown at best altitude and Mach number.
- o 30 minutes in holding pattern at 4572 m (15000 ft) altitude.
- o Allowance for headwinds and off-nominal operation equal to 7 percent of trip fuel.
- o Missed approach - no allowance.

These off-nominal operation capabilities are based on fuel reserves established by FAR 121.648 modified for holding altitude. Current FAR reserve fuel regulations governing international flight include a requirement for 30 minutes at 457 m (1500 ft). During SCAR studies it was found that for supersonic aircraft, which are designed to operate efficiently at higher speeds and altitudes, increasing the hold altitude to 4572 m (15000 ft) would result in about a one percent range improvement and significantly improve noise. This is the basis for the hold altitude modification which is used in this study.

The foregoing criteria establish the mission profile on which basis the mission performance analysis is based. Mission profiles for each of the SSXJET aircraft evaluation appear in Figures 94 through 98.

During the engine and aircraft sizing studies, engine thrust to weight ratios (t/w) ranging from .35 to .55 were evaluated. With the exception of noise criteria, the major parameters affecting power plant sizing are as follows:

- o Takeoff field length
- o Safety rules during takeoff which include balanced field length and maintaining a specified minimum rate of climb with one engine inoperative.
- o Climb ceiling resulting from inadequate thrust which would prevent the aircraft from reaching optimum cruise altitude.
- o Adequate acceleration power to attain desired cruise speed, particularly through high drag transonic region.
- o Cruise efficiency, lowest fuel consumption.
- o Determination of engine performance due to above normal ambient temperatures, high power extraction to operate accessory systems or airbleed for special features such as surface blowing or boundary layer control.
- o Safety regulations during landing and approach climb capability with one inoperative engine.

The performance of SSXJET, SSXJET I, and SSXJET II series are based on use of scaled advanced dry turbojet engines operated at standard +80C day temperature conditions. Aircraft and engine sizing are based on hot day operating conditions. SSXJET III performance is based on use of GE21/J11-B10 variable cycle operating at standard day conditions.

The program analyzes each segment of the selected mission profile and provides en-route details such as required fuel, thrust, altitude, speed, and time for each segment. These data, along with other pertinent aerodynamic, weight, and propulsion parameters, are all recorded on a computer printout and are available for investigation at any discrete point along the mission. The mission profile used in this study is composed of the following segments:

1. Takeoff fuel allowance consisting of ten minutes taxi (idle power setting) plus one minute at full takeoff thrust with no credit for distance.

2. Climb and accelerate in accordance with the Mach-altitude climb schedule shown in Figure 99. The program automatically determines optimum cruise altitude for maximum range unless thrust available is inadequate to reach that altitude, and a climb ceiling is established.

3. Cruise begins at either optimum altitude or climb ceiling. The program determines the Brequet range factor, V/SFC L/D, for begin and end cruise, and determines an average range factor value which is applied over the entire cruise range.

4. Descent is not calculated by the program; however, previously determined values for descent distance, time, and fuel are used as input. A descent range of 370 km (200 n. mi.) and a descent time of 20 minutes were selected for use in this analysis. The fuel estimate was based on 20 minutes of fuel flow at idle power at the average descent altitude and speed.

Results of the mission performance evaluation are summarized in Tables VIII through XII.

Off-Design Operation

Since it is not possible to operate a supersonic aircraft at cruise speeds for all missions, particularly overland, the aircraft was evaluated for subsonic range performance. Although no mixed cruise missions were investigated, missions with all subsonic cruise segments were evaluated to determine range. A transcontinental flight, New York to San Francisco, at Mach .95 is feasible, and it was determined that the SSXJET has a subsonic range adequate to fly this range at maximum payload. A hypothetical mission could be to fly from San Francisco to New York subsonic at Mach .95, refuel and continue from New York to London or Paris at supersonic cruise at Mach 2.2 (Figure 100). A supersonic cruise mission between a city-pair, (Los Angeles to Honolulu) having a range of 4074 km (2200 n. mi.) which is less than the SSXJET long-range cruise capability, but so located as to make possible an all supersonic (Mach 2.2) cruise leg.

An all supersonic cruise mission between the city-pair of Los Angeles-Honolulu was investigated to determine the gross takeoff weight required to fly the 4074 km (2200 n. mi.) range. The takeoff gross weight for the SSXJET is determined to be 30209 kg (66600 lbm).

Performance Sensitivity

Recent technological advances have made available a unique new titanium material processing and construction technique called superplastic forming and diffusion bonding (SPF/DB), reference 34, which yields promising airframe weight savings through increased structural efficiency. This process is described in more detail in the Mass Properties section of this report. A 10 percent reduction in operating weight (OW) could be achieved if SPF/DB were used resulting in a 9 percent increase in range. The effects of changes in operating weight on range for constant gross weight and payload are displayed in the Range Sensitivity Diagram, Figure 101.

The effects on range were also investigated and found to be 37 km (20 n. mi.) per count of drag. The change in drag versus range curve is also displayed in Figure 101. The uncertainty in calculated wave drag can result in a range variation of up to 741 km (400 n. mi.).

TAKEOFF PERFORMANCE

This section presents the predicted takeoff performance characteristics for both a SSXJET powered by two advanced turbojet engines and a SSXJET III powered by two GE21/J11-B10 double bypass turbofan engines. The SSXJET has a gross take-off weight of 35,720 kg (78,750 lbm) and a wing reference area of 89.65 m^2 (965 ft^2). The SSXJET has a nominal installed T/W of 0.39 on a standard day corresponding to an installed SLTO thrust of 67,577N (15192 lbf) per engine. The gross takeoff weight of the SSXJET III is 36,031 kg (79,545 lbm) and the wing reference area is 105.0 sq.m. (1130 sq.ft.). The SSXJET III has a nominal installed T/W of 0.51 on a standard day which corresponds to a SLTO thrust of 90,210 N (20,280 lbf) per engine.

For supersonic transport configurations, there are no existing takeoff performance rules; however, the subsonic transport take-off requirements set forth in FAR 25 (reference 32) were used as a guide. Because of the high lift-off velocities of supersonic arrow-wing transport configurations, the velocity and climb out requirements set forth in FAR 25 (reference 32) are not the limiting criteria in sizing the engines for take-off. All take-off field length analyses of supersonic transport configurations are conducted on a standard +8^{o}C day rather than standard day. The installed engine thrust level of the SSXJET is decreased from the nominal value of 67,577 N (15,192 lbf) to 64,279 N (14,540 lbf) per engine. Similarly the installed engine thrust of the SSXJET III is reduced from the nominal value of 90,210 N (20,280 lbf) to 86,416 N (19,427 lbf) per engine.

TAKEOFF ANALYSIS METHODOLOGY

The takeoff method used in this study predicts the aircraft takeoff profile from the start of takeoff roll, through lift-off and through climb out to a specified altitude. The method has been programmed and is described in reference 33. Figure 102 shows the significant parameters required to define a takeoff profile for an arrow-wing supersonic transport configuration. The first segment shown in figure 102 is the total takeoff distance obtained by accelerating the aircraft from the start of takeoff roll to a predetermined rotation velocity, at which time the airplane is allowed to increase its angle of attack at a specified pitch rate. The airplane continues to accelerate and rotate until the lift-off point is reached as shown on figure 102. After lift-off, the aircraft continues to accelerate and rotate to a maximum allowable angle of attack and climbs to clear a 10.7 m (35 ft.) obstacle. The all engine takeoff field length in accordance with FAR 25 (ref. 32) is the distance from the start of takeoff roll or brake release to the 10.7 m (35 ft.) obstacle as shown in figure 102. The reference 33 takeoff program requires the all engine takeoff field length to be input and iterates on the rotation velocity to obtain the desired result. Also, the program provides a minimum all engine takeoff field length for a particular aircraft configuration. From the obstacle, the aircraft follows an adjusted climb gradient to reach a climb out point defined by an altitude and a downrange distance from start of takeoff roll as shown on figure 102. At the start of climb out the aircraft angle of attack is gradually reduced until the desired climb gradient is obtained. Also, during this segment of climb out, the aircraft acceleration rate must be positive. Because of the high lift-off velocities of supersonic arrow-wing transport configurations, the velocity and climb out requirements are not the limiting criteria in sizing the engines. At this defined climb out point, the wing trailing-edge flaps are partially retracted to a lower angle and the engine power is reduced to that power setting required for level flight with one engine out. After cutback, the aircraft climb gradient and velocity are maintained constant for the remainder of takeoff as shown on figure 102.

To compute the takeoff profile, the aircraft low-speed aerodynamic characteristics and the engine low-speed performance characteristics are required. The necessary low-speed aerodynamic characteristics include the variation of lift coefficient and drag coefficient with angle of attack at each wing trailing-edge flap setting for out-of-ground effect. For the aircraft near the ground the lift coefficient and drag coefficient are modified using DeYoung's arrow-wing ground effect equations from reference 12 and are shown in the low-speed aerodynamics section. These equations require pertinent aircraft data such as the wing area, wing aspect ratio, the gear height, the gear drag, and the angle of attack while on the ground.

The engine thrust characteristics are also required to compute the takeoff. The variation of net thrust with altitude and forward velocity must be defined for full power on a hot day (standard 8^{0} C day) to determine the minimum engine size to meet the prescribed takeoff field length from the start of takeoff roll to the 10.7 m (35 ft.) obstacle. In accordance with FAR 25 (ref. 32), the all engine takeoff field length must be increased

15 percent to define the balanced field length, which is the actual minimum runway length required for safety. Thus, for the SSXJET and the SSXJET III, where the defined balanced field length is 1931 m (6500 ft), the all engine takeoff length is 1723 m (5652 ft).

TAKEOFF FIELD LENGTH FOR SSXJET AND SSXJET III

The SSXJET is powered by two advanced turbojet engines which have an installed SLTO thrust of 64279 N (14540 lbf) per engine on a standard +8°C day. The leading-edge flaps of the SSXJET L_1 and L_2 were set at 0.523 radians (30°) and 0.785 radians (45°), respectively, and the outboard aileron T_3 was set at 0.087 radians (5°). These flap settings were maintained constant for all takeoffs of both the SSXJET and SSXJET III. The wing trailing-edge flaps T_1 and T_2 were set at 0.349 radians (20°), 0.436 radians (25°), and 0.523 radians (30°) for the SSXJET and both the all engine takeoff field length (distance from start of takeoff roll to clear a 10.7 m (35 ft) obstacle and the balanced field length were computed for the standard +8°C day using the takeoff method previously described. The results are listed below:

SSXJET FIELD LENGTHS

Wing Trailing-Edge Flap Angle	All Engine Takeoff Field Length	Balanced Field Length
0.349 radians (20°)	1859 m (6100 ft)	2138 m (7015 ft)
0.436 radians (25°)	1753 m (5750 ft)	2015 m (6612 ft)
0.523 radians (30°)	1658 m (5440 ft)	1907 m (6256 ft)

From the above table it was determined that for the SSXJET to meet the balanced field length requirement at 1981 m (6500 ft), the wing trailing-edge flap angles must be set greater than 0.463 radians (26.5°).

The SSXJET III is powered by two GE21/J11-B10 double bypass turbofan engines which have an installed SLTO thrust of 86416 N (19427 lbf) per engine on a standard +8°C day for the GE21/J11-B10 engines, the actual all engine takeoff field length and the balanced field length cannot be ascertained for the SSXJET III. However, the installed T/W ratio of the SSXJET III is 32 percent greater than the installed T/W of the SSXJET and the wing loading is 14 percent less than the wing loading of the SSXJET. Therefore, the all engine takeoff field length and the balanced field length of the SSXJET III will be considerably less than the SSXJET.

Summary

The advanced turbojet powered SSXJET does meet the balanced field length requirement of 1931 m (6500 ft.) with the wing trailing-edge flaps set at angles equal to or greater than 0.463 radians (26.5^{o}).

The GE21/J11-B10 double bypass turbofan powered SSXJET III has considerably more available thrust than the turbojet powered SSXJET and, therefore, meets the balanced field length requirement of 1981 m (6500 ft.).

NOISE PREDICTION

This section presents the predicted takeoff noise levels for the SSXJET and the SSXJET III as well as a discussion of the FAR 36 (ref. 29) noise rules and the noise prediction methodology.

For supersonic transport aircraft configurations, jet exhaust takeoff noise levels are a severe problem as evidenced by the Concorde. The jet exhaust noise level is mainly dependent on the jet exhaust gas velocity. Thus to reduce the noise levels, it is desirable to reduce the jet exhaust velocity, which in turn reduces engine thrust. The thrust loss, however, can be compensated for by oversizing the engines. Recently, both Pratt and Whitney (ref. 27) and General Electric (ref. 28) have conducted tests under contracts with NASA/Lewis Research Center to evaluate noise reductions of an inverted flow turbofan engine, where the outside flow has a higher velocity than the inside or core flow. The test results with these coannular jets have shown gains up to 10.0 dB relative to single jets with only the high velocity flow. Thus, for the SSXJET III which uses the double bypass turbofan GE21/J11B10 engines with the inverted exhaust jet profile, there are predicted takeoff noise levels with no coannular noise benefits and predicted noise levels using this coannular noise benefit.

Significant performance improvement is available through application of more recent supersonic cruise technology advancements. Advanced titanium fabrication methods (superplastic forming/diffusion bonding) and application of high temperature composite materials could significantly reduce structural weight and initial cost. A higher compressor pressure ratio turbojet engine sized with a retractable mechanical suppressor should be studied. A parametric sizing study is required to understand the trades between performance, noise, and field length. Finally, advanced takeoff and landing procedures (automatic flap retraction, autothrottling, acceleration in climbout, decelerating approach) could significantly reduce noise beyond the values estimated herein.

There are currently no existing noise rules for supersonic transport configurations, however, the FAR 36 rules will be used as a guide for evaluation of the SSXJET and SSXJET III noise levels. The initial FAR 36 rules were set in 1969 and define maximum allowable aircraft noise levels in terms of effective noise level (EPNL) which is a time average history of the perceived noise

level at the observer station. Per FAR 36 (reference 29), the take-off noise levels are measured at two stations. The first is along the runway centerline at 6486 m (3.5 n.mi.) from the start of take-off roll and the second is along a sideline 463 m (0.25 n.mi.) from the centerline, where the noise level after liftoff is greatest. Figure 103 shows the location of the prescribed measurement stations.

For take-off noise analyses, the engine thrust data is required at full power and at part power on a standard +10°C day per FAR 36 (ref. 29) rather than standard +8°C day required for engine sizing and take-off field length evaluation. For the SSXJET and the SSXJET III, the all-engine take-off field length was set at 1981 m (6500 ft.). If a safety problem does develop during take-off, the engine power levels can always be increased to full throttle and the noise rules can be disregarded. To evaluate the jet noise characteristics for a particular take-off, the jet exhaust flow properties must be defined, including area, mass flow, velocity, and temperature. These values are required at several flight conditions along the take-off path. The flight conditions include aircraft altitudes, velocity, and engine thrust level.

It should be noted that the amount of take-off data supplied by the engine manufacturers is very limited, usually three or four points, so that considerable extrapolation is required to obtain the necessary information. The propulsion section presents the take-off propulsion data required.

Noise Requirements

For supersonic transport configurations, there are currently no existing noise rules; however, the subsonic aircraft noise rules of FAR 36 (ref. 29) will definitely serve as a guideline for supersonic transport aircraft. The initial FAR 36 rules were set in 1969 and define maximum allowable aircraft noise levels in terms of effective perceived noise level (EPNL) as presented in the noise prediction methodology. Figure 103 shows the location of the prescribed measurement stations. Per the 1969 version of FAR 36 rules (ref. 29), the maximum allowable noise limit is dependent on the gross take-off weight of the airplane as shown in figures 104 and 105. Also, per the 1969 version of FAR 36, the engine power was allowed to be cutback at altitudes greater than 700 feet. The amount of cutback is defined as that power required to maintain level flight with one engine out. For a four-engine aircraft, the amount of cutback power can be considerably less than for a two-engine aircraft such as the SSXJET.

In 1977, FAA modified FAR 36 by reducing the maximum allowable noise limits. In addition, thrust cutback from the initial power setting was disallowed. However, for supersonic transport configurations of arrow wing design, it has been maintained that thrust cutback is reasonable and in addition, the configuration has been allowed to change by partial retraction of the wing trailing edge flaps at the cutback point. Per the 1977 version of FAR 36, the maximum allowable noise limits are not only dependent on aircraft gross take-off weight, but also on the number of engines. The allowable noise limits for a two-engine aircraft like the SSXJET are less than for a four-engine aircraft

as shown in figures 106 and 107. Thus, the two-engine aircraft is doubly penalized because it requires higher engine thrust and thus higher exhaust jet velocities and must meet reduced noise level requirements.

Noise Prediction Methodology

The aircraft observed jet noise levels are dependent on the engine jet exhaust nozzle flow characteristics, the aircraft velocity, and the aircraft position relative to the observer. The engine exhaust flow characteristics include jet area, mass flow, velocity, and total temperature. In accordance with FAR 36 (ref. 29) all take-off performance characteristics are evaluated on a standard +10°C day.

The take-off profile was divided into nine segments and the average engine exhaust flow characteristics, aircraft velocity, and altitude were calculated separately for each segment. These average properties were then employed to obtain the variation of engine source noise sound pressure level (SPL) over a range of frequency and directivity angles at a radius of 45.7 m (150 ft.) from the center of the exit nozzle plane, using reference 30 (Stone's Interim Prediction Method for Jet Noise (NASA TM X-71618)). It should be noted that Stone (ref. 30) does not include noise benefits of inverted flow coannular jets where the outside jet flow has a greater velocity than the center or primary jet flow.

For an observer located on the ground, at a particular instant in time, there is a particular directivity angle between the observer and the engine exhaust jet, and at this directivity angle, the engine exhaust jet source noise SPL's are computed over the range of frequencies from 50 to 10,000 hz at a distance of 45.7 m (150 ft.).

The source noise SPL's are extrapolated from the source noise distance to the observer distance using the FAR 36 (ref. 29) correction techniques. These include effects of spherical divergence, atmospheric attenuation, extra ground attenuation, and ground reflection. Spherical divergence is the dissipation of the sound pressure over a spherical surface area, as the sound wave expands outward from the source. Atmospheric attenuation is the dissipation of the sound pressure by the air molecules and varies with air temperature, air humidity, the frequency level of the noise, and the distance. The higher frequency noise levels are dissipated considerably more than the lower frequency noise levels. Extra ground attenuation is thought to be due to a combination of sound wave refraction due to wind and temperature gradients in the atmosphere and dispersion due to the turbulent boundary layer of the earth. The extra ground attenuation is predicted as a function of the distance, elevation angle, frequency, and wind direction. Ground reflection is the increase in observed noise levels near the ground due to the reflection off the ground of indirect sound waves from the source. Ground reflection is dependent on aircraft/observer geometry, frequency, ground impedance, ground roughness, and the wave number ratio (ratio of the speed of sound on the ground to the speed of sound at altitude). The final consideration in extrapolation of the source noise to the observer is the multiengine shielding effect. This is the

dissipation of noise from engines which are partly shielded from the observer by the engine noise source closest to the observer. The multi-engine shielding depends on the number of engines and the sideline elevation angle.

Thus, at a particular time, the variation of SPL with frequency at the observer station is computed. These SPL's are then added logarithimically to obtain a perceived noise level (PNL) at the observer station. As the aircraft travels along the flight path, both the distance between the aircraft and the observer, and the directivity angle vary. Thus, corresponding to each time during the take-off there is an observed perceived noise level (PNL). As the aircraft approaches the observer location and passes by the observer location, the perceived noise level increases to a maximum level (PNL_{MAX}) and then as the aircraft travels away from the observer, the PNL decreases again. The effective perceived noise level is obtained by integrating the PNL's over the time that the PNL first reaches 10 dB below the maximum PNL until the time the PNL last reaches 10 dB less than the maximum PNL. This integrated PNL-time level is then divided by a time interval of 10 seconds to obtain the effective perceived noise level (EPNL) in accordance with FAR 36 (ref. 29).

Take-Off Flight Profiles for Noise Evaluation

For the noise evaluation study of the SSXJET and the SSXJET III, the all engine take-off field length was set at 1931 m (6500 ft.), and the engine performance characteristics were defined for a standard +10°C day. The wing trailing edge flaps of the SSXJET were set at 0.523 radians (30°) and the two advanced turbojet engines were set at a 92 percent power setting which corresponds to a SLTO installed thrust of 58,660 N (13,187 lbf) per engine on a standard +10°C day.

The lift-off distance for the SSXJET is 1568 m (5144 ft.) from start of take-off roll, and the aircraft velocity at lift-off is 91.4 mps (177.6 kts). The distance to the 10.7 m (35 ft.) obstacle is 1981 m (6500 ft.) and the aircraft velocity at the obstacle is 96.7 mps (187.8 kts.). For minimum take-off noise levels of the SSXJET it was judged that the cutback point be set at an altitude of 529 m (1736 ft.) and the cutback distance from the start of take-off roll was 5943 m (19,500 ft.). At cutback the aircraft velocity was 117.5 mps (228.3 kts.) and the climb gradient was 0.133 radians (7.64 degrees). At cutback the wing trailing edge flap angles were retracted from 0.523 radians (30°) to 0.349 radians (20°) and the engine thrust level was reduced from 55,821 N (12,549 lbf) per engine to 47,307 N (10,635 lbf) per engine. After cutback the aircraft acceleration was reduced to zero and the climb angle increased from 0.133 radians (7.64°) to 0.161 radians (9.25°) even though the engines were throttled back. This climb angle increase can partly be attributed to the increased lift to drag ratio obtained by retracting the flaps from 0.523 radians (30°) to 0.349 radians (20°). The low speed aerodynamic section of this report shows that at low velocities and thus high values of C_L, the 0.523 radians (30°) flaps yield higher L/D ratios than obtained with 0.349 radians (20°) flaps. However, as the velocity increases, the C_L required to fly decreases, and at the cutback point where the C_L is 0.477, the L/D with 0.349 radians (20°) flaps is 8.84 as opposed to an L/D of 8.19 obtained with

0.523 radians (30°) flap position. To meet the takeoff field length requirements it is necessary to have high wing trailing edge flap settings, whereas to minimize the engine power levels at cutback, it is necessary to reduce the wing trailing edge flap settings.

The minimum allowable cutback thrust is defined in the 1969 version of FAR 36 rules (ref. 29) as that power to maintain level flight with one engine out. For the two-engine SSXJET, this power setting is considerably higher than for a four-engine aircraft.

The altitude at the 6,486 m (3.5 n.mi.) point is 617.6 m (2026.3 ft.) and the aircraft velocity is 117.5 mps (228.3 kts.). Figure 108 shows the takeoff profile of the SSXJET used for evaluating the noise characteristics.

The SSXJET III has a nominal installed thrust of 86,060 N (19,347 lbf) per engine on a standard +10°C day, which corresponds to an installed T/W of 0.486 for the 36,031 kg (79,545 lbm) gross takeoff weight. Like the SSXJET, the SSXJET III has all all engine takeoff field length of 1981 m (6500 ft.) on a standard +10°C day and the wing trailing edge flaps were initially set at 0.523 radians (30°). The GE21/J11B10 double bypass turbofan engines were operated at power settings ranging from 63 percent to 75 percent to reduce the takeoff noise levels. The cutback distance was set at 5944 m (19,500 ft) from the start of takeoff roll and the cutback altitude was varied from 244 m (800 ft.) to 363 M (2250 ft.). From the matrix of cases run, it was determined that the minimum takeoff noise levels were obtained at an initial takeoff power setting of 75 percent, which corresponds to an installed engine thrust level of 64,544 N (14,510 lbf) per engine. The lift-off distance for the SSXJET III is 1594 m (5231 ft.) and the lift-off velocity is 95.7 mps 196.0 kts.). At the 10.7 m (35 ft.) obstacle, the velocity of the SSXJET III is 101.4 mps (19619 kts.). The takeoff noise levels of the SSXJET III were minimized at a cutback altitude of 533.4 m (1750 ft.) and the cutback distance was set at 5944 m (19,500 ft.) from the start of takeoff roll. The aircraft velocity at cutback was 126.7 mps (246.2 kts.) and the climb angle was 0.133 radians (7.63°). At cutback, the wing trailing edge flaps were partially retracted from 0.523 radians (30°) to 0.349 radians (20°) and the engines were throttled back from 57,208 N (12,861 lbf) per engine to 39,738 N (8933 lbf) per engine. After cutback, the climb angle increased to 0.142 radians (8.12°). At the 6486 m (3.5 n.mi.) point, the altitude is 610.8 m (2004 ft.) and the aircraft velocity is 126.7 mps (246.2 kts.). Figure 109 shows the takeoff profile of the SSXJET III which minimizes the takeoff noise levels.

Predicted Jet Exhaust Takeoff Noise Levels of SSXJET and SSXJET III

For the advanced turbojet powered SSXJET configuration, the jet exhaust effective preceived noise levels (EPNL's) at the prescribed takeoff measurement station were computed to be 116.3 dB at the centerline measurement station (measurement point 1) and 119.7 dB at the sideline measurement station (measurement point 2). The noise levels for the 35,720 kg (78,750 lbm) SSXJET are shown on figures 104 through 107 and tabulated in Table XIII.

Together with the reference 3 limits, it can be seen from figures 104 and 105 that the SSXJET exceeds the 1969 version of reference 29 rules by 17.6 dB on the sideline and 23.0 dB on the centerline. Figures 106 and 107 show that it exceeds the 1977 version of reference 3 rules by 27.3 dB on the centerline and 25.7 dB on the sidelines.

For the GE21/J11B10 double bypass turbofan powered SSXJET III configuration, the jet exhaust EPNL's at the prescribed take-off measurement stations were computed to be 97.1 dB on the centerline and 105.9 dB on the sideline with no coannular suppression effects. Based on study results by Pratt and Whitney (ref. 27) and General Electric (ref. 28) the amount of coannular suppression could range from 5.0 dB to 10.0 dB. Thus for the SSXJET III, the noise level at the centerline measurement station could be as low as 87.1 dB and the noise level at the sideline measurement station could be as low as 95.9 dB. The jet exhaust noise levels with and without coannular suppression for the 36,031 kg (79,545 lbm) SSXJET III are shown on figures 104 through 107 and tabulated in Table XIII, together with the reference 29 limits. From Table XIII and figures 104 through 107, it can be seen that with no coannular suppression effect, the jet noise levels of the SSXJET III exceed both the 1969 version and the 1977 version of reference 29 rules. However, with coannular suppression effects, the noise levels are below the 1969 version of reference 29 rules and the centerline noise level is below the 1977 version of reference 29 rules, whereas the sideline noise level exceeds the reference 29 rules by 1.8 dB.

Predicted Take-Off Airframe Nose Levels

The airframe overall sound pressure levels (OASPL) of the SSXJET and the SSXJET III were computed using Fink's equation (equation 1) from reference 31.

$$OASPL = 50 \log (V/100) + 10 \log (s/h^2) + 100.3 \qquad (1)$$

On the runway centerline at the 6486 m (3.5 n.mi.) point the values used in equation 1 above are as follows:

	SSXJET	SSXJET III
C-mps (fps)	117.5 (335.6)	126.6 (415.0)
S-m^2 (ft^2)	89.6 (965)	103.0 (1130)
h-m (ft)	617.6 (2250)	611.0 (2004)

Using these values the airframe OASPL of the SSXJET is 67.5 dB and the airframe OASPL of the SSXJET III is 69.9 dB.

Summary

The turbojet powered SSXJET exceeds the FAR 36 (ref. 29) noise rules by a considerable margin. However, by increasing the engine size so that the

installed T/W is the same as the SSXJET III and employing a mechanical suppressor, the take-off noise levels of the SSXJET could be reduced considerably.

The double bypass turbofan powered SSXJET III is viable from a take-off noise standpoint in that with coannular suppression it could meet the FAR 36 (ref. 29) noise limits if reduced take-off thrust is allowed.

The current 1977 version of FAR 36 noise rules (ref. 29) should be modified for supersonic transport configurations, to make the SSXJET a viable aircraft. The modifications should include not imposing stricter noise limits for two-engine aircraft than for four-engine aircraft and allowing thrust cutback at altitudes above some minimum altitude, such as 304.8 m (1000 ft.).

The coannular jet suppression effect should be investigated to ascertain the exact jet noise level of the SSXJET III.

CONCLUDING REMARKS

A preliminary design study has been conducted to determine the impact of advanced supersonic technologies on the performance and characteristics of a supersonic executive aircraft. Four configurations with different engine locations and wing/body blending were studied with an advanced non-afterburning turbojet engine. One configuration incorporated an advanced General Electric variable cycle engine and two-dimensional inlet with internal ducting. A M 2.2 design Douglas scaled arrow-wing was used throughout this study with Learjet 35 accommodations (eight passengers). Performance results are summarized in Table XIV. All four configurations with turbojet engines meet the performance goals of 5926 km (3200 n.mi.) range, 1981 meters (6500 feet) take-off field length, and 77 meters per second (150 knots) approach speed. The benefits shown for wing-body blending are within the uncertainty to which wave drag can be calculated for this class of aircraft. Noise levels of turbojet configurations are excessive. The variable-cycle engine configuration is deficient in range 555 km (300 n.mi.), but meets the most stringent noise rules (FAR 36 1977 edition), if coannular noise relief is assumed. All configurations are in the 33,566 to 36,287 kg (74,000 to 80,000 lbm) take-off gross weight class when incorporating current titanium manufacturing technology.

While the performance results to date are encouraging, some uncertainties exist mainly in the prediction of aerodynamic characteristics, which can be resolved only by extensive wind tunnel tests through the Mach number range. Validated low-speed data is vital to the establishment of low noise levels, low approach speeds, and short field lengths. Supersonic aerodynamic data is mandatory to the transatlantic range goal and to demonstrate confidence in the applicability of the methods used herein. Further detailed system integration studies to the depth described in this status report should await the completion of planned experimental programs.

REFERENCES

1. Dutton, Donnell W., Georgia Institute of Technology "Preliminary Studies of a Supersonic Business Jet". SAE Paper 670246, Business Aircraft Conference, Wichita, Kansas, April 5-7, 1967.

2. Catholic University, Department of Space Science and Applied Physics, Aviation Week and Space Technology, May 1, 1967, p. 77.

3. Proceedings of SCAR Conference, NASA CP-001, Langley Research Center, Hampton, Virginia, November 9-12, 1976.

4. Radkey, R. L., Welge, H. R., and Felix, J. R.: "Aerodynamic Characteristics of a Mach 2.2 Advanced Supersonic Cruise Configuration at Mach Numbers from 0.5 to 2.4". McDonnel Douglas Corporation, Douglas Aircraft Company, February, 1977.

5. Keith, A. L., Jr.: Effects of Variable Turbine Areas on Subsonic Cruise Performance of Turbojets Designed for Supersonic Application. NASA TN D-5962, October, 1970.

6. Baber, H. T., Jr. and Swanson, E. E.: Advanced Supersonic Technology Concept AST-100 Characteristics Developed in a Baseline-Update Study. NASA TM X-72815, January 16, 1976.

7. Smeltzer, Donald B. and Sorensen, Norman E.: Tests of a Mixed Compression Axisymmetric Inlet with Large Transonic Mass Flow at Mach Number 0.6 to 2.65. NASA TN D-6971, December, 1972.

8. The General Electric Company: Preliminary Study Data GE21/J11-B10 Study Al Turbojet Propulsion System for use in Advanced Supersonic System Technology Study. Report No. R72AEG329 (Contract NAS3-16950) November, 1972.

9. Keith, A. L., Jr.: Unpublished Computer Program developed by NASA Langley Research Center for computing the performance of a single rotor turbojet engine with or without afterburning.

10. Coe, Paul L., Jr. and McLemore, Clyde: Effects of Upper Surface Blowing and Thrust Vectoring on Low-Speed Aerodynamic Characteristics of a Large-Scale Supersonic Transport Model, NASA TM X-72792, November, 1975.

11. Margason, Richard J. and Lamar, John E.: Vortex Lattice Fortran Program for Estimating Subsonic Aerodynamic Characteristics of Complex Planforms, NASA TN D-6142, 1971.

12. LTV Aerospace Corp., HTC: Advanced Supersonic Technology Concept Study, Reference Characteristics, NASA CR-132374, 1973.

13. Lockwood, Vernard E. and Huffman, Jarrett K.: The Aerodynamic Characteristics of a Fixed Arrow-Wing Supersonic Configuration (SCAT 15-F-9898) Part I. Stability and Performance Characteristics in the Landing and Take-Off Configuration, LWP-766, 1969.

14. USAF Stability and Control DATCOM: Characteristics at Angle of Attack Air Force Flight Dynamics Laboratory, dated October, 1960, revised January, 1975.

15. Hoerner, S. F.: Fluid Dynamic Drag, 1958.

16. Lockwood, Vernard E.: The Aerodynamic Characteristics of a Fixed Arrow-Wing Supersonic Transport Configuration (SCAT 15-F-9898) Part IA. Additional Studies of the Stability and Performance Characteristics in the Landing and Take-Off Configuration, LWP-842, January, 1970.

17. Quartero, C. B.: Subsonic Parasite Drag Computer Program. Vought Corporation, Hampton Technical Center, July, 1975.

18. Sommer, Simon C. and Short, Barbara J.: Free Flight Measurements of Turbulent Boundary Layer Skin Friction in the Presence of Severe Aerodynamic Heating at Mach numbers from 2.8 to 7.0. NASA TN 3391, 1955.

19. Harris, Roy V.: An Analysis and Correlation of Aircraft Wave Drag. NASA TM X-947, 1963.

20. Carlson, Harry W. and Miller, David S.: Numerical Methods for the Design and Analysis of Wings at Supersonic Speeds. NASA TN D-7713, 1974.

21. Mack, Robert J.: A Numerical Method for Evaluation and Utilization of Supersonic Nacelle-Wing Interference. NASA TN D-5057, 1968.

22. Middleton, Wilbur D. and Carlson, Harry W.: A Numerical Method of Estimating and OptimizingSupersonic Aerodynamic Characteristics of Arbitrary Planform Wings. J. Aircraft, Vol. 2, No. 4, July-August, 1965, pp. 261-265.

23. Sorrells, Russell B., III and Landrum, Emma Jean: Theoretical and Experimental Study of Twisted and Cambered Delta Wings Designed for Mach Number of 3.5. NASA TN D-8247, 1976.

24. Mack, Robert J.: Effects of Leading-Edge Sweep Angle and Design Lift Coefficient on Performance of a Modified Arrow-Wing at a Design Mach Number of 2.6. NASA TN D-7753, 1974.

25. Carlson, H. W. and Maglieri, D. J.: Review of Sonic Boom Generation Theory and Prediction Methods, J. Acoust. Soc. Ameri. 51, 675-685, (1972).

26. Ferri, Antonio: Possibilities and Goals for the Future SST, AIAA Paper 75-254, 1975.

27. NASA CR-2628, Aerodynamic and Acoustic Tests of Duct Burning Turbofan Exhaust Nozzles, Hilary Kozlowski and Allen B. Packman, Pratt and Whitney Aircraft, December, 1976.

28. Acoustic Test of Ducting-Burning Turbofan Jet Noise Simulation, Final Technical Report, October, 1975, P. R. Knott et al, General Electric.

29. Department of Transportation, Federal Aviation Administration Noise Standards; Aircraft Type and Airworthiness Certification, Federal Aviation Regulations, Part 36.

30. NASA TM X-71618, Interim Prediction Method for Jet Noise, J. R. Stone, Lewis Research Center.

31. AIAA Paper 76-526, Approximate Prediction of Airframe Noise, by Martin, R. Fink, presented at the Third AIAA Aero-Acoustics Conference, Palo Alto, California, July, 1976.

32. Department of Transportation, Federal Aviation Administration Airworthiness Standards; Transport Category Airplane, Federal Aviation Regulation, Part 25.

33. Unpublished Computer Program, TAKEOFF, to Calculate Profiles for Noise Analysis for SCAR Aircraft Configuration.

34. Pulley, John: "Evaluation of Low-Cost Titanium Structure for Advanced Aircraft", Rockwell International Los Angeles Aircraft Division, dated October 22, 1976.

COMPARATIVE WEIGHT SUMMARY

MODEL	BOEING 960-5128				LOCKHEED TASK II				MCDAC 3230-2.0-64			
Item or Group Description	Boeing	Vought	Wt. Lbs.	Variation %	Lockheed	Vought	Wt. Lbs.	Variation %	McDAC	Vought	Wt. Lbs.	Variation %
WING	43436	42078	- 1358	- 3.14	41088	41398	+ 310	+ .75	34137	36247	+ 2070	+ 6.06
HORIZONTAL TAIL	2962	1939	- 1023	- 34.54	3606	3298	- 308	- 8.54	1796	2371	+ 575	+ 32.02
VERTICAL TAIL - BODY MTD	1143	1404	+ 256	+ 22.30	1179	1557	+ 378	+ 32.06	1727	1893	+ 166	+ 9.61
VERTICAL FIN - WING MTD	1506	1511	+ 5	+ .33	1270	993	- 277	- 21.81	0	0	0	0
CANARD	0	0	0	0	0	0	0	0	0	0	0	0
FUSELAGE	25485	23751	- 1714	- 6.73	19106	22848	+ 3742	+ 19.59	21642	23349	+ 1707	+ 7.89
LANDING GEAR - MAIN	16928	13466	- 5162	- 27.73	12428	12963	- 926	- 5.99	16689	13749	- 2940	- 17.62
- NOSE	1706				1361							
NACELLE	8655	5506	- 3149	- 36.38	11293	9355	- 1938	- 17.16	6681	7575	+ 894	+ 13.38
STRUCTURE TOTAL	(101866)	(89650)	(-12156)	(- 11.94)	(91331)	(92412)	(+ 1081)	(+ 1.18)	(82712)	(85184)	(+ 2472)	(+ 2.99)
ENGINES	20502	20502	0	0	23189	23189	0	0	30812	30812	0	0
REVERSERS AND SUPPRESSORS	0	0	0	0	0	0	0	0	0	0	0	0
MISCELLANEOUS SYSTEMS	1102	807	- 295	- 26.77	3178	807	+ 1943	+ 61.14	1026	807	+ 301	+ 10.91
FUEL SYSTEM - TANKS AND PLUMBING	4132	2495	- 1637	- 39.62		4314			1733	2253		
- INSULATION	0	0	0	0	0	0	0	0	0	0	0	0
PROPULSION TOTAL	(25736)	(23804)	(- 1932)	(- 7.51)	(26367)	(28310)	(+ 1943)	(+ 7.37)	(33571)	(33872)	(+ 301)	(+ .90)
FLIGHT CONTROLS	6668	4456	- 2212	- 33.17	3856	4456	+ 600	+ 15.57	4134	4456	+ 322	+ 7.79
AUXILIARY POWER	113	0	- 113	-100.00	0	0	0	0	431	0	- 431	-100.00
INSTRUMENTS	846	1542	+ 696	+ 82.27	558	1542	+ 984	+176.00	557	1542	+ 985	+176.84
HYDRAULICS AND PNEUMATIC	2629	2540	- 89	- 3.38	2585	2540	- 45	- 1.74	2578	2540	- 38	- 1.47
ELECTRICAL	2341	2291	- 50	- 2.14	2064	2291	+ 227	+ 11.00	2200	2291	+ 91	+ 4.14
AVIONICS	1309	1220	- 89	- 6.80	842	1220	+ 358	+ 41.53	1250	1220	- 30	- 2.40
FURNISHINGS AND EQUIPMENT	8623	11390	+ 2767	+ 32.09	5216	11390	+ 6174	+118.37	11144	11390	+ 246	+ 2.21
ENVIRONMENTAL CONTROL SYSTEM	5139	3719	- 1420	- 27.63	3765	3719	- 46	- 1.22	2806	3719	+ 913	+ 32.54
ANTI-ICING	61	95	+ 34	+ 55.74	0	95	+100.00		222	95	- 127	- 57.21
SYSTEMS AND EQUIPMENT TOTAL	(27729)	(27253)	(- 476)	(- 1.72)	(18906)	(27253)	(+ 8347)	(+ 44.15)	(25322)	(27253)	(+ 1931)	(+ 7.63)
OPTIONS	1134	0	- 1134	-100.00	898	0	- 898	-100.00	1297	0	- 1297	-100.00
MANUFACTURERS EMPTY WEIGHT	156400	140707	-15698	- 10.04	137502	147975	+10473	+ 7.62	142902	146309	+ 3407	+ 2.38
CREW AND BAGGAGE - FLIGHT	2386	306	- 240	- 10.06	4853	306	+ 1707	+ 35.17	3672	306	+ 3656	+ 99.56
- CABIN		513				513				674		
UNUSABLE FUEL		1079				1053				980		
ENGINE OIL		248				386				323		
PASSENGER SERVICE	3719	3213	- 628	+ 16.89		3213				3748		
CARGO CONTAINERS		1134				1089				1297		
OPERATING WEIGHT	162510	147200	-15310	- 9.42	142355	154535	+12180	+ 8.56	146574	153637	+ 7063	+ 4.82
PASSENGERS	17513	17513	0	0	22226	17513	- 43	- 0.19	20432	20432	0	0
PASSENGER BAGGAGE	4670	4670	0	0		4670			5445	5449	0	0
CARGO	0	0	0	0	0	0	0	0	0	0	0	0
ZERO FUEL WEIGHT	184693	169383	-15310	- 8.29	164581	176718	+12137	+ 7.37	172455	179518	+ 7063	+ 4.10
MISSION	155501	170811	+15310	+ 9.85	175613	163476	-12137	- 6.91	167739	160676	- 7063	- 4.21
TAKEOFF GROSS WEIGHT	340194	340194	0	0	340194	340194	0	0	340194	340194	0	0

TABLE I(a)

COMPARATIVE WEIGHT SUMMARY

MODEL	BOEING 969-5126				LOCKHEED TASK II				McDAC 3230-2.2-5A			
Item or Group Description	Boeing	Vought	Wt. Lbs.	Variation %	Lockheed	Vought	Wt. Lbs.	Variation %	McDAC	Vought	Wt. Lbs.	Variation %
WING	95760	92756	- 3004	- 3.14	90584	91268	+ 684	+ .75	75347	79913	+ 4566	+ 6.06
HORIZONTAL TAIL	6530	4274	- 2256	- 34.55	7950	7271	- 679	- 8.54	3960	5227	+ 1267	+ 31.99
VERTICAL TAIL - BODY MTD	2530	3095	+ 565	+ 22.33	2600	3432	+ 832	+ 32.00	3807	4173	+ 366	+ 9.61
VERTICAL FIN - WING MTD	3320	3331	+ 11	+ .33	2800	2189	- 611	- 21.82				
CANARD												
FUSELAGE	56140	52361	- 3779	- 6.73	42122	50372	+ 8250	+ 19.59	47713	51477	+ 3764	+ 7.89
LANDING GEAR - MAIN	37320	29638	-11392	- 27.73	27400	28579	- 1821	- 5.99	36792	30312	- 6480	- 17.61
- NOSE	3760				3000							
NACELLE	19080	12139	- 6941	- 36.38	24897	20625	- 4272	- 17.16	14730	16700	+ 1970	+ 13.37
STRUCTURE TOTAL	(224440)	(197644)	(-26796)	(- 11.94)	(201353)	(203735)	(- 2382)	(+ 1.18)	(182349)	(187802)	(+ 5453)	(+ 2.99)
ENGINES	45200	45200	0	0	51124	51124	0	0	67928	67928	0	0
REVERSERS AND SUPPRESSORS												
MISCELLANEOUS SYSTEMS	2430	1780	- 650	- 26.75	7007	1780	+ 4283	+ 61.12	2262	1780	+ 666	+ 10.95
FUEL SYSTEM-TANKS AND PLUMBING	9110	5500	- 3610	- 39.63		9510			3820	4968		
-INSULATION												
PROPULSION TOTAL	(56740)	(52430)	(- 4260)	(- 7.51)	(58131)	(62414)	(+ 4283)	(+ 7.37)	(74010)	(74676)	(+ 666)	(+ .90)
FLIGHT CONTROLS	14700	9824	- 4876	- 33.17	8500	9824	+ 1324	+ 15.58	9115	9824	+ 709	+ 7.78
AUXILIARY POWER	250		- 250	-100.00					950	0	- 950	-100.00
INSTRUMENTS	1865	3400	+ 1535	+ 82.31	1230	3400	+ 2170	+176.00	1227	3400	+ 2173	+177.10
HYDRAULICS AND PNEUMATIC	5795	5600	- 195	- 3.36	5700	5600	- 100	- 1.75	5684	5600	- 84	- 1.48
ELECTRICAL	5160	5050	- 110	- 2.13	4550	5050	+ 500	+ 10.99	4850	5050	+ 200	+ 4.12
AVIONICS	2885	2690	- 195	- 6.76	1900	2690	+ 790	+ 41.58	2756	2690	- 66	- 2.39
FURNISHINGS & EQUIPMENT	21910	25111	+ 3201	+ 14.61	11500	25111	+13611	+118.36	24563	25111	+ 543	+ 2.21
ENVIRONMENTAL CONTROL SYSTEM	8430	8200	- 230	- 2.73	8300	8200	- 100	- 1.20	6186	8200	+ 2014	+ 32.56
ANTI-ICING	135	210	+ 75	+ 55.56	0	210	+ 210	+100.00	489	210	- 279	- 57.06
SYSTEMS AND EQUIPMENT TOTAL	(61130)	(60085)	(- 1045)	(- 1.71)	(41680)	(60085)	(+18405)	(+ 44.16)	(55825)	(60085)	(+ 4260)	(+ 7.63)
OPTIONS	2500	0	- 2500	-100.00	1980	0	- 1980	-100.00	2860	0	- 2860	-100.00
MANUFACTURERS EMPTY WEIGHT	344810	310209	-34601	- 10.03	303144	326235	+23091	+ 7.62	315044	322563	+ 7519	+ 2.39
CREW AND BAGGAGE-FLIGHT,	[3]	[3] 675			[3]	[3] 675			[3]	675		
-CABIN,	[7] 5260	[7] 1130	- 531	- 10.10	[7]	[7] 1130			[9]	1485		
UNUSABLE FUEL		2378			10700	2322	+ 3762	+ 35.16	8096	2160	+ 8060	+ 99.89
ENGINE OIL		546				852				712		
PASSENGER SERVICE	8200	7083	+ 1383	+ 16.87		7083				8264		
CARGO CONTAINERS,	[5]	[5] 2500			[5]	[5] 2400			[6]	2860		
OPERATING WEIGHT	358270	324521	-33749	- 9.42	313844	340697	+26853	+ 8.56	323140	338719	+ 15579	+ 4.82
PASSENGERS,	[234] 38610	33610	0	0	[234] 38610	38610	0	0	[273] 45045	45045	0	0
PASSENGER BAGGAGE	10296	10296	0	0	10390	10296	- 94	- .19	12012	12012	0	0
CARGO												
ZERO FUEL WEIGHT	407176	373427	-33479	- 8.29	362844	389603	-26759	+ 7.37	380197	395776	+ 15579	+ 4.10
MISSION FUEL	342824	346573	+33749	+ 9.84	387156	360397	-26759	- 6.91	369803	354224	- 15579	- 4.21
TAKE-OFF GROSS WEIGHT	750000	750000	0	0	750000	750000	0	0	750000	750000	0	0

TABLE 1(b)

MASS SUMMARY

MODEL	SSXJET		SSXJET I		SSXJET II & II TANDEM		SSXJET III	
Description	Kilograms	Pounds	Kilograms	Pounds	Kilograms	Pounds	Kilograms	Pounds
STRUCTURE	9469.6	20877	8990.7	19821	8830.5	19468	10299.3	22706
PROPULSION	3700.9	8159	3633.7	8011	3475.0	7661	4261.5	9395
SYSTEMS	2799.1	6171	2781.0	6131	2781.0	6131	3155.6	6957
WEIGHT EMPTY	15969.6	35207	15405.4	33963	15086.5	33260	17716.4	39058
OPERATING ITEMS	351.1	774	350.6	773	349.3	770	377.4	832
OPERATING WEIGHT	16320.7	35981	15755.9	34736	15435.7	34030	18093.8	39890
PAYLOAD	725.8	1600	725.8	1600	725.8	1600	725.8	1600
ZERO FUEL WEIGHT	17046.5	37581	16481.7	36336	16161.5	35630	18819.5	41490
MISSION FUEL	18673.9	41169	18444.9	40664	17404.3	38370	17261.5	38055
TAKE-OFF-GROSS WEIGHT	35720.4	78750	34926.6	77000	33565.8	74000	36081.0	79545
NORMAL LANDING WEIGHT	20289.2	44730	20150.8	44425	19225.5	42385	22473.2	49545

TABLE II

GROUP WEIGHT SUMMARY

	SEXJET		SEXJET I		SEXJET II & II TANDEM		SEXJET III	
	Kilograms	Pounds	Kilograms	Pounds	Kilograms	Pounds	Kilograms	Pounds
WING	3598.8	7934	3357.9	7403	3055.9	6737	2863.1	6312
HORIZONTAL TAIL	191.9	423	191.9	423	191.9	423	235.9	520
VERTICAL TAIL	289.4	638	289.4	638	289.4	638	374.2	825
FUSELAGE	3494.0	7703	3298.5	7272	3513.5	7746	3476.3	7664
LANDING GEAR	1390.7	3066	1359.9	2998	1306.8	2881	1400.2	3087
NACELLE	504.8	1113	493.1	1087	473.1	1043	1949.5	4298
STRUCTURE TOTAL	(9469.6)	(20877)	(8990.7)	(19821)	(8830.5)	(19468)	(10299.3)	(22706)
ENGINES	3015.5	6648	2948.3	6500	2833.1	6246	3655.0	8058
THRUST REVERSERS	0.0	0	0.0	0	0.0	0	0.0	0
MISCELLANEOUS SYSTEMS	59.0	130	59.0	130	59.0	130	59.0	130
FUEL SYSTEM - TANKS AND PLUMBING	626.4	1381	626.4	1381	582.9	1285	547.5	1207
PROPULSION TOTAL	(3700.9	(8159)	(3633.7)	(8011)	(3475.0)	(7661)	(4261.5)	(9395)
SURFACE CONTROLS	564.3	1244	552.0	1217	530.2	1169	573.3	1264
AUXILIARY POWER	0.0	0	0.0	0	0.0	0	0.0	0
INSTRUMENTS	205.9	454	205.9	454	205.9	454	212.3	468
HYDRAULICS	266.3	587	260.4	574	249.9	551	270.3	596
ELECTRICAL	444.5	980	444.5	980	444.5	980	444.5	980
AVIONICS	453.6	1000	453.6	1000	453.6	1000	453.6	1000
FURNISHINGS AND EQUIPMENT	417.3	920	417.3	920	417.3	920	790.2	1742
AIR CONDITIONING	352.0	776	352.0	776	384.2	847	316.2	697
ANTI-ICING	95.3	210	95.3	210	95.3	210	95.3	210
SYSTEMS AND EQUIPMENT TOTAL	(2799.1)	(6171)	(2781.0)	(6131)	(2781.0)	(6131)	(3155.6)	(6957)
WEIGHT EMPTY	15969.6	35207	15405.4	33963	15086.5	33260	17716.4	39058
CREW & BAGGAGE - FLIGHT, 2	181.4	400	181.4	400	181.4	400	181.4	400
UNUSABLE FUEL	99.3	219	99.3	219	99.3	219	112.5	248
ENGINE OIL	33.6	74	33.1	73	31.8	70	46.7	103
PASSENGER SERVICE	36.7	81	36.7	81	36.7	81	36.7	81
OPERATING WEIGHT	16320.7	35981	15755.9	34736	15435.7	34030	18093.8	39890
PASSENGERS, 8	616.9	1360	616.9	1360	616.9	1360	616.9	1360
PASSENGER BAGGAGE	108.9	240	108.9	240	108.9	240	108.9	240
ZERO FUEL WEIGHT	17046.5	37581	16481.7	36336	16161.5	35630	18819.5	41490
MISSION FUEL	18673.9	41169	18444.9	40664	17404.3	38370	17261.5	38055
TAKE-OFF GROSS WEIGHT	35720.4	78750	34926.6	77000	33565.8	74000	36081.0	79545

TABLE III

MASS INERTIA DATA SUMMARY

ITEM	MODEL	SEXJET		SEXJET I		SEXJET II & II TANDEM		SEXJET III	
Description	Condition	Take-off Gross Weight	Normal Landing Weight	Take-off Gross Weight	Normal Landing Weight	Take-off Gross Weight	Normal Landing Weight	Take-off Gross Weight	Normal Landing Weight
MASS, kg		35720.4	20289.2	34926.6	20150.8	33565.8	19225.5	36081.0	22473.2
lbm		78750	44730	77000	44425	74000	42385	79545	49545
HORIZONTAL c.g., m		17.361	17.165	16.525	16.530	17.186	16.772	18.453	18.567
in.		683.5	675.8	650.6	650.8	676.6	660.3	726.5	731.0
percent of M.A.C.		57.08	54.98	53.98	53.99	58.5	54.0	50.85	52.00
ROLL INERTIA, I_x, kg-m^2		6.440×10^4	5.559×10^4	7.348×10^4	6.833×10^4	6.101×10^4	3.932×10^4	10.385×10^4	5.559×10^4
slug-ft^2		4.75×10^4	4.10×10^4	5.42×10^4	5.04×10^4	4.50×10^4	2.90×10^4	7.66×10^4	4.10×10^4
PITCH INERTIA, I_y, kg-m^2		225.717×10^4	210.511×10^4	195.077×10^4	94.874×10^4	209.990×10^4	155.896×10^4	257.102×10^4	193.50×10^4
slug-ft^2		166.49×10^4	88.89×10^4	143.89×10^4	69.98×10^4	154.89×10^4	114.99×10^4	189.64×10^4	142.73×10^4
YAW INERTIA, I_z, kg-m^2		228.618×10^4	124.294×10^4	198.521×10^4	99.904×10^4	213.257×10^4	157.442×10^4	263.447×10^4	197.68×10^4
slug-ft^2		168.63×10^4	91.68×10^4	146.43×10^4	73.69×10^4	157.30×10^4	116.13×10^4	194.32×10^4	145.81×10^4
PRODUCT OF INERTIA, I_{xz}, kg-m^2		2.847×10^4	2.603×10^4	$.691\times10^4$	$.813\times10^4$	3.200×10^4	2.983×10^4	7.280×10^4	5.708×10^4
slug-ft^2		2.10×10^4	1.92×10^4	$.51\times10^4$	$.60\times10^4$	2.36×10^4	2.20×10^4	5.37×10^4	4.21×10^4
PRINCIPAL AXIS ANGLE OF INCLINATION, θ	rad.	.0134	.0220	.0037	.0089	.0154	.0195	.0288	.0297
	des.	.77	1.26	.21	.51	.88	1.12	1.65	1.70

TABLE IV

TABLE V

SSXJET Low-Speed Zero-Lift Drag Buildup

S_{REF} = 89.65 m^2 (965. Ft^2)

Item	Drag Coefficient
Wing-Body (including interference)	.005652
Empennage	.000764
Nacelles (including nacelle-fuselage-empennage interference)	.001073
Propulsion bleed and air-conditioning drag	.000533
Landing gear	.007678
SSXJET total zero-lift drag:	
gear up	.008022
gear down	.015700

TABLE VI

SSXJET I Low-Speed Zero-Lift Drag Buildup

S_{REF} = 89.65 m^2 (965. Ft^2)

Item	Drag Coefficient
Wing-body (including interference)	.005652
Empennage	.000764
Nacelles (including wing-nacelle interference)	.003603
Propulsion bleed and air-conditioning	.000533
Landing gear	.007678
SSXJET I total zero-lift drag:	
gear up	.010552
gear down	.018230

TABLE VIII

MISSION PERFORMANCE

MISSION: Design Supersonic Cruise Mach 2.2

MODEL NO.: SSXJET

AIRCRAFT CHARACTERISTICS

Take-off gross weight	kg (lbm)	35720	(78750)
Operating weight empty	kg (lbm)	16320	(35980)
Payload-No. Passengers		8	8
Cargo	kg (lbm)	0	0
Total Weight	kg (lbm)	726	(1600)
Wing area - reference	m^2 (ft^2)	89.65	(965)
- gross	m^2 (ft^2)	89.65	(965)
Advanced Turbojet (2) ;sea level static (std. day +8° C) installed thrust per engine, N (lbf)		64677	(14540)
Initial installed thrust to weight ratio		.3693	.3693
Initial wing loading - reference,	N/m^2 (lbm/ft^2)	3907.4	(81.61)
- actual	N/m^2 (lbm/ft^2)	3907.4	(81.61)

Design Mission

	OPERATING WEIGHTS, kg (lbm)		Δ FUEL kg (lbm)	Δ RANGE km (n. mi.)	ΔTIME minutes
Take-off	35720	(78750)			
			317.5 (700)	0 (0)	0
Start Climb	35403	(78050)			
			4343.6 (9576)	746 (403)	29
Start Cruise	31059	(68474)			
			10644.5 (23467)	5075 (2740)	128
End Cruise	20415	(45007)			
			102.1 (225)	370 (200)	20
End Descent	20313	(44782)			
			117.9 (260)	0 (0)	5
Taxi-in	20195	(44522)			
Block Fuel and Time			15525.6 (34228)		182
Trip Range				6191 (3343)	

NOTES: 1. Taxi-in fuel taken out of reserves at destination.

2. C.A.B. range corresponding to block time and fuel equals trip range minus traffic allowances as will be specified for supersonic aircraft.

TABLE VII - SSXJET SERIES WETTED AREAS SUMMARY

	SSXJET AND SSXJET I		SSXJET II SIDE/SIDE		SSXJET II TANDEM		SSXJET III	
COMPONENT	A_{WET}	$\frac{A_{WET}}{A_{TOTAL}}$	A_{WET}	$\frac{A_{WET}}{A_{TOTAL}}$	A_{WET}	$\frac{A_{WET}}{A_{TOTAL}}$	A_{WET}	$\frac{A_{WET}}{A_{TOTAL}}$
WING	135.15 (1454.7)	.4328	95.81 (1031.3)	.3067	95.81 (1031.3)	.3121	162.52 (1749.3)	.4099
FUSELAGE	118.32 (1273.6)	.3789	157.71 (1697.6)	.5049	152.33 (1639.7)	.4962	118.49 (1275.4)	.2989
NACELLES (2)	32.47 (349.5)	.1040	32.47 (349.5)	.1040	32.47 (349.5)	.1058	81.88 (881.3)	.2065
VERTICAL TAIL	14.06 (151.3)	.0450	14.06 (151.3)	.0450	14.06 (151.3)	.0458	18.32 197.2)	.0462
HORIZONTAL TAIL	12.30 (132.4)	.0394	12.30 (132.4)	.0394	12.30 (132.4)	.0401	15.24 164.0)	.0385
TOTAL	312.30 (3361.5)		312.35 (3362.1)		306.97 (3304.2)		396.45 (4267.3)	

NOTE: WETTED AREAS IN SQUARE METERS WITH SQUARE FEET IN PARENTHESES.

TABLE VIII - concluded

Model No.: SSXJET

Reserve Fuel Breakdown, kg (lbm):

1. 7% Trip Fuel	1079	(2378)
2. Missed Approach	-	-
3. 482 km (260 n. m.) to alternate airport	1329	(2930)
4. 30 min. holding at 457 m. (15000 ft)	835	(1841)
Total Reserve	3243	(7149)

Initial Cruise Conditions:

Lift Coefficient	.08738	
Drag Coefficient	.01495	
Lift/Drag	5.84	
TSFC, kg/hr/N (lbm/hr/lbf)	.130	1.276
Altitude, m(ft)	15240	(50000)

TABLE IX

MISSION PERFORMANCE

MISSION: Design Supersonic Cruise Mach 2.2

MODEL NO.: SSXJET I

AIRCRAFT CHARACTERISTICS

Take-off gross weight	kg (lbm)	34927	(77000)
Operating weight empty	kg (lbm)	15756	(34736)
Payload-No. Passengers		8	8
Cargo	kg (lbm)	0	0
Total Weight	kg (lbm)	726	(1600)
Wing area - reference	m^2 (ft^2)	89.65	(965)
- gross	m^2 (ft^2)	89.65	(965)
Advanced Turbojet (2) ;sea level static (std. day +8°C) installed thrust per engine, N (lbf)		60878	(13686)
Initial installed thrust to weight ratio		.3555	.3555
Initial wing loading - reference,	N/m^2 (lbm/ft^2)	3820.6	(79.79)
- actual	N/m^2 (lbm/ft^2)	3820.6	(79.79)

Design Mission

	OPERATING WEIGHTS, kg (lbm)	Δ FUEL kg (lbm)	Δ RANGE km (n. mi.)	ΔTIME minutes
Take-off	34927 (77000)			
		318 (700)	0 (0)	0
Start Climb	34609 (76300)			
		4689 (10338)	989 (534)	35
Start Cruise	29920 (65962)			
		10160 (22399)	4745 (2562)	155
End Cruise	19759 (43562)			
		99 (218)	370 (200)	20
End Descent	19661 (43345)			
		188 (260)	0 (0)	5
Taxi-in	19543 (43085)			
Block Fuel and Time		15384 (33915)		180
Trip Range			6104 (3296)	

NOTES: 1. Taxi-in fuel taken out of reserves at destination.

2. C.A.B. range corresponding to block time and fuel equals trip range minus traffic allowances as will be specified for supersonic aircraft.

TABLE IX - concluded

Model No.: SSXJET I

Reserve Fuel Breakdown, kg (lbm):

1. 7% Trip Fuel	1069	(2356)
2. Missed Approach	0	(0)
3. 482 km (260 n. m.) to alternate airport	1300	(2865)
4. 30 min. holding at 457 m. (15000 ft)	798	(1759)
Total Reserve	3166	(6980)

Initial Cruise Conditions:

Lift Coefficient	.10170	
Drag Coefficient	.01622	
Lift/Drag	6.27	
TSFC, kg/hr/N (lbm/hr/lbf)	.135	1.320
Altitude, m(ft)	15240	(50000)

TABLE X

MISSION PERFORMANCE

MISSION: Design Supersonic Cruise Mach 2.2

MODEL NO.: SSXJET II

AIRCRAFT CHARACTERISTICS

Take-off gross weight	kg (lbm)	33566	(74000)
Operating weight empty	kg (lbm)	15436	(34030)
Payload-No. Passengers		8	8
Cargo	kg (lbm)	0	0
Total Weight	kg (lbm)	726	(1600)
Wing area - reference	m^2 (ft^2)	89.65	(965)
- gross	m^2 (ft^2)	89.65	(965)
Advanced Turbojet (2) ;sea level static (std. day +8° C) installed thrust per engine, N (lbf)		60878	(13686)
Initial installed thrust to weight ratio		.370	.370
Initial wing loading - reference,	N/m^2 (lbm/ft^2)	3671.7	(76.68)
- actual	N/m^2 (lbm/ft^2)	3671.7	(76.68)

Design Mission

	OPERATING WEIGHTS, kg (lbm)	Δ FUEL kg (lbm)	Δ RANGE km (n. mi.)	ΔTIME minutes
Take-off	33566 (74000)			
		318 (700)	0 (0)	0
Start Climb	33248 (73300)			
		4033 (8892)	754 (400)	29
Start Cruise	29215 (64408)			
		9880 (21782)	4982 (2690)	126
End Cruise	19626 (43268)			
		97 (213)	370 (200)	20
End Descent	19528 (43052)			
		118 (260)	0 (0)	5
Taxi-in	19410 (42792)			
Block Fuel and Time		14446 (31847)		180
Trip Range			6106 (3297)	

NOTES: 1. Taxi-in fuel taken out of reserves at destination.

2. C.A.B. range corresponding to block time and fuel equals trip range minus traffic allowances as will be specified for supersonic aircraft.

TABLE X - concluded

Model No.: SSXJET II

Reserve Fuel Breakdown, kg (lbm):

1.	7% Trip Fuel	1003 (2211)
2.	Missed Approach	- -
3.	482 km (260 n. m.) to alternate airport	1277 (2815)
4.	30 min. holding at 457 m. (15000 ft)	784 (1728)
	Total Reserve	3064 (6754)

Initial Cruise Conditions:

Lift Coefficient	.08222	
Drag Coefficient	.01428	
Lift/Drag	5.83	
TSFC, kg/hr/N (lbm/hr/lbf)	.130	(1.276)
Altitude, m(ft)	15240	(50000)

TABLE XI

MISSION PERFORMANCE

MISSION: Design Supersonic Cruise Mach 2.2

MODEL NO.: SSXJET II TANDEM

AIRCRAFT CHARACTERISTICS

Take-off gross weight	kg (lbm)	33566	(74000)
Operating weight empty	kg (lbm)	15436	(34030)
Payload-No. Passengers		8	8
Cargo	kg (lbm)	0	0
Total Weight	kg (lbm)	726	(1600)
Wing area - reference	m^2 (ft^2)	89.65	(965)
- gross	m^2 (ft^2)	89.65	(965)
Advanced Turbojet (2) ;sea level static (std. day +8° C) installed thrust per engine, N (lbf)		60878	(13686)
Initial installed thrust to weight ratio		.370	.370
Initial wing loading - reference,	N/m^2 (lbm/ft^2)	3671.7	(76.68)
- actual	N/m^2 (lbm/ft^2)	3671.7	(76.68)

Design Mission

	OPERATING WEIGHTS, kg (lbm)	Δ FUEL kg (lbm)	Δ RANGE km (n. mi.)	ΔTIME minutes
Take-off	33566 (74000)			
		318 (700)	0 (0)	0
Start Climb	33248 (73300)			
		3975 (8763)	743 (401)	29
Start Cruise	29273 (64537)			
		9931 (21897)	5086 (2746)	128
End Cruise	19341 (42640)			
		97 (213)	370 (200)	20
End Descent	19245 (42427)			
		118 (260)	0 (0)	5
Taxi-in	19127 (42167)			
Block Fuel and Time		14439 (31833)		182
Trip Range			6199 (3347)	

NOTES: 1. Taxi-in fuel taken out of reserves at destination.

2. C.A.B. range corresponding to block time and fuel equals trip range minus traffic allowances as will be specified for supersonic aircraft.

TABLE XI - concluded

Model No.: SSXJET II TANDEM

Reserve Fuel Breakdown, kg (lbm):

1. 7% Trip Fuel	1002	(2210)
2. Missed Approach	-	-
3. 482 km (260 n. m.) to alternate airport	1277	(2816)
4. 30 min. holding at 457 m. (15000 ft)	784	(1729)
Total Reserve	3064	(6756)

Initial Cruise Conditions:

Lift Coefficient	.08237	
Drag Coefficient	.01412	
Lift/Drag	5.83	
TSFC, kg/hr/N (lbm/hr/lbf)	.130	(1.276)
Altitude, m(ft)	15240	(50000)

TABLE XII

MISSION PERFORMANCE

MISSION: Design Supersonic Cruise Mach 2.2

MODEL NO.: SSXJET III

AIRCRAFT CHARACTERISTICS

Take-off gross weight	kg (lbm)	36081	(79545)
Operating weight empty	kg (lbm)	18094	(39089)
Payload-No. Passengers		8	8
Cargo	kg (lbm)	0	0
Total Weight	kg (lbm)	726	(1600)
Wing area - reference	m^2 (ft^2)	104.98	(1130)
- gross	m^2 (ft^2)	104.98	(1130)
GE21/J11-B10 engines (2); sea level static (std. day) installed thrust per engine, N (lbf)		90209	(20280)
Initial installed thrust to weight ratio		.510	.510
Initial wing loading - reference,	N/m^2 (lbm/ft^2)	3370.5	(70.39)
- actual	N/m^2 (lbm/ft^2)	3370.5	(70.39)

Design Mission

	OPERATING WEIGHTS, kg (lbm)	Δ FUEL kg (lbm)	Δ RANGE km (n. mi.)	ΔTIME minutes
Take-off	36081 (79545)			
		318 (700)	0 (0)	0
Start Climb	35763 (78845)			
		2608 (5750)	193 (104)	9
Start Cruise	33155 (73095)			
		10547 (23252)	4812 (2598)	124
End Cruise	22608 (49843)			
		113 (250)	370 (200)	20
End Descent	22495 (49593)			
		118 (260)	0 (0)	5
Taxi-in	22377 (49333)			
Block Fuel and Time		13704 (30212)		158
Trip Range			5375 (2902)	

NOTES: 1. Taxi-in fuel taken out of reserves at destination.

2. C.A.B. range corresponding to block time and fuel equals trip range minus traffic allowances as will be specified for supersonic aircraft.

TABLE XII - concluded

Model No.: SSXJET III

Reserve Fuel Breakdown, kg (lbm):

1. 7% Trip Fuel	951	(2097)
2. Missed Approach	-	-
3. 482 km (260 n. m.) to alternate airport	1651	(3640)
4. 30 min. holding at 457 m. (15000 ft)	1074	(2367)
Total Reserve	3676	(8104)

Initial Cruise Conditions:

Lift Coefficient	.07865	
Drag Coefficient	.01448	
Lift/Drag	5.43	
TSFC, kg/hr/N (lbm/hr/lbf)	.126	(1.237)
Altitude, m(ft)	15240	(50000)

TABLE XIII

NOISE LIMITS AND PREDICTED NOISE LEVELS FOR SSXJET AND SSXJET III

REFERENCE 29 - CENTERLINE NOISE MEASUREMENT POINT

	PREDICTED JET NOISE LEVEL	1969 LIMIT	NOISE EXCEEDENCE	1977 LIMIT	NOISE EXCEEDENCE	PREDICTED AIRFRAME NOISE LEVEL
SSXJET	116.3	93.1	23.2	89.0	27.3	67.5
*SSXJET III	97.1	93.4	3.7	89.0	8.1	69.9
**SSXJET III	87.1- 92.1	93.4	-	89.0	0-3.1	-

REFERENCE 29 - SIDELINE NOISE MEASUREMENT POINT

	PREDICTED JET NOISE LEVEL	1969 LIMIT	NOISE EXCEEDENCE	1977 LIMIT	NOISE EXCEEDENCE
SSXJET	119.7	102.0	17.7	94.0	25.7
*SSXJET III	105.9	102.2	3.7	94.1	11.8
**SSXJET III	95.9 - 100.9	102.2	-	94.1	1.8 - 6.8

*SSXJET III JET EXHAUST PREDICTED NOISE LEVELS DO NOT INCLUDE EFFECTS OF COANNULAR SUPPRESSIONS.

**SSXJET III JET EXHAUST PREDICTED NOISE LEVELS WITH COANNULAR SUPPRESSION EFFECTS INCLUDED.

AIRCRAFT MISSION SUMMARY

MODEL SSXJET

		Basic	I	II	II T	III
TAKE-OFF GROSS WEIGHT	lbm	78750	77000	74000	74000	79545
	kg	35720	34927	33566	33566	36081
OPERATING WEIGHT EMPTY	lbm	35980	34736	34030	34030	39089
	kg	16320	15756	15436	15436	18024
PAYLOAD	lbm	1600	1600	1600	1600	1600
	kg	726	726	726	726	726
TOTAL FUEL	lbm	41170	40664	38370	38370	38055
	kg	18674	18445	17404	17404	17261
WING AREA						
REFERENCE	ft^2	965	965	965	965	1130
	m^2	89.65	89.65	89.65	89.65	104.98
GROSS	ft^2	965	965	965	965	1130
	m^2	89.65	89.65	89.65	89.65	104.98
INITIAL WING LOADING						
REFERENCE	lbf/ft^2	81.61	79.79	76.68	76.68	70.39
	N/m^2	3907.4	3820.6	3671.7	3671.7	3370.5
GROSS	lbf/ft^2	81.61	79.79	76.68	76.68	70.39
	N/m^2	3907.4	3820.6	3671.7	3671.7	3370.5
PROPULSION SYSTEM						
TYPE		Adv. Turbojet	Adv. Turbojet	Adv. Turbojet	Adv. Turbojet	GE21/ J11-B10
NUMBER		2	2	2	2	2
CONDITIONS		Std +8°C	Std +8°C	Std +8°C	Std +8°C	Std
INSTALLED THRUST/ENGINE	lbf	14540	13686	13686	13686	20280
	N	64677	60878	60878	60878	90209
INSTALLED T/W	lbf/lbm	.369	.356	.370	.370	.510
	N/kg	3.621	3.486	3.627	3.627	5.000
TAKE-OFF FIELD LENGTH	ft	6500	6500	6500	6500	6500
	m	1981	1981	1981	1981	1981
START CRUISE ALTITUDE	ft	54600	54500	56300	56600	58000
	m	16642	16612	17160	17252	17678
END CRUISE ALTITUDE	ft	65200	63400	64900	65300	66000
	m	19873	19324	19782	19903	20117
RANGE	n. mi.	3343	3296	3297	3347	2902
	km	6191	6104	6106	6199	5375
TRIP FUEL	lbm	33966	33655	31587	31573	29952
	kg	15407	15266	14328	14321	13586
TRIP TIME	min	182	180	180	182	158
RESERVE FUEL						
7 % TRIP FUEL	lbm	2378	2356	2211	2210	2097
	kg	1079	1069	1003	1002	951
260 n.mi. / 482 km. ALT. AIRPORT	lbm	2930	2865	2815	2816	3640
	kg	1329	1300	1277	1277	1651
30 min. HOLD @ 15,000 ft. / 4,572 m.	lbm	1841	1759	1728	1729	2367
	kg	835	798	784	784	1074
TOTAL	lbm	7149	6980	6754	6756	8104
	kg	3243	3166	3064	3064	3676
INITIAL CRUISE CONDITIONS						
C_L		.08738	.10170	.08222	.08237	.07865
C_D		.01495	.01622	.01428	.01412	.01448
L/D		5.84	6.27	5.83	5.83	5.43
TSFC	lbm/hr/lbf	1.276	1.320	1.276	1.276	1.237
	kg/hr/N					

TABLE XIV

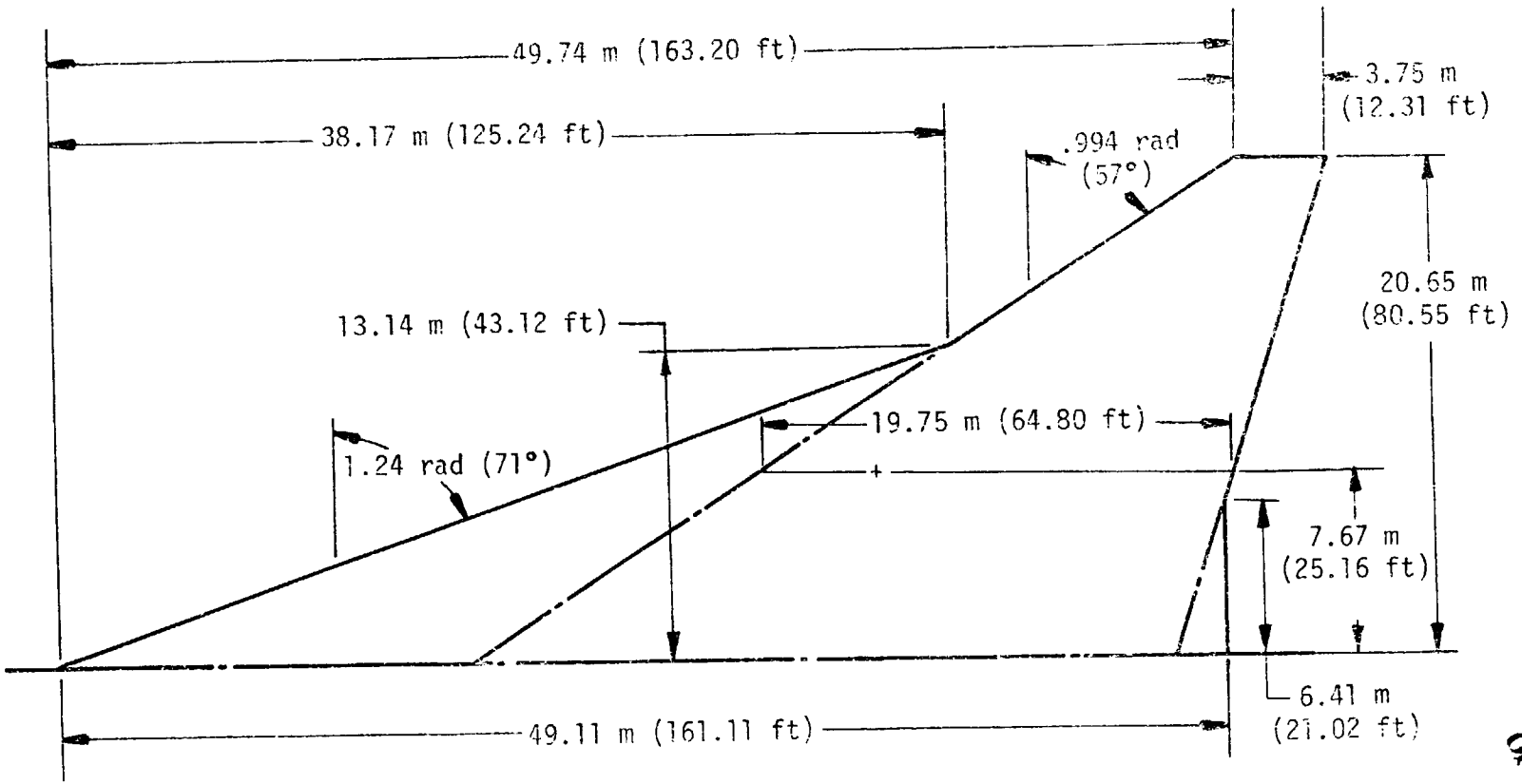

Figure 1. - McDonnell Douglas Mach 2.2 wing planform

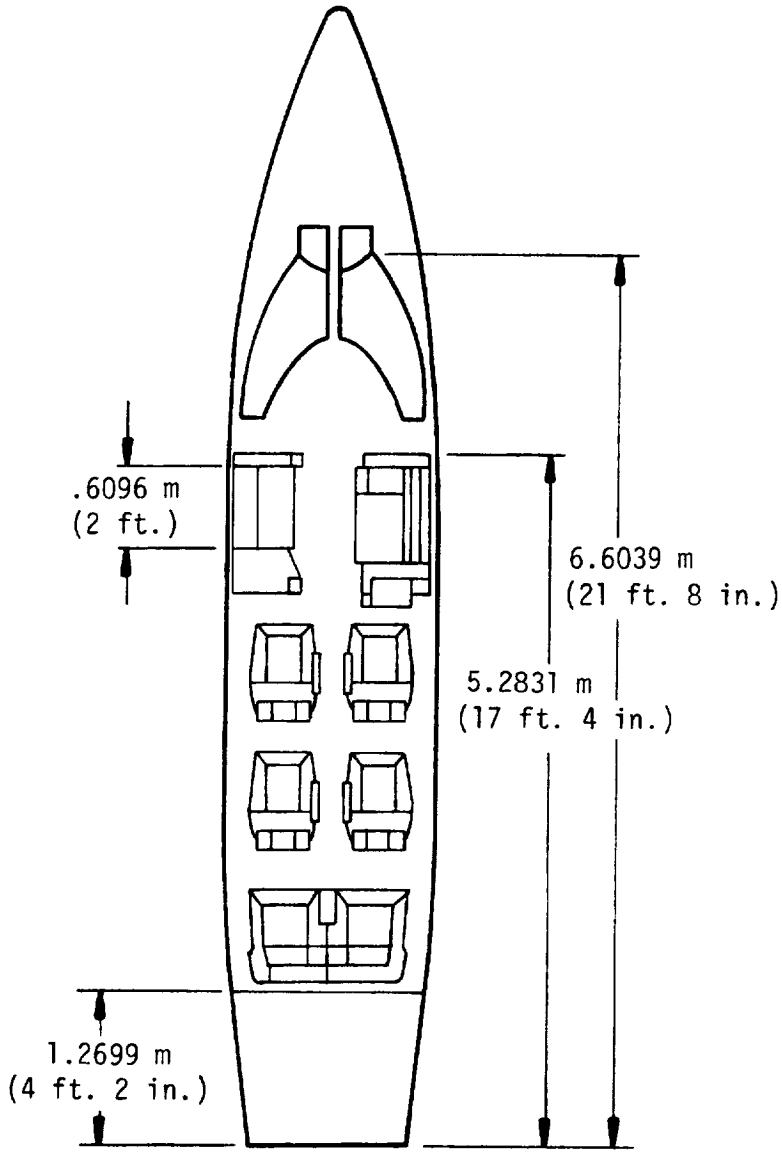

Figure 2. - LEARJET 35 Seating arrangement

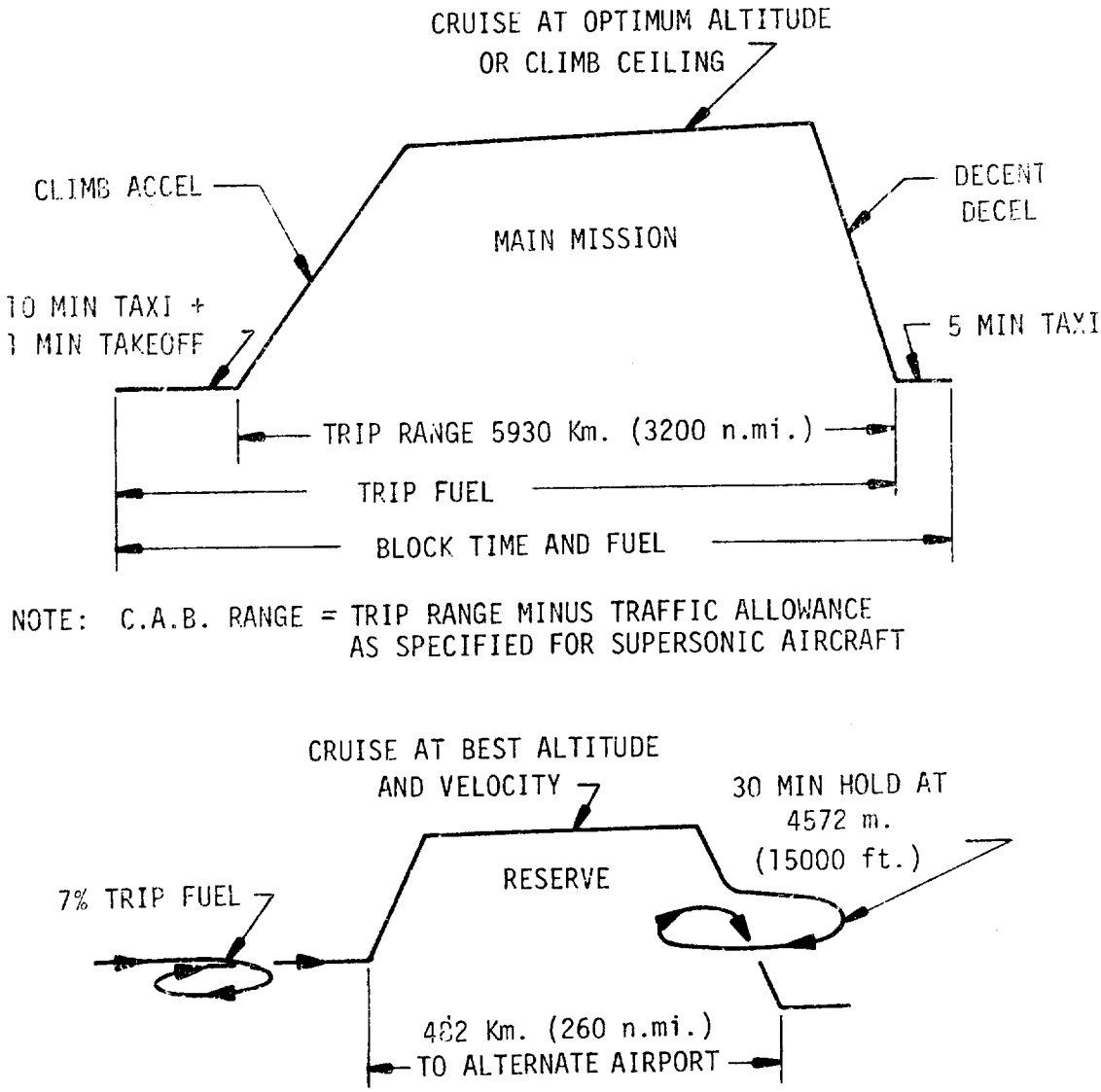

Figure 3. - Mission profile

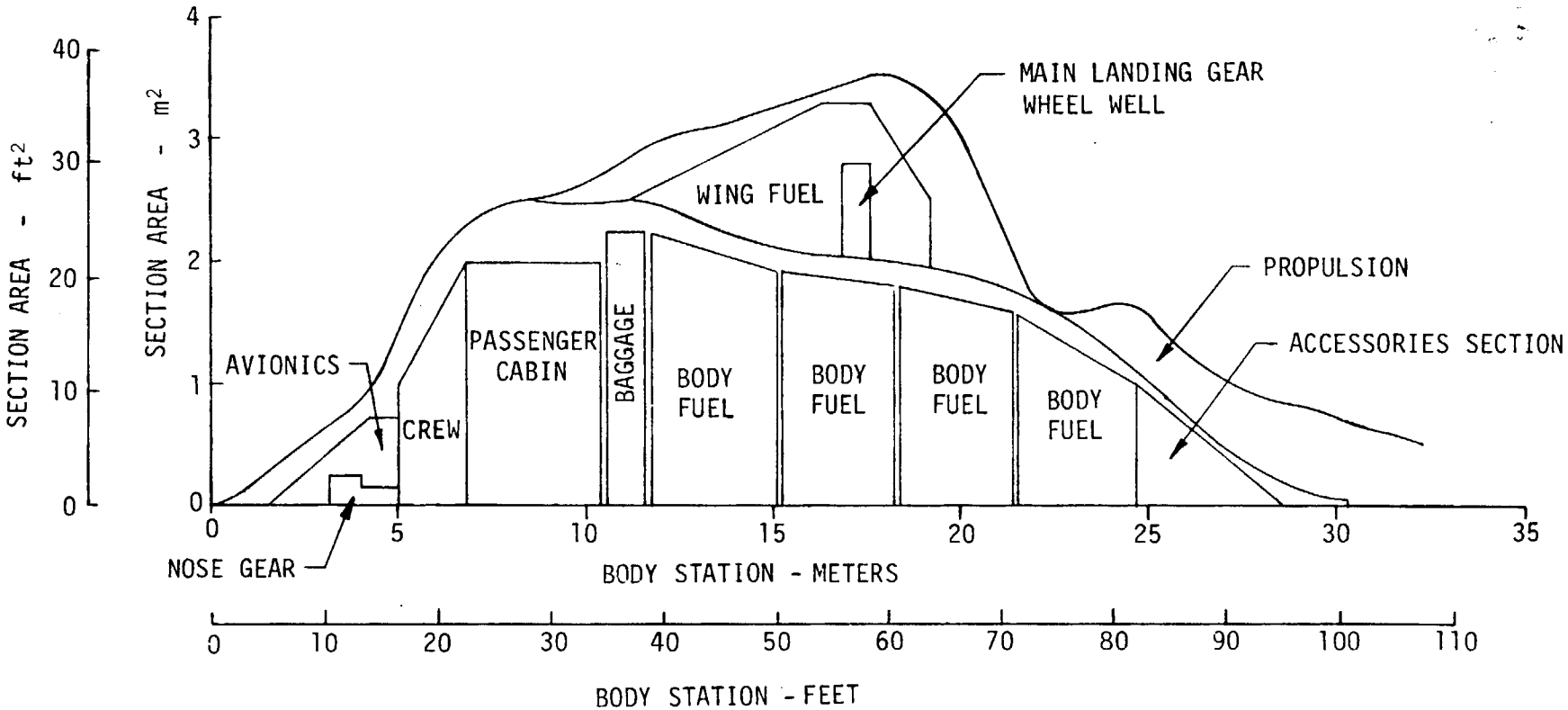

Figure 4. - SSXJET Volume utilization

GEOMETRY	WING	HORIZONTAL	VERTICAL
AREA (GROSS) S (m²)	89.651 (965)	6.038 (65)	6.967 (75)
MAC (GROSS) c̄ (m)	9.316 (30.565)	2.051 (6.730)	3.961 (12.997)
SPAN b (m)	12.833 (42.105)	3.297 (10.817)	1.866 (6.124)
ASPECT RATIO	1.84	1.8	.50
SWEEP Λ_{LE} (DEG)	71.57	60	65
ROOT CHORD (m)	15.254 (50.048)	2.930 (9.614)	5.332 (17.496)
TIP CHORD (m)	1.165 (3.822)	.732 (2.404)	2.132 (6.998)
ROOT T/C %		3.0	3.0
TIP T/C %		3.0	3.0
TAPER RATIO		.25	.40
DIHEDRAL (DEG)		10	

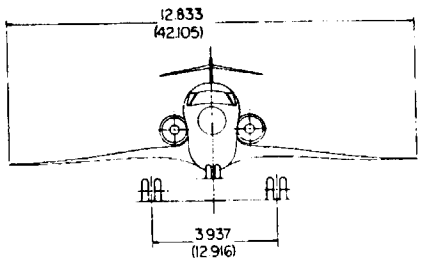

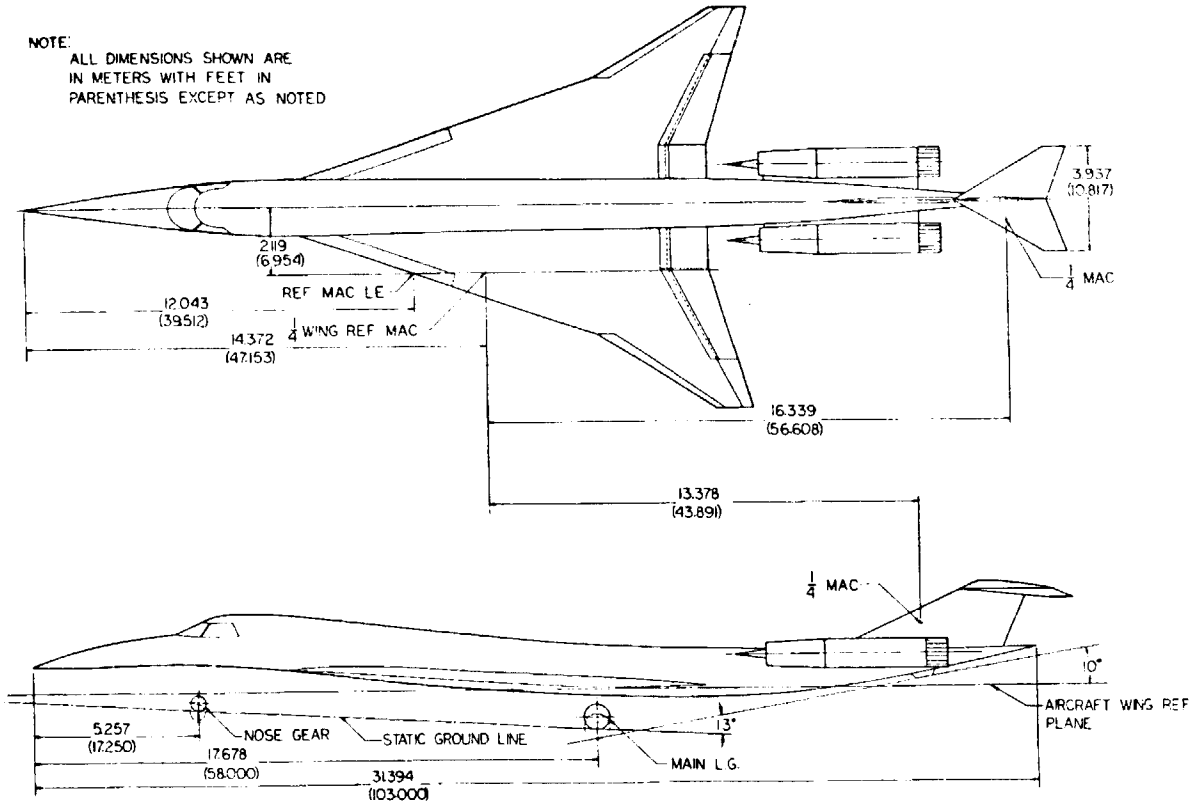

Figure 5. - SSXJET General arrangement.

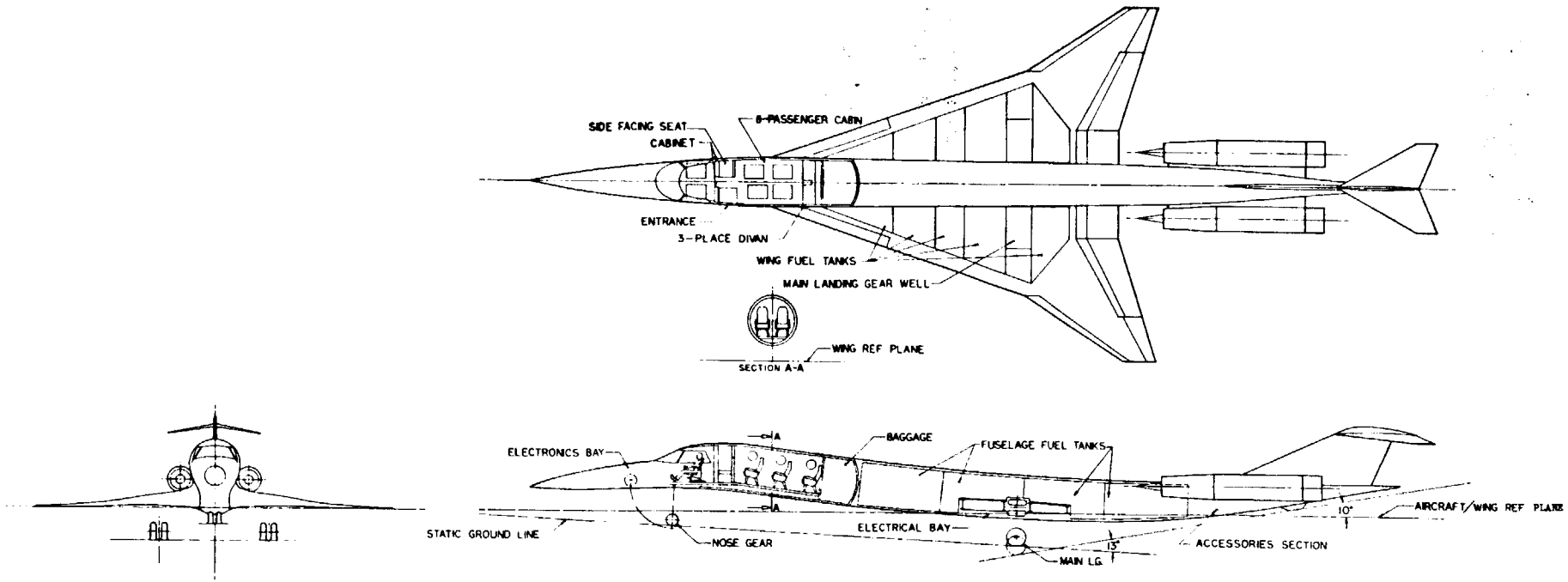

Figure 6. - SSXJET Inboard profile.

GEOMETRY	WING	HORIZ	VERT
AREA (GROSS) S (m²)	89.65 (965)	60.38 (65)	67.67 (73)
MAC (GROSS) c (m)	9.315 (30.565)	2.05 (6.730)	5.961 (12.997)
SPAN b (m)	12.833 (42.105)	3.749 (10.817)	5.646 (18.524)
ASPECT RATIO (GROSS)	1.84	1.80	.50
SWEEP Λ_{LE} (DEG)	71 57	60	65
ROOT CHORD (m)	15.254 (50.048)	2.950 (9.681)	5.332 (17.496)
TIP CHORD (m)	1.65 (5.823)	.737 (2.494)	2.32 (6.994)
ROOT T/C %	—	3.03	3.00
TIP T/C %	—	3.03	3.00
TAPER RATIO λ	—	.25	.40
DIHEDRAL (DEG)	—	10	—

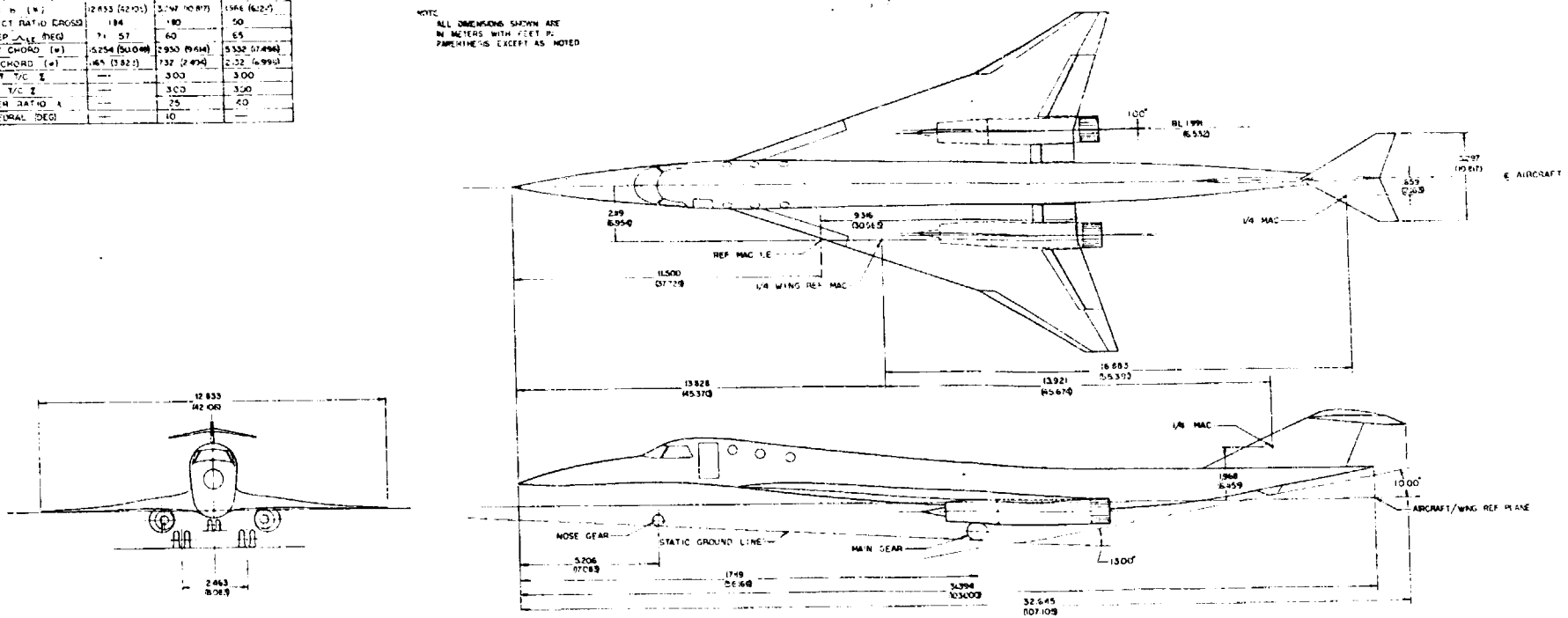

Figure 7. - SSXJET I General arrangement.

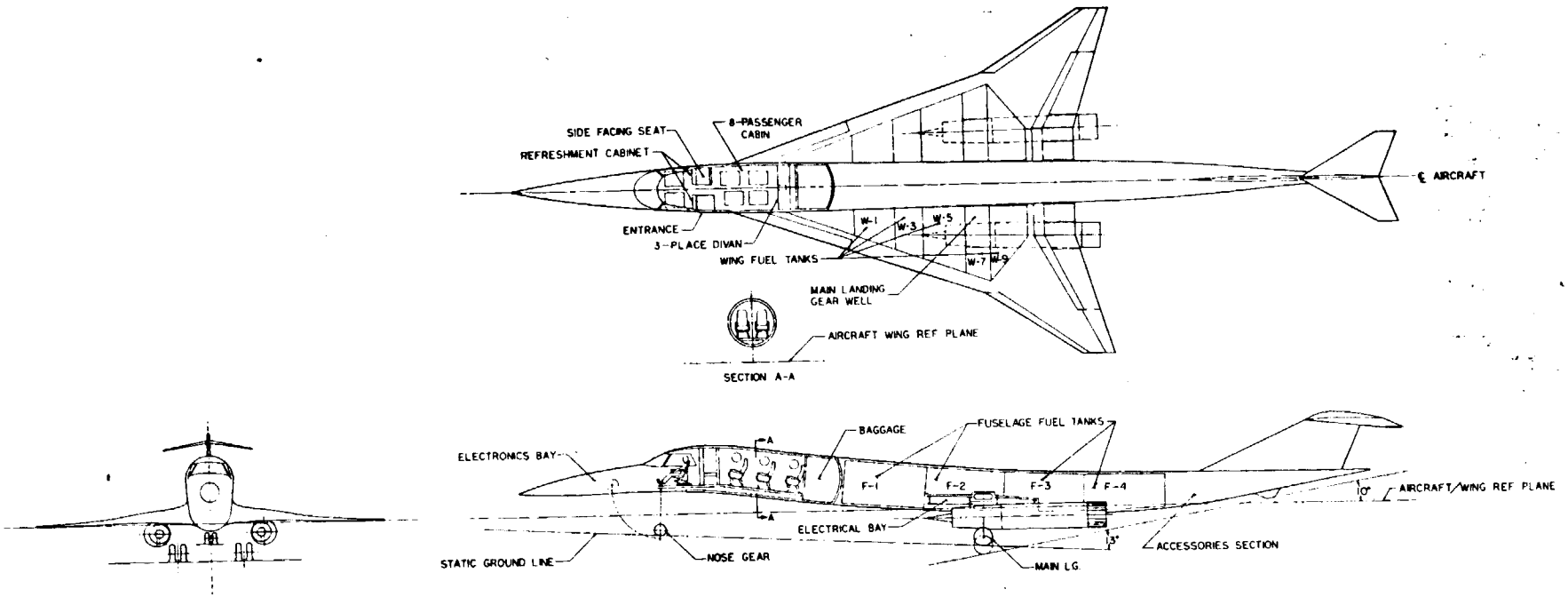

Figure 8. - SSXJET I Inboard profile.

GEOMETRY	WING	HORIZONTAL	VERTICAL
AREA (GROSS) S (m²)	89.654 (965)	6.038 (65)	6.967 (75)
MAC (GROSS) c̄ (m)	9.346 (30.565)	2.054 (6.730)	3.961 (12.997)
SPAN b (m)	12.833 (42.105)	3.297 (10.817)	1.866 (6.124)
ASPECT RATIO	1.84	1.80	5.0
SWEEP $\Lambda_{c/4}$ (DEG)	71 57	60	65
ROOT CHORD (m)	15.254 (50.048)	2.930 (9.614)	5.332 (17.496)
TIP CHORD (m)	1.165 (3.822)	.732 (2.404)	2.132 (6.998)
ROOT T/C %		3.0	5.0
TIP T/C %		3.0	3.0
TAPER RATIO		.25	.40
DIHEDRAL (DEG) λ		10	

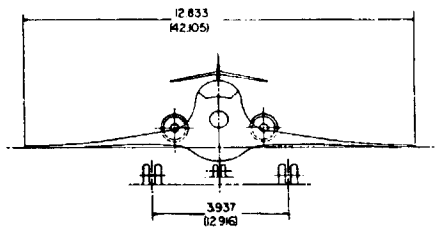

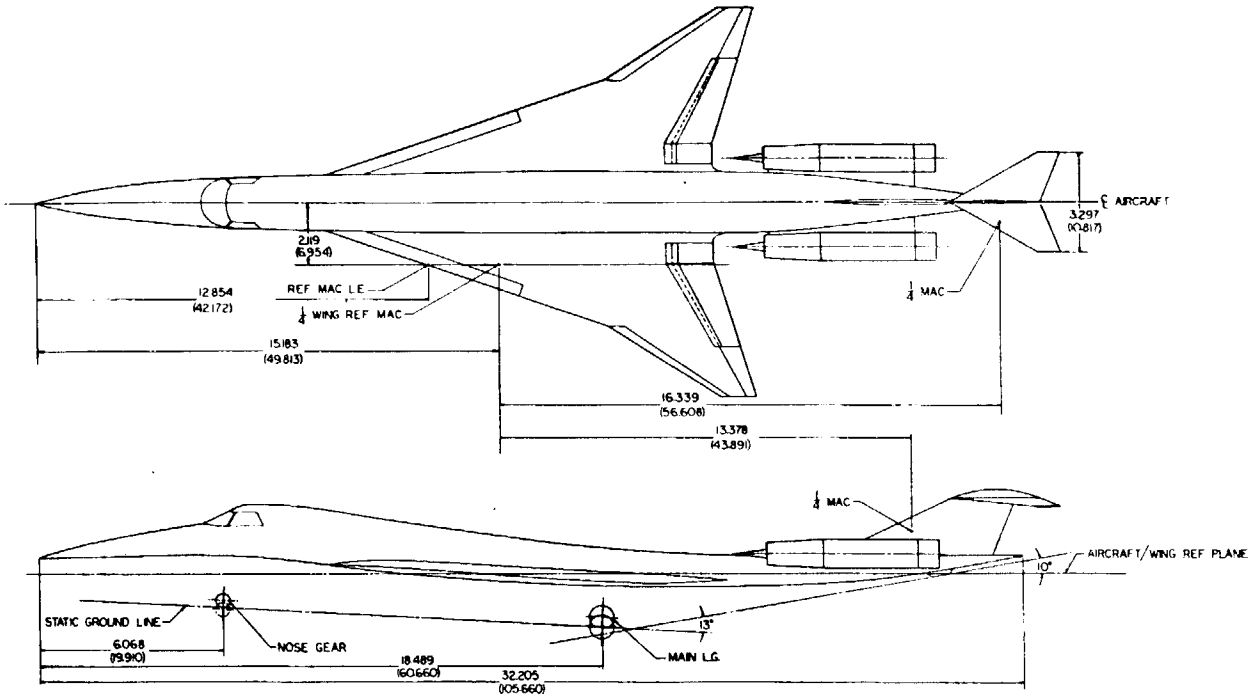

Figure 9. - SSXJET II General arrangement.

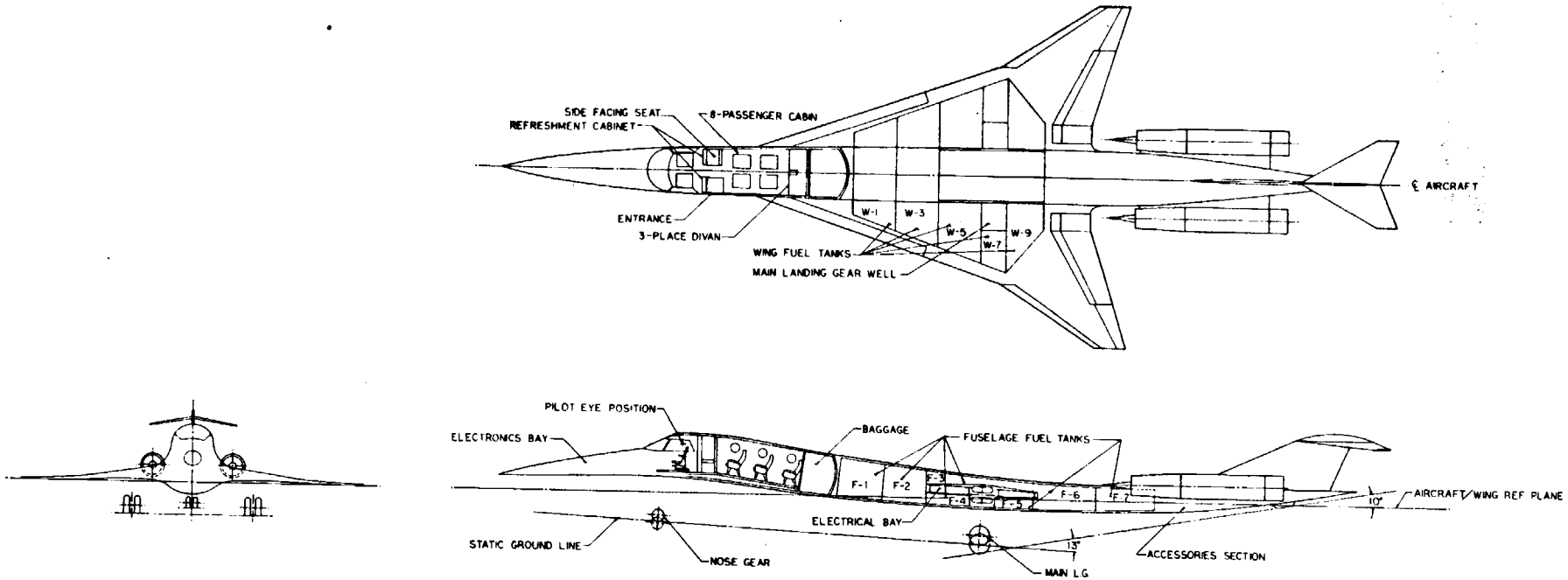

Figure 10. - SSXJET II Inboard profile

GEOMETRY	WING	HORIZONTAL	VERTICAL
AREA (GROSS) S (m²)	8965 (965)	6038 (65)	6967 (75)
MAC (GROSS) $\bar{c}$ (m)	9316 (305.65)	2051 (67.30)	3961 (12.937)
SPAN b (m)	12833 (42.105)	3297 (10.817)	1866 (6.124)
ASPECT RATIO	84	18	50
SWEEP Λ_{LE} (DEG)	71.52	60	65
ROOT CHORD (m)	15.254 (50.034)	2.930 (9.614)	5.332 (17.496)
TIP CHORD (m)	1.655 (5.822)	732 (2.404)	2.132 (6.998)
ROOT T/C %		3.000	3.000
TIP T/C %		3.000	3.000
TAPER RATIO λ		250	.30
DIHEDRAL (DEG)		10	

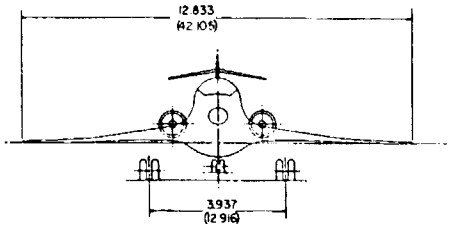

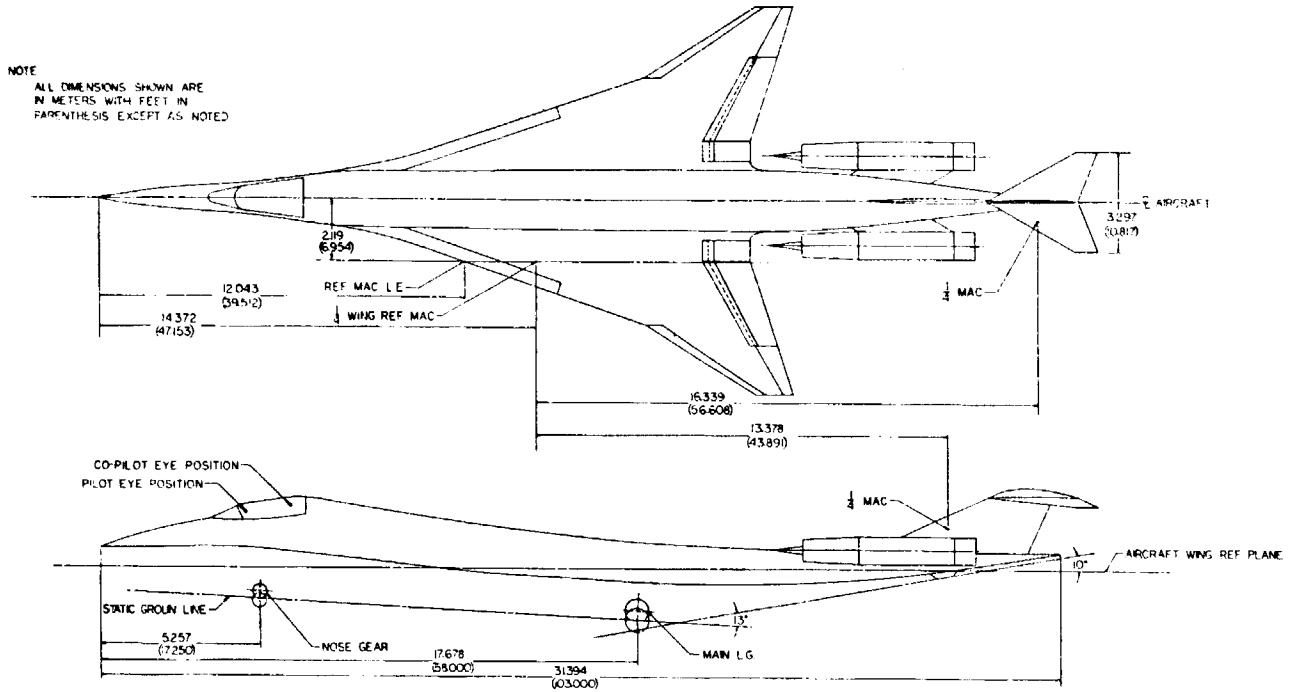

Figure 11. - SSXJET II T General arrangement.

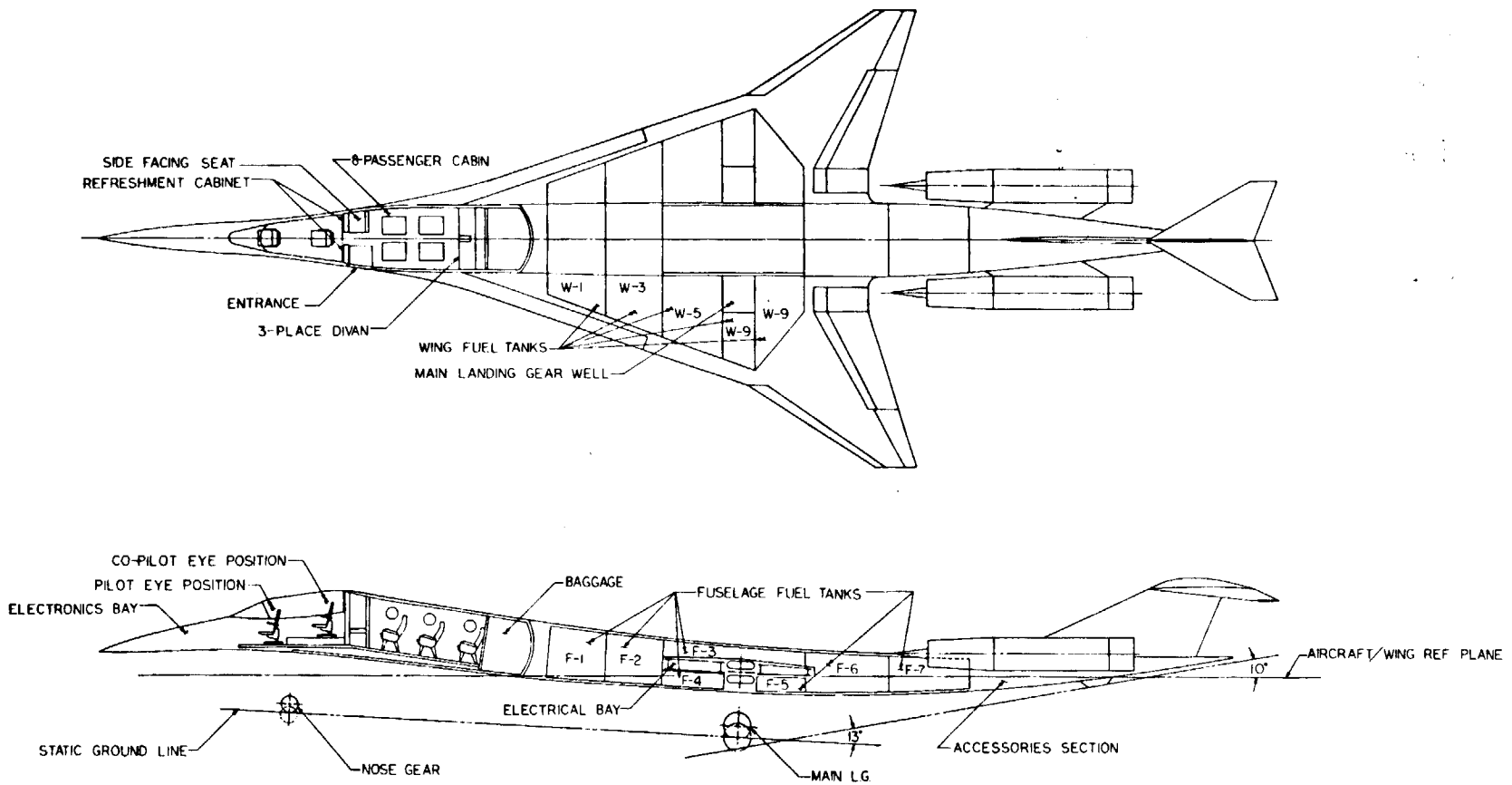

Figure 12. - SSXJET II T Inboard profile.

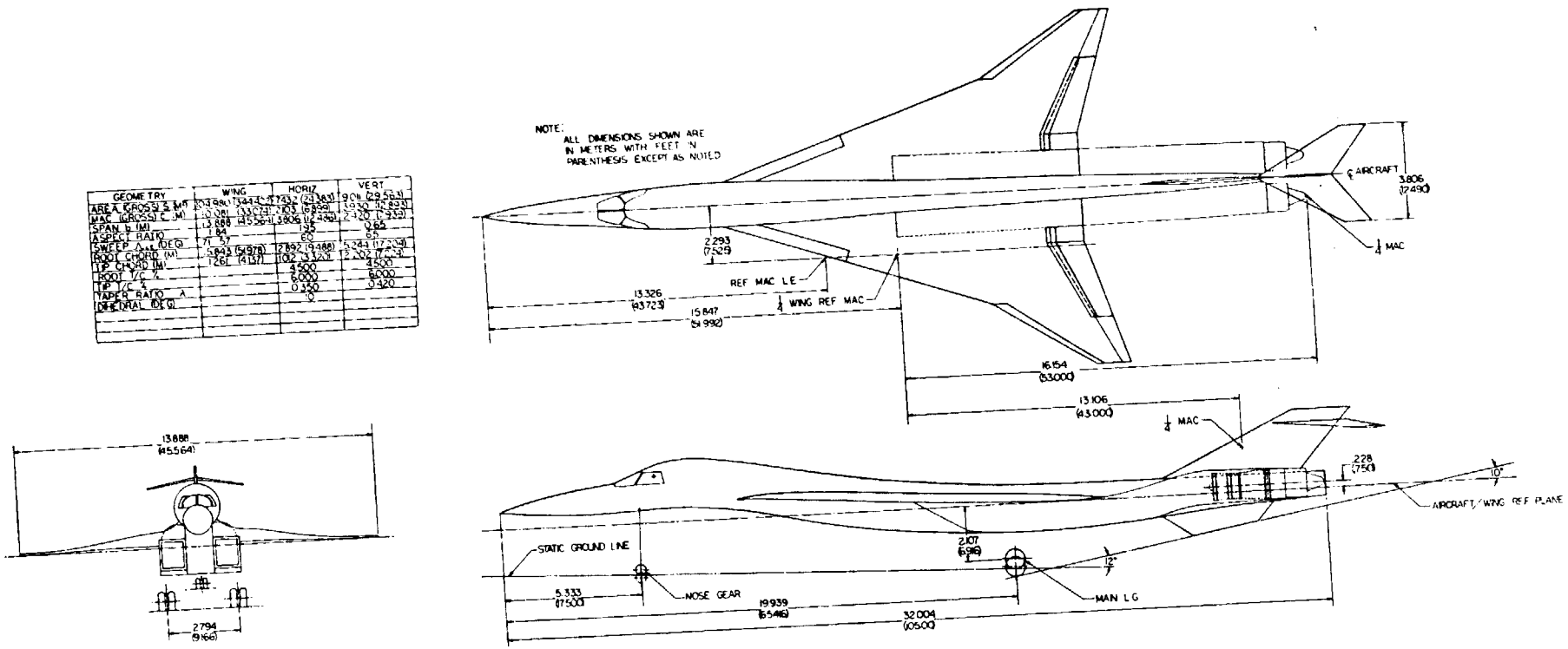

Figure 13. - SSXJET III General arrangement.

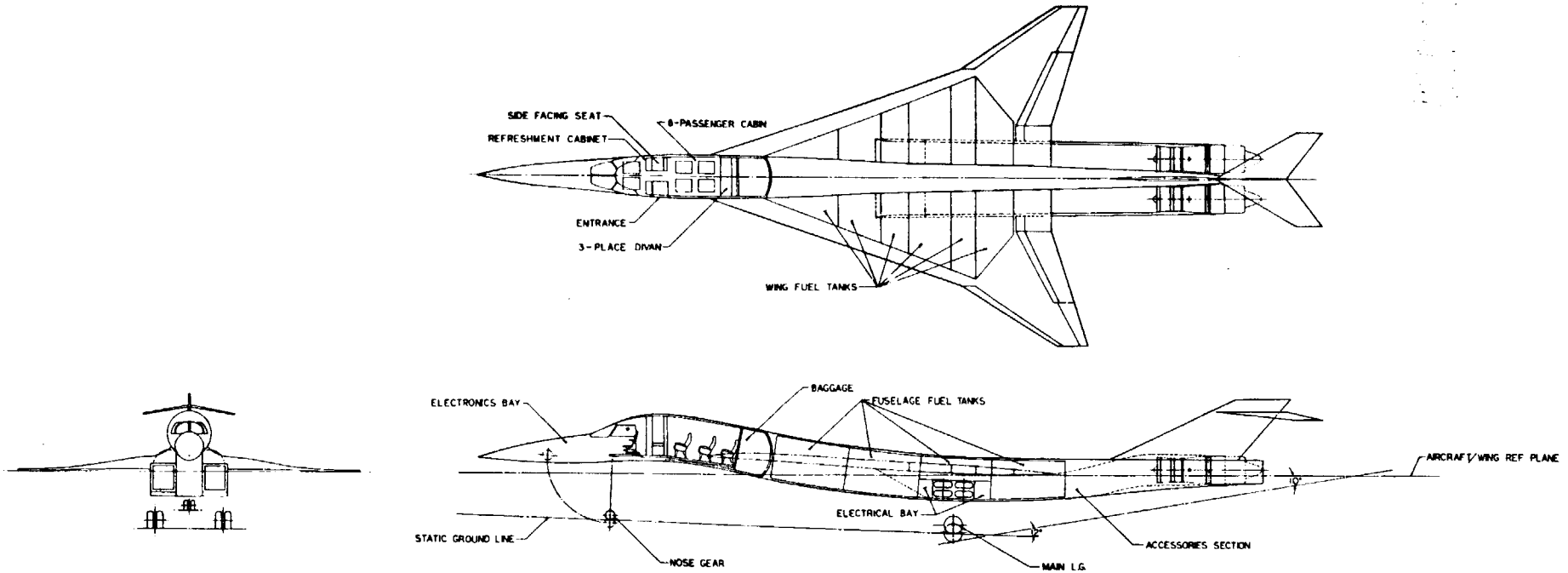

Figure 14. - SSXJET III Inboard profile.

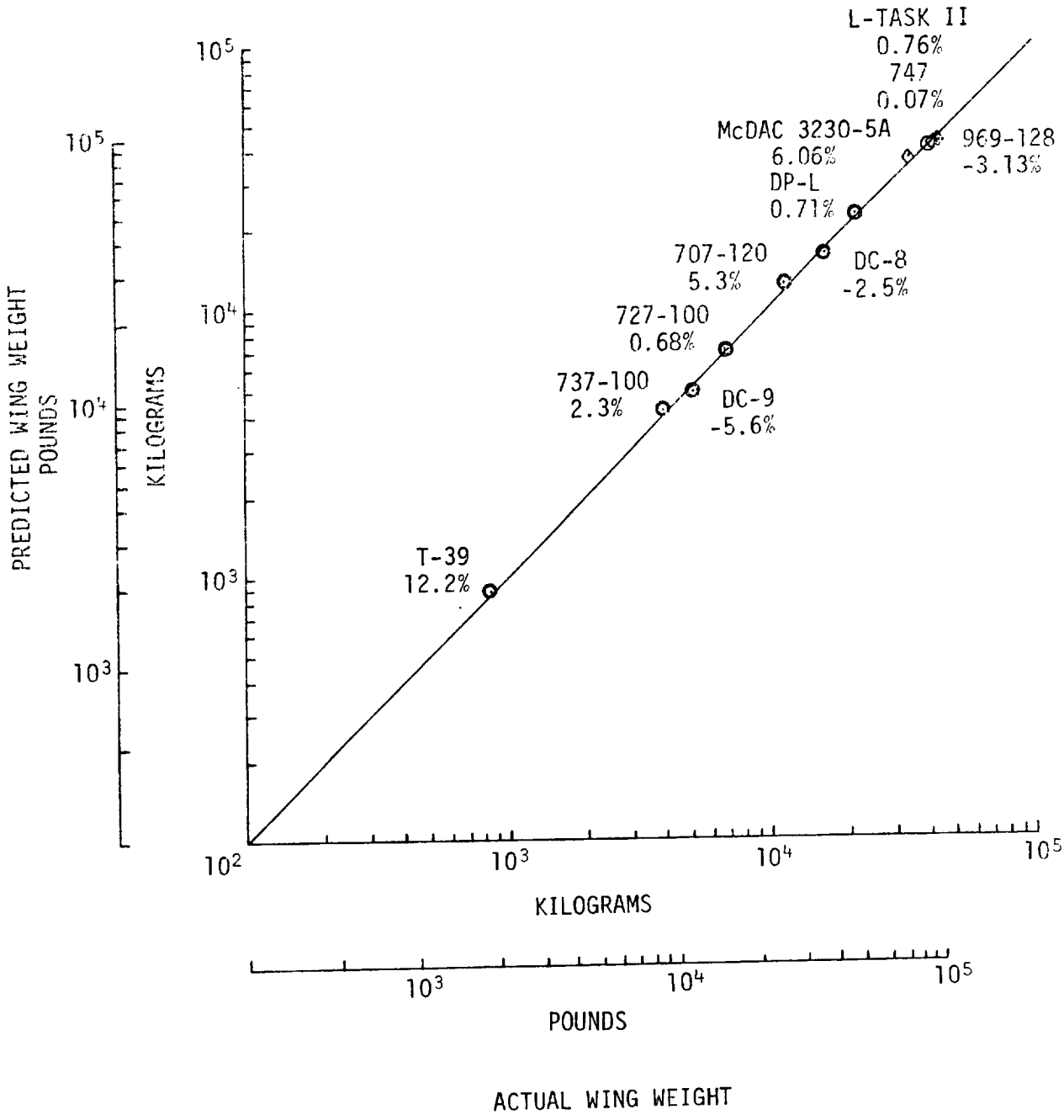

Figure 15. - Wing weight estimation method correlation

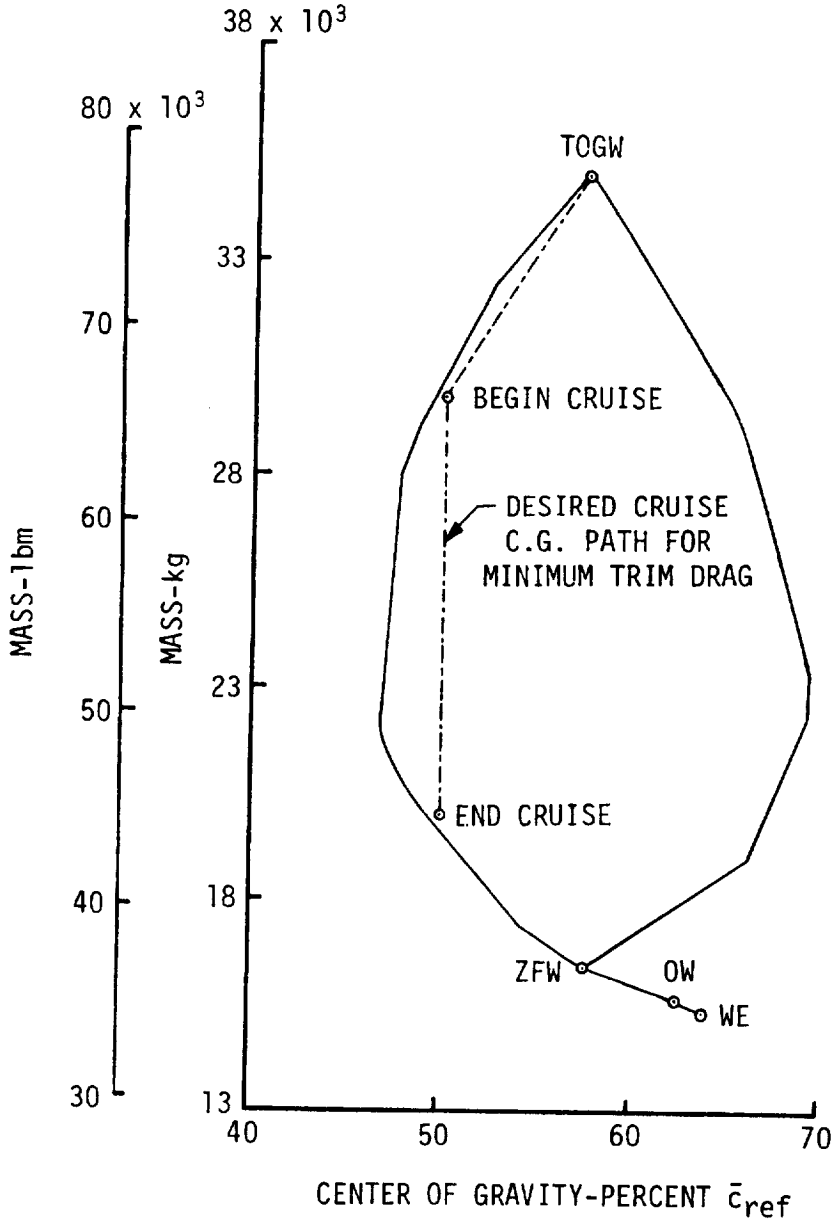

Figure 16. - SSXJET Center-of-gravity envelope.

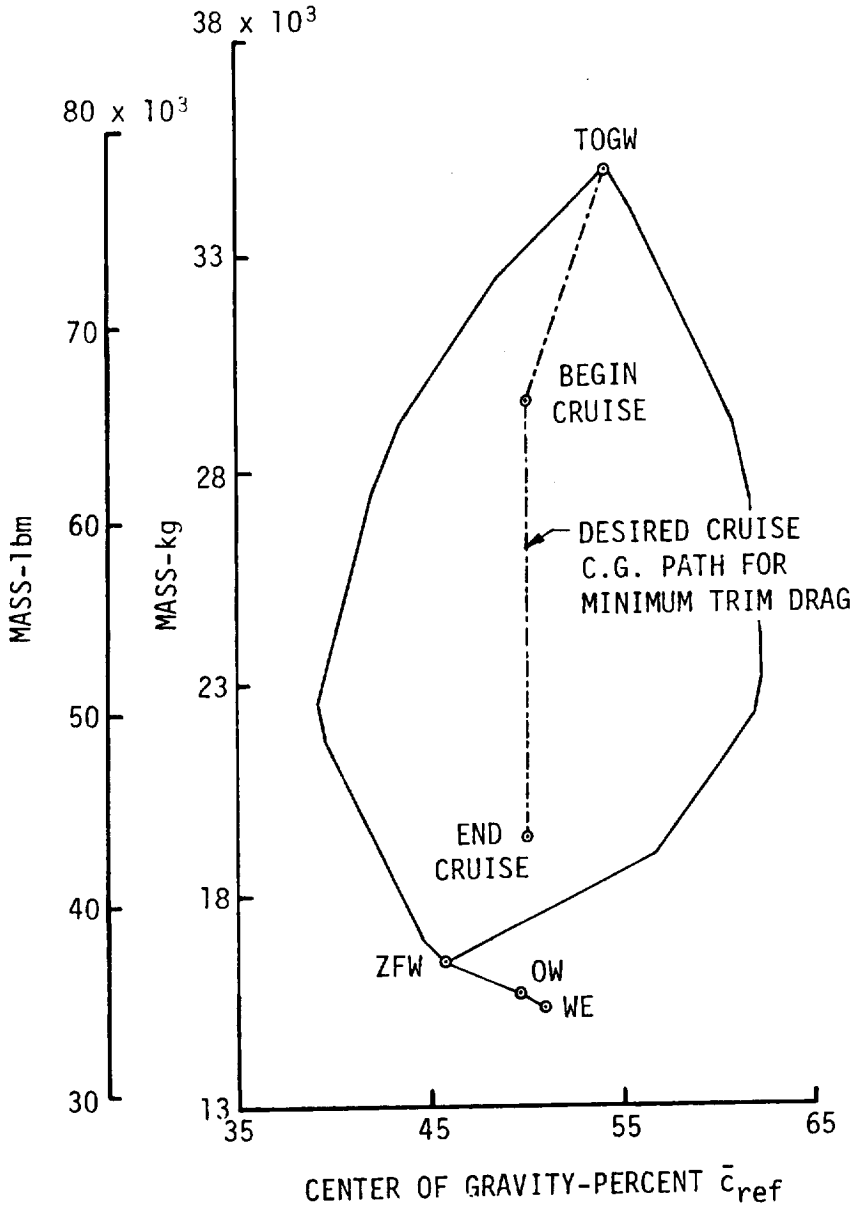

Figure 17. - SSXJET I Center-of-gravity envelope.

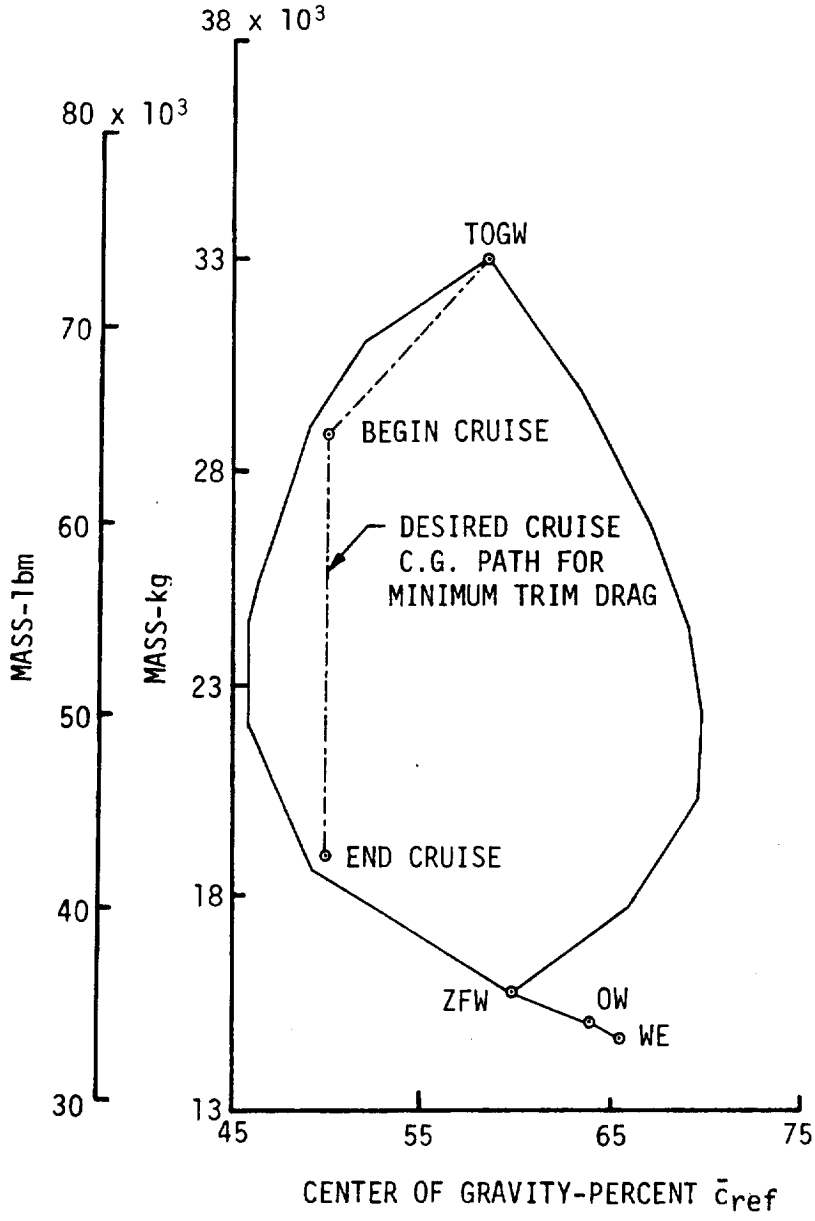

Figure 18. - SSXJET II Center-of-gravity envelope.

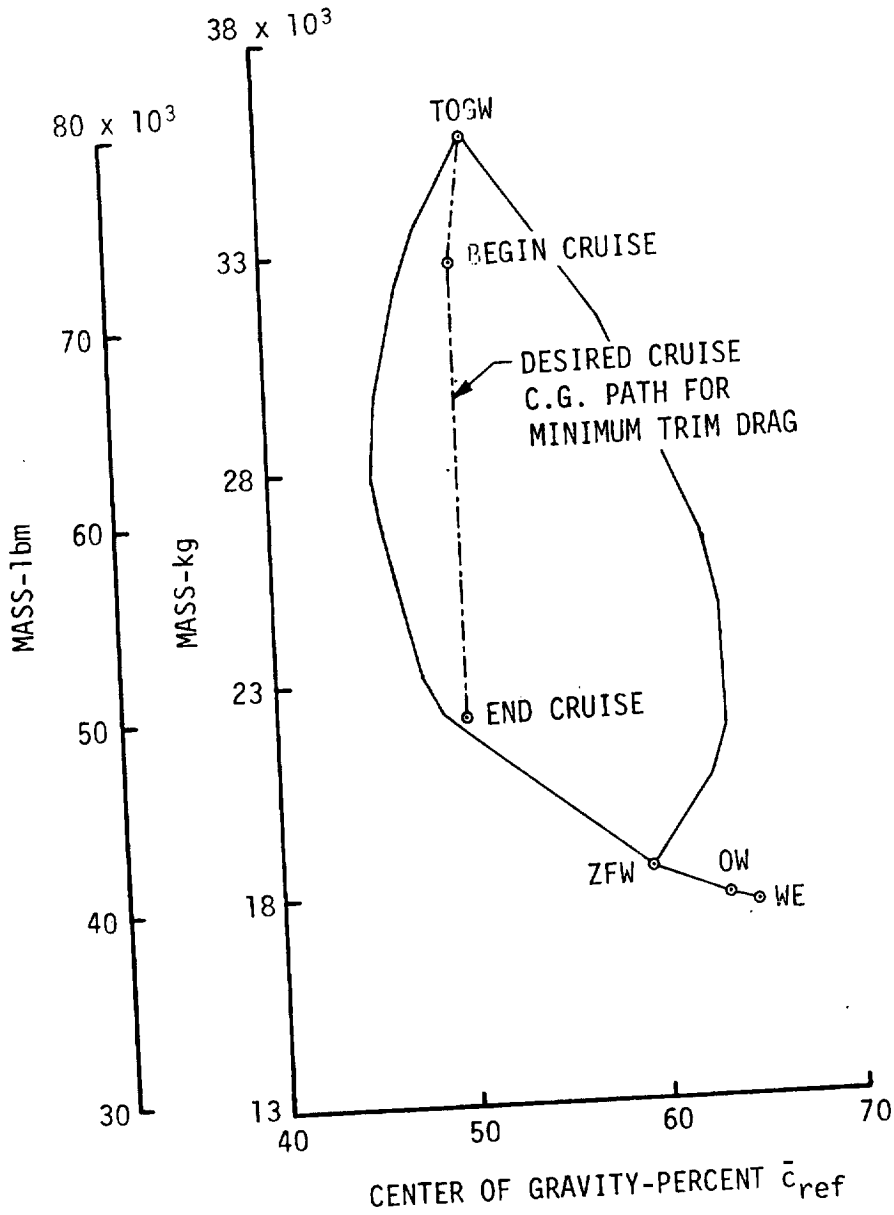

Figure 19. - SSXJET III Center-of-gravity envelope.

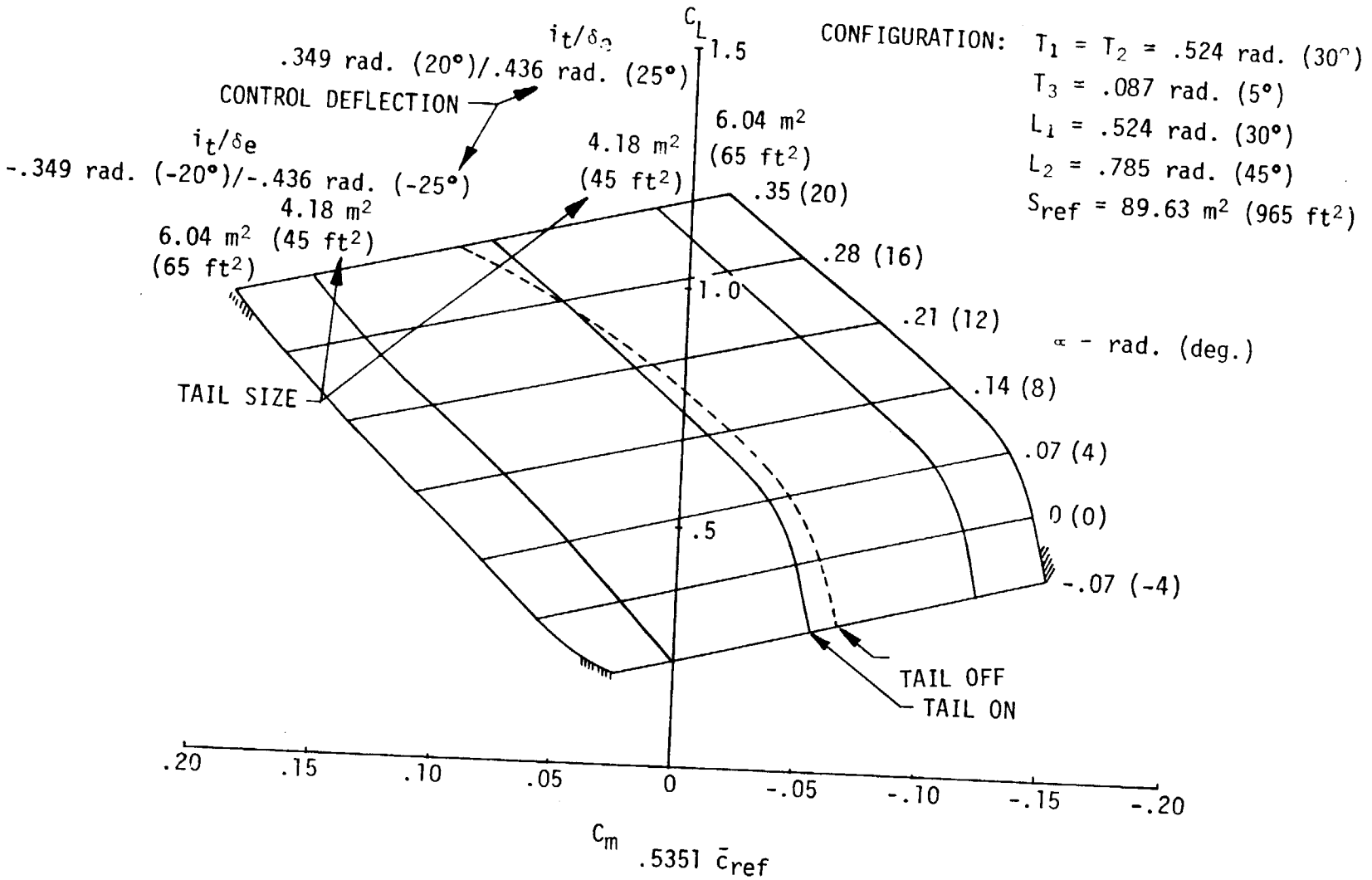

Figure 20. - Effect of horizontal tail size and maximum control deflection on stability and trim, and out of ground effect.

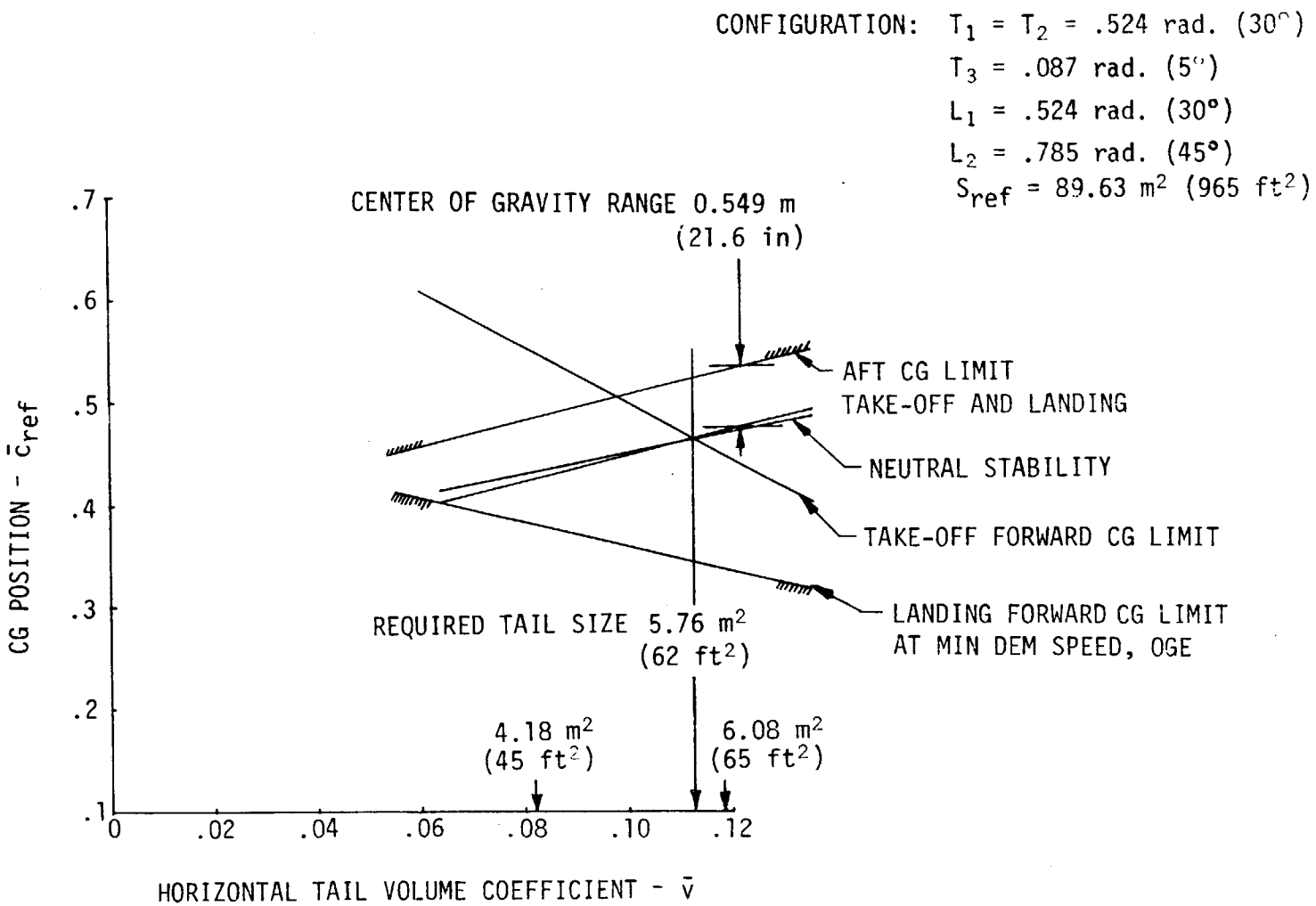

Figure 21. - Center of gravity limits for take-off, approach, and landing.

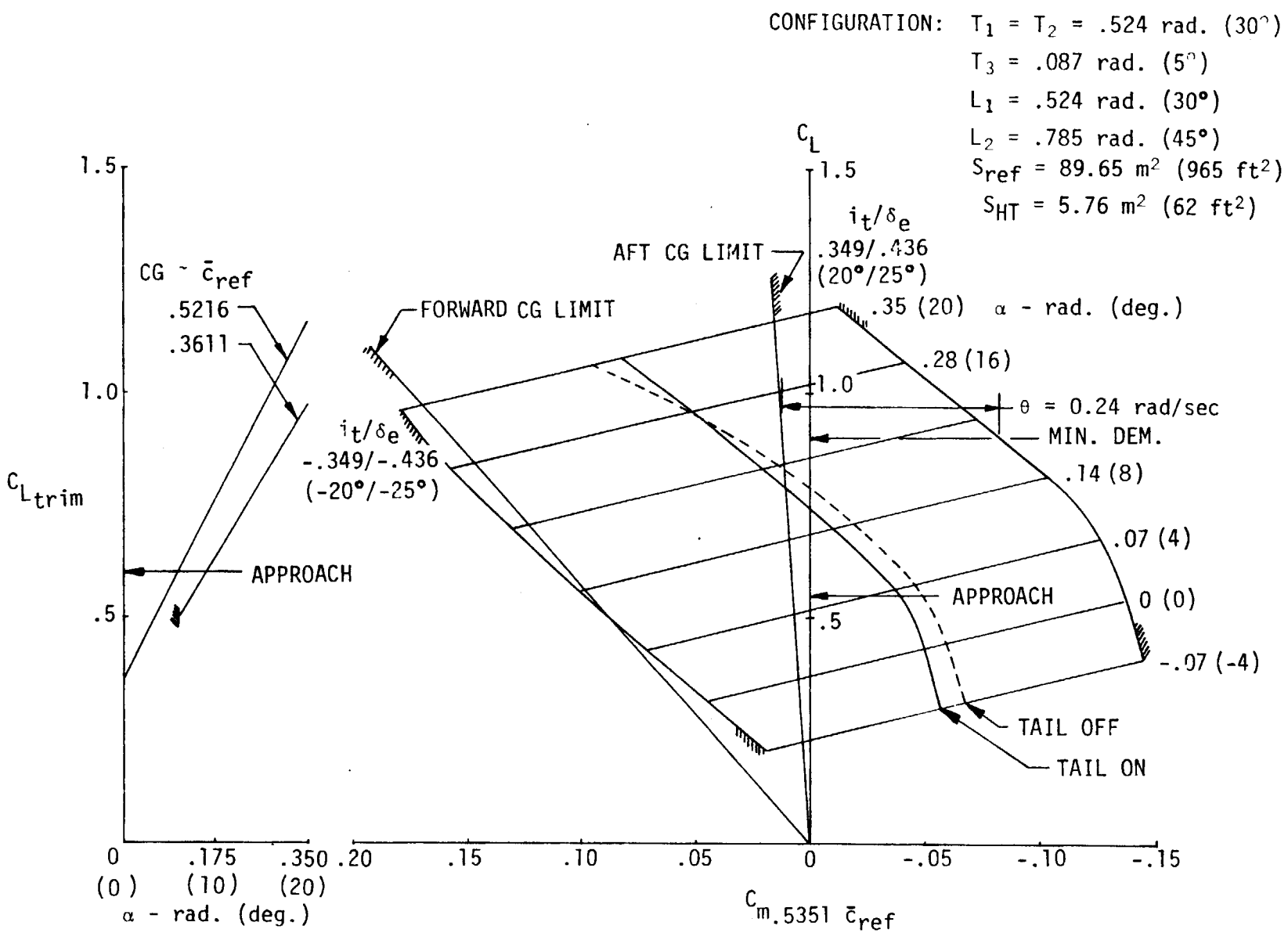

Figure 22. - Final approach trim and stability, out of ground effect

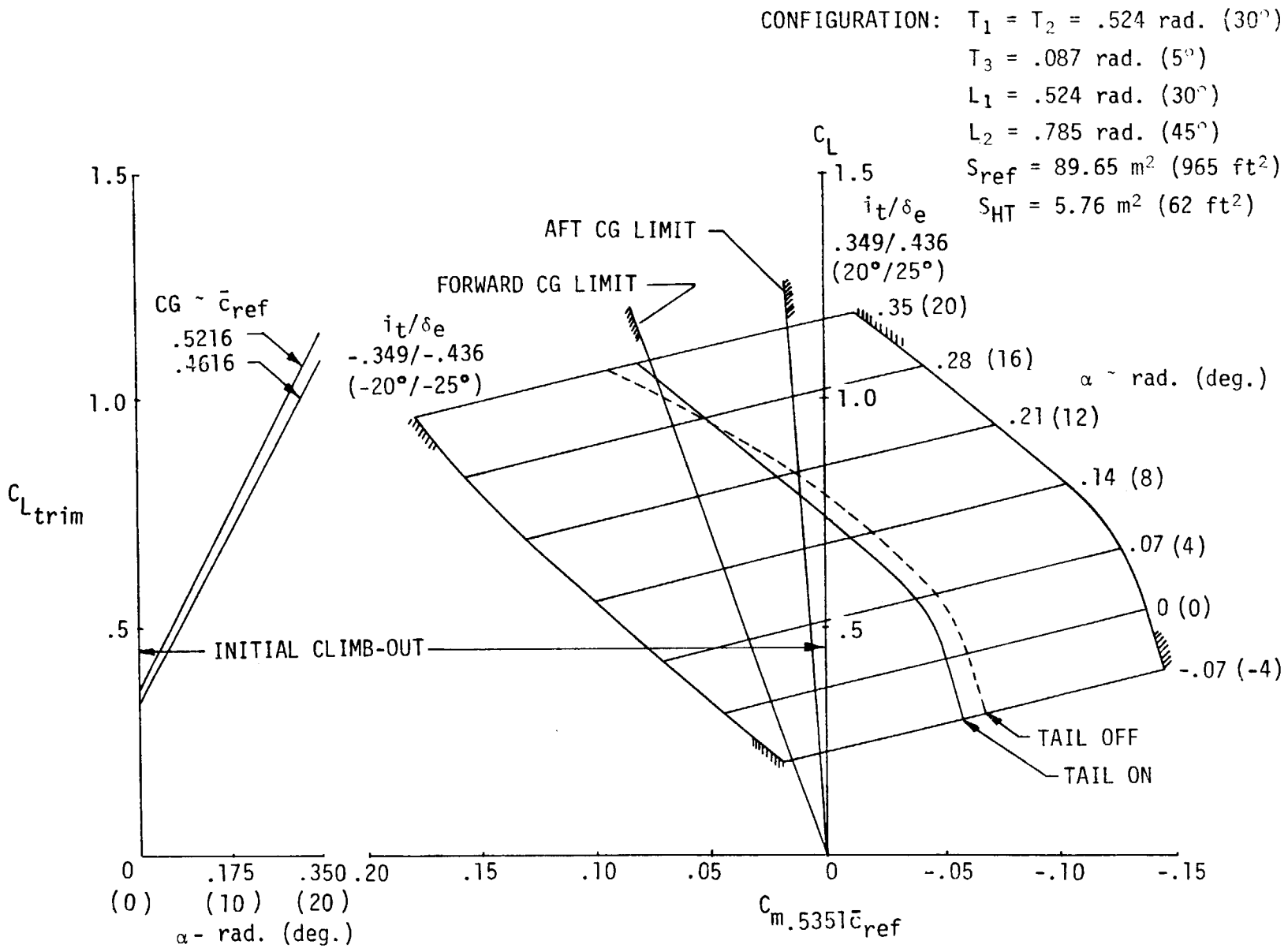

Figure 23. - Climb-out trim and stability, out of ground effect

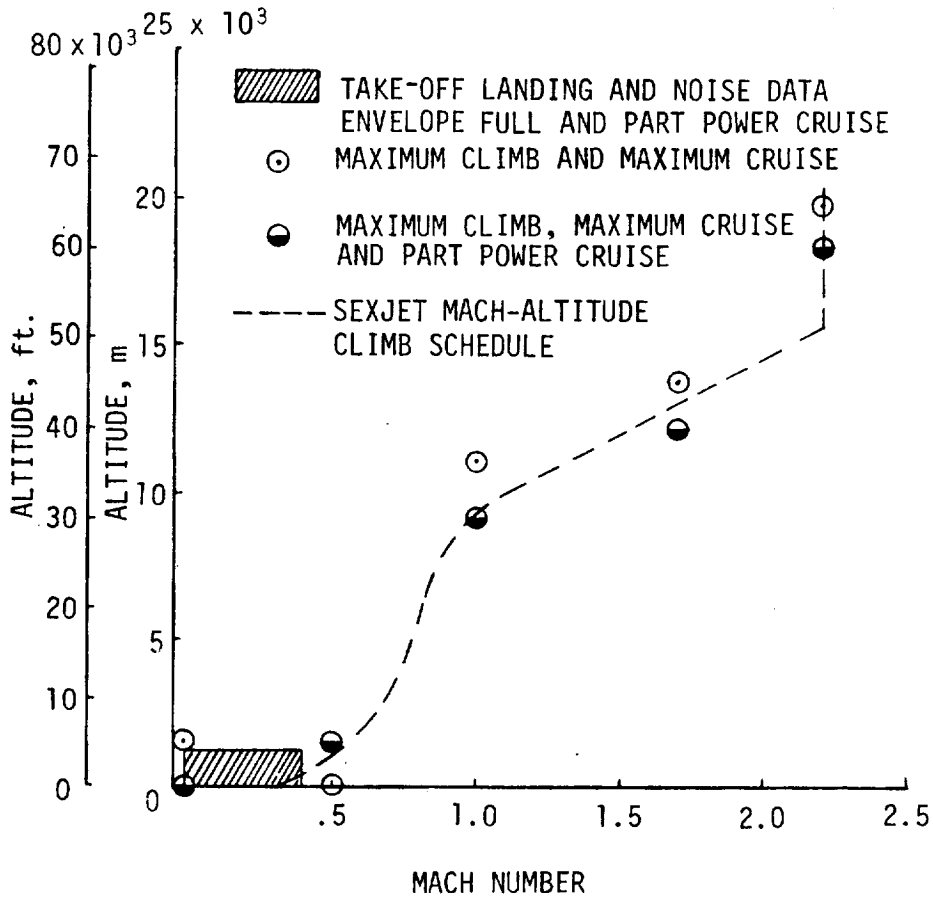

Figure 24. - Minimum required engine performance

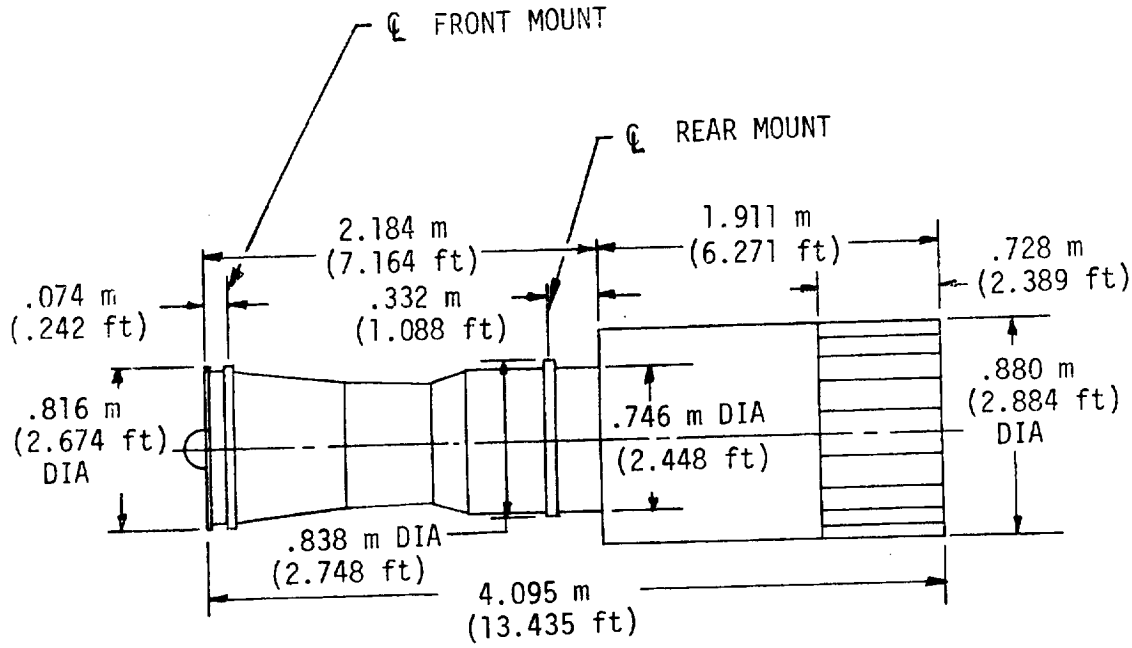

Figure 25. - Turbojet engine

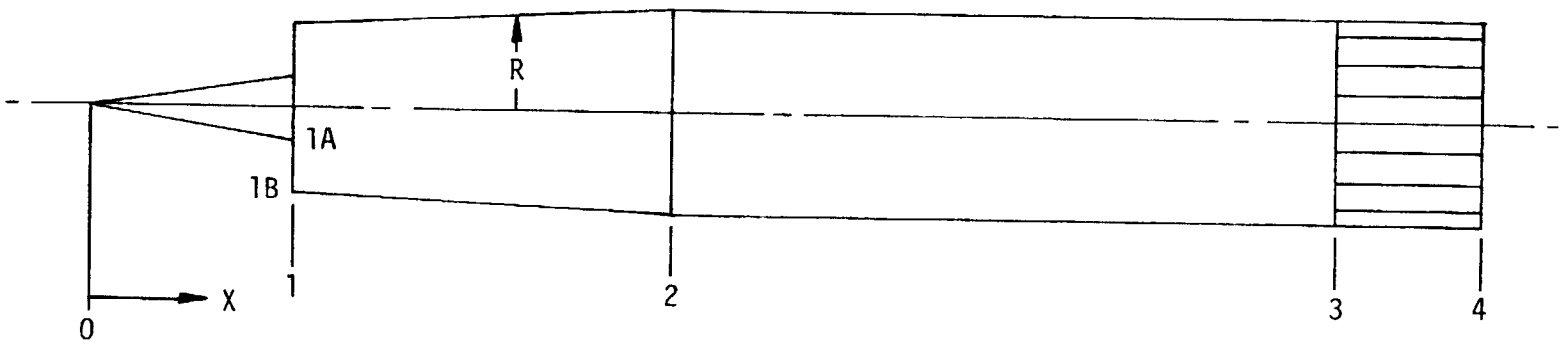

NACELLE DIMENSIONS

STATION NUMBER	X		R		AREA	
	m	ft.	m	ft.	m^2	ft^2
0	0	0	0	0	0	0
1A	1.047	3.434	.147	.482	.068	.730
1B	1.047	3.434	.395	1.294	.490	5.260
2	2.987	9.800	.440	1.442	.608	6.533
3	6.354	20.846	.440	1.442	.608	6.533
4	7.082	23.235	.440	1.442	.608	6.533

Figure 26. - Turbojet engine nacelle.

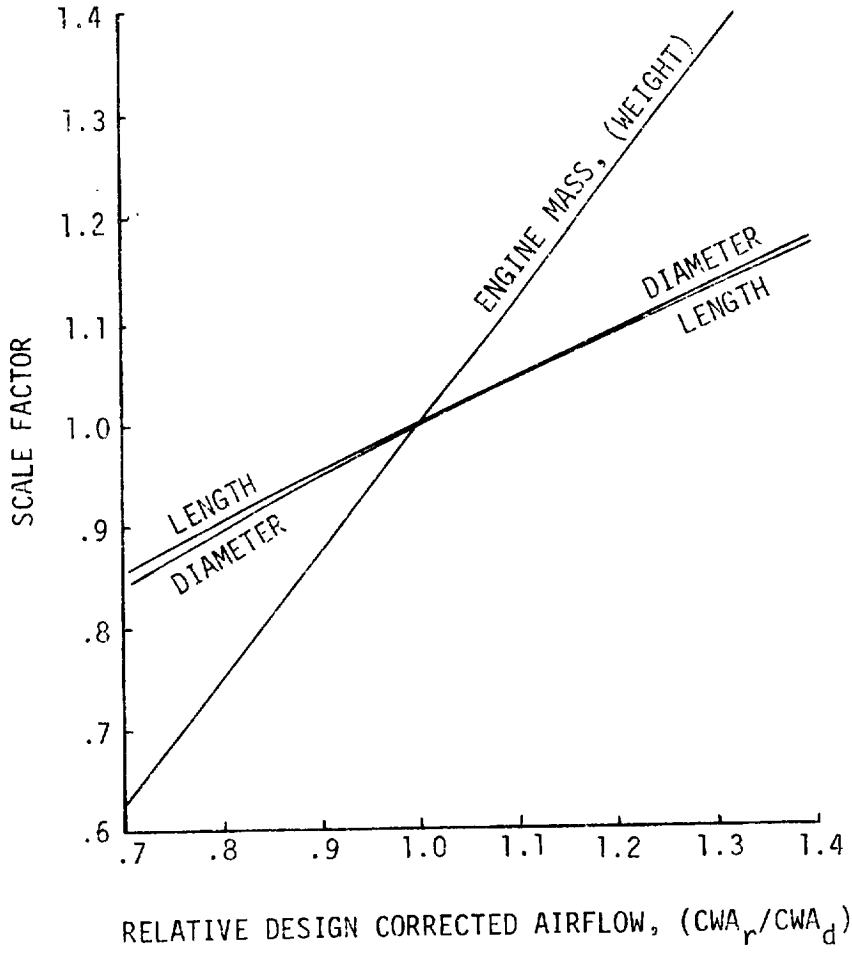

Figure 27. - NASA Turbojet engine and nacelle scaling factors.

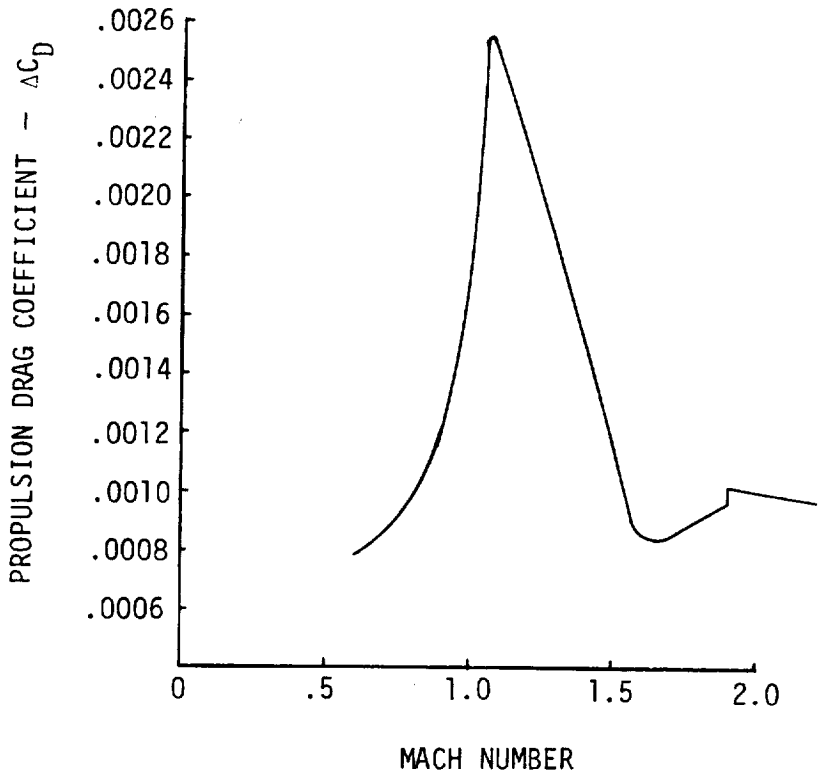

Figure 28. - NASA Turbojet total propulsion drag increment.

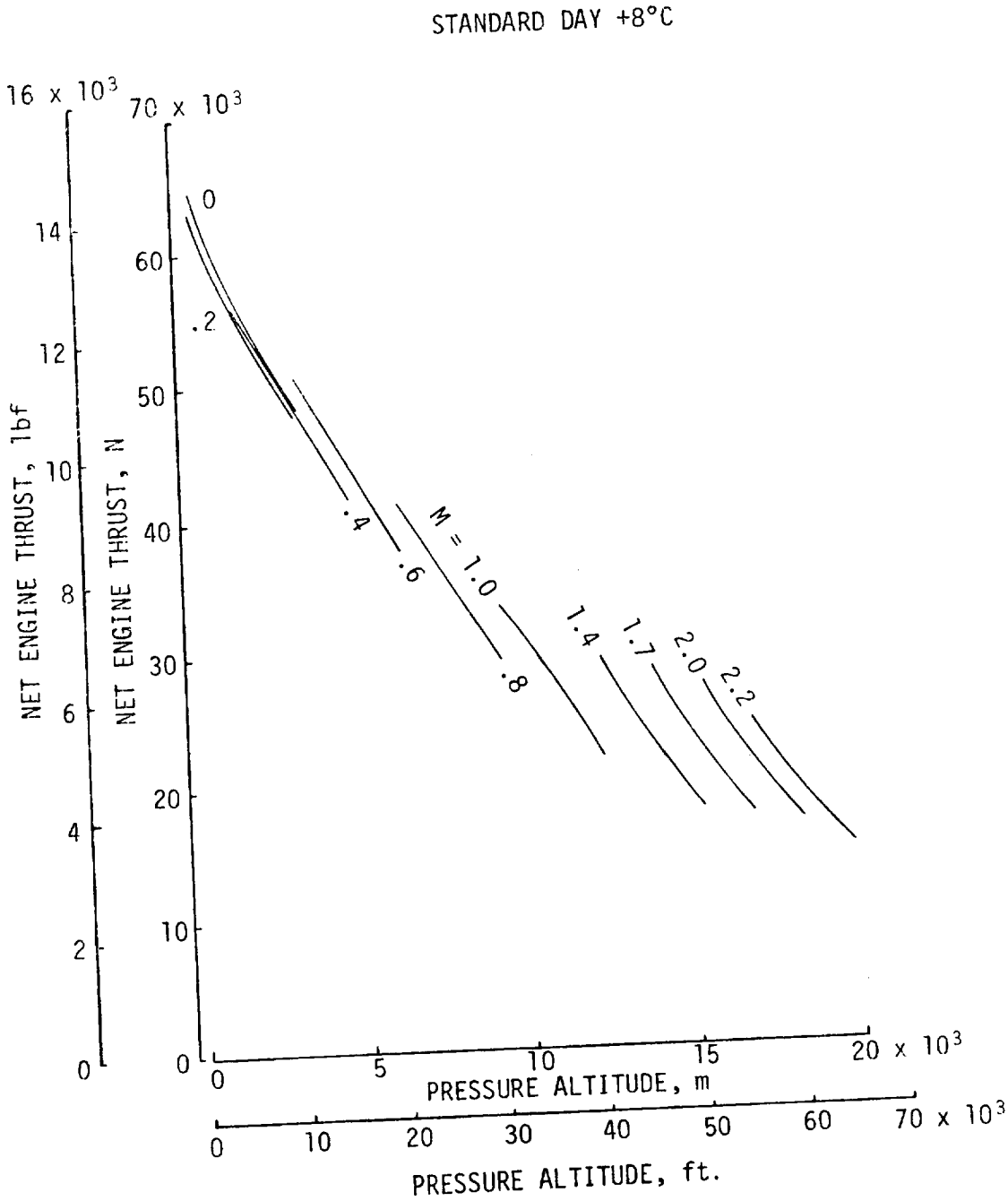

Figure 29. - Installed turbojet net engine thrust for maximum climb and cruise.

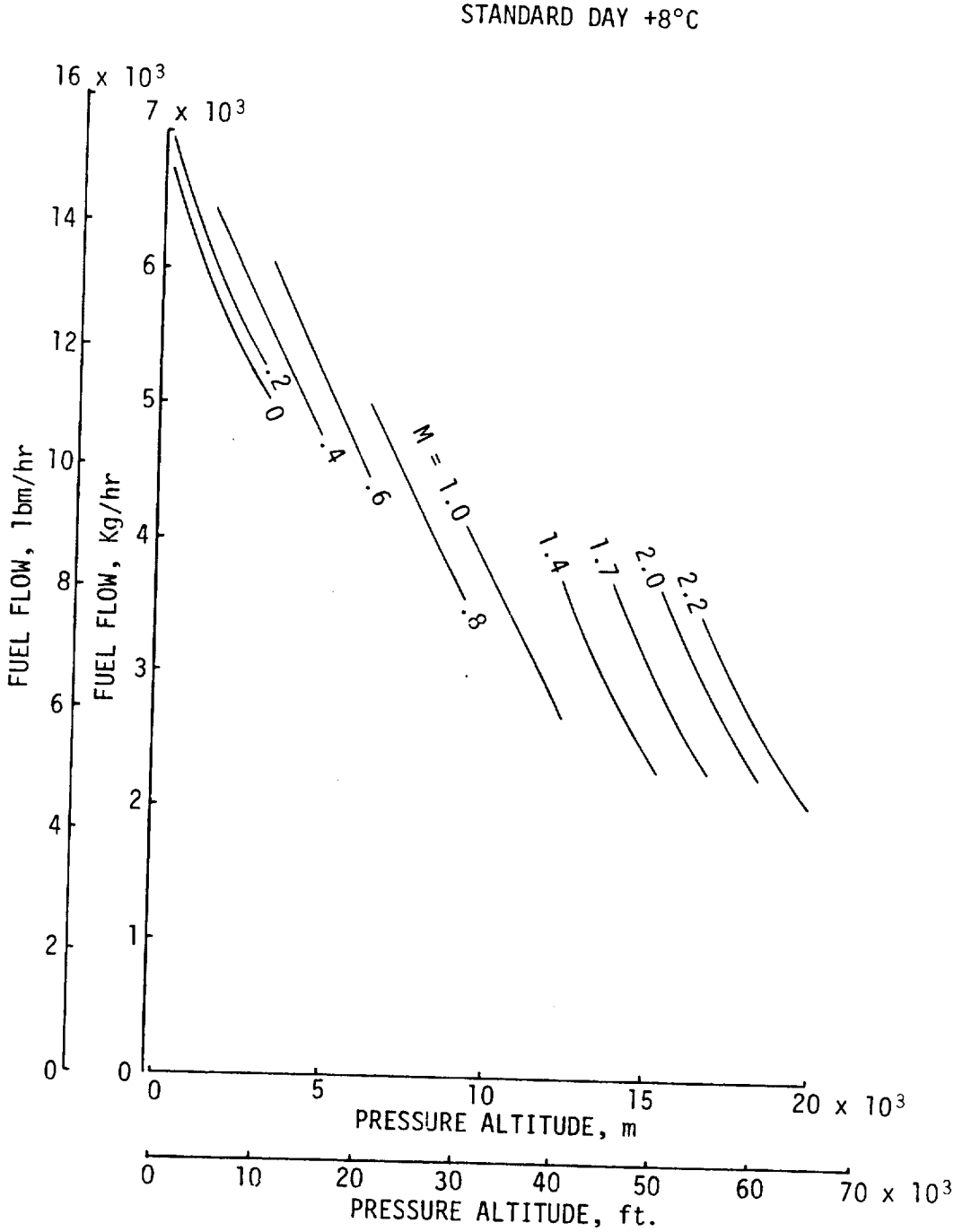

Figure 30. - Installed turbojet fuel flow for maximum climb and cruise.

STANDARD +8°C DAY

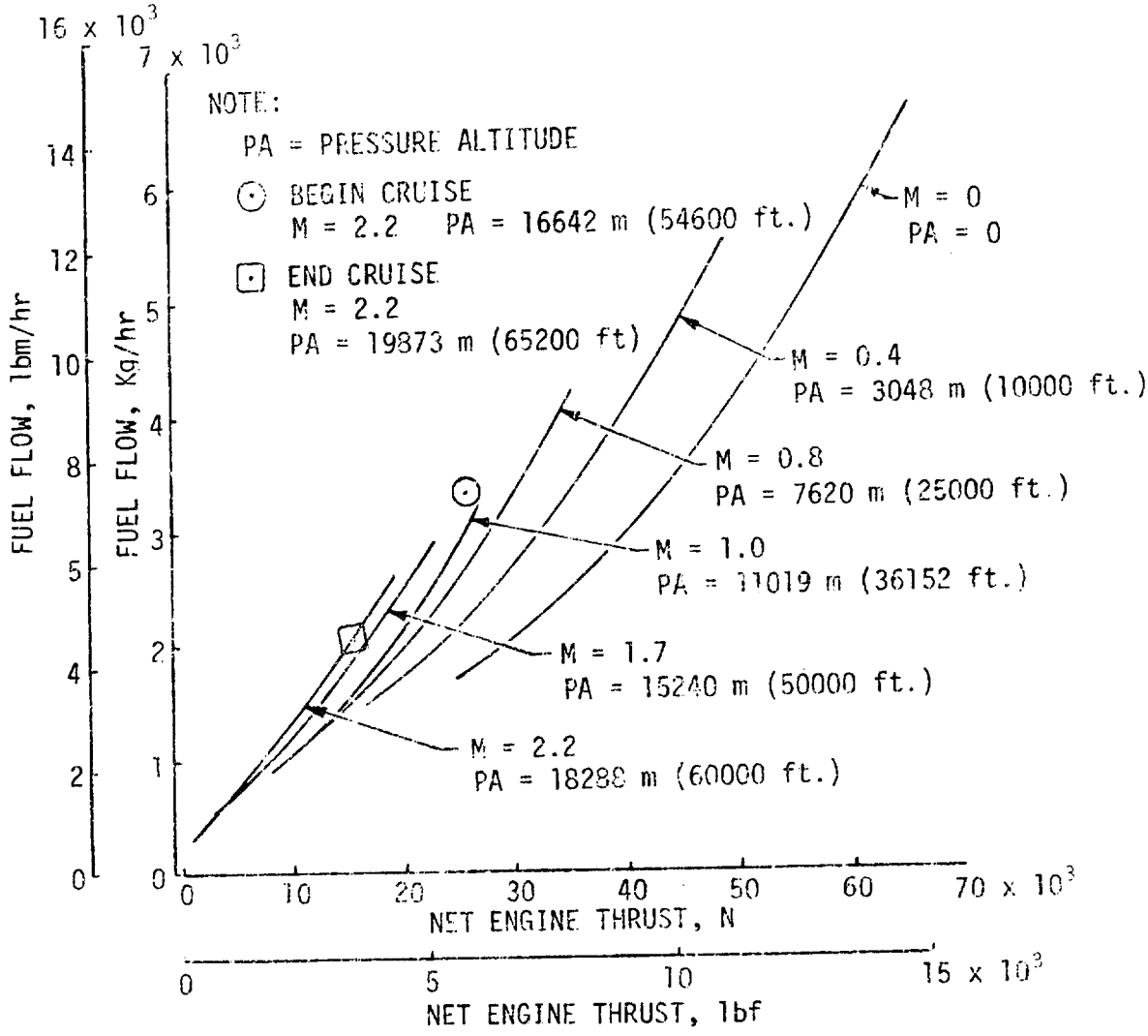

Figure 31. - Installed turbojet fuel flow for maximum and part power cruise.

STANDARD +10°C DAY

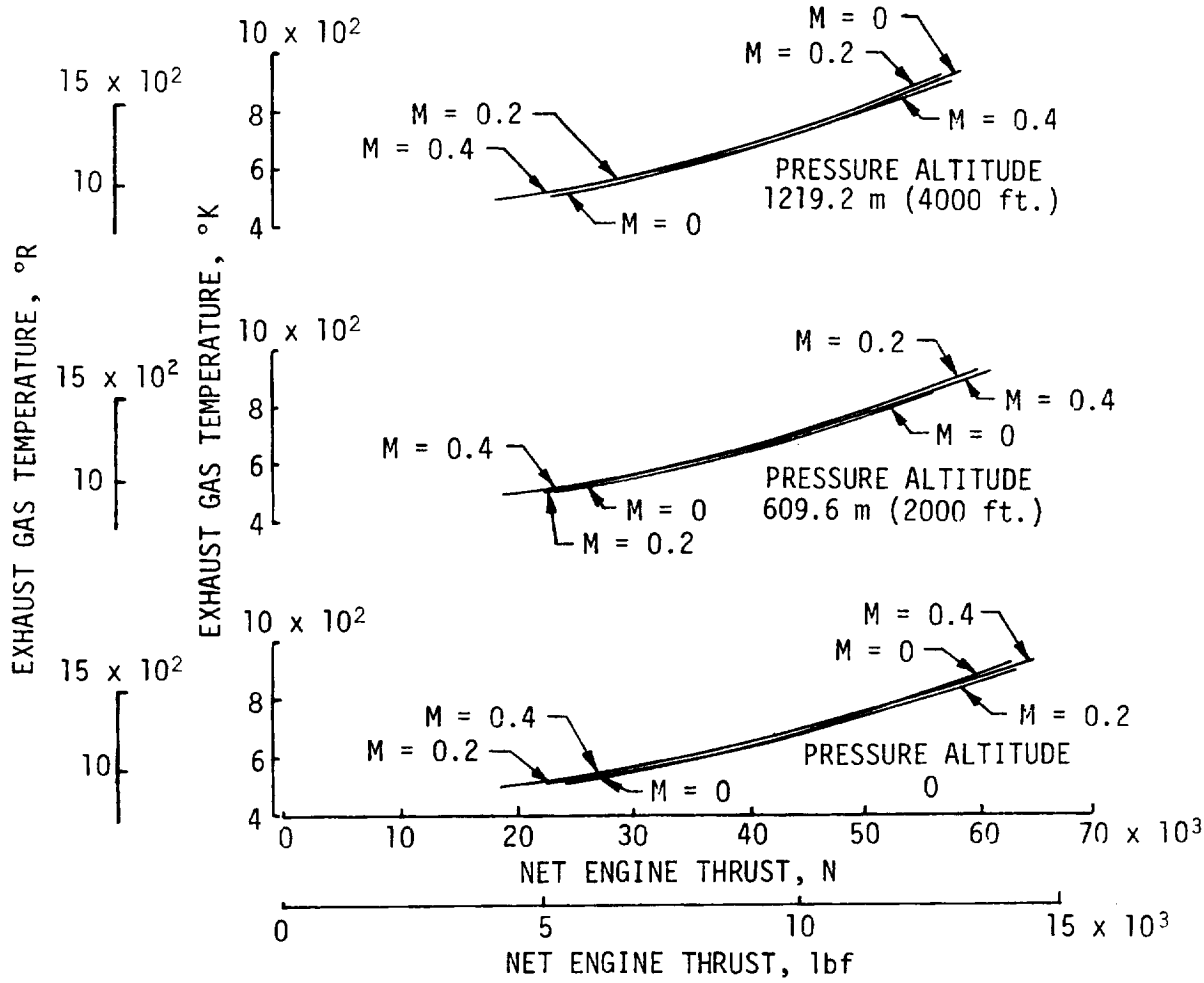

Figure 32. - Installed turbojet exhaust gas temperature for take-off and part power cruise.

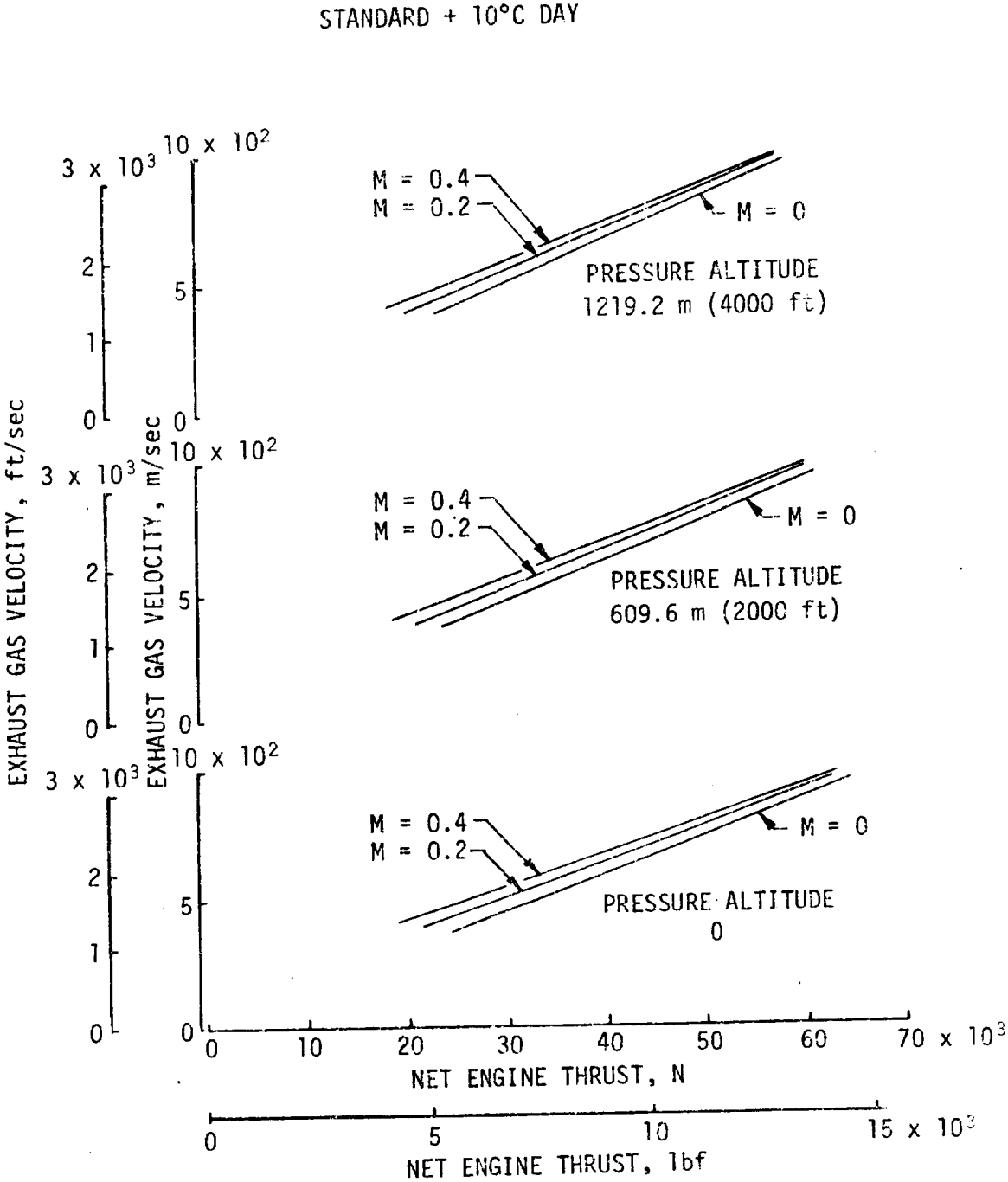

Figure 33. - Installed turbojet exhaust gas velocity for take-off and part power cruise.

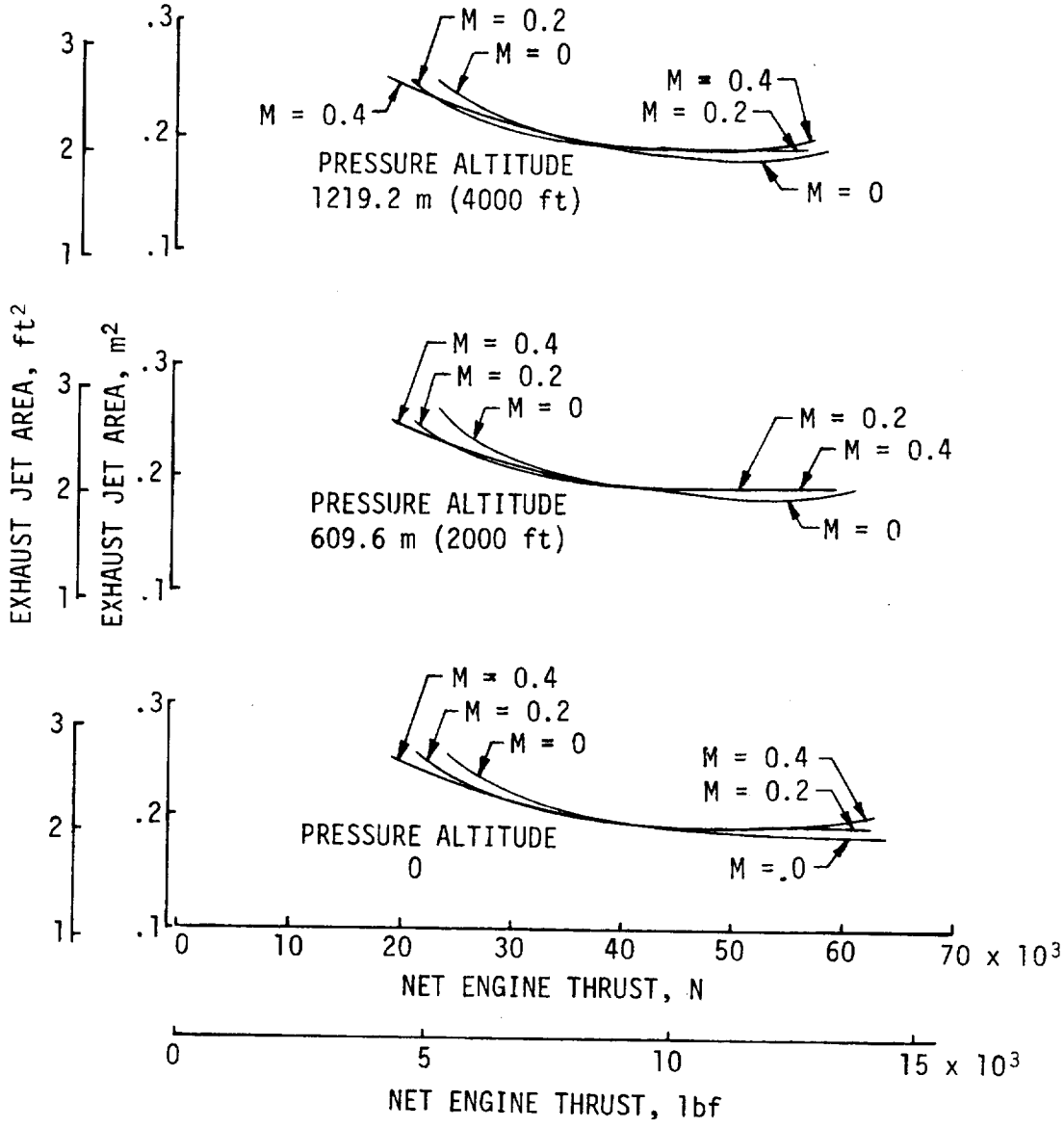

Figure 34. - Installed turbojet nozzle exit area for take-off and part power cruise.

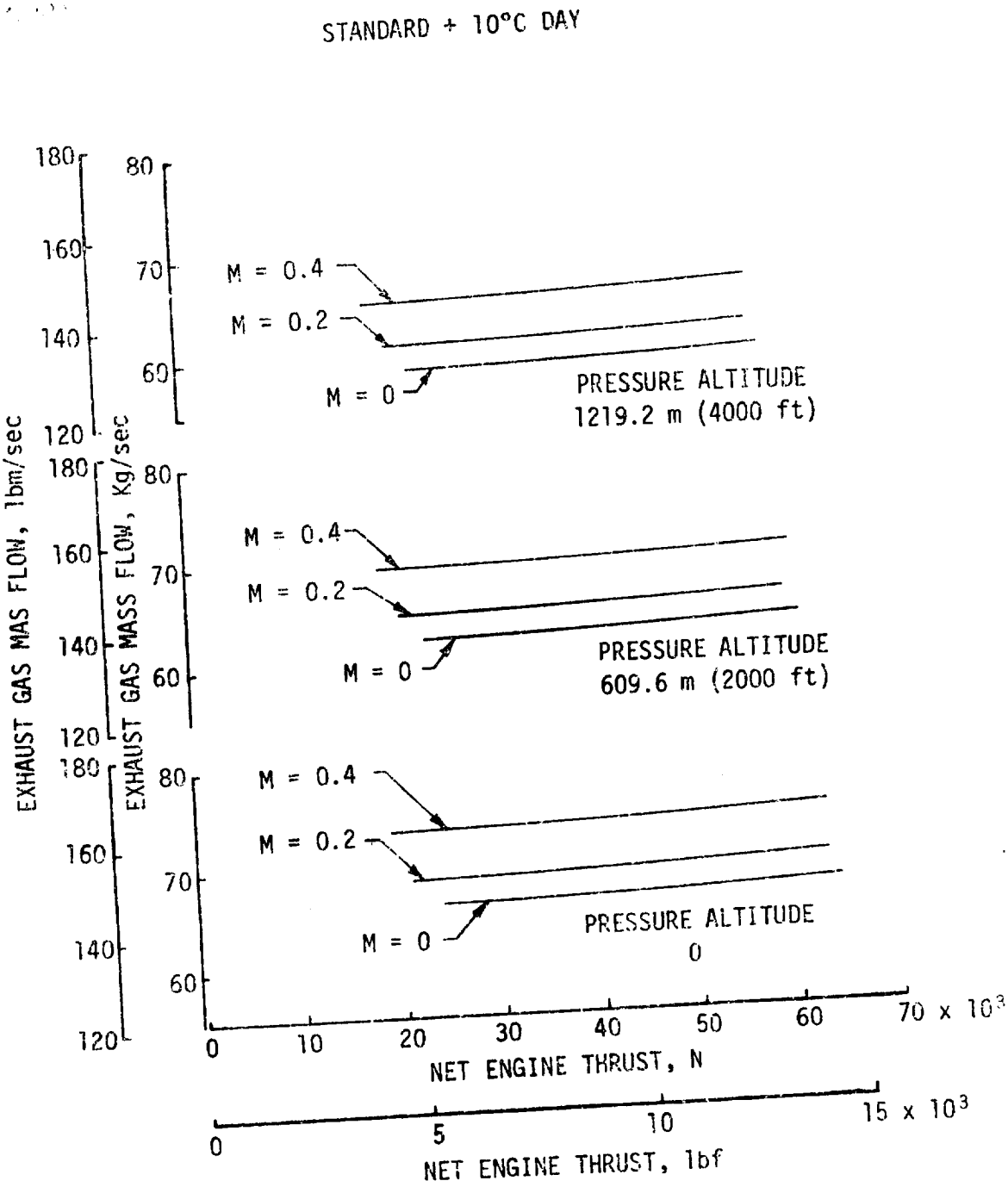

Figure 35. - Installed turbojet exhaust gas mass flow for take-off and part power cruise.

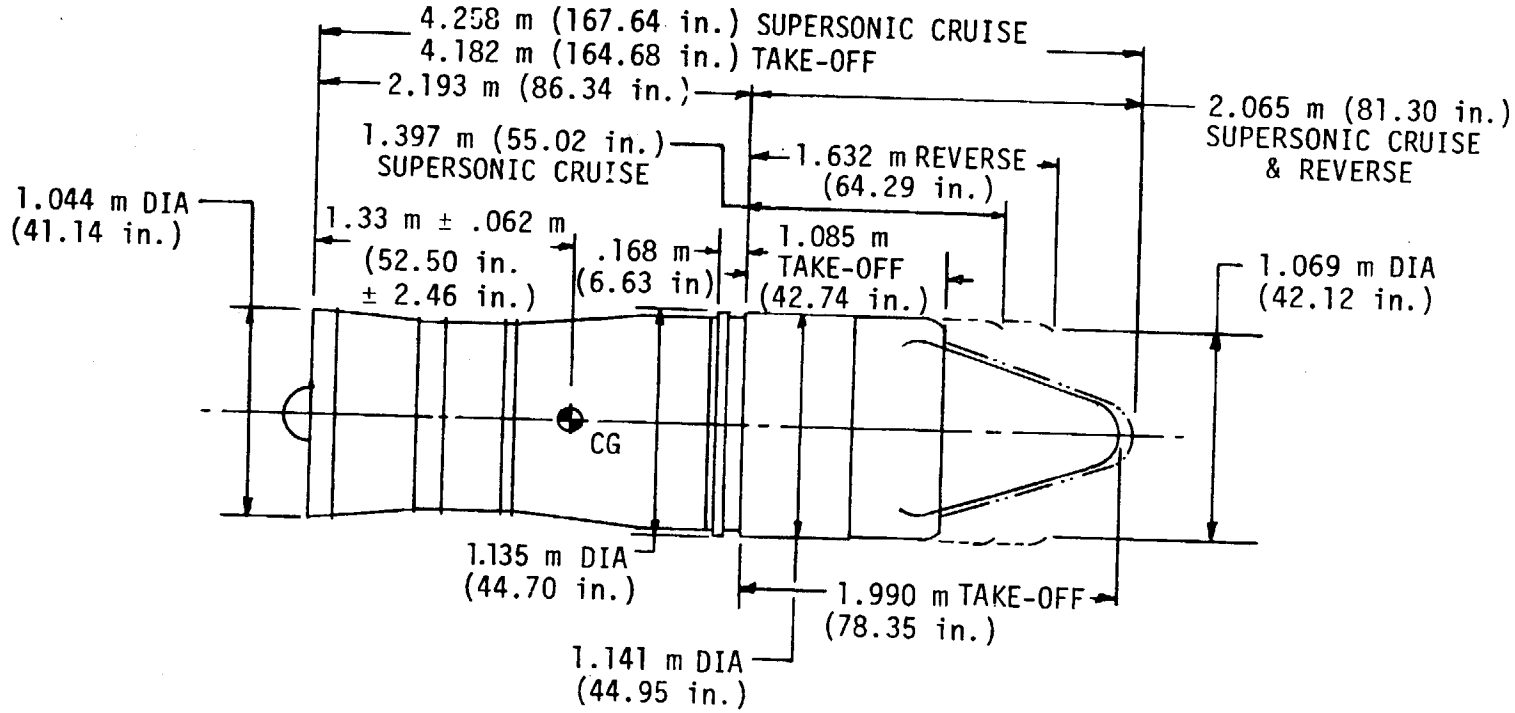

Figure 36. - GE21/J11-B10 engine scaled to SSXJET III

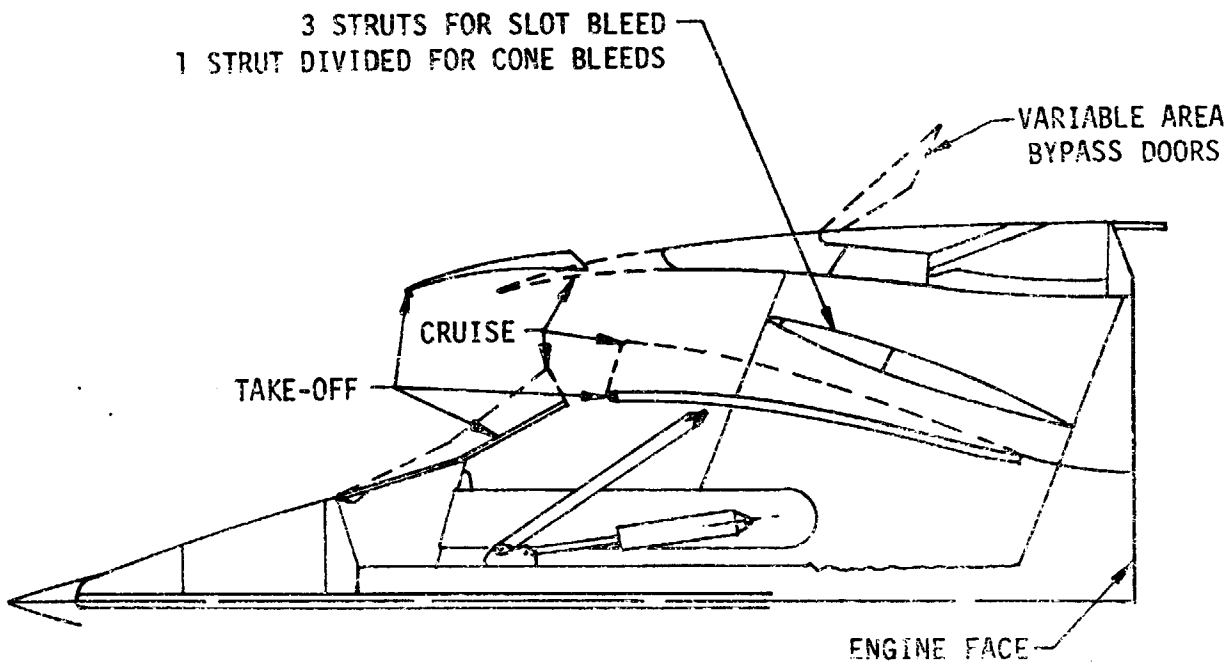

Figure 37. - Douglas Aircraft Co. External compression inlet.

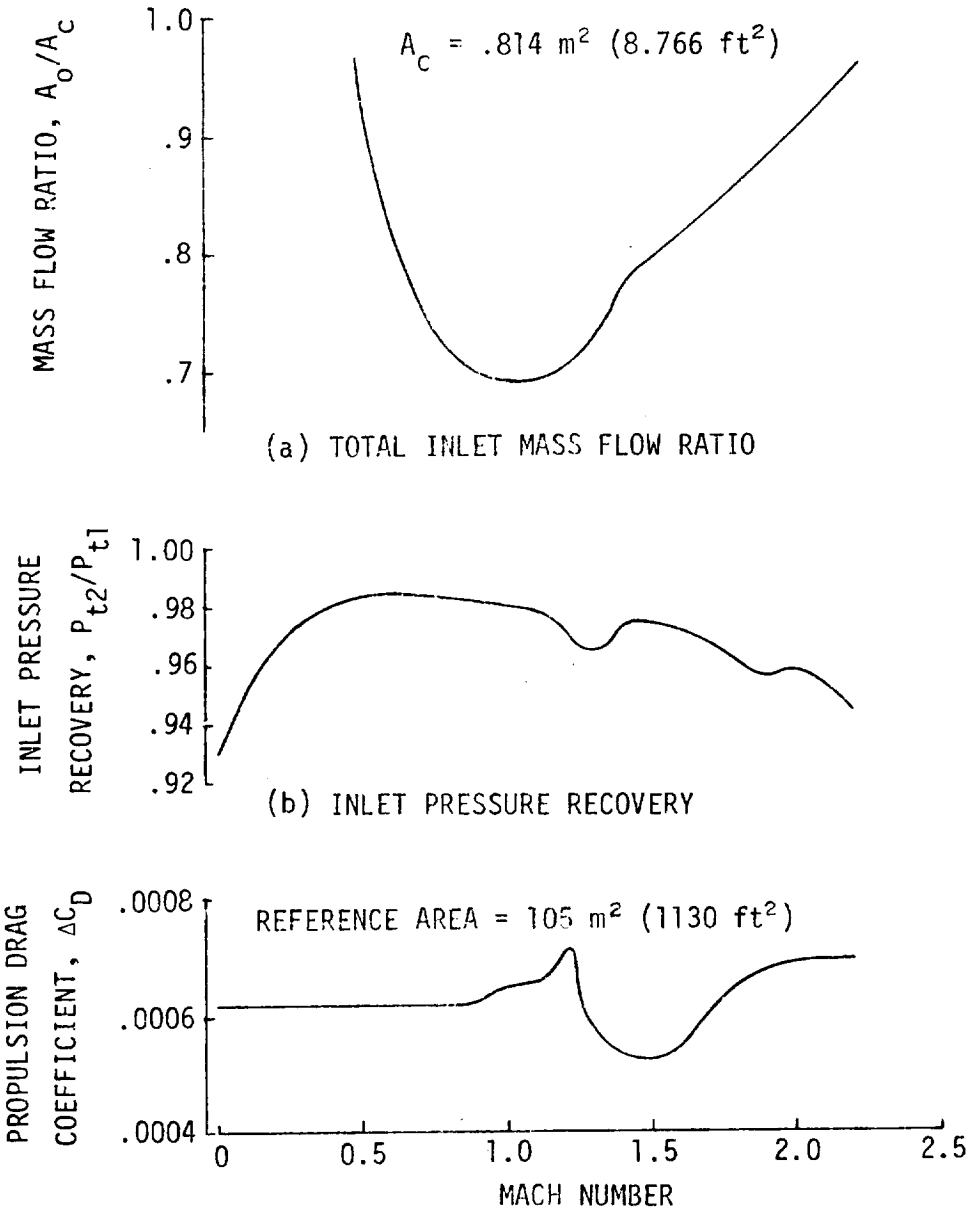

Figure 38. - Douglas Aircraft Co. External compression inlet performance.

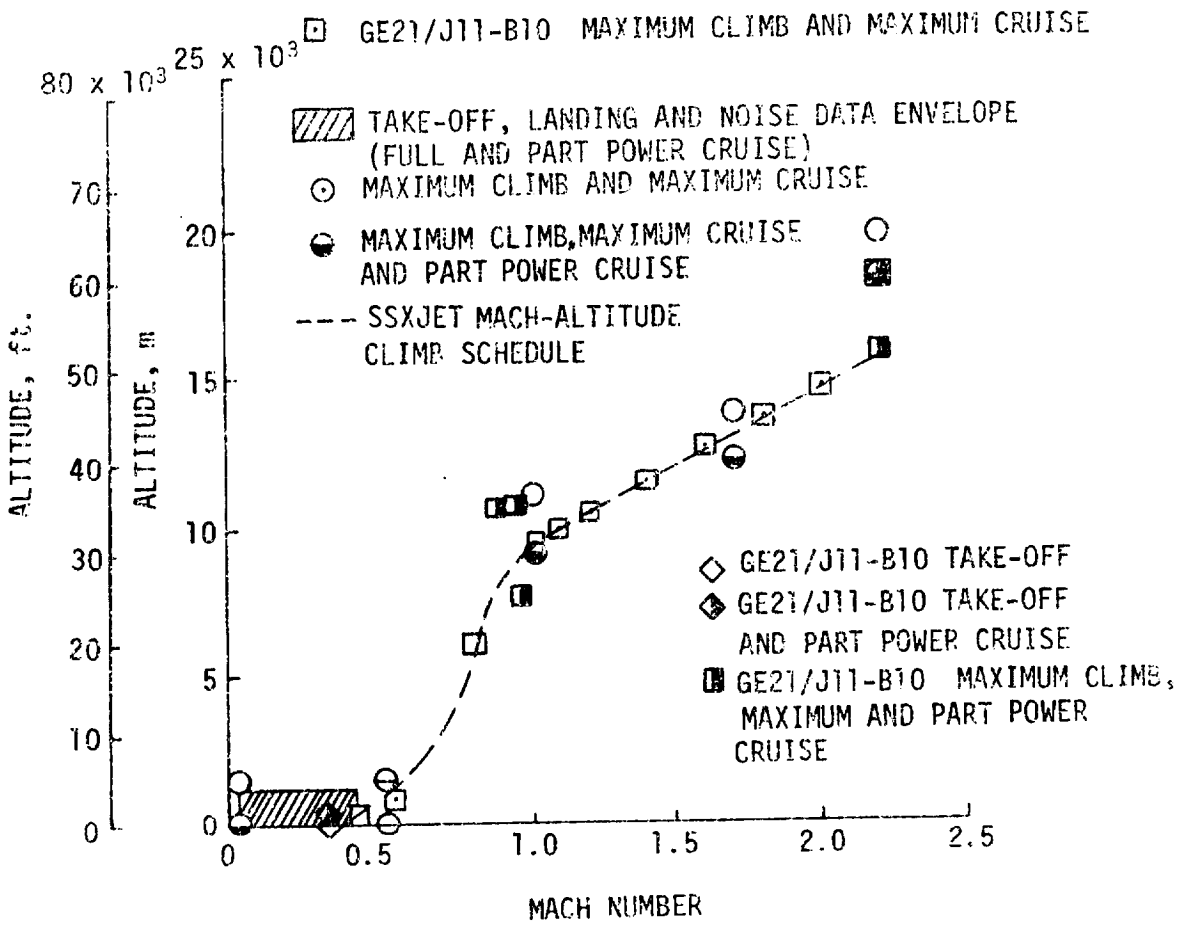

Figure 39. - GE21/J11-B10 data supplied relative to minimum data required.

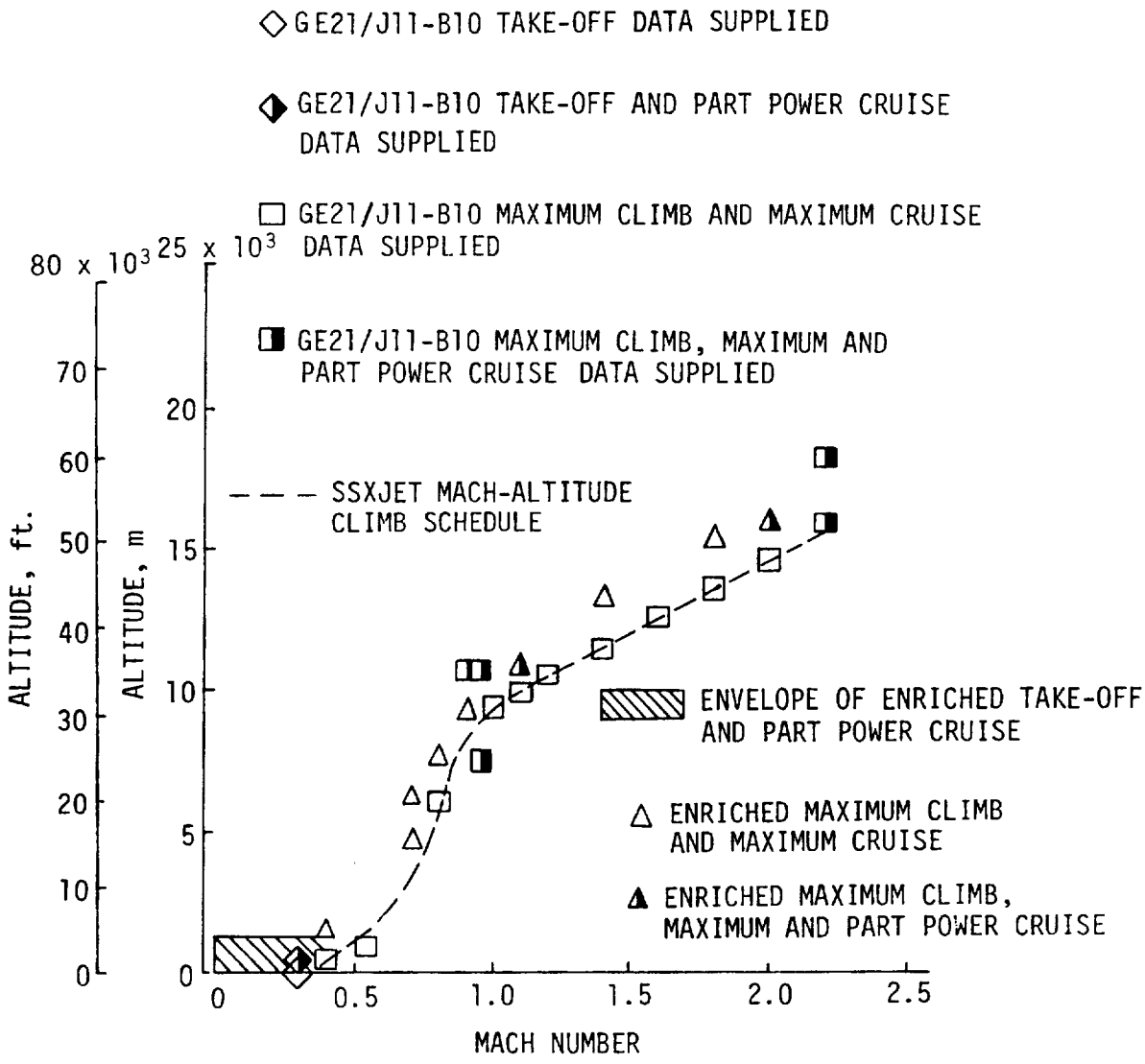

Figure 40. - GE21/J11-B10 data as enriched by Vought Hampton relative to data supplied.

STANDARD DAY

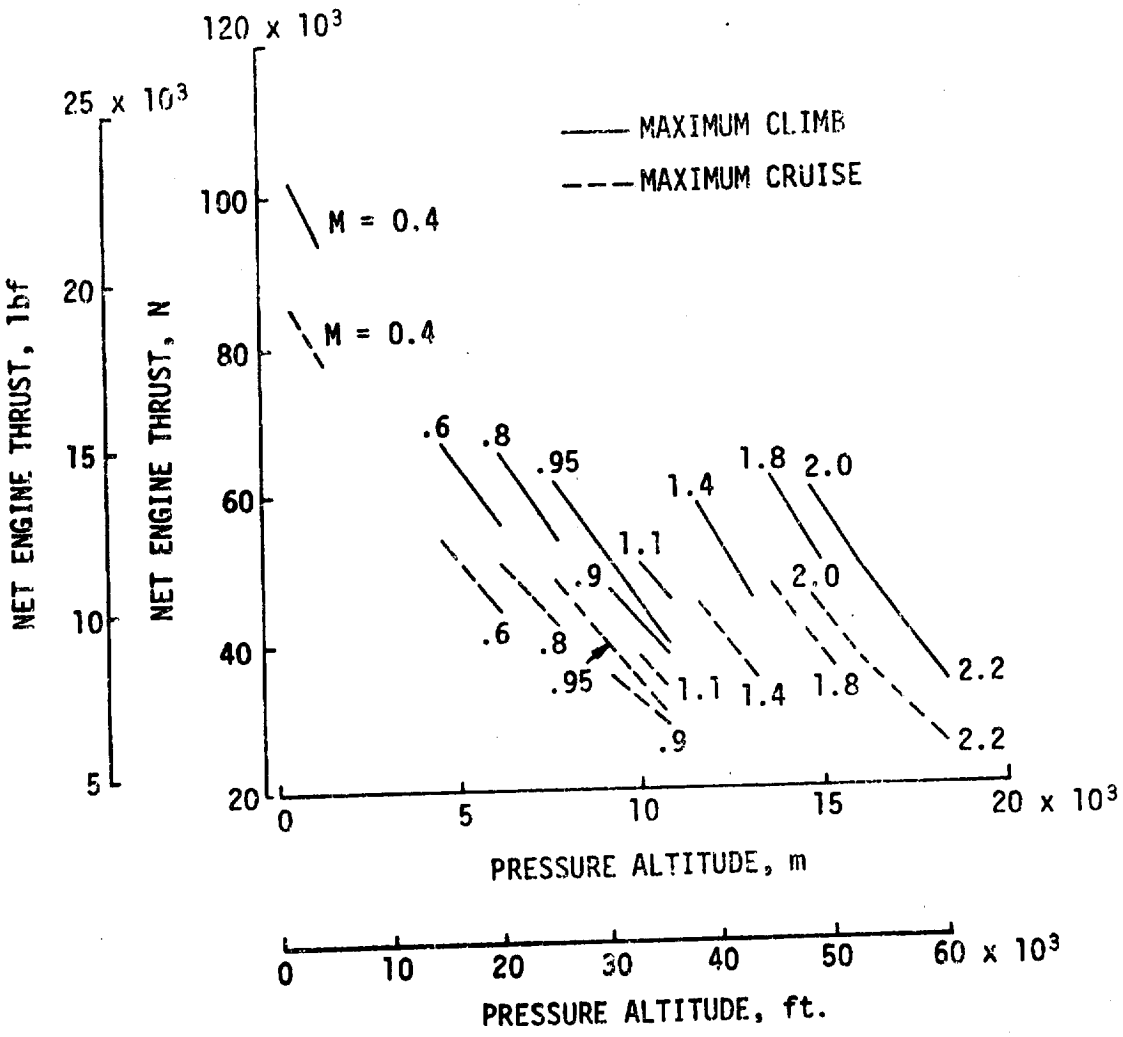

Figure 41. - G.E. 21/J11B10 Installed net thrust for maximum climb and maximum cruise.

STANDARD DAY

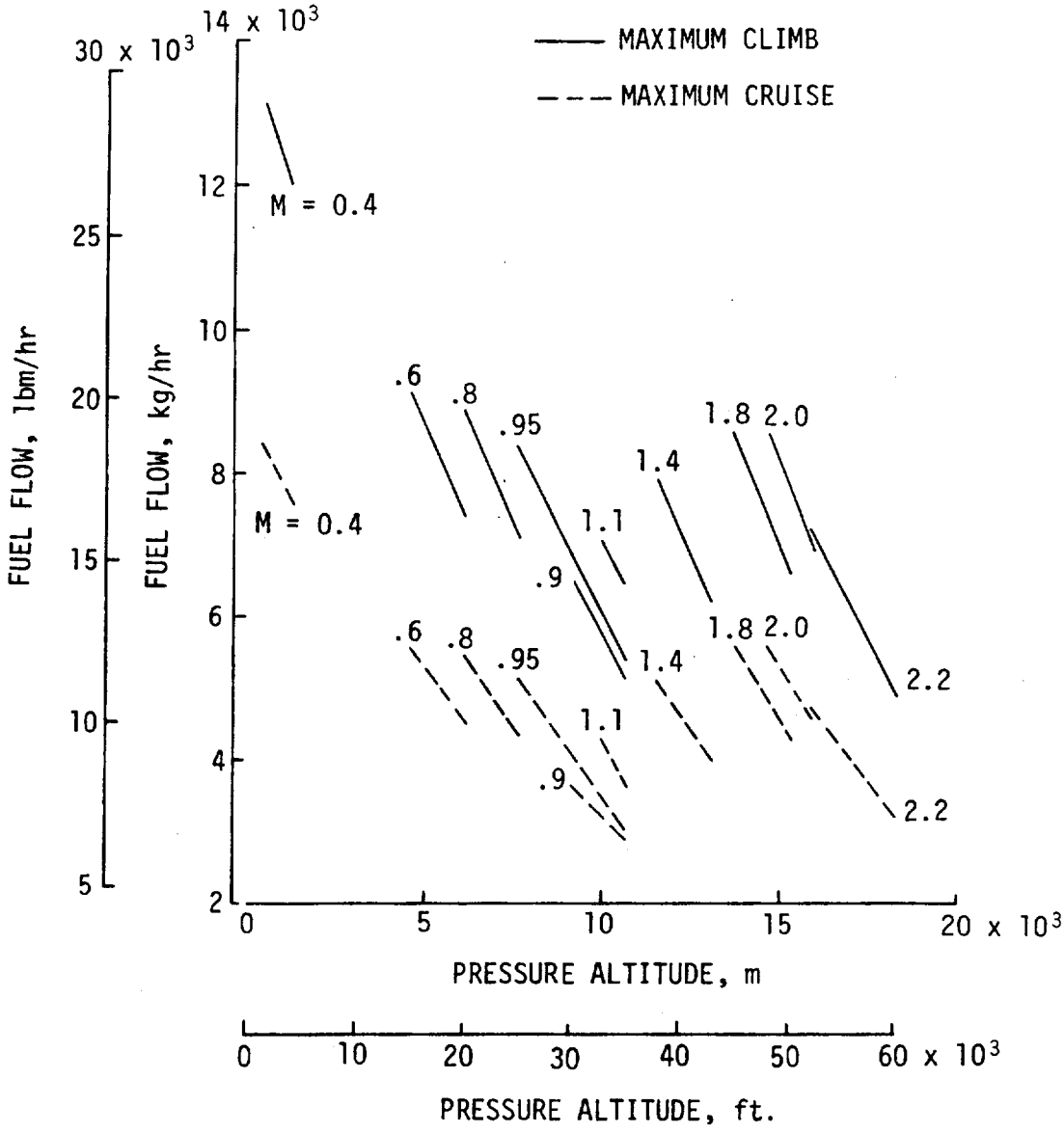

Figure 42. - G.E. 21/J11B10 Installed fuel flow for maximum climb and maximum cruise.

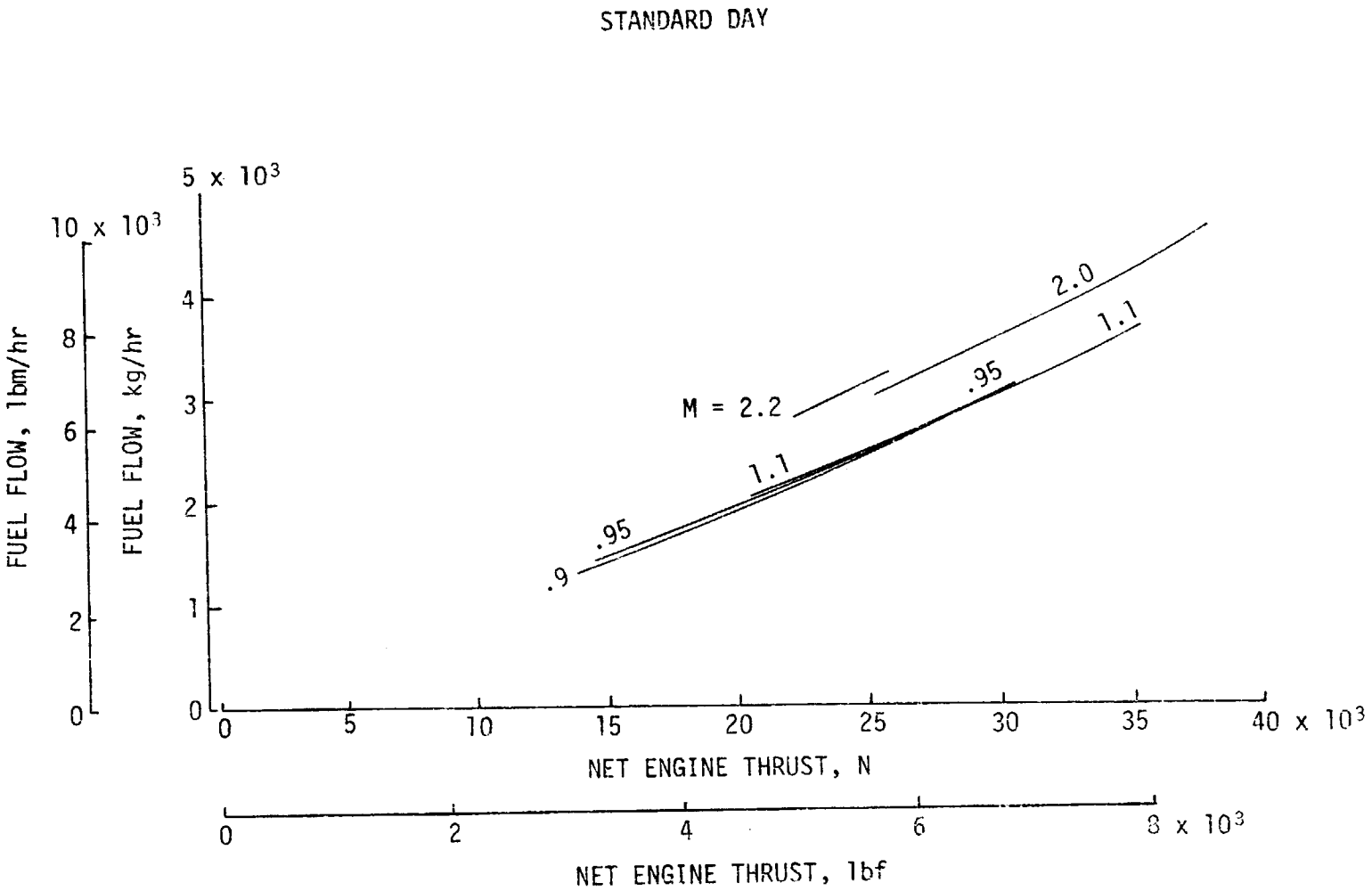

Figure 43. - G.E. 21/J11B10 Installed fuel flow for maximum and part power cruise.

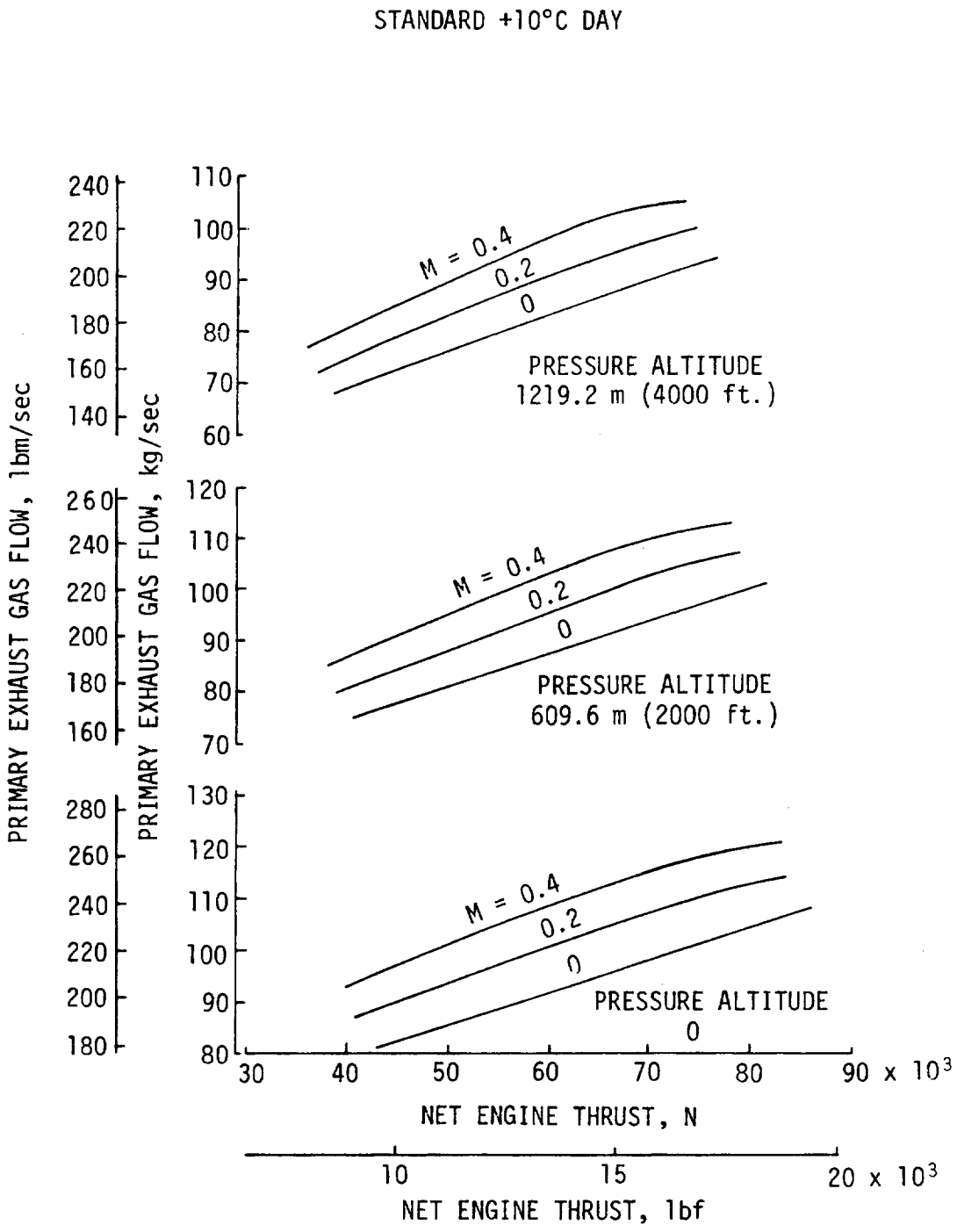

Figure 44. - Installed G.E. 21/J11B10 primary exhaust gas flow for take-off and part power cruise.

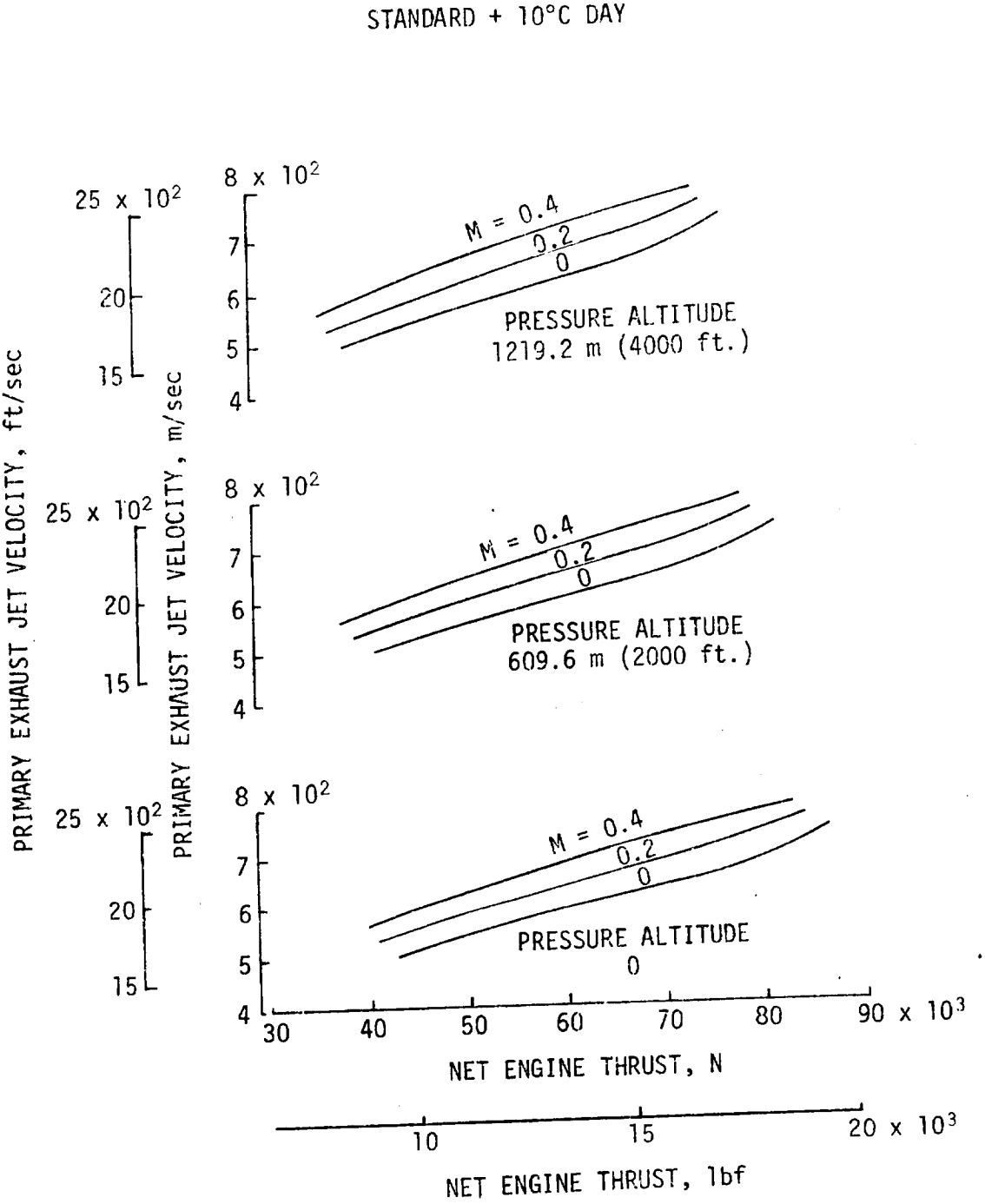

Figure 45. - Installed G.E. 21/J11B10 primary exhaust jet velocity for take-off and part power cruise.

STANDARD + 10°C DAY

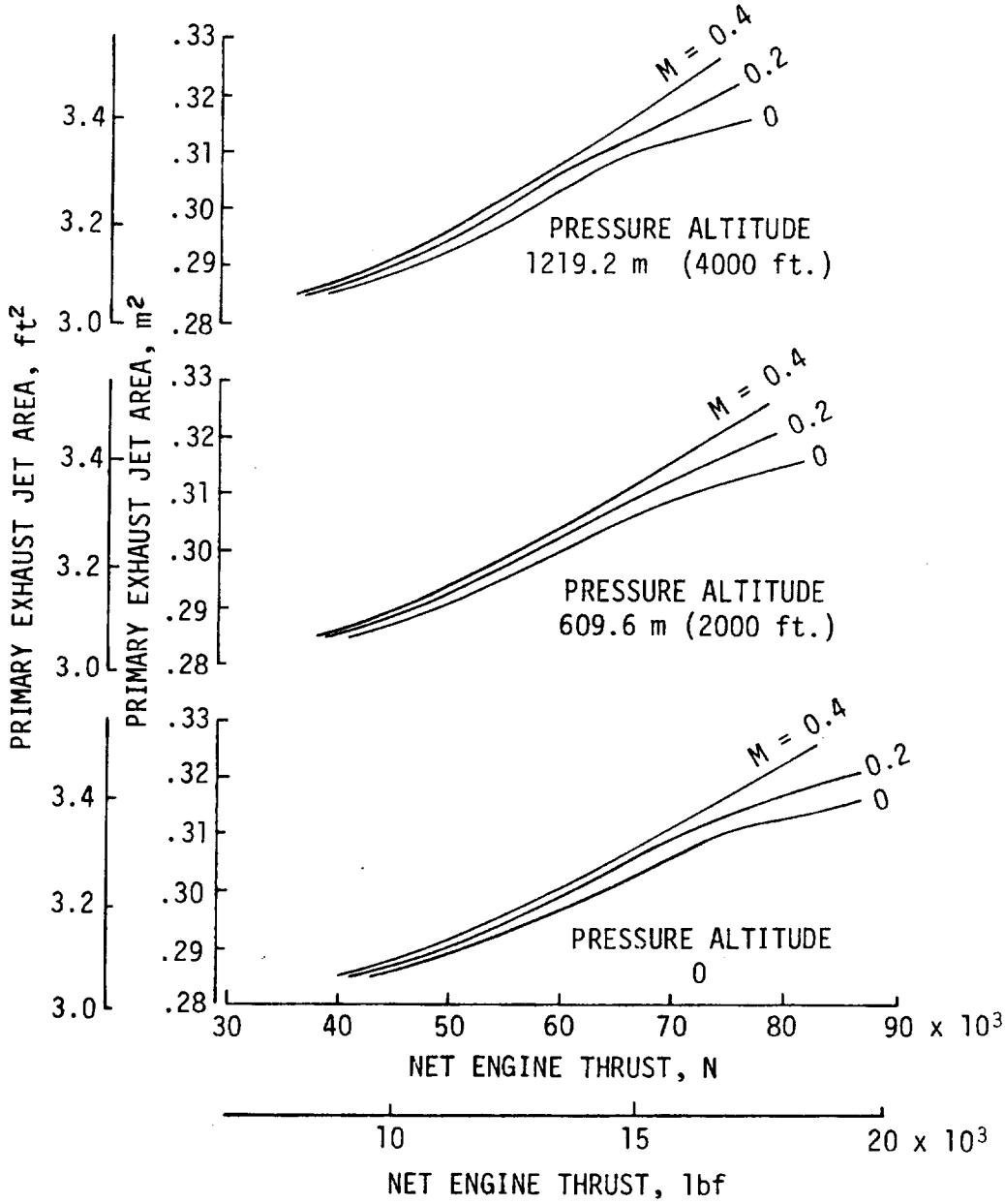

Figure 46. - Installed G.E. 21/J11B10 primary exhaust jet area for take-off and part power cruise.

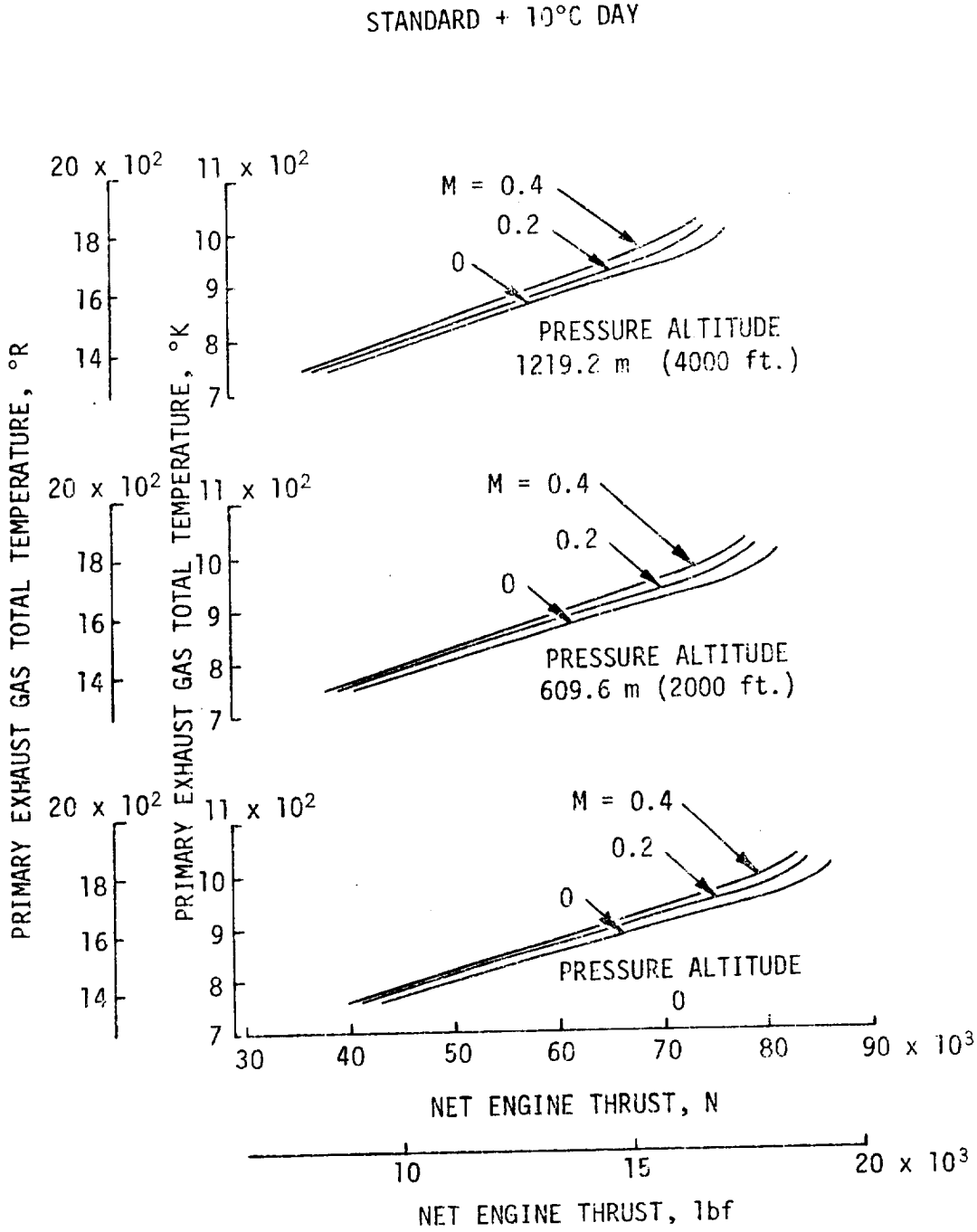

Figure 47. - Installed G.E. 21/J11B10 primary exhaust gas total temperature for take-off and part power cruise.

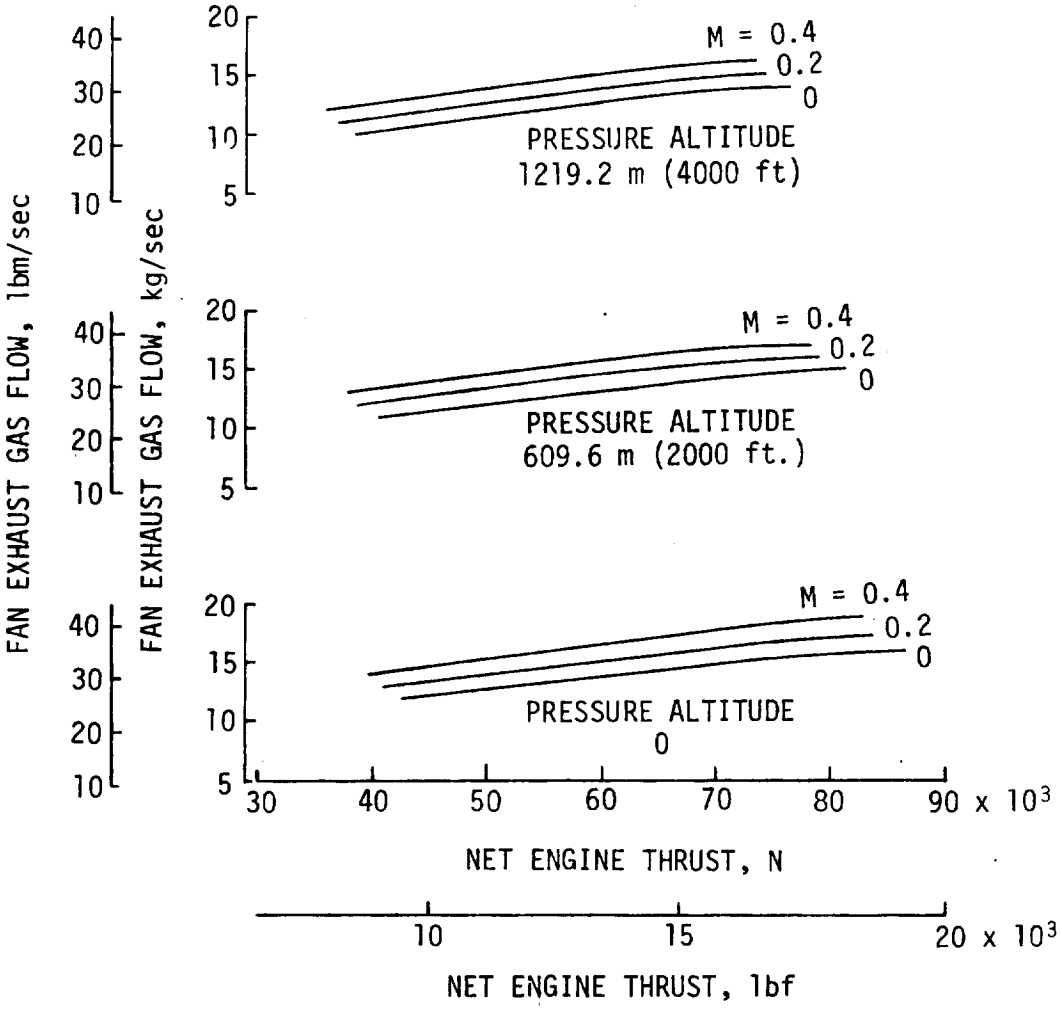

Figure 48. - Installed G.E. 21/J11B10 fan exhaust gas flow for take-off and part power cruise.

STANDARD + 10° DAY

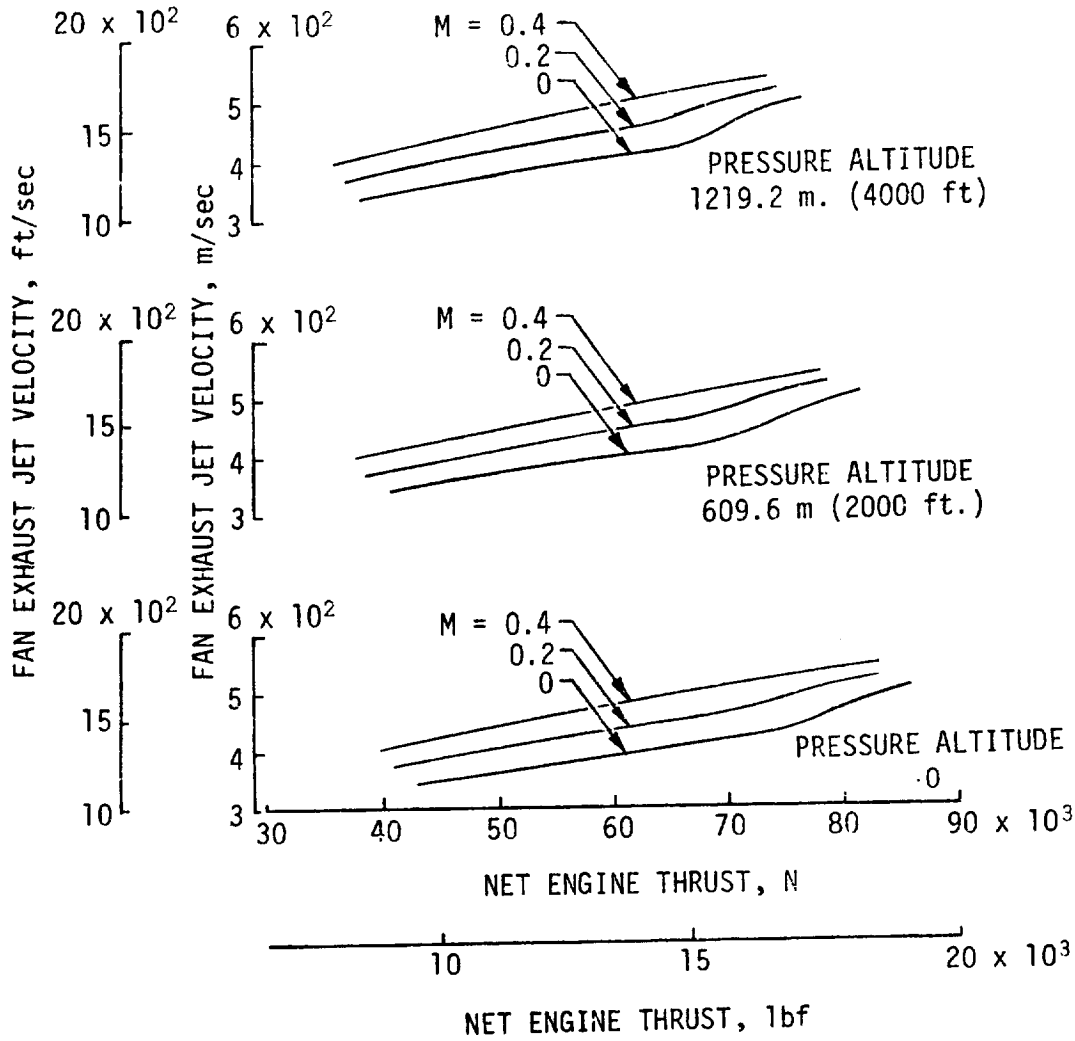

Figure 49. - Installed G.E. 21/J11B10 fan exhaust jet velocity for take-off and part power cruise.

STANDARD + 10°C DAY

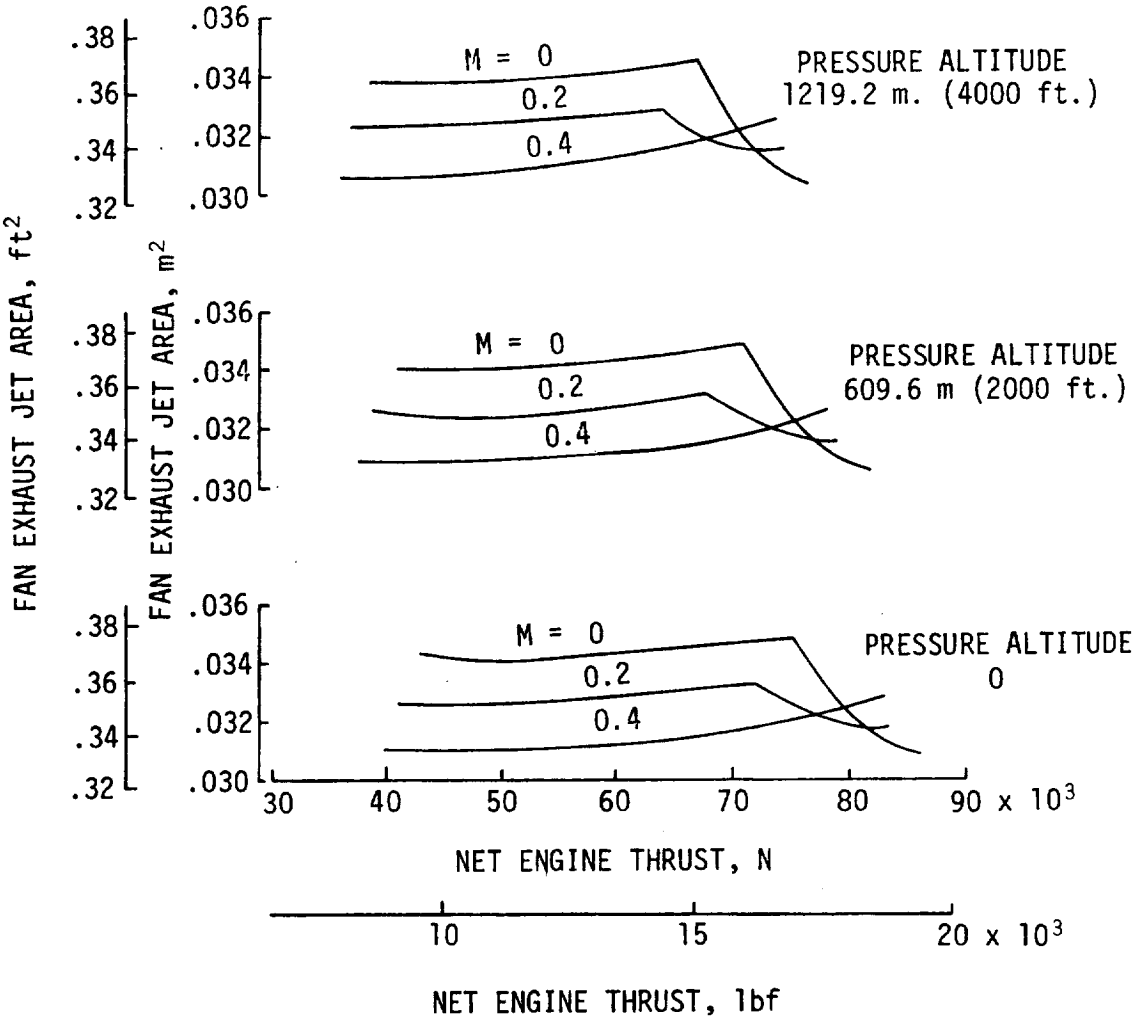

Figure 50. - Installed G.E. 21/J11B10 fan exhaust jet area for take-off and part power cruise.

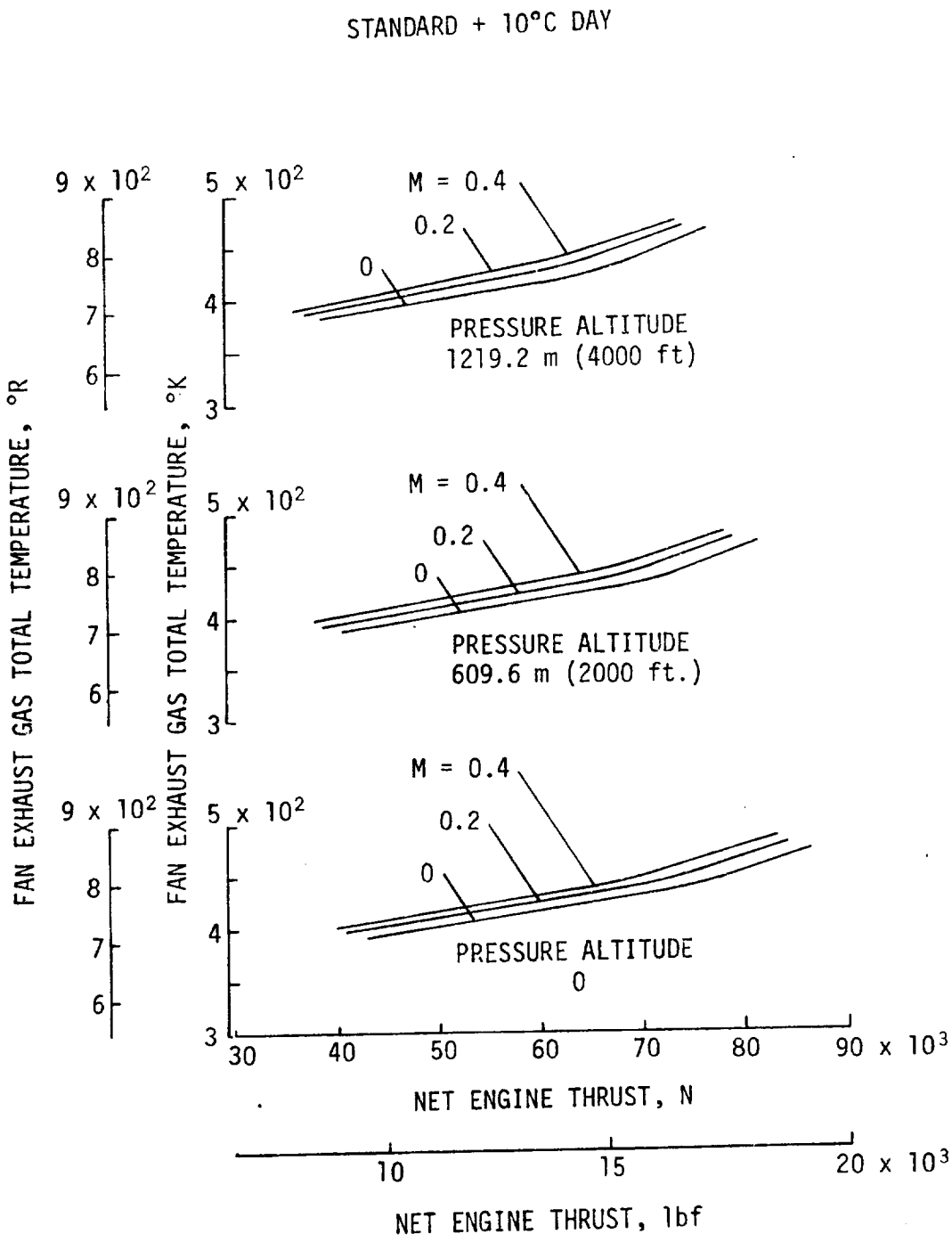

Figure 51. - Installed G.E. 21/J11B10 fan exhaust gas total temperature for take-off and part power cruise.

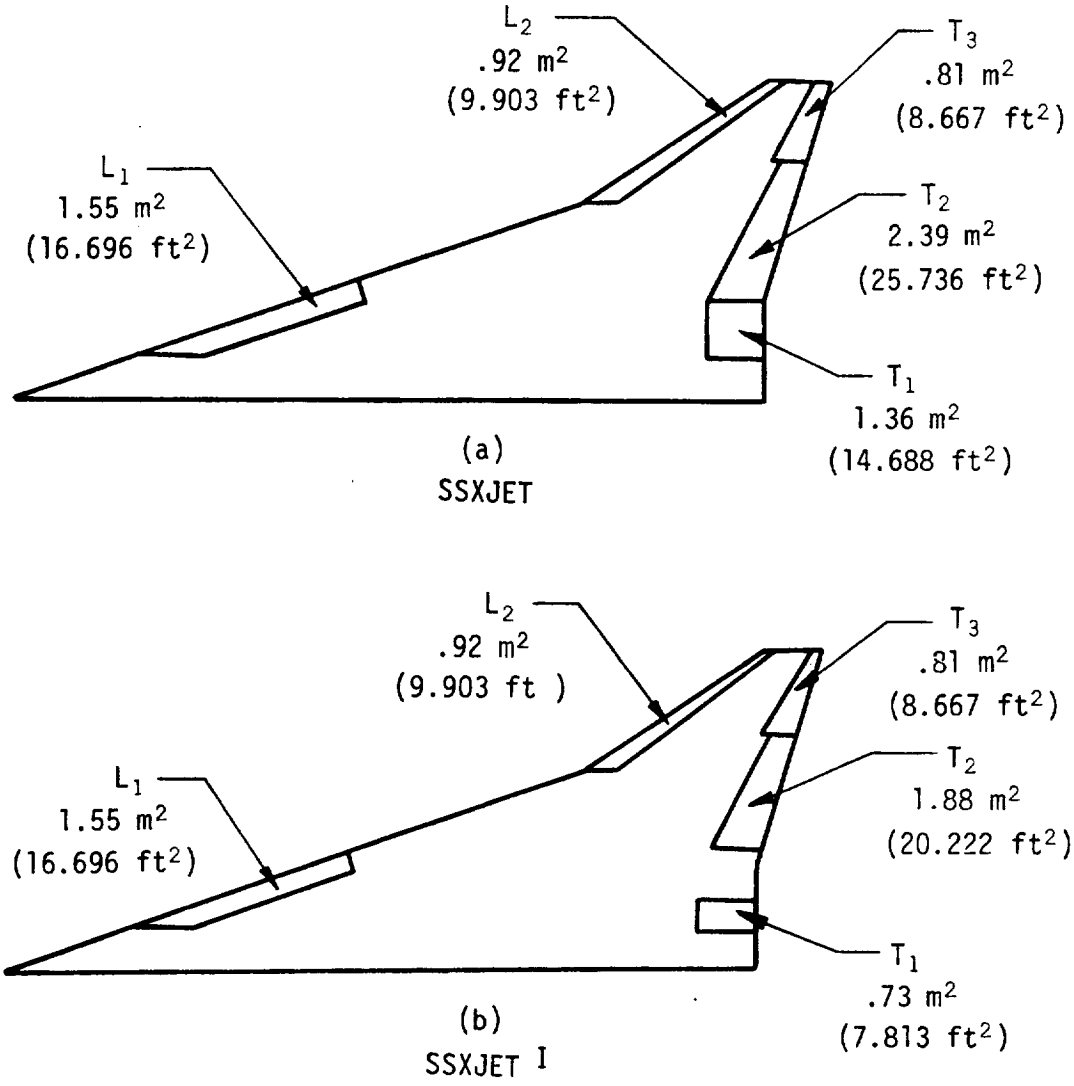

Figure 52. - High-lift system geometry.

Figure 53. - Three-quarter rear view of the model with upper-surface engines mounted for tests in the Langley full-scale tunnel.

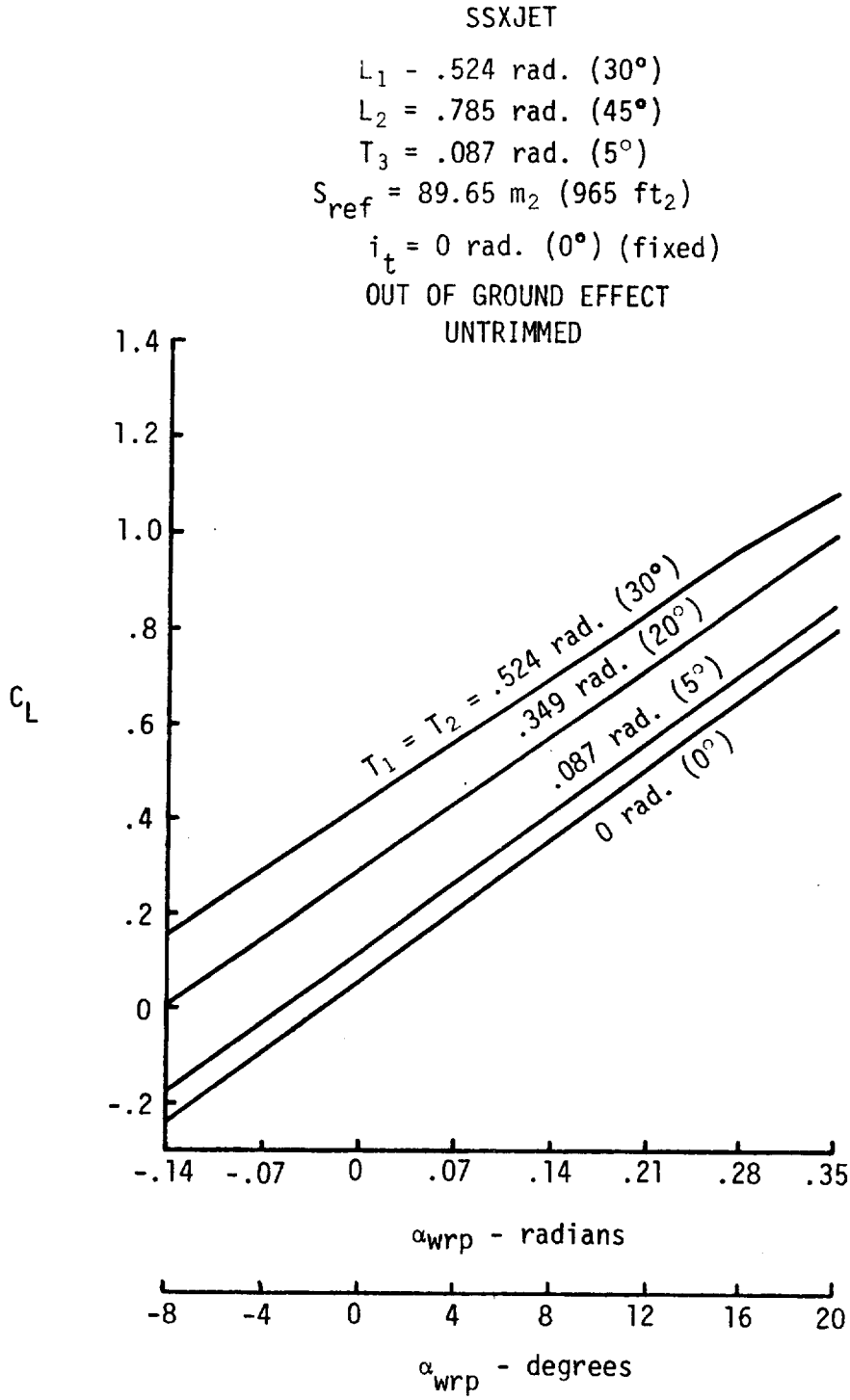

Figure 54. - SSXJET lift curves.

SSXJET I

L_1 = .524 rad. (30°)
L_2 = .785 rad. (45°)
T_3 = .087 rad. (5°)
S_{ref} = 89.65 m (965 ft)
i_t = 0 rad. (0°) (fixed)
OUT OF GROUND EFFECT
UNTRIMMED

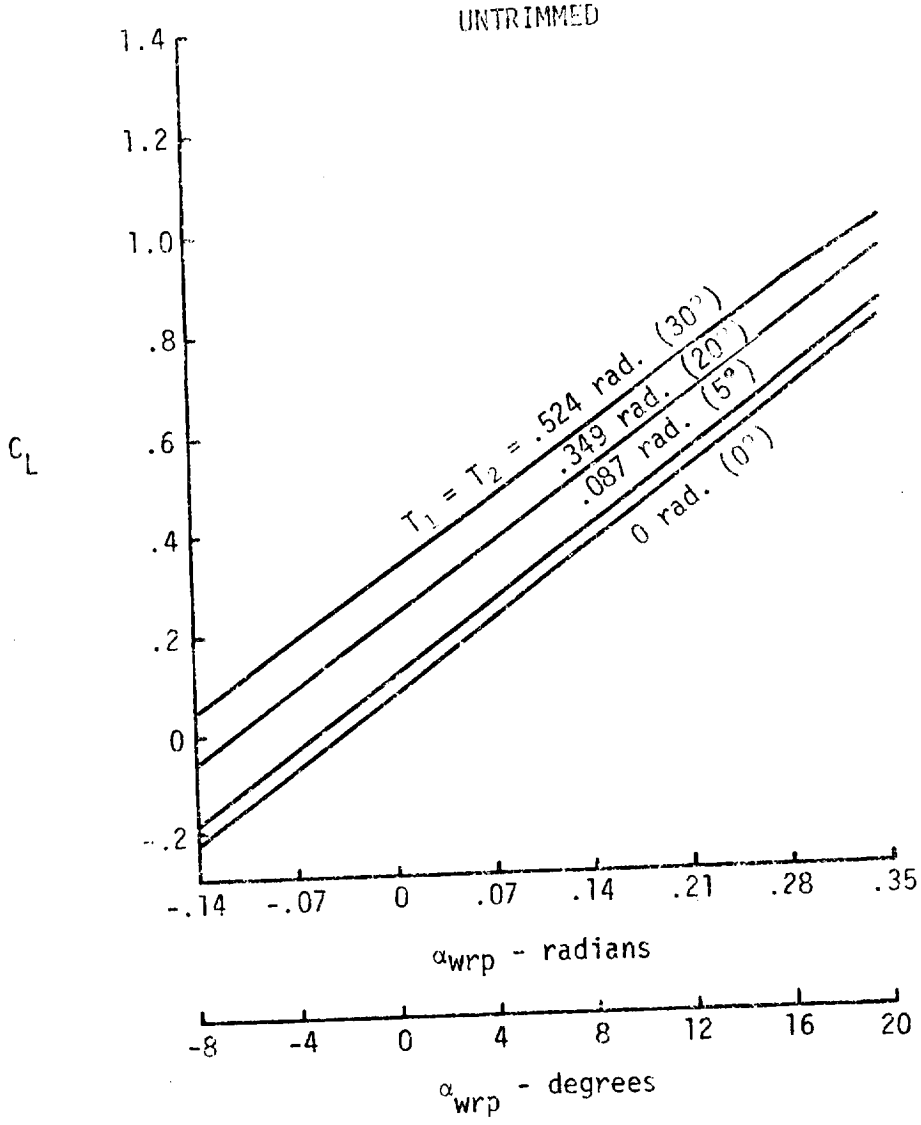

Figure 55. - SSXJET I Lift curves.

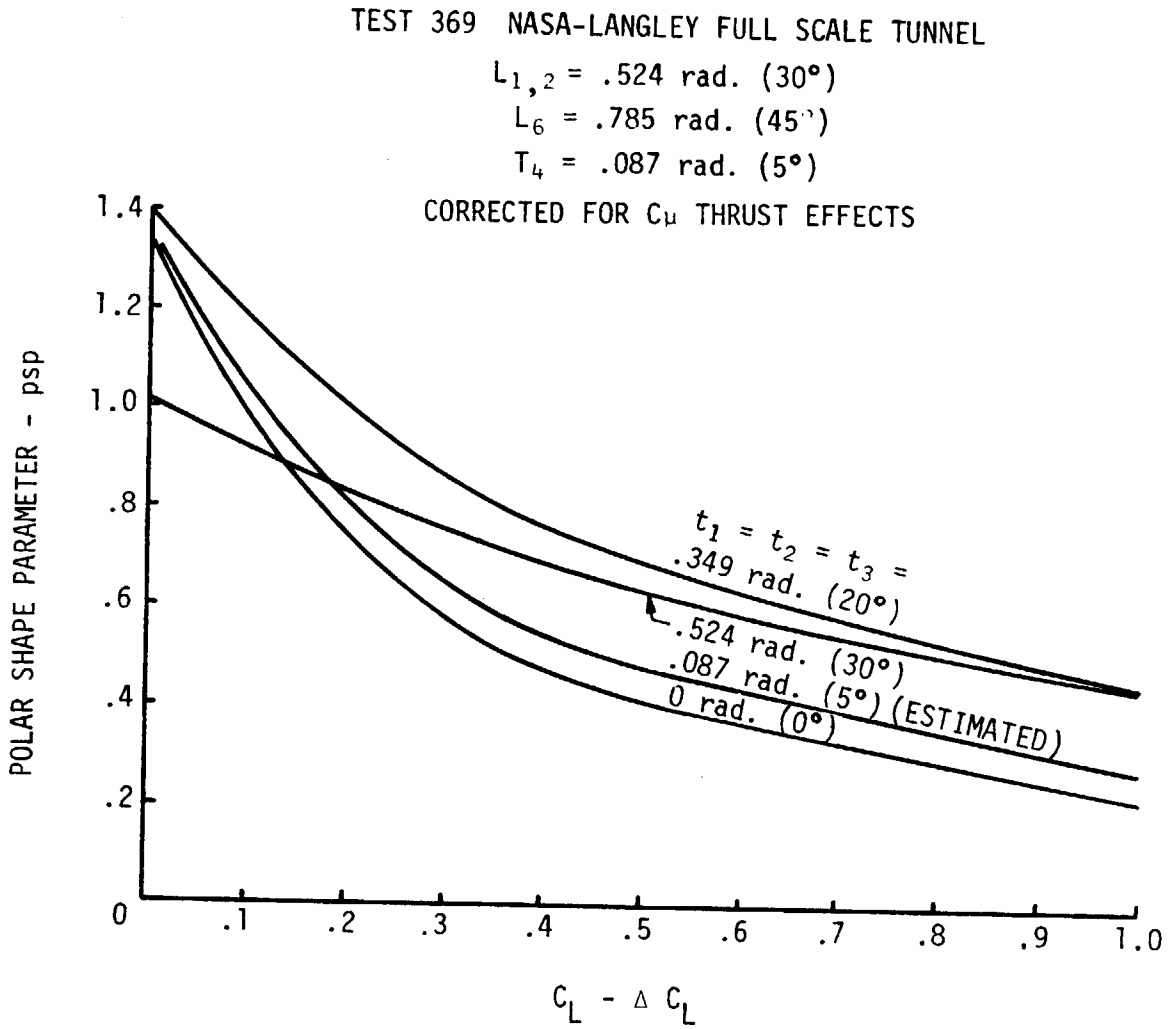

Figure 56. - Polar shape parameters developed for SSXJET

SSXJET

L_1 = .524 rad. (30°)
L_2 = .785 rad. (45°)
T_3 = .087 rad. (5°)
S_{ref} = 89.65 m^2 (965 ft^2)
i_t = 0 rad. (0°) (fixed)
OUT OF GROUND EFFECT
UNTRIMMED

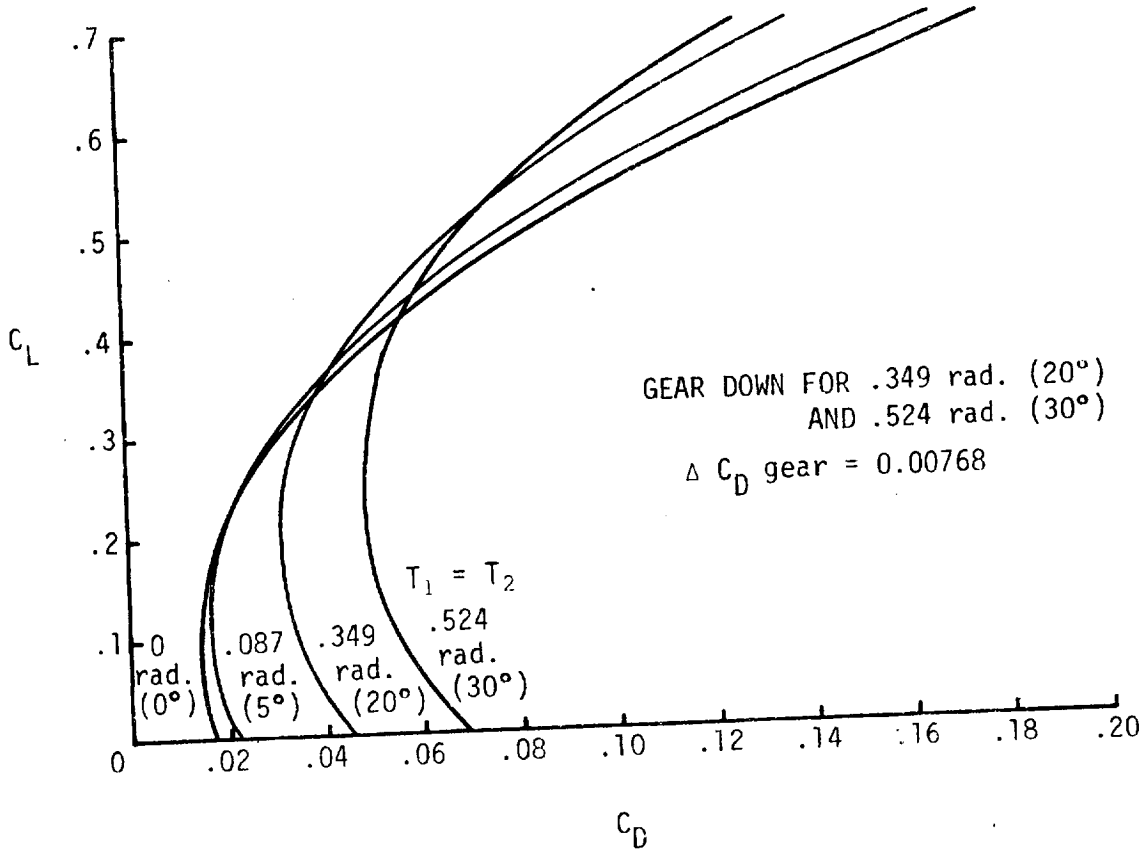

Figure 57. - SSXJET Drag polars.

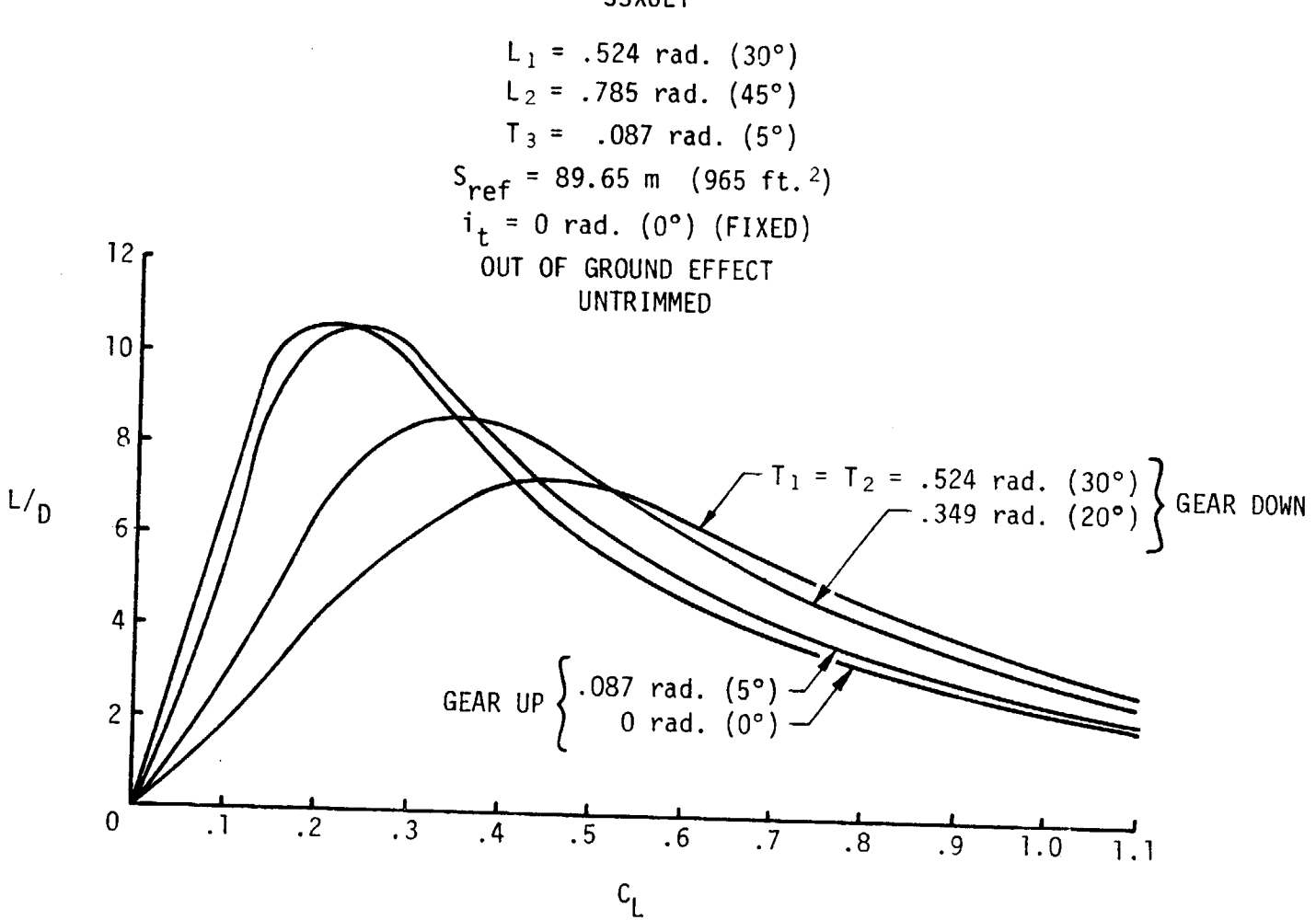

Figure 58. - SSXJET $L/_D$ performance.

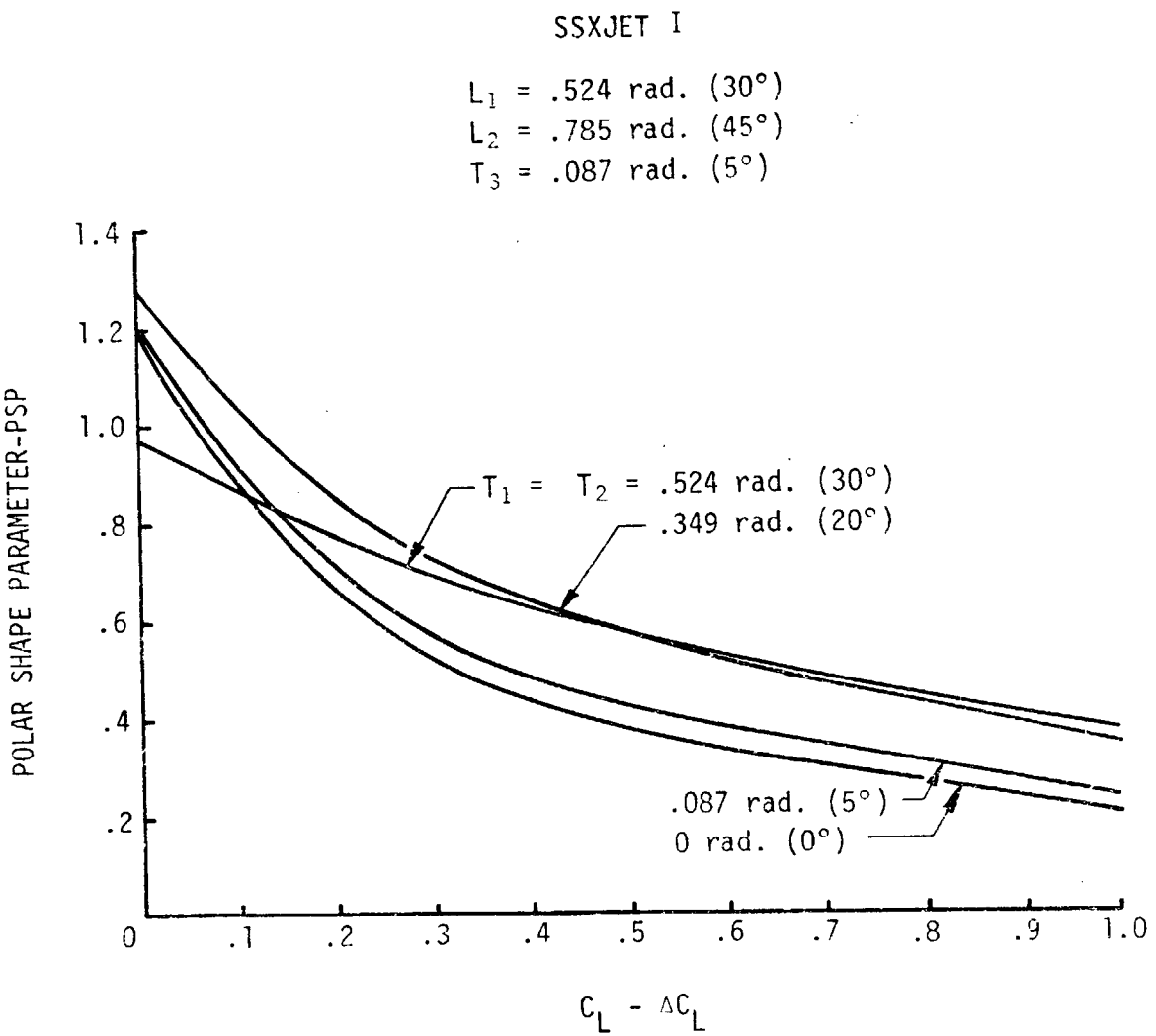

Figure 59. - Polar shape parameters for SSXJET I.

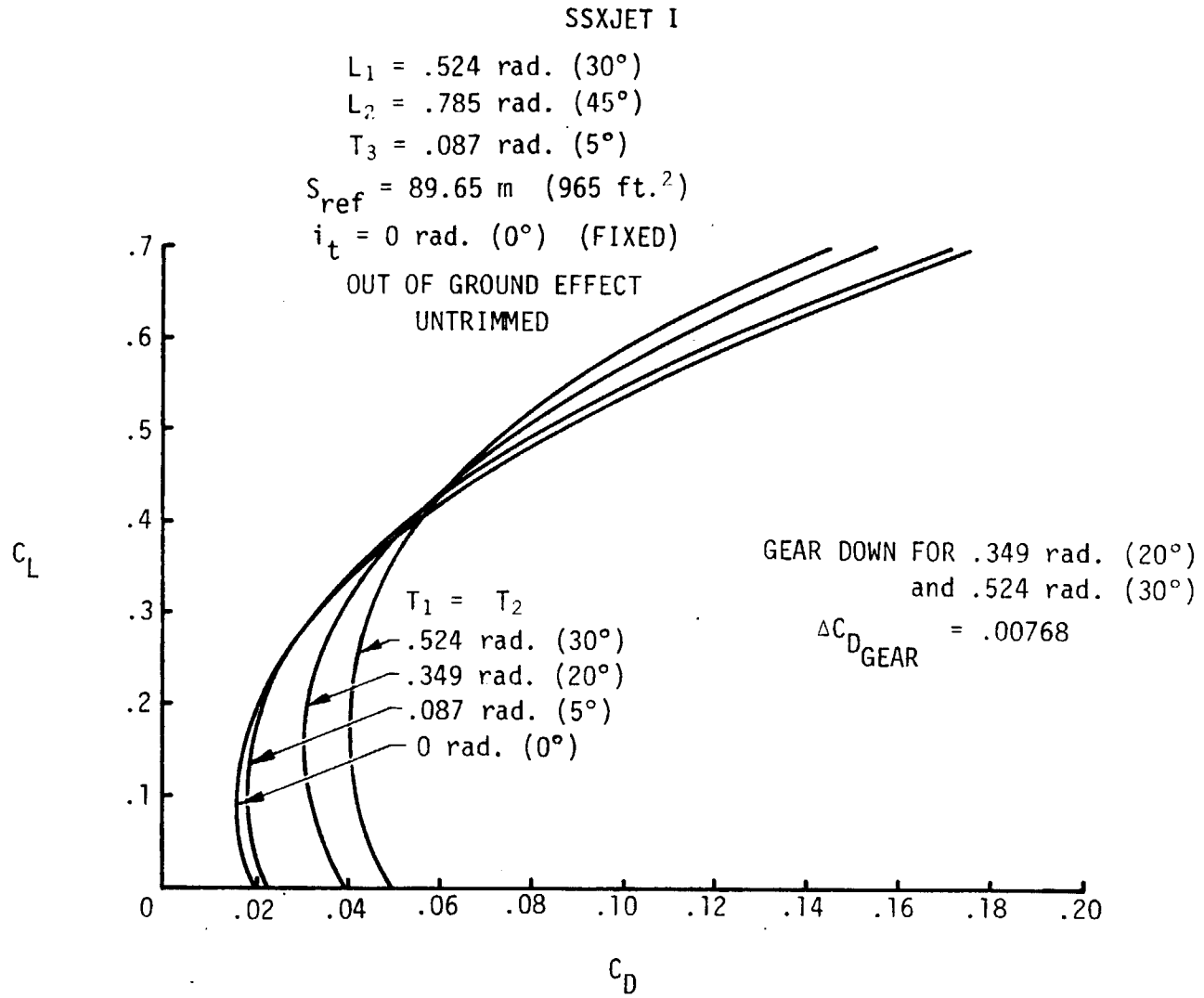

Figure 60. - SSXJET I drag polars.

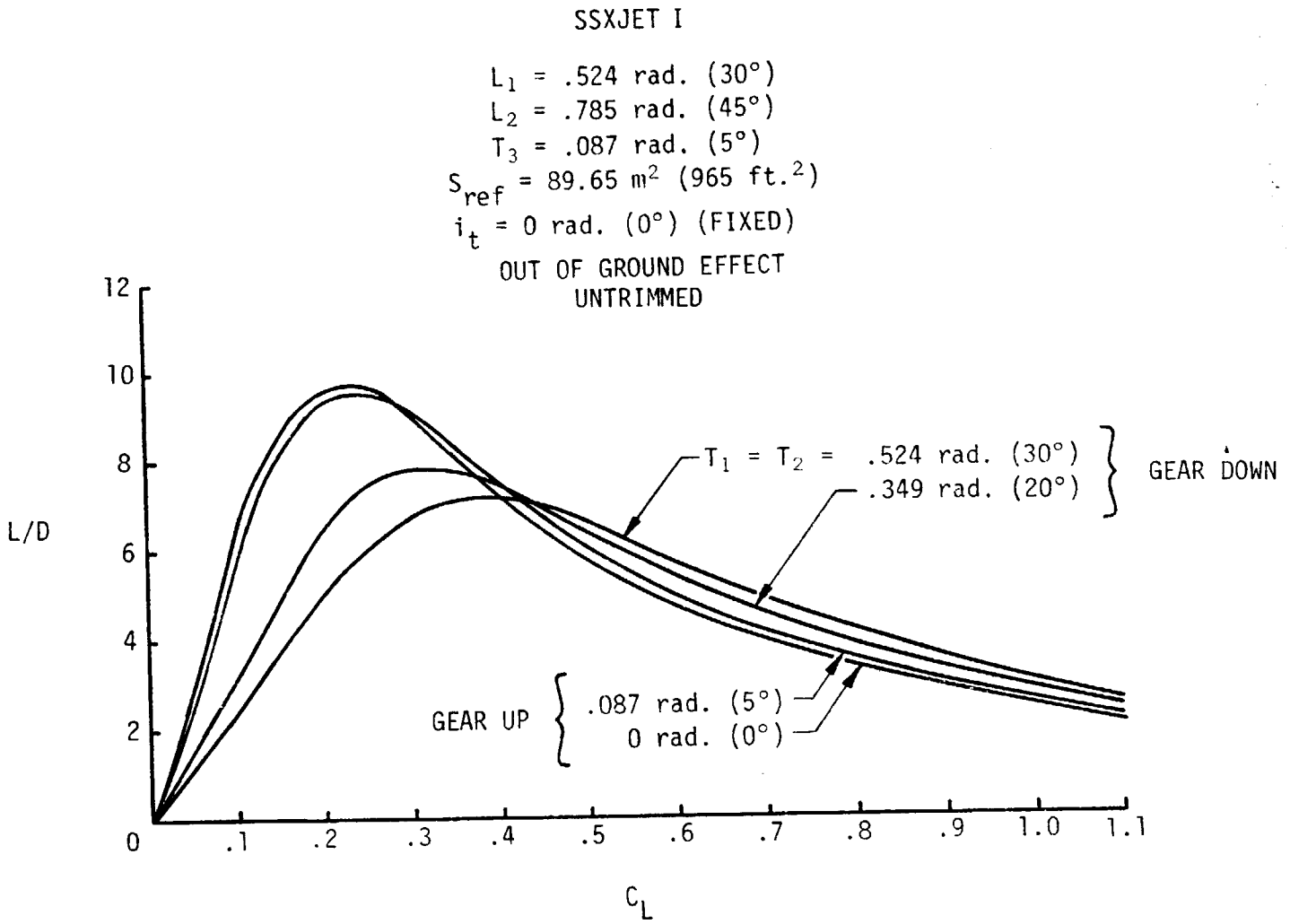

Figure 61. - SSXJET I L/D performance.

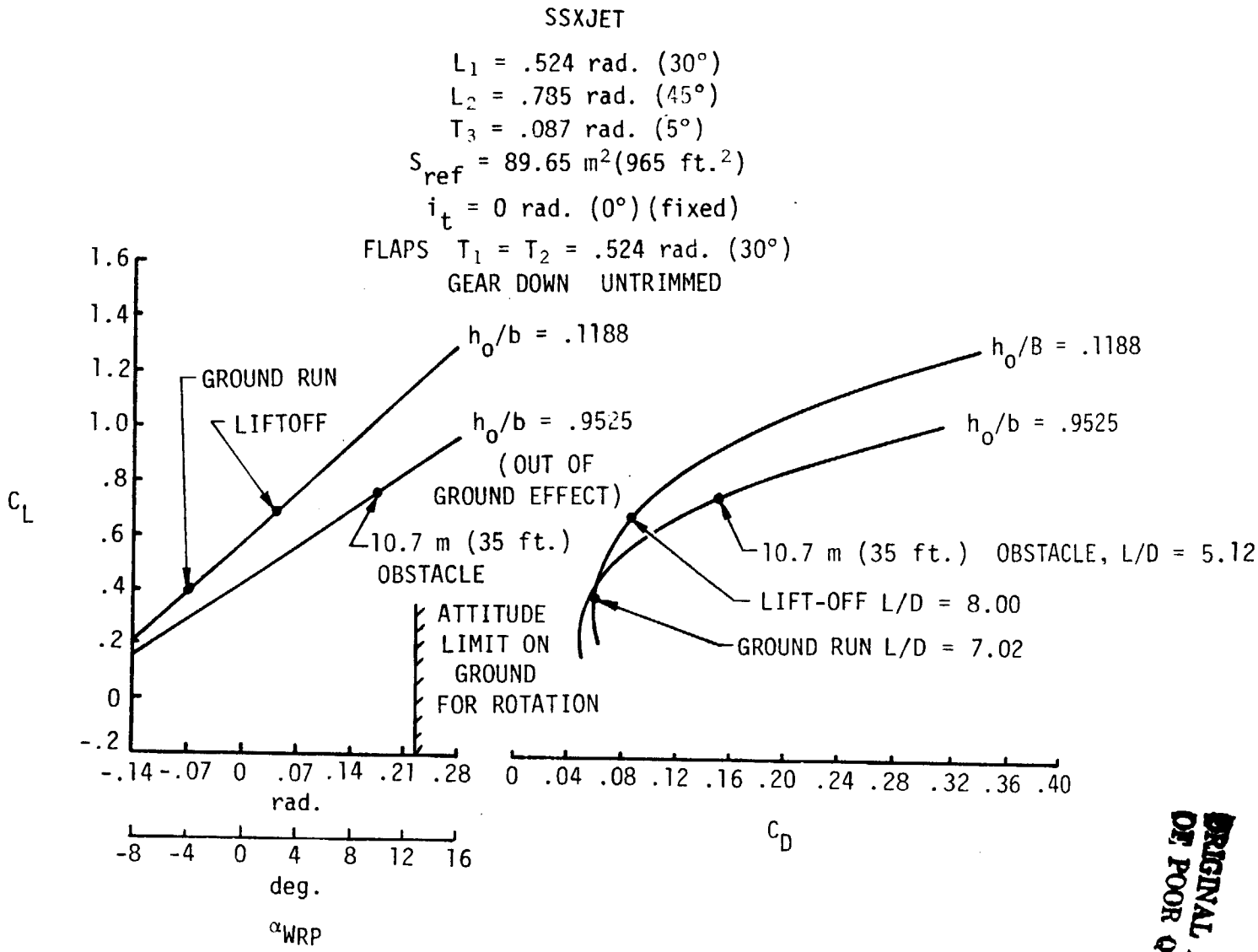

Figure 62. - SSXJET aerodynamics in ground effect.

SSXJET
TWO ENGINES

S_{ref} = 89.65 m^2 (965 $ft.^2$)

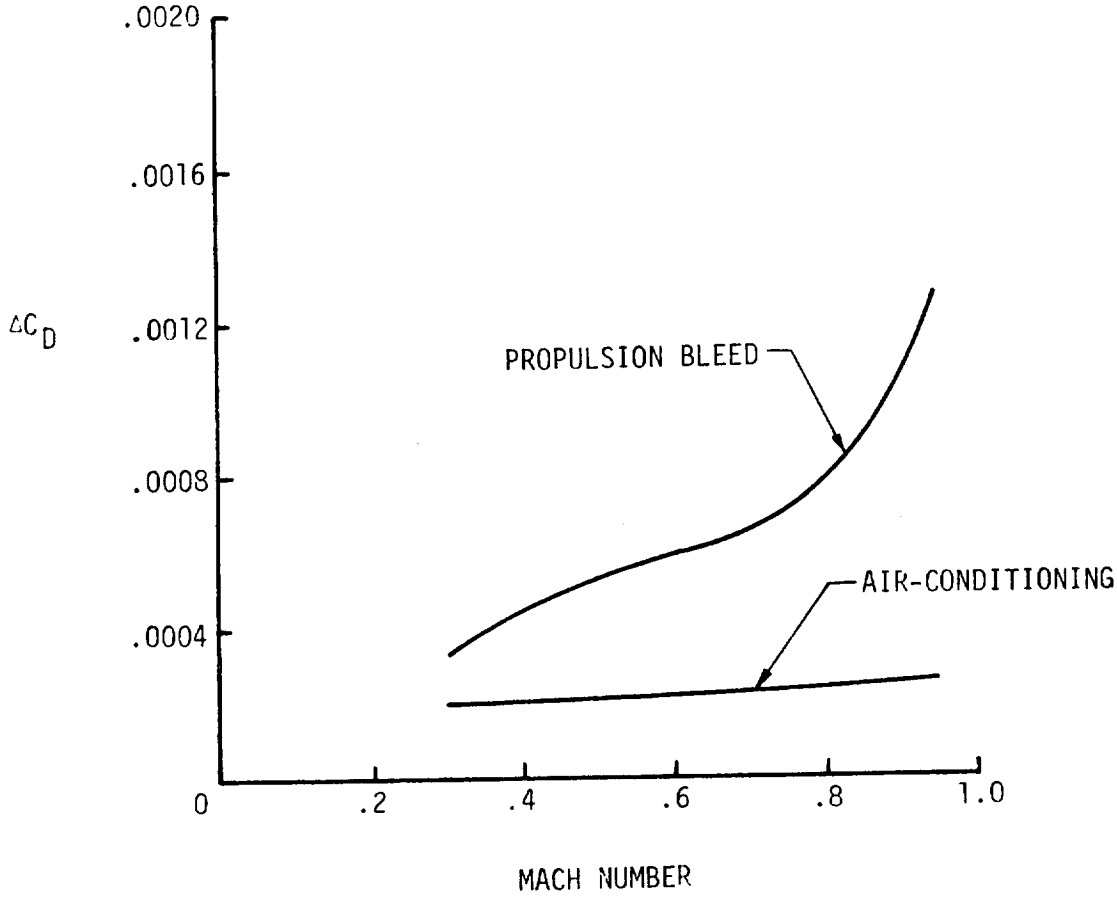

Figure 63. - Propulsion bleed and air-conditioning drag increments.

SSXJET

S_{ref} = 89.65 m^2(965 ft.^{2})

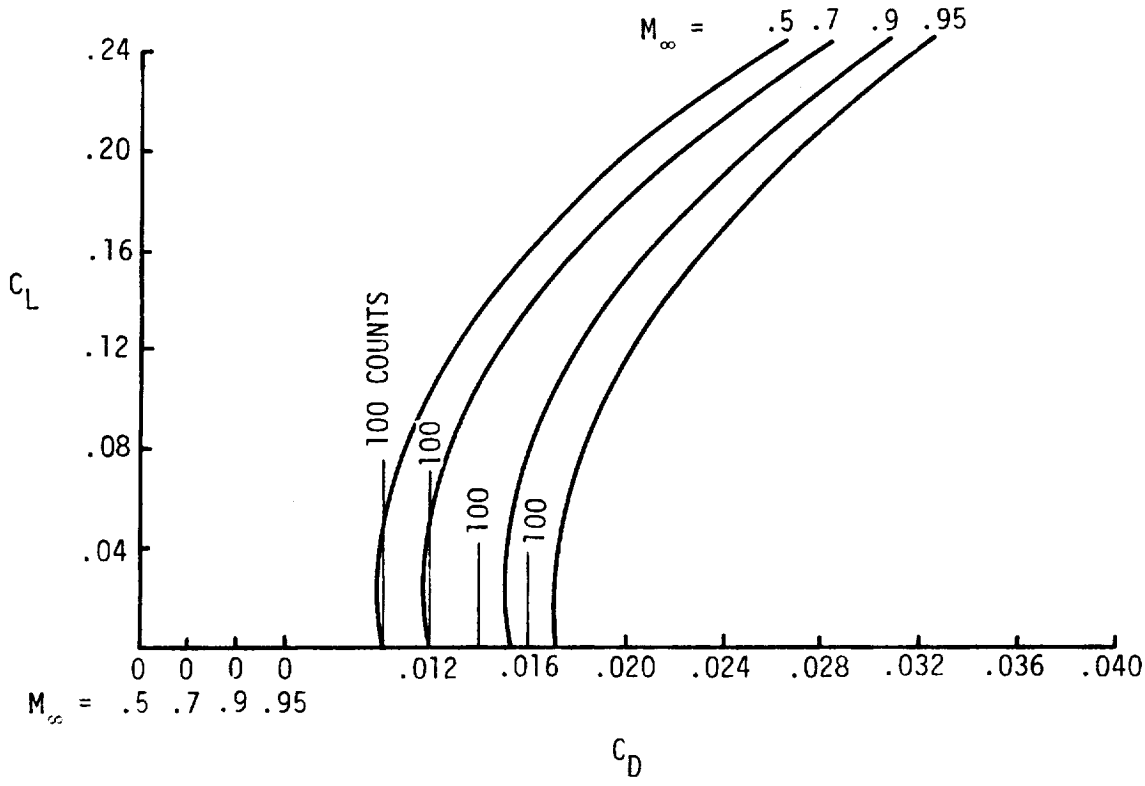

Figure 64. - Subsonic/transonic SSXJET polars.

SSXJET III

S_{ref} = 104.98 m^2(1130 $ft.^2$)

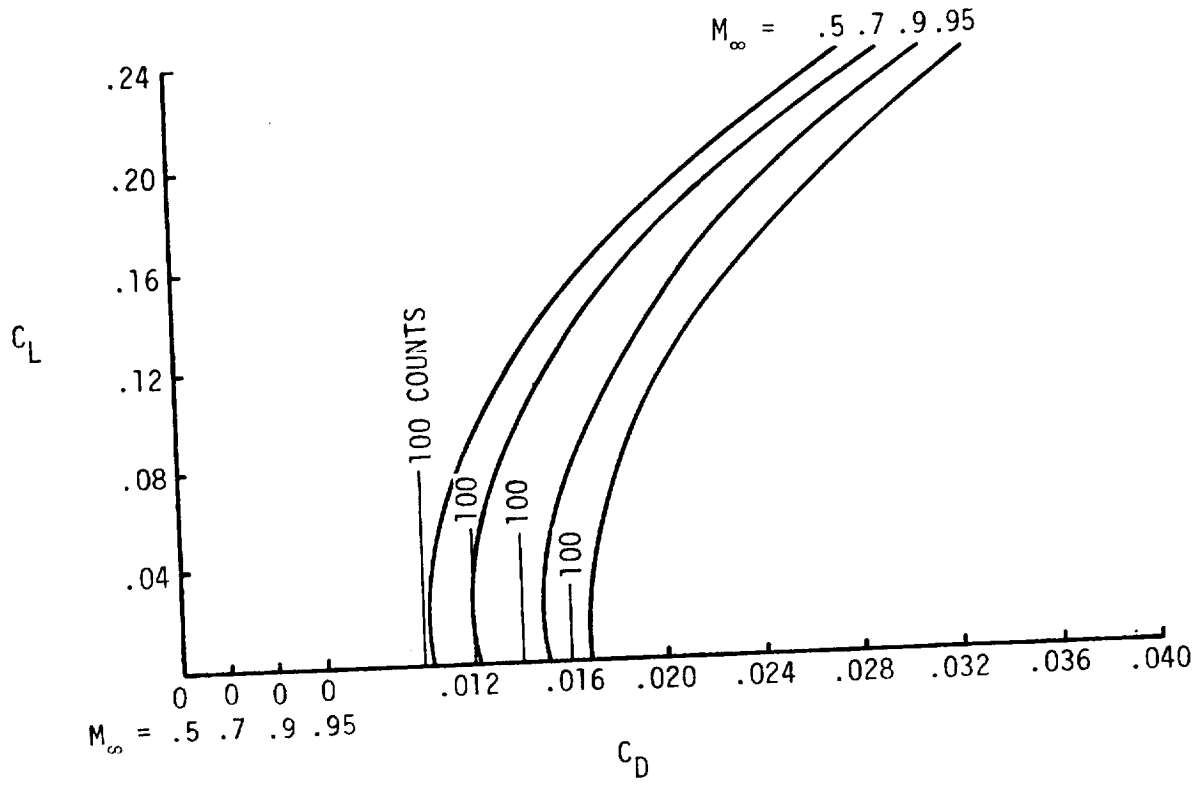

Figure 65. - SSXJET III subsonic/transonic polars.

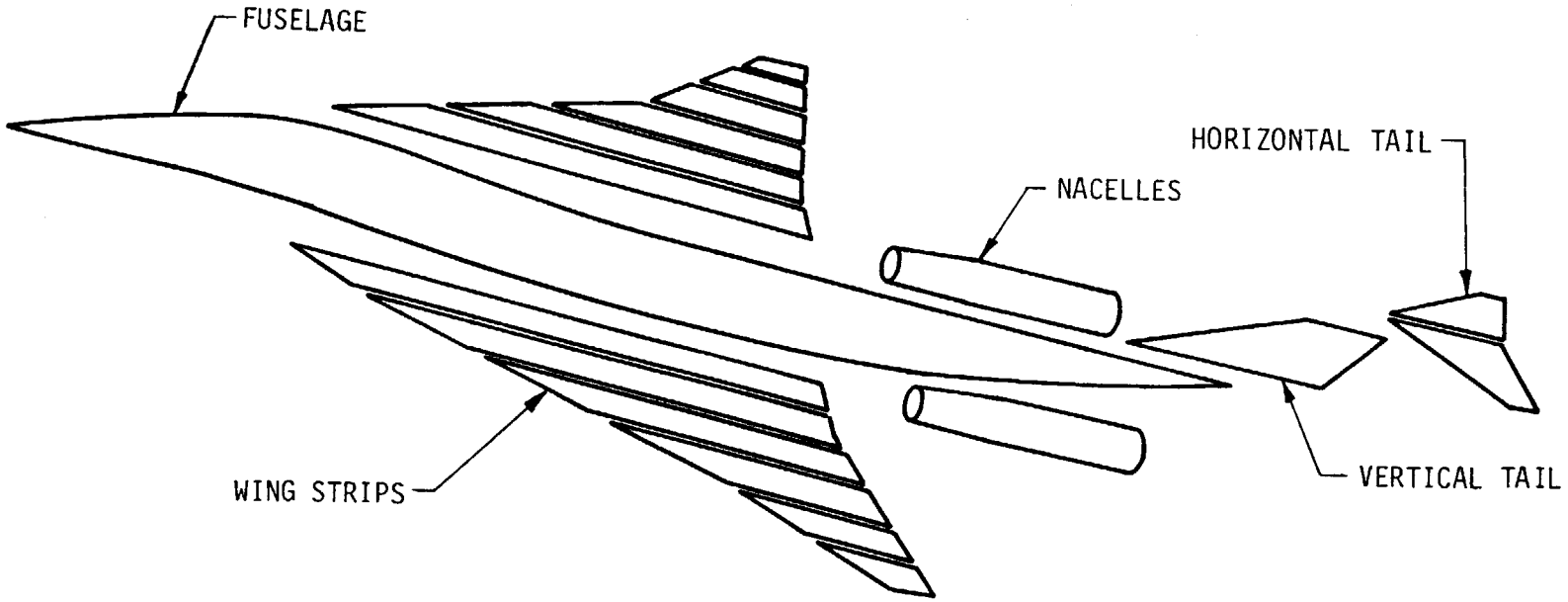

Figure 66. - Configuration breakdown for skin friction calculation.

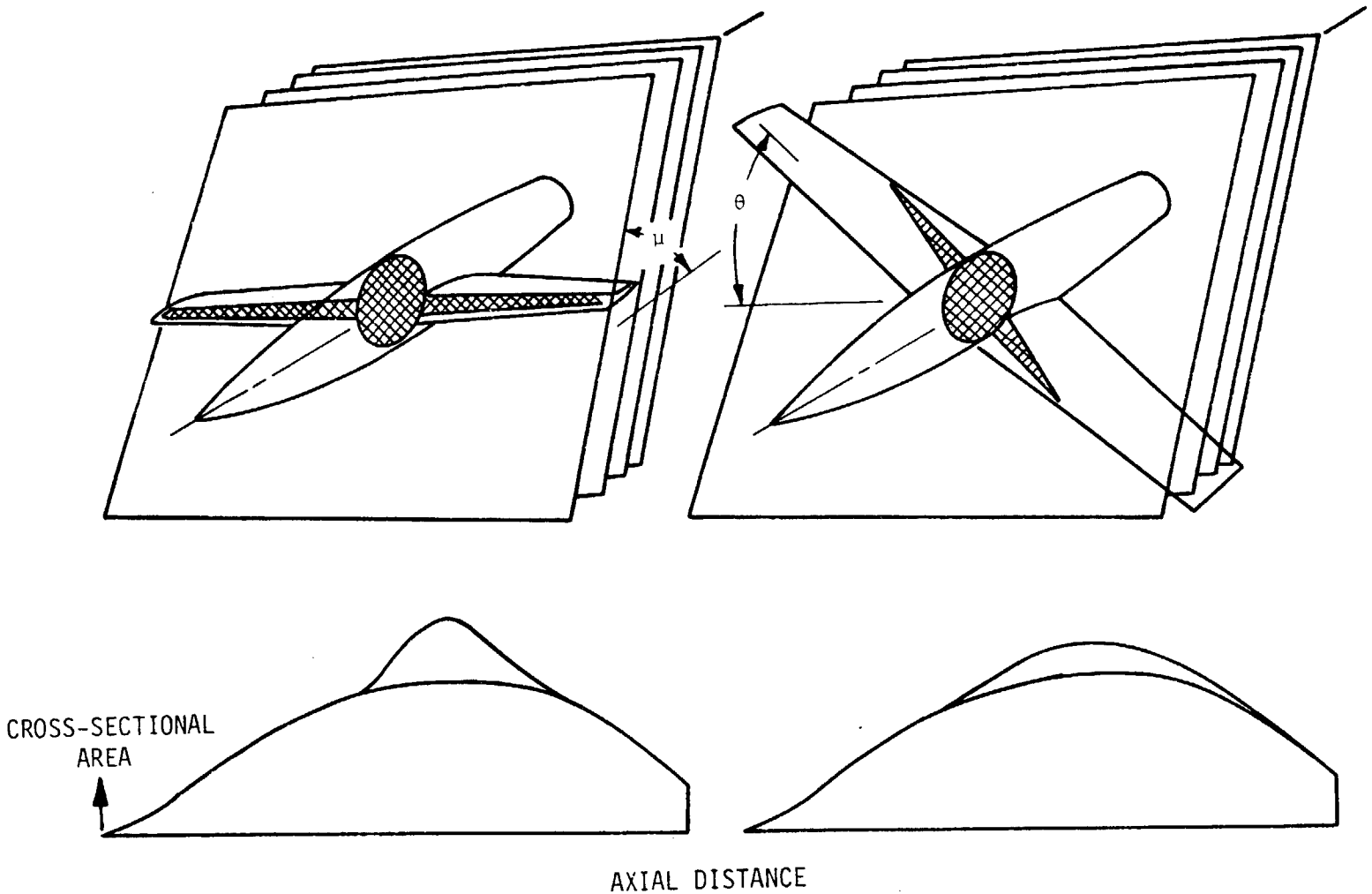

Figure 67. - Illustration of procedure for determining area developments related to wave drag at supersonic Mach numbers.

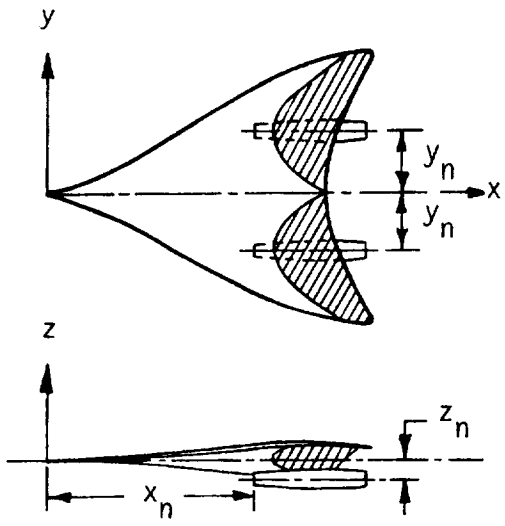

(b) Modeling of the nacelle-wing interference problem. Shaded areas represent interference regions.

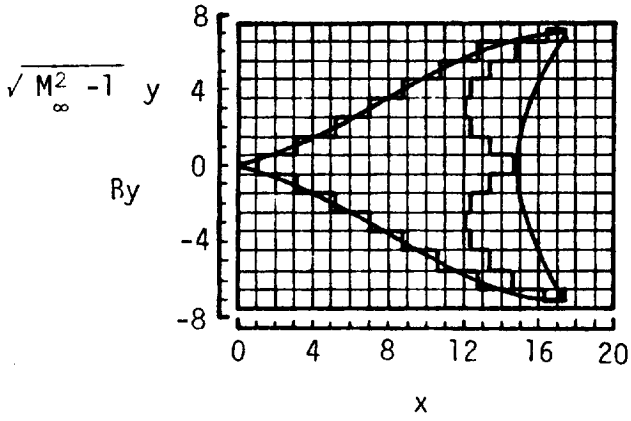

(a) Grid system for nacelle interference and wing analysis computations.

Figure 68. - Nacelle interference and wing analysis techniques.

Figure 69. - Douglas model installed in the 4 x 7 tunnel at the NASA-AMES Research Center

.015 Scale Douglas AST model

—— Theory

o Test

S_{ref} = .209 m^2 (324 in^2)

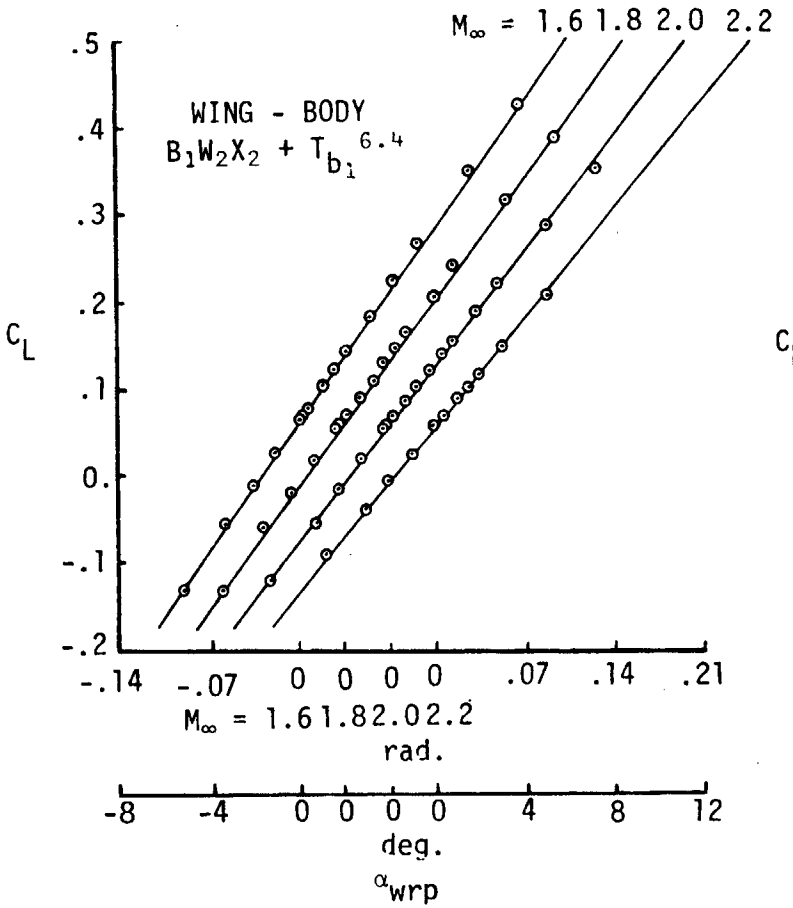

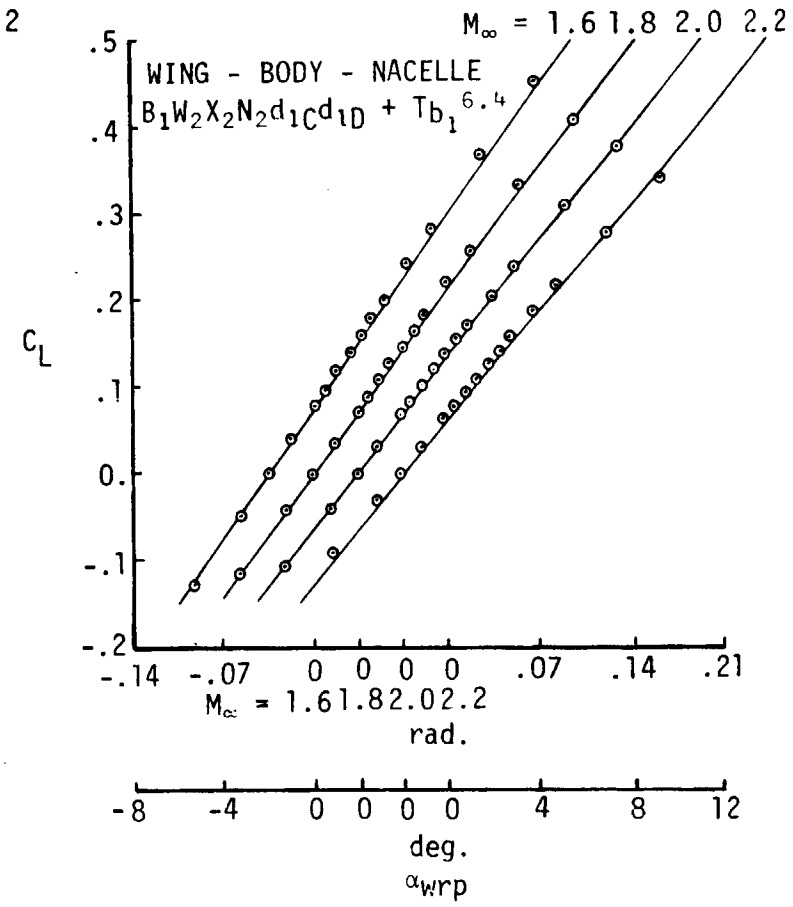

Figure 70. - Lift correlation for Douglas AST model.

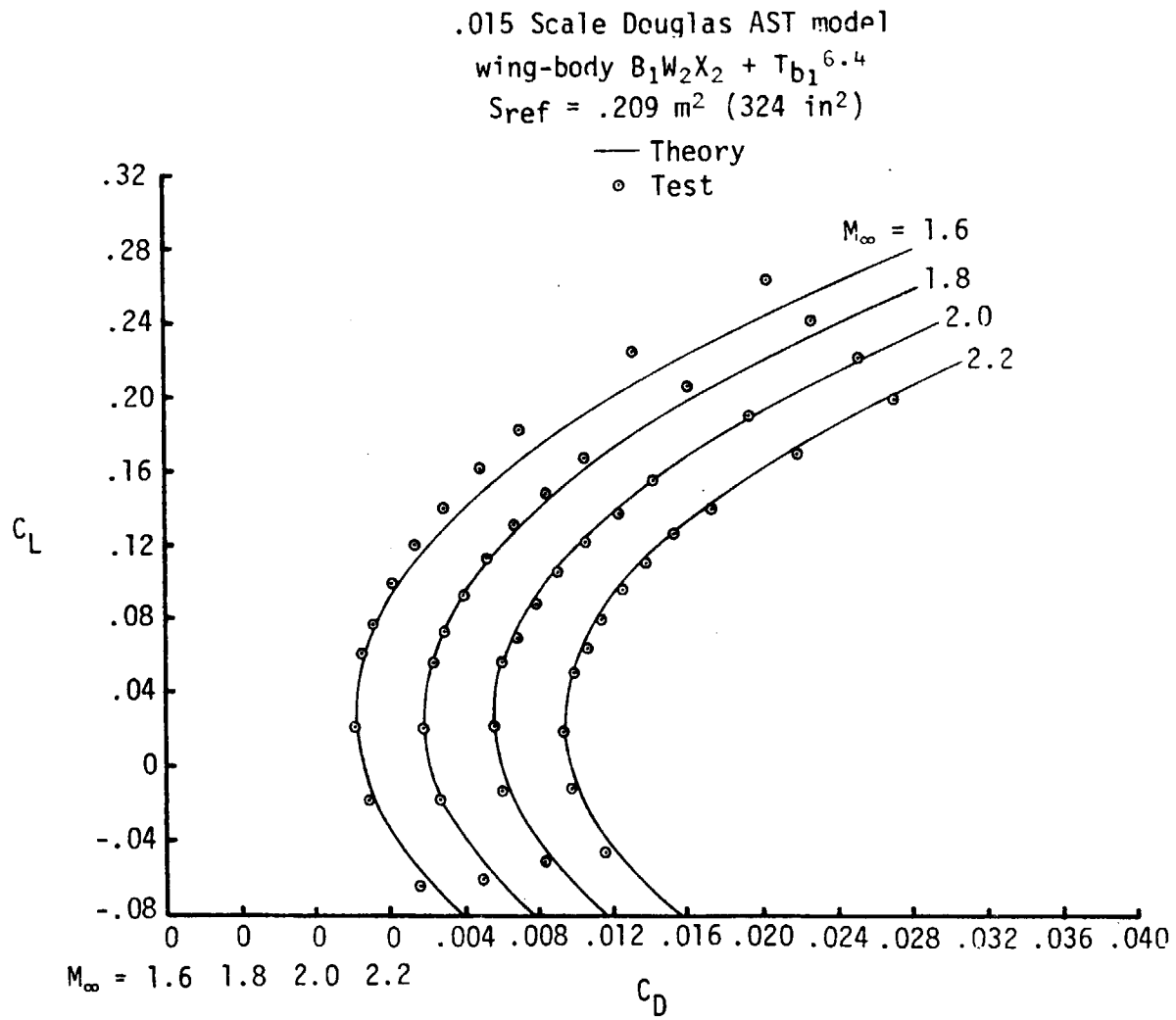

Figure 71. - Drag correlation for the wing-body configuration.

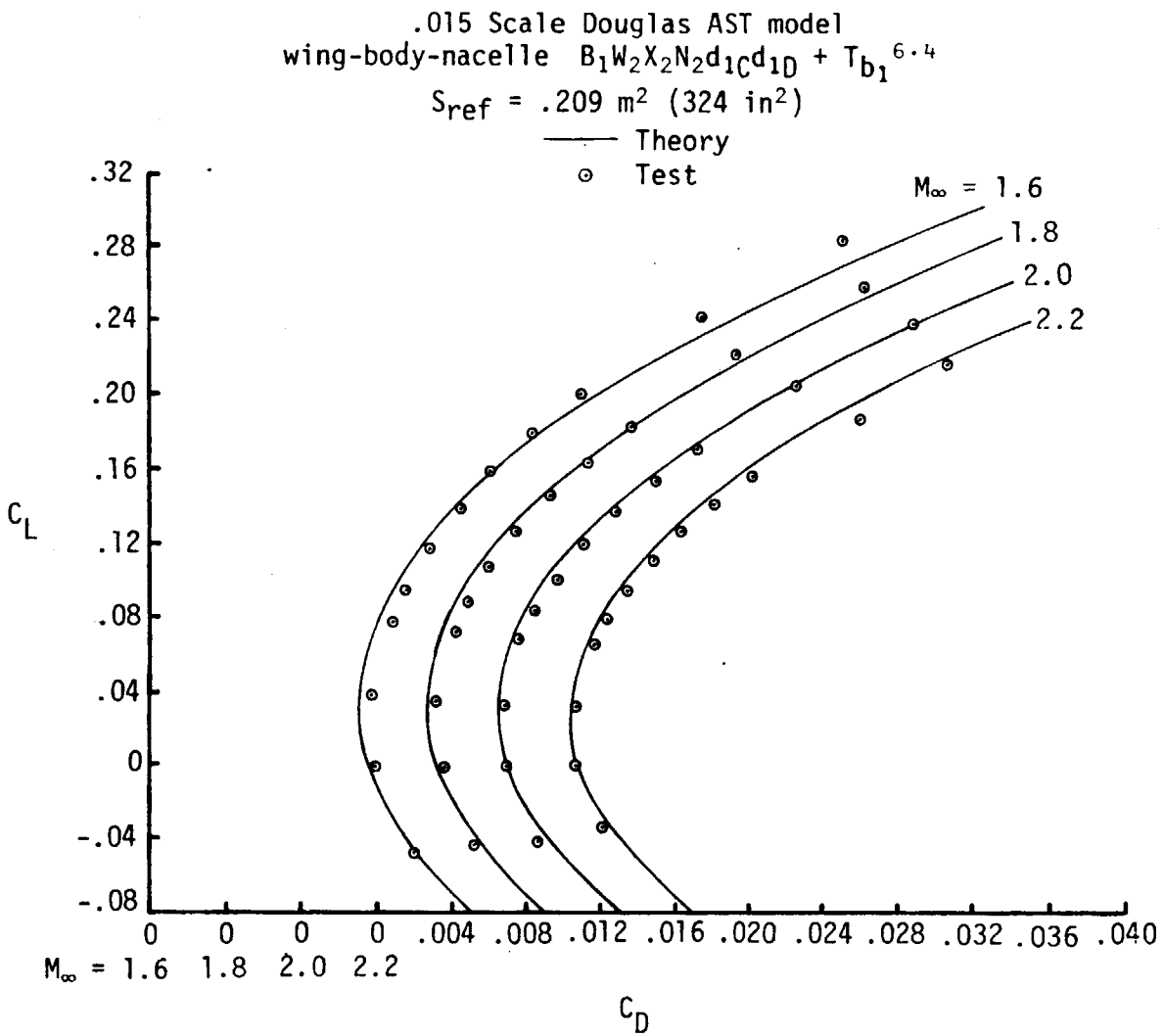

Figure 72. - Drag correlation for the wing-body-nacelle configuration.

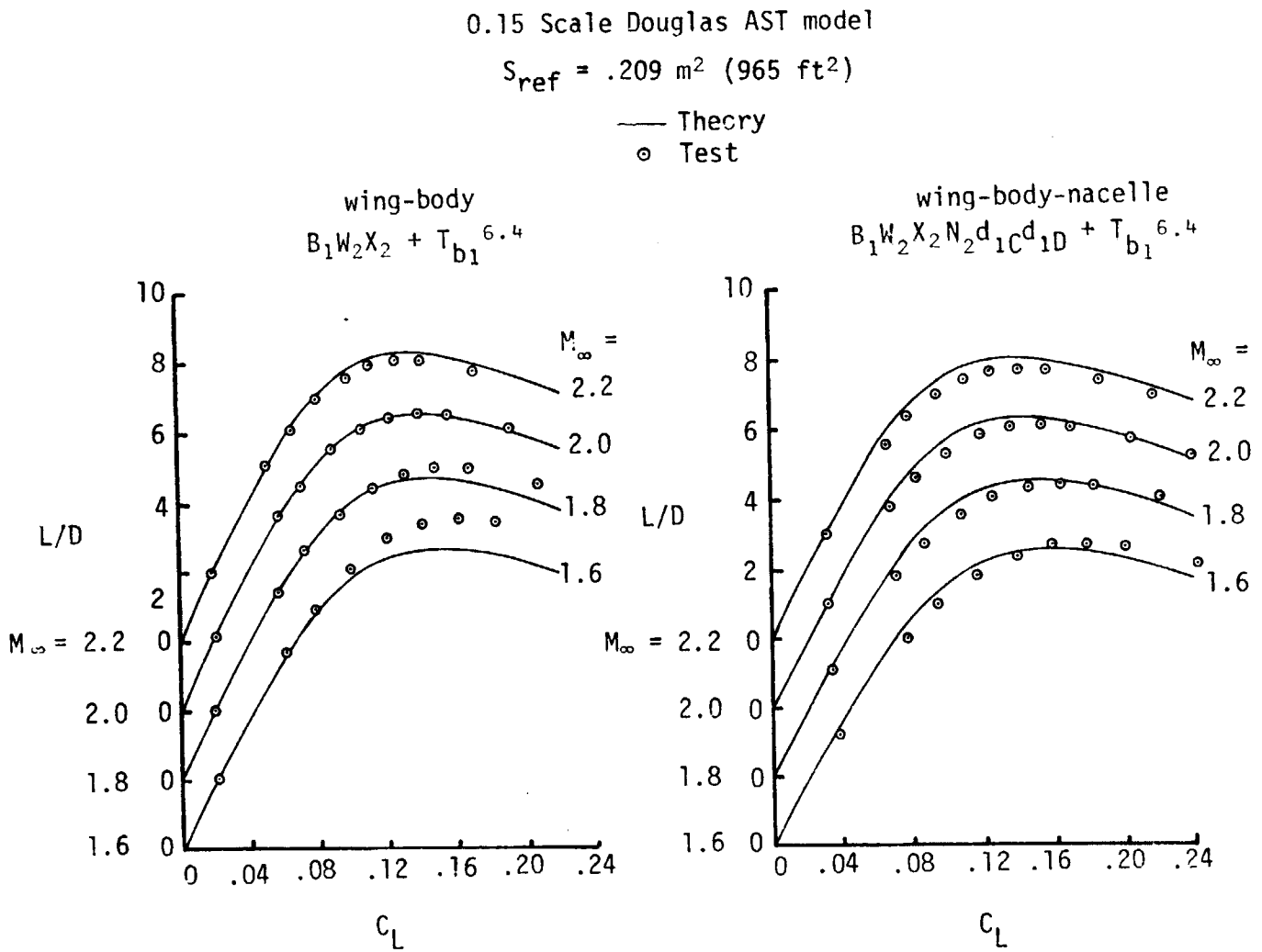

Figure 73. - L/D correlations for the Douglas model.

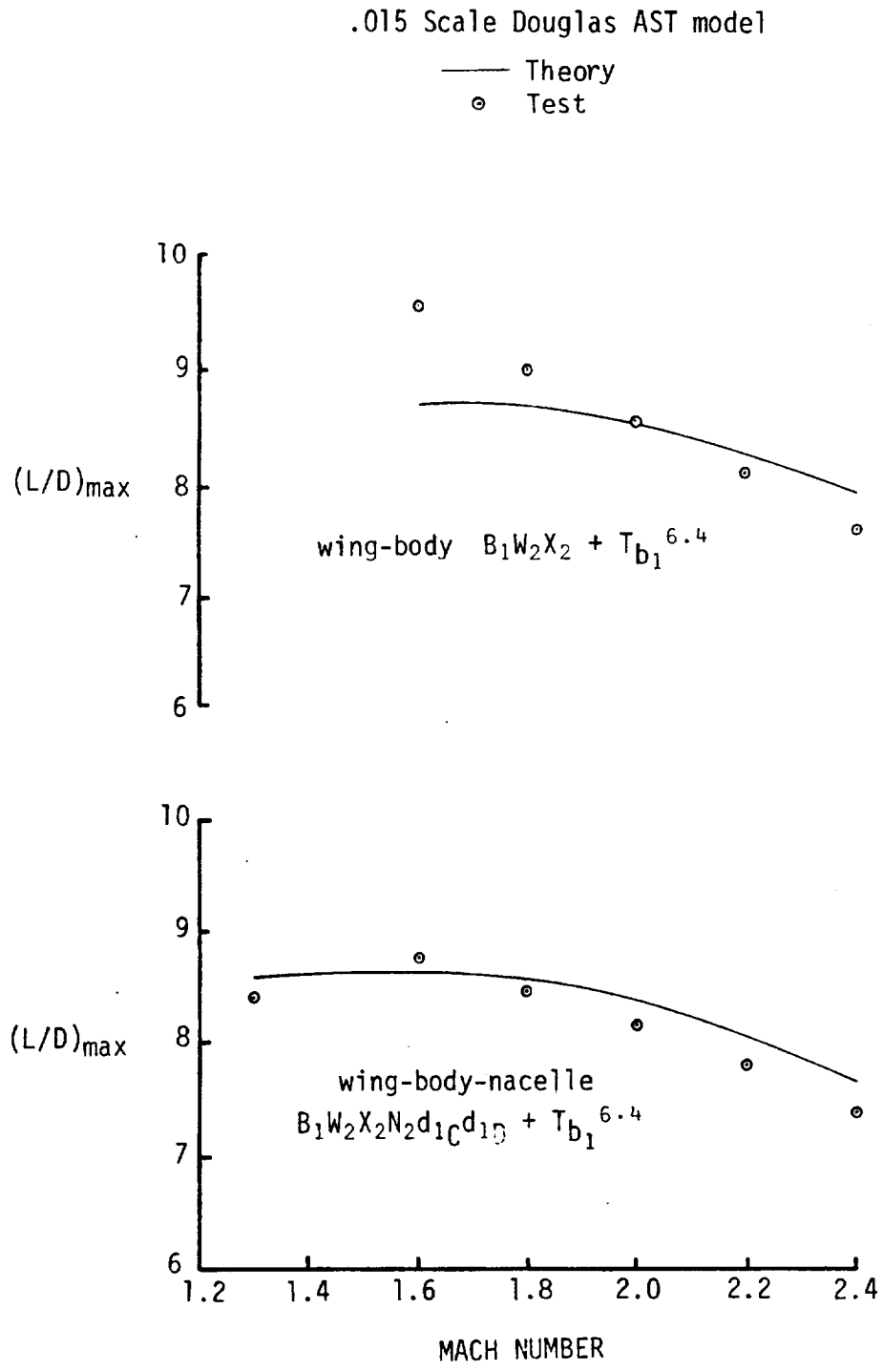

Figure 74. - Correlation of maximum lift-to-drag ratio performance for the Douglas model.

SSXJET

S_{ref} = 89.65 m^2 (965 ft^2)

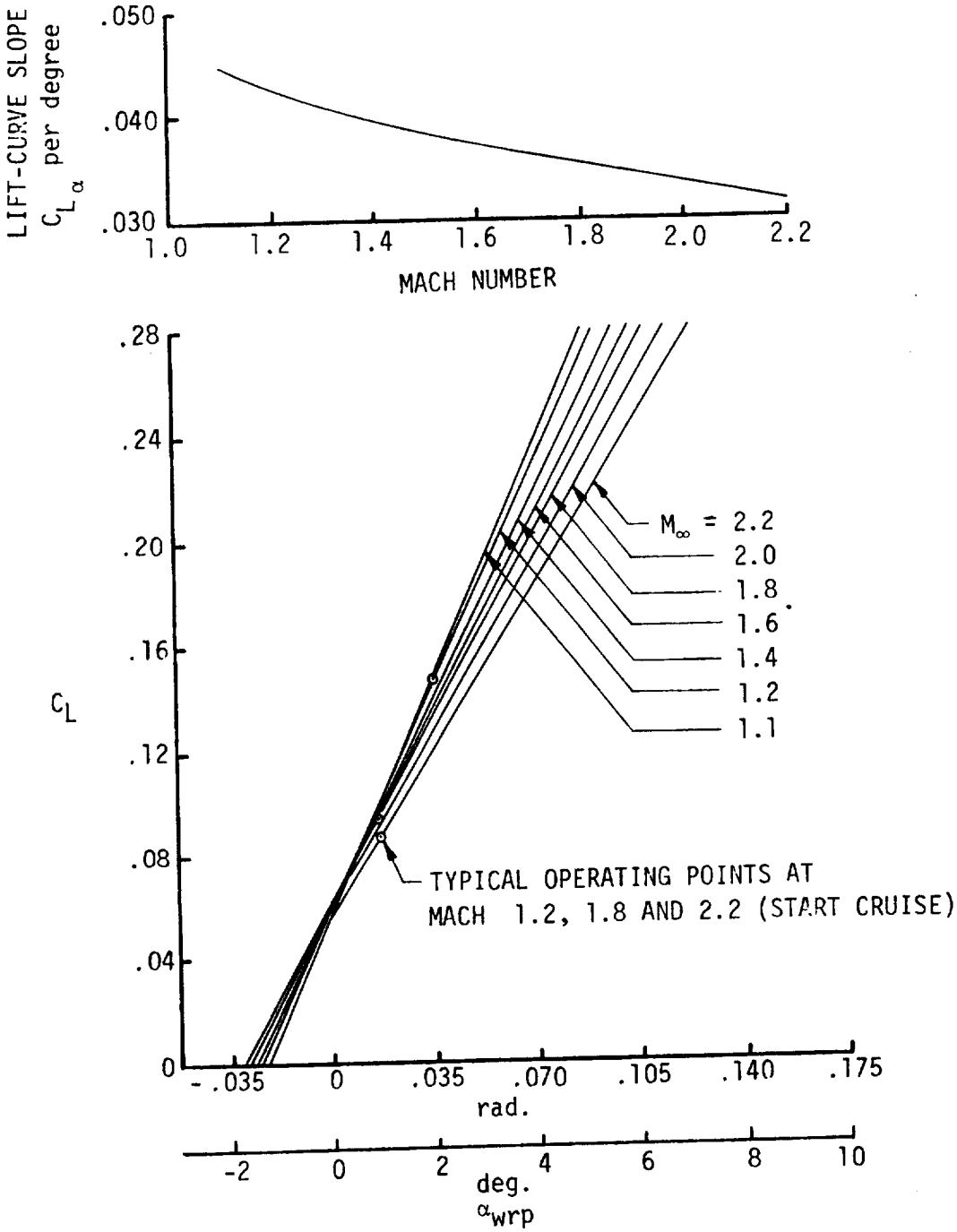

Figure 75. - SSXJET lift characteristics.

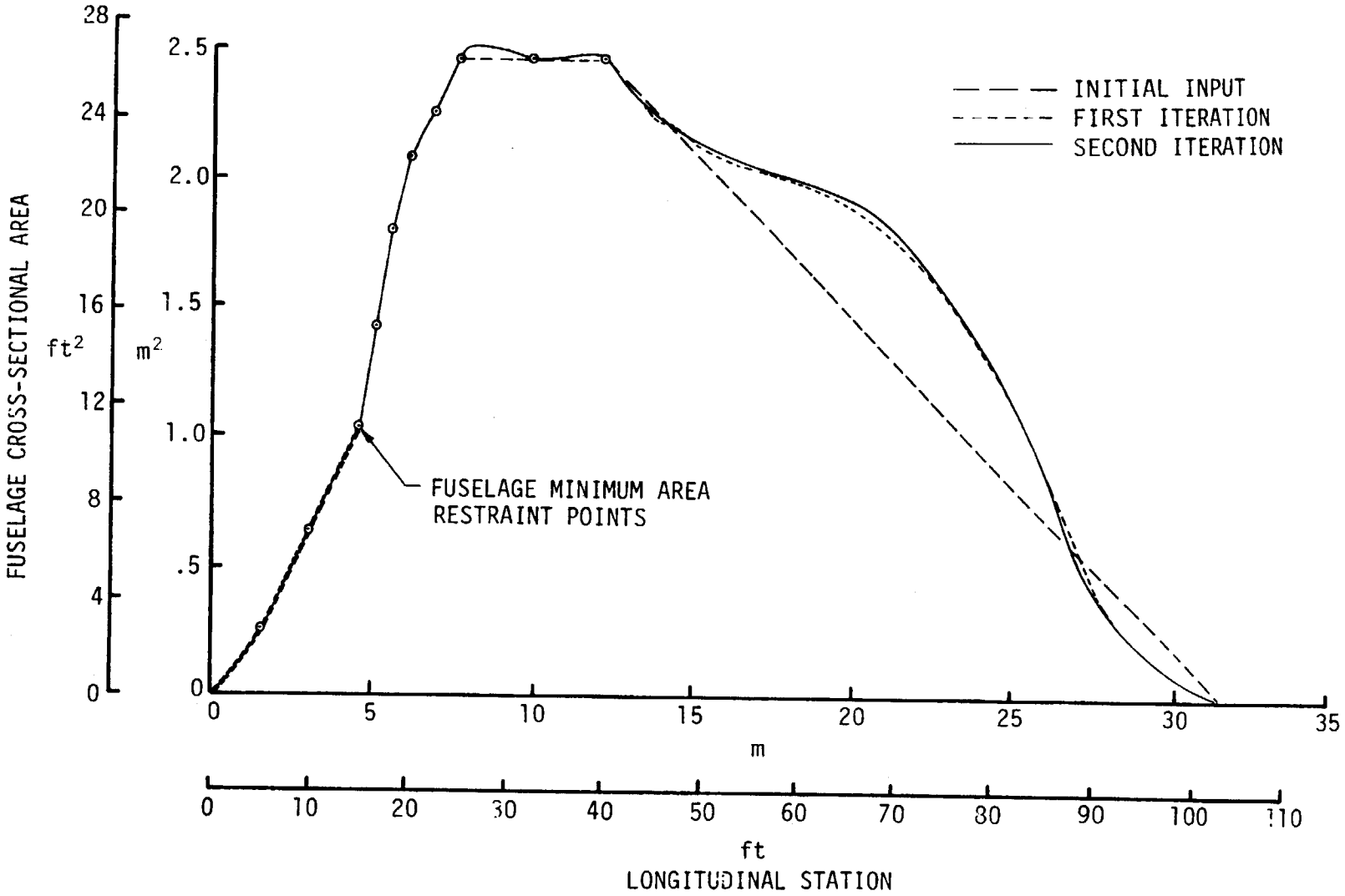

Figure 76. - SSXJET Fuselage optimization

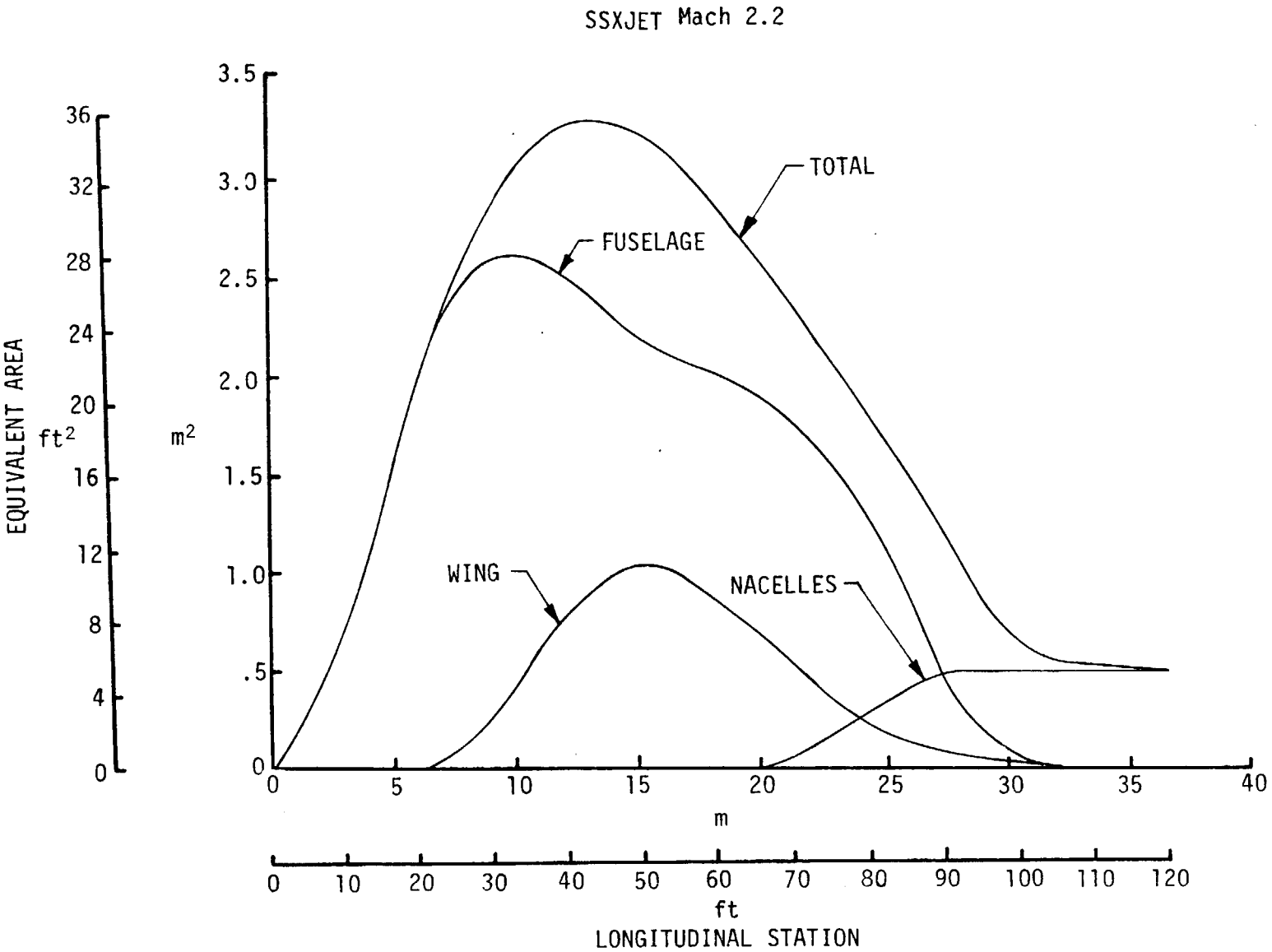

Figure 77. - SSXJET Mach 2.2 equivalent area distribution

SSXJET

S_{ref} = 89.65 m^2 (965 ft^2)

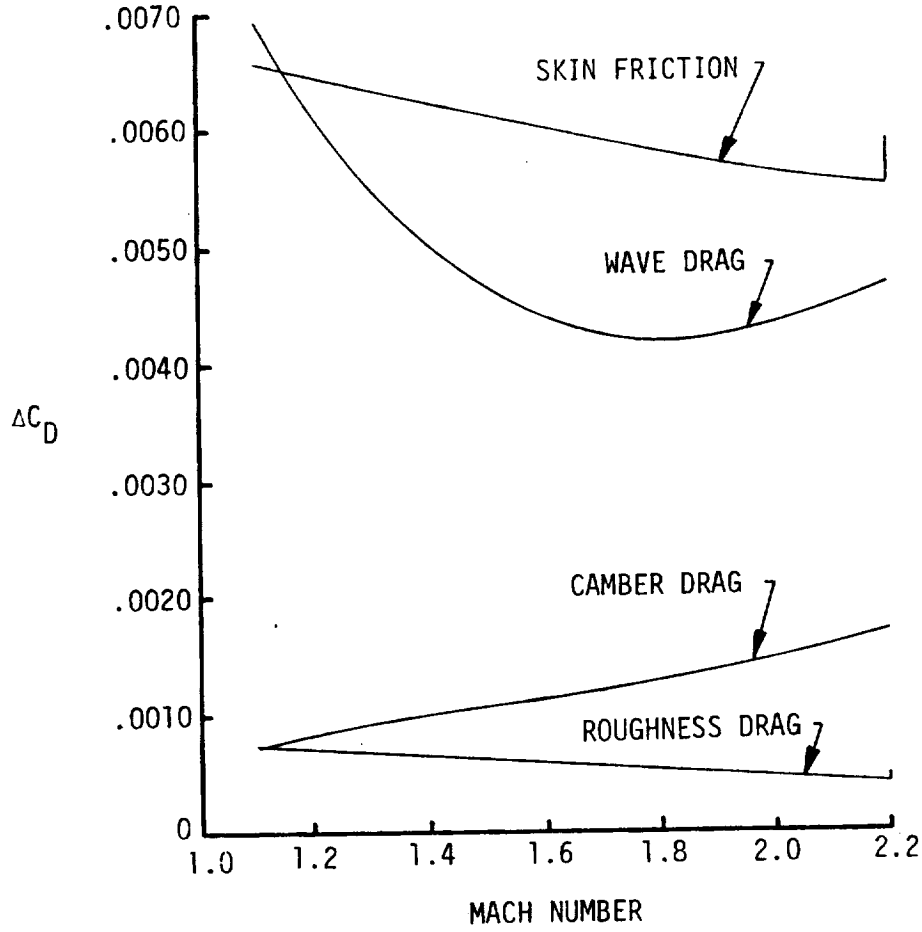

Figure 78. - SSXJET zero-lift drag components

SSXJET

$M_\infty = 2.2$ $N\theta = 16$

$S_{ref} = 89.65\ m^2\ (965\ ft^2)$

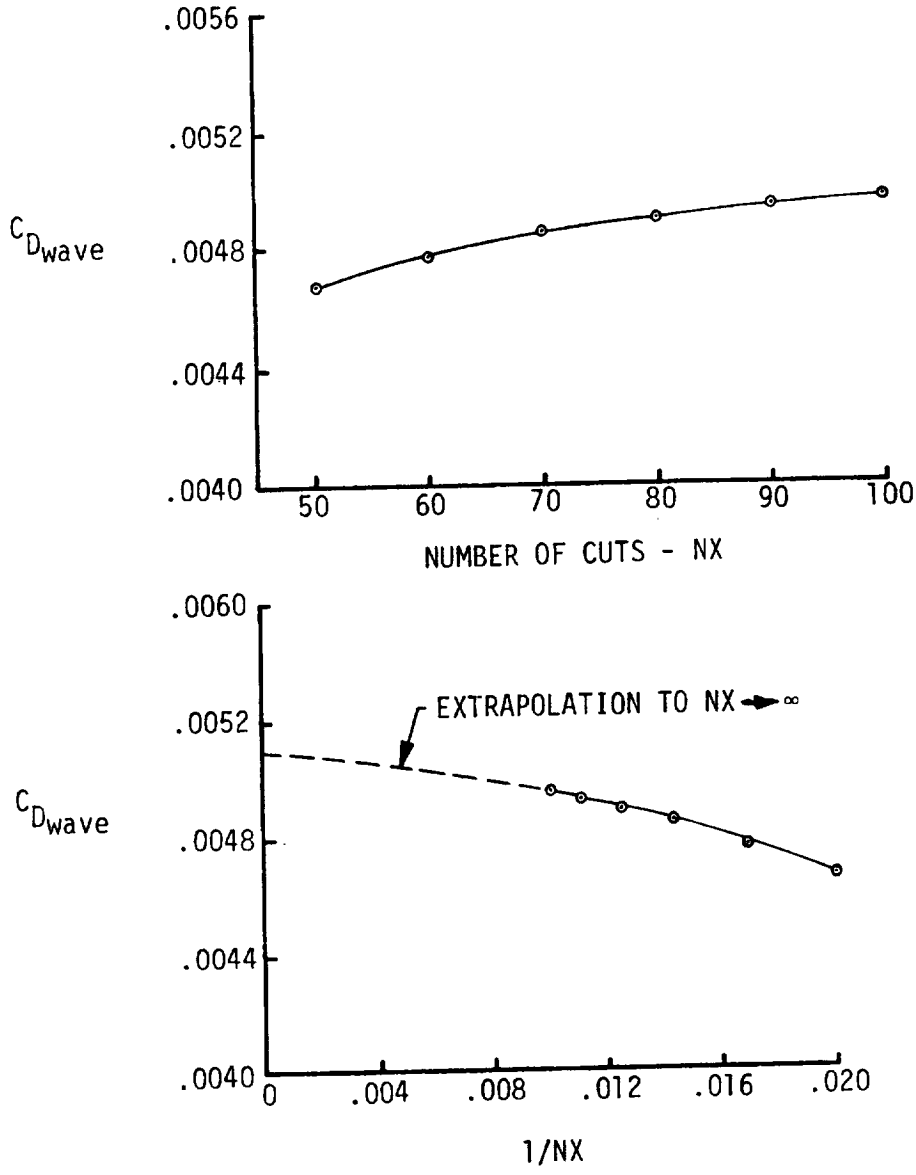

Figure 79. - Convergence characteristics of the FAR-field wave drag method.

SSXJET

Two engines
S_{ref} = 89.65 m^2 (965 ft^2)

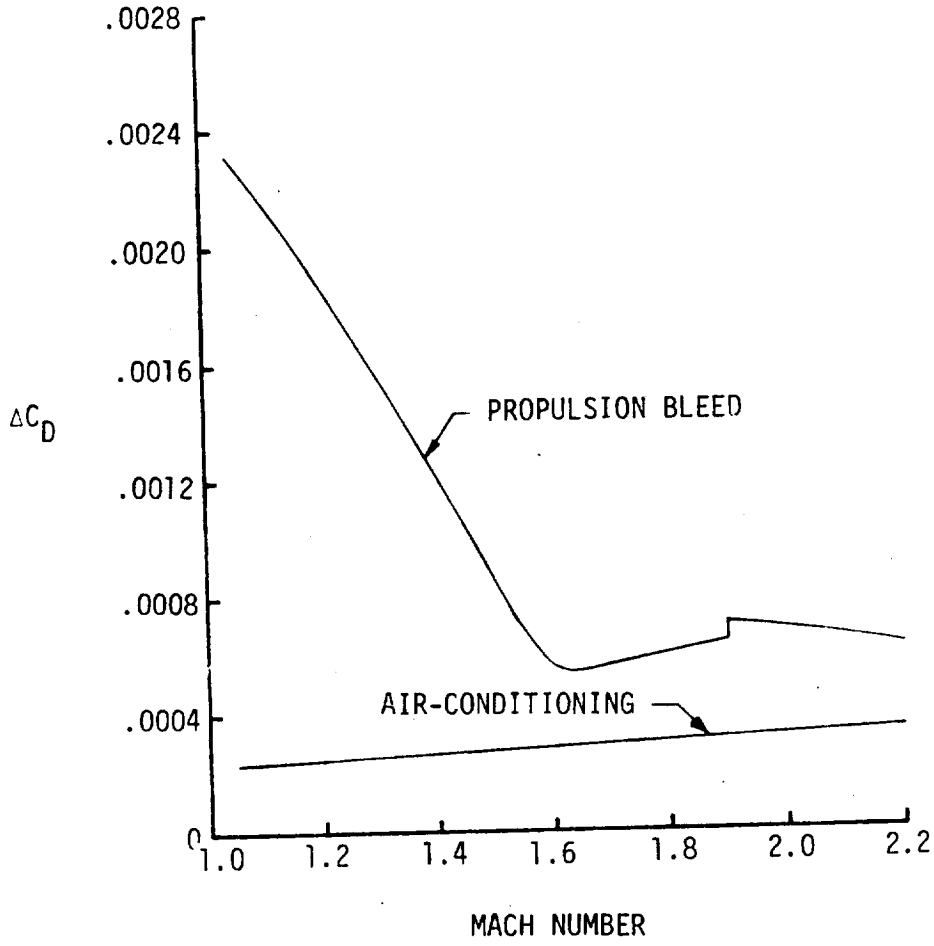

Figure 80. - Propulsion bleed and air conditioning drag.

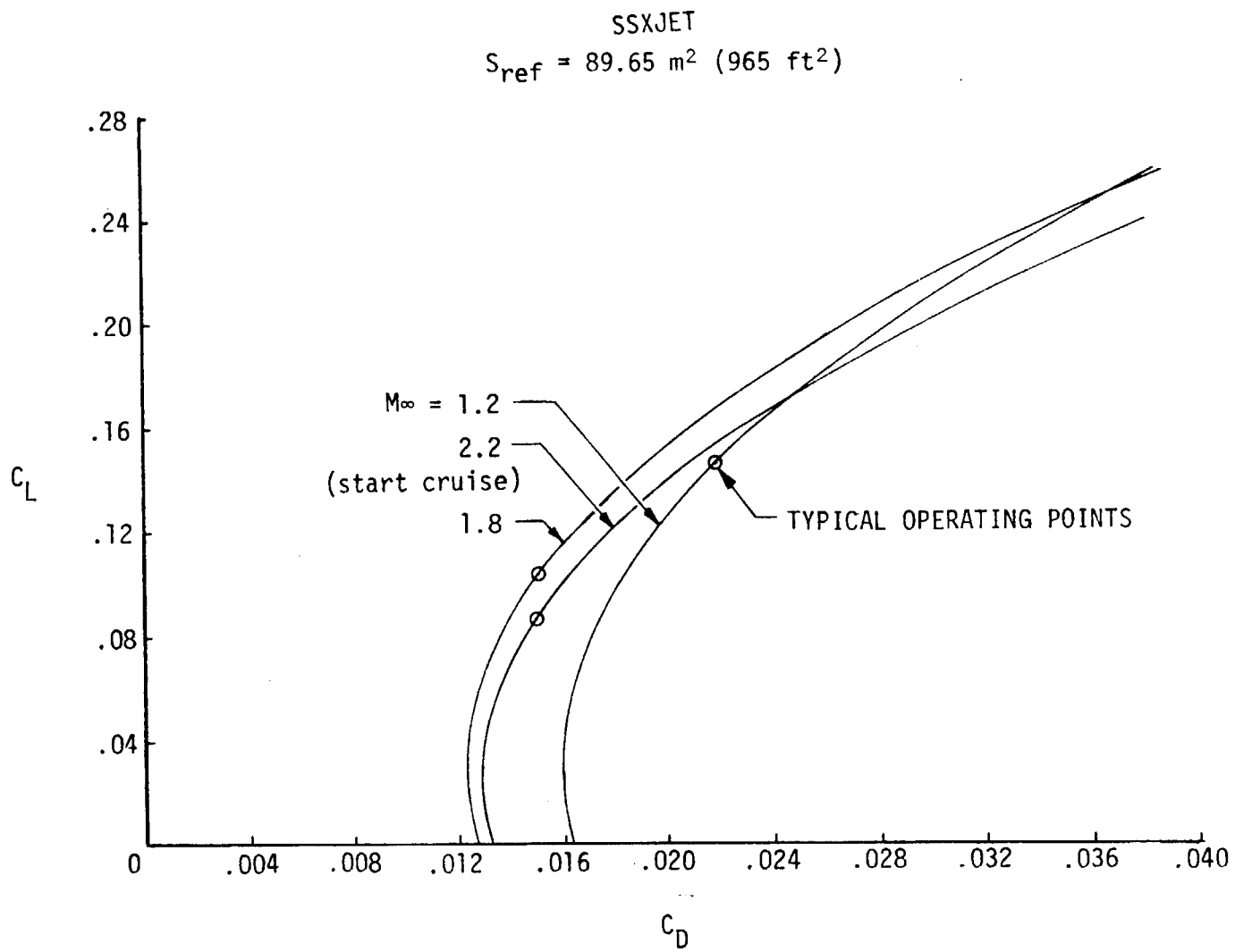

Figure 81. - SSXJET drag polars

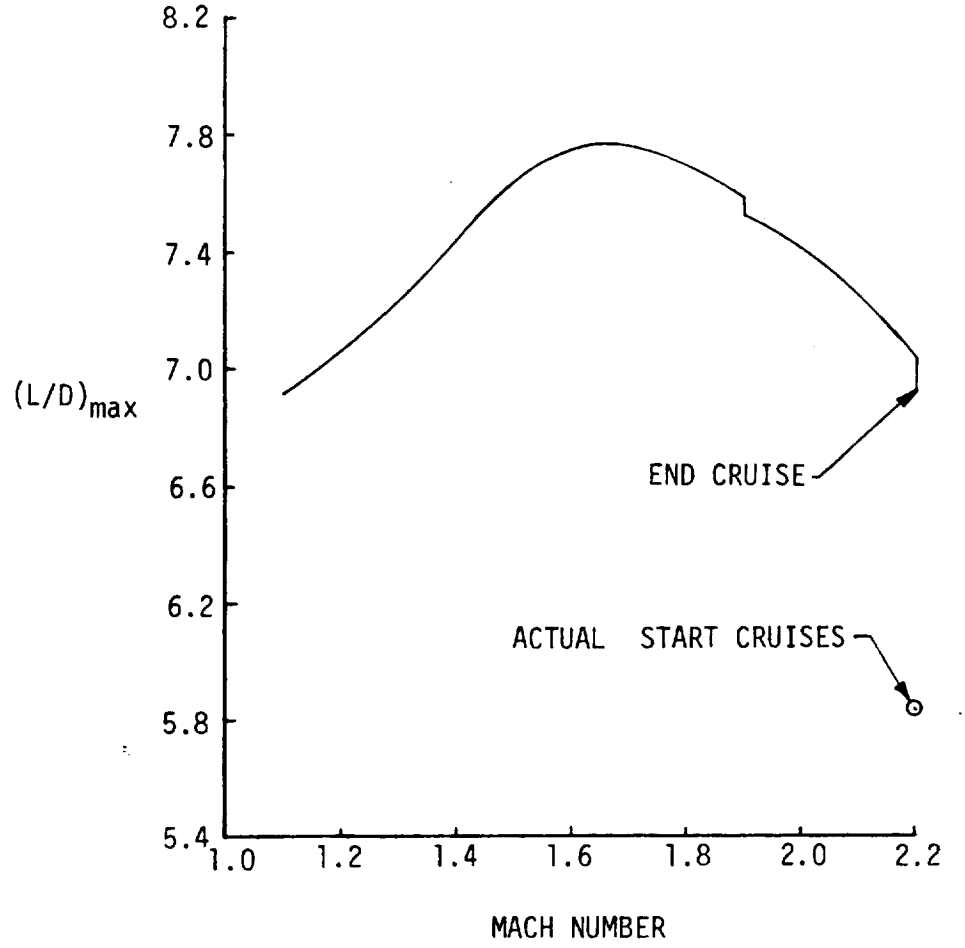

Figure 82. - SSXJET $(L/D)_{max}$ performance.

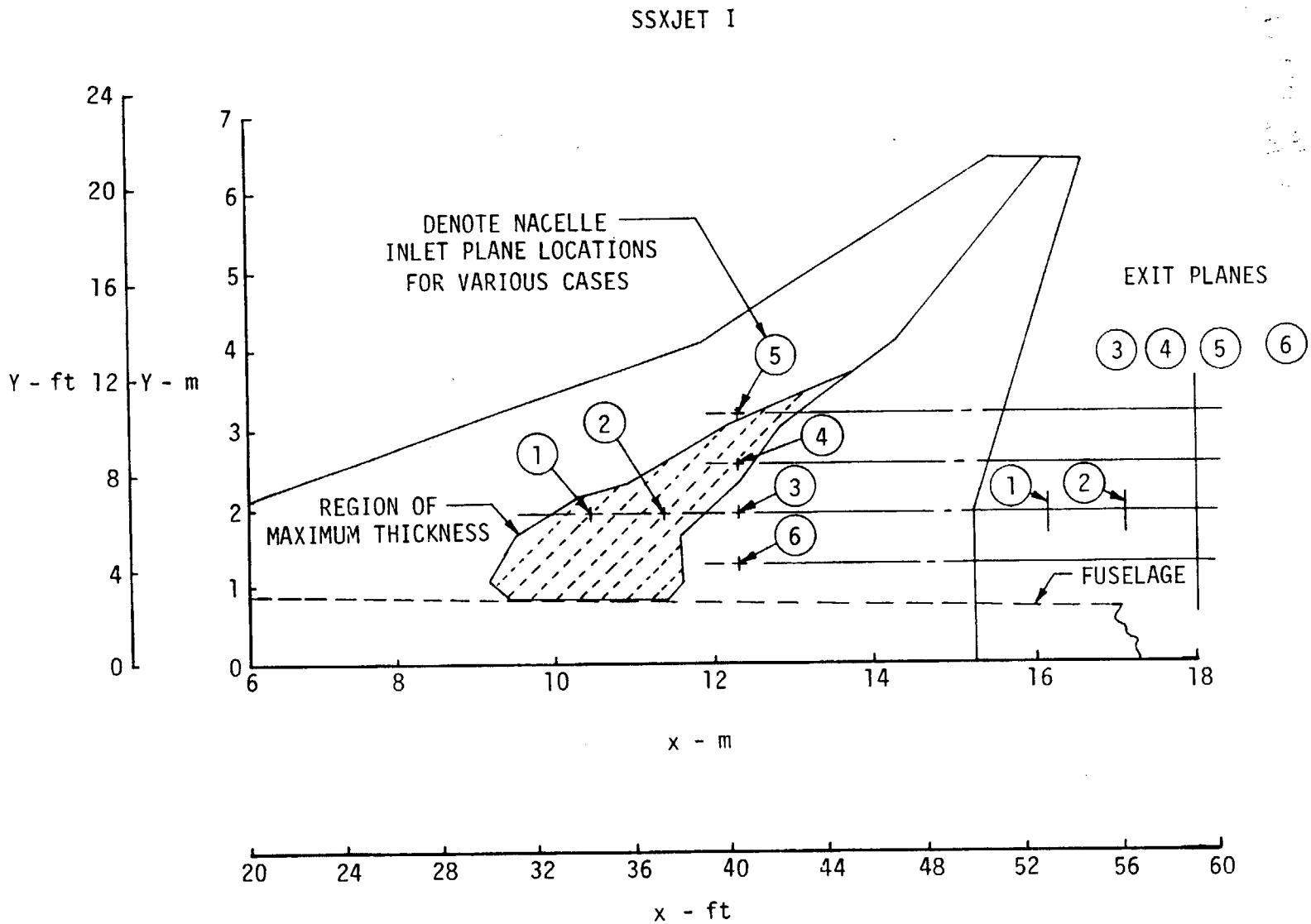

Figure 83. - Case definition for SSXJET I nacelle location study.

SSXJET I

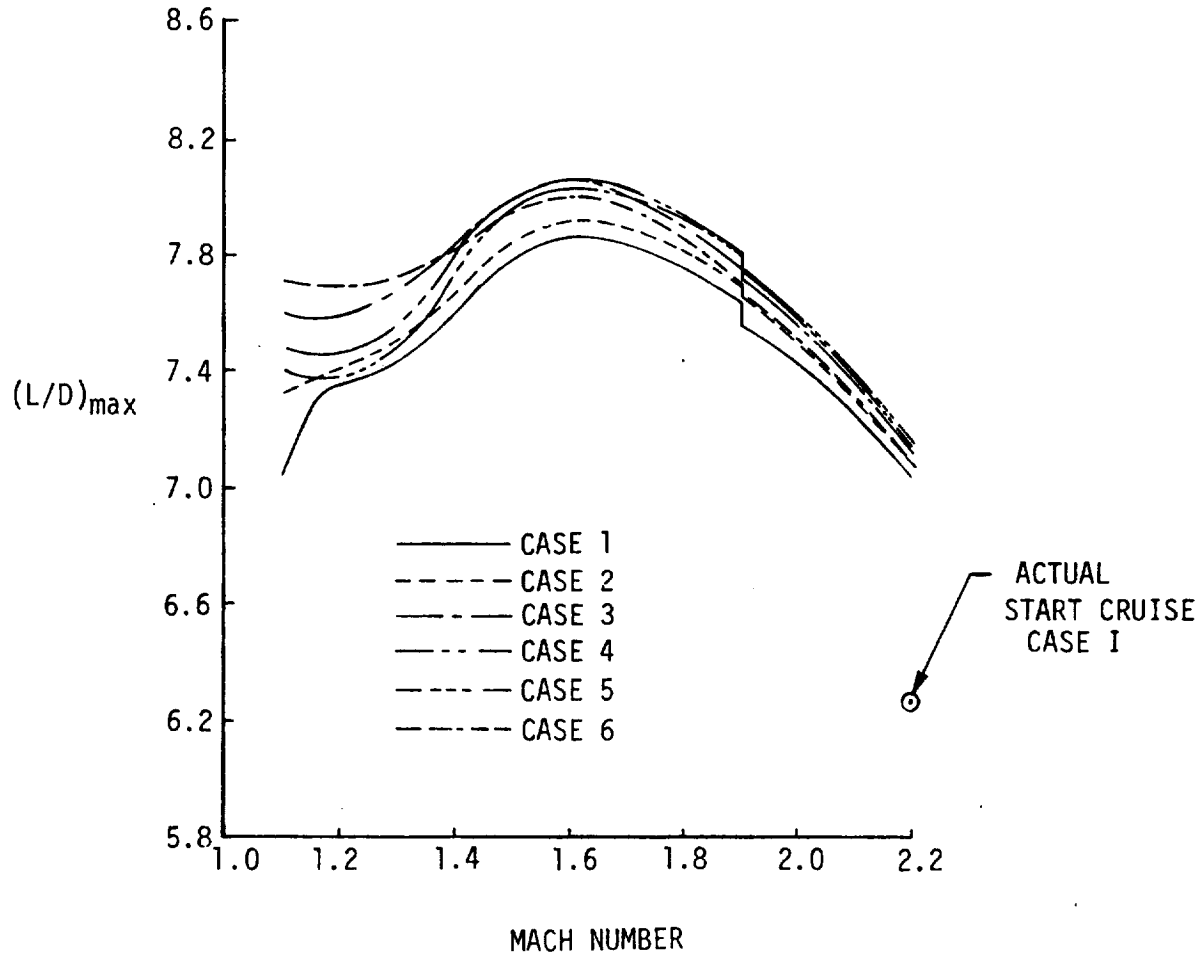

Figure 84. - $(L/D)_{max}$ performance for various SSXJET I configurations.

SSXJET I

S_{ref} = 89.65 m^2 (965 ft^2)

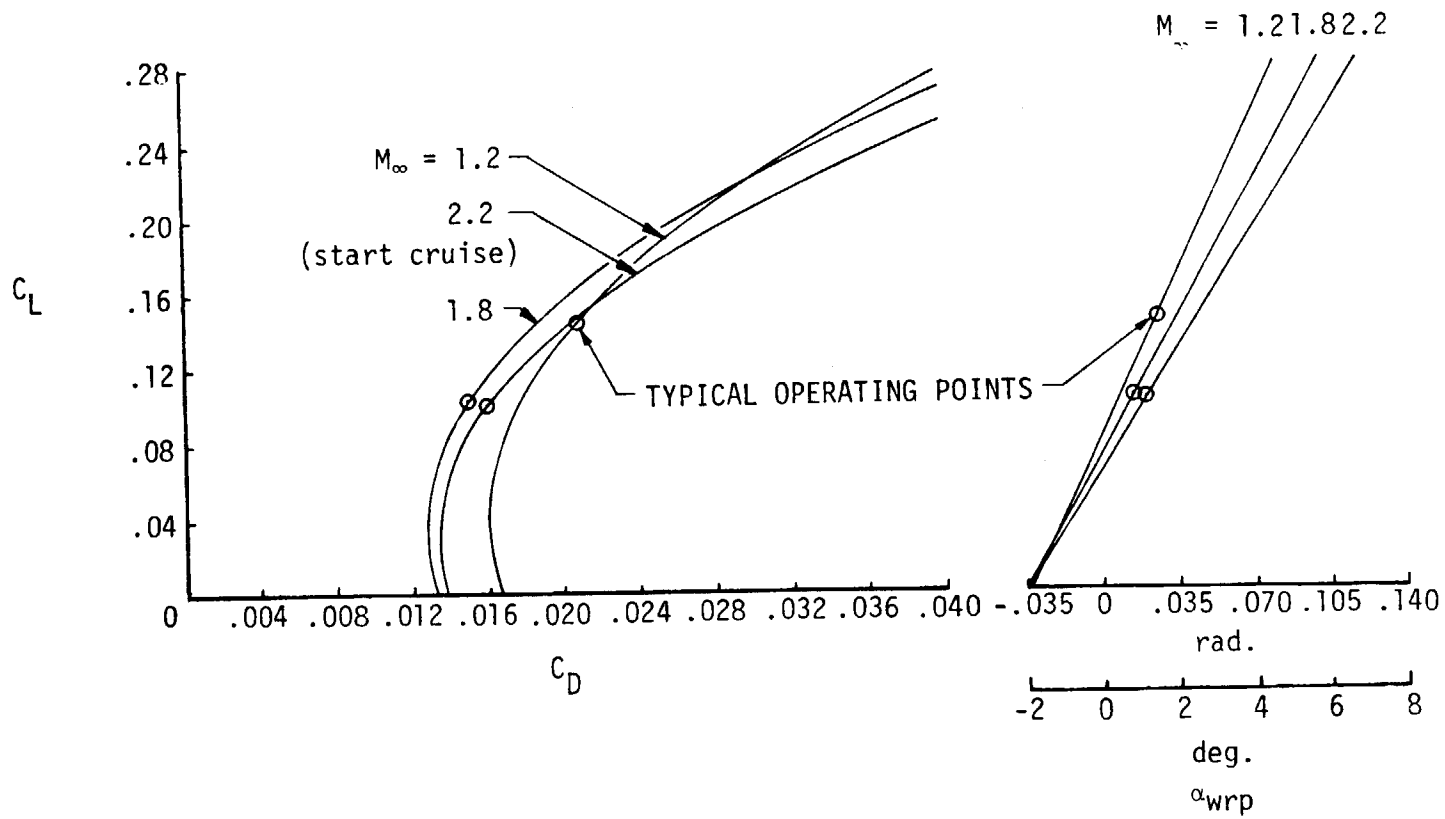

Figure 85. - Lift-drag summary for SSXJET I.

SSXJET II

S_{ref} = 89.65 m^2 (965 ft^2)

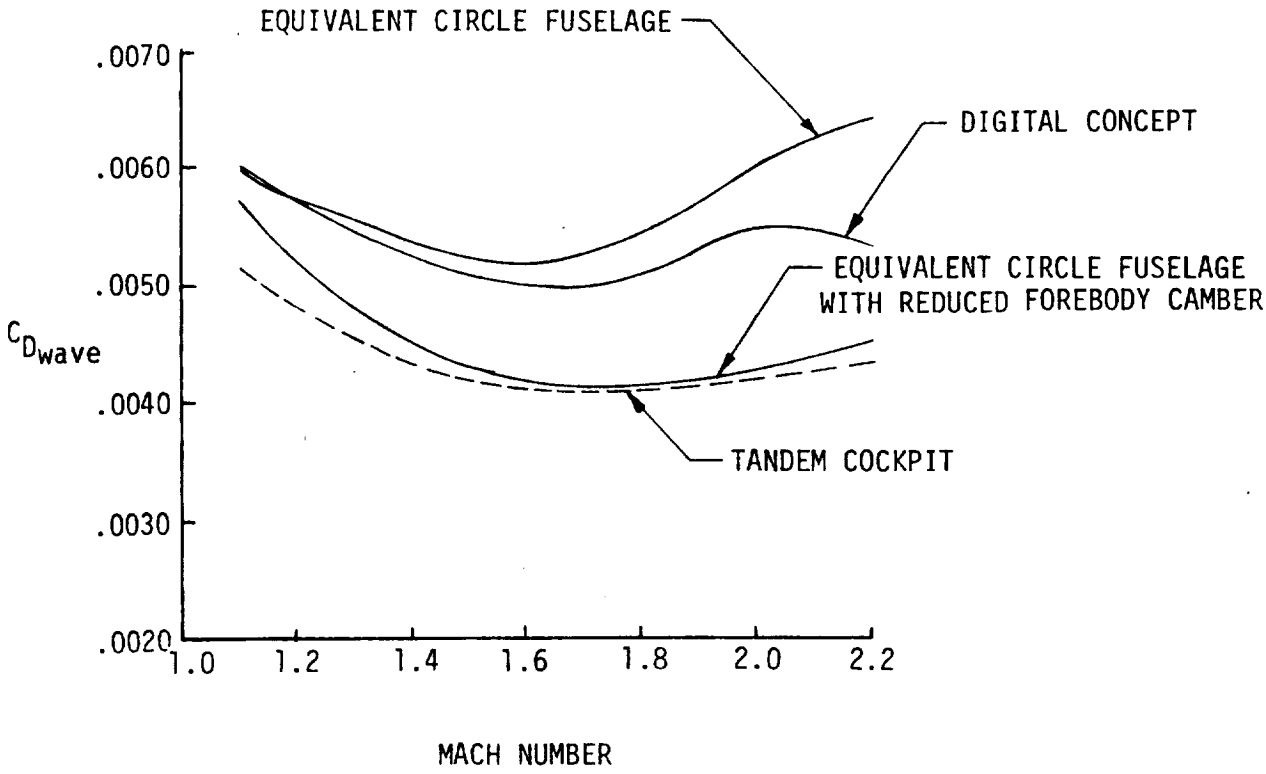

Figure 86. - SSXJET II wave drag analysis.

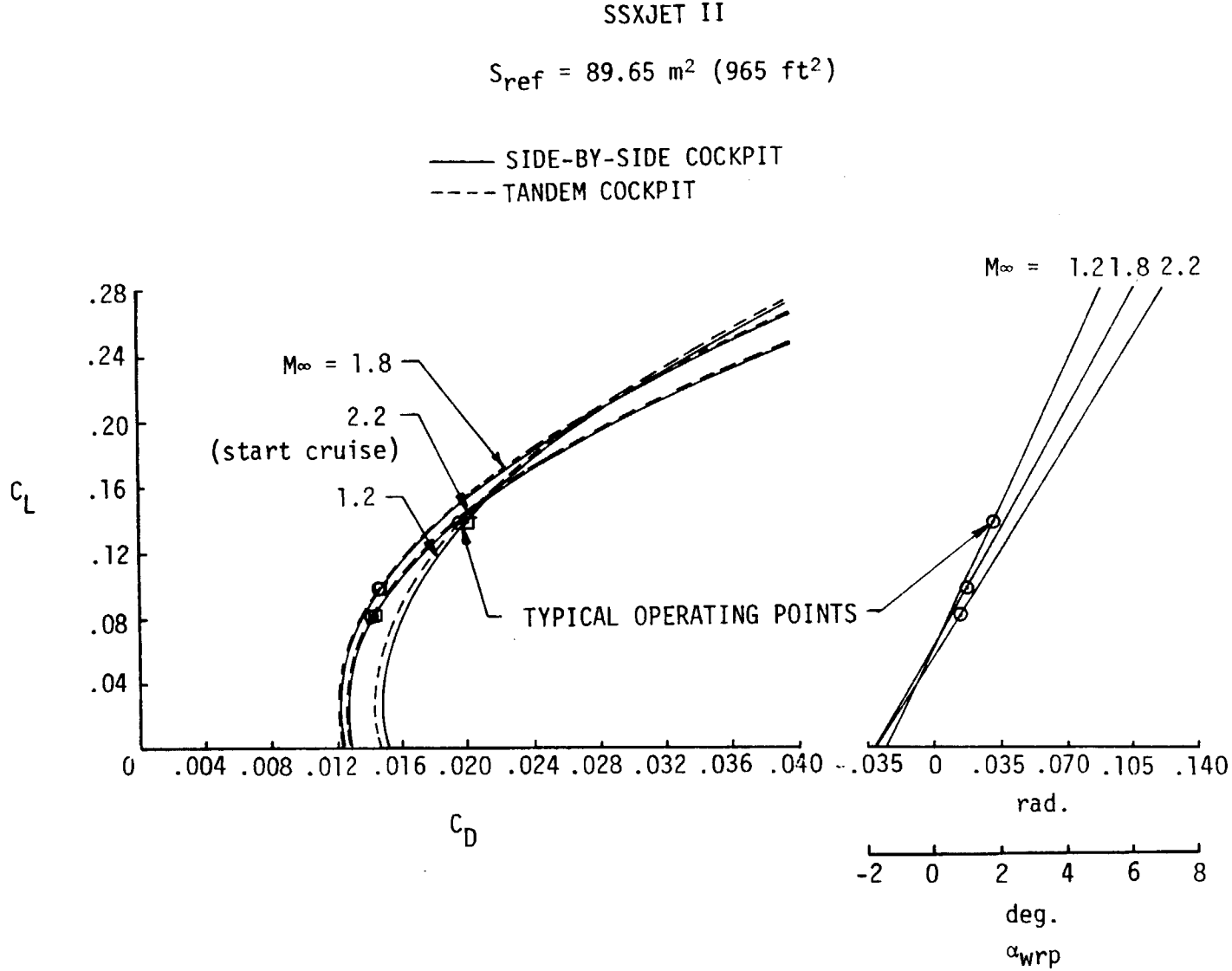

Figure 87. - SSXJET II lift-drag summary

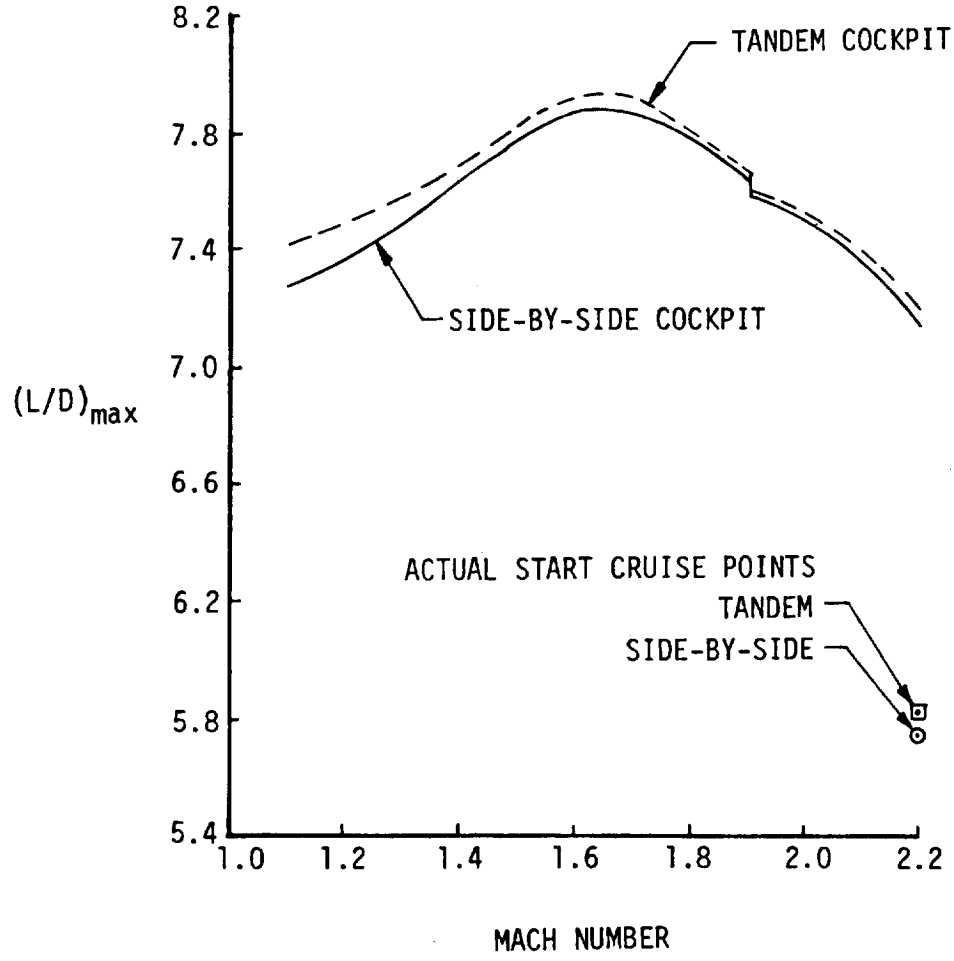

Figure 88. - Maximum L/D performance for the SSXJET II concepts.

SSXJET III

GE21/J11-B10 ENGINES

S_{ref} = 104.98 m^2 (1130 ft^2)

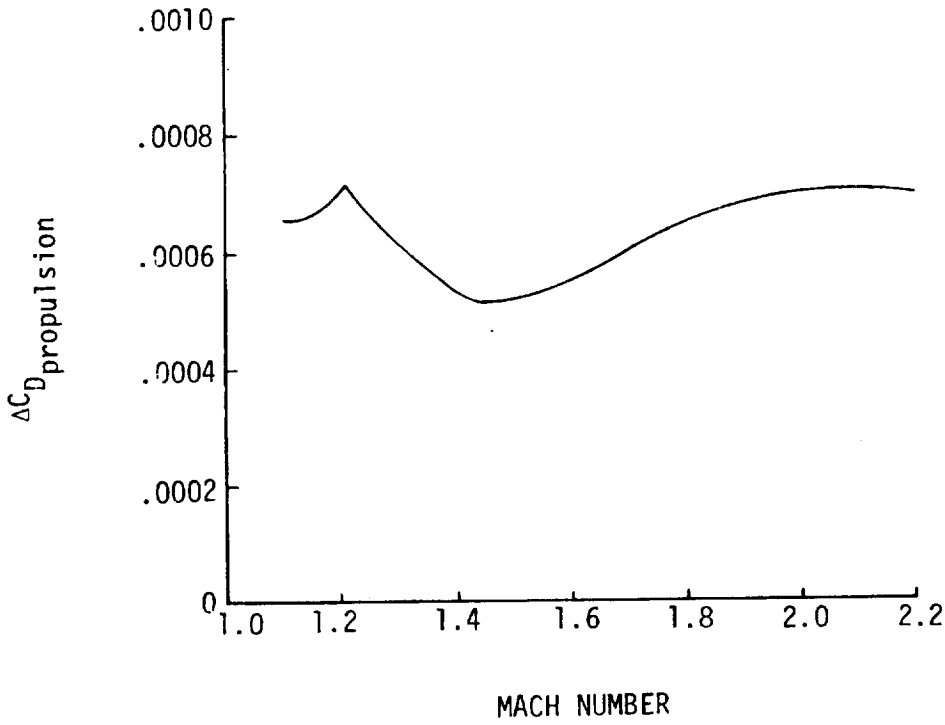

Figure 89. - Additive propulsion drag for the SSXJET III

SSXJET III

S_{ref} = 104.98 m^2 (1130 ft^2)

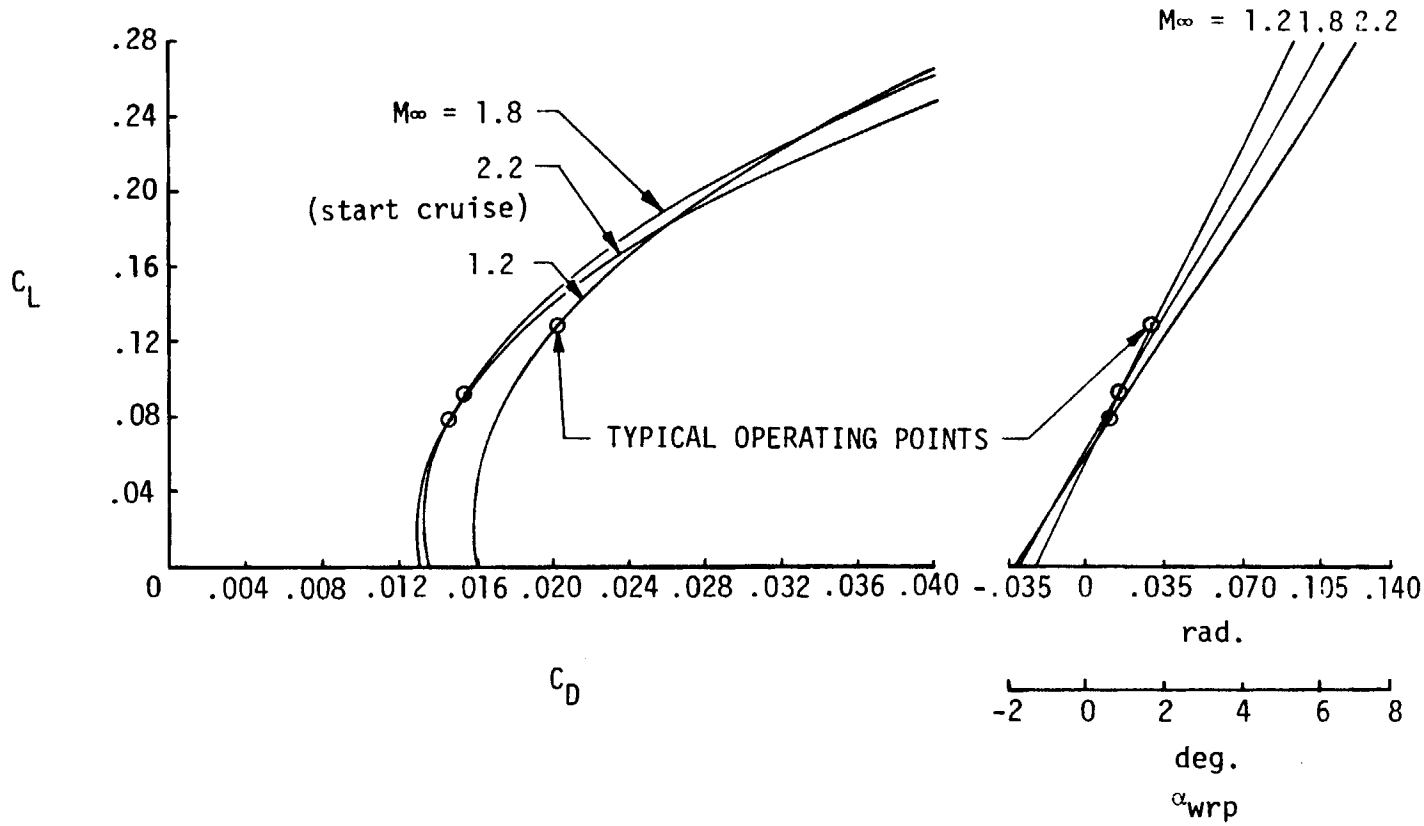

Figure 90. - Lift-drag summary for SSXJET III

SSXJET III

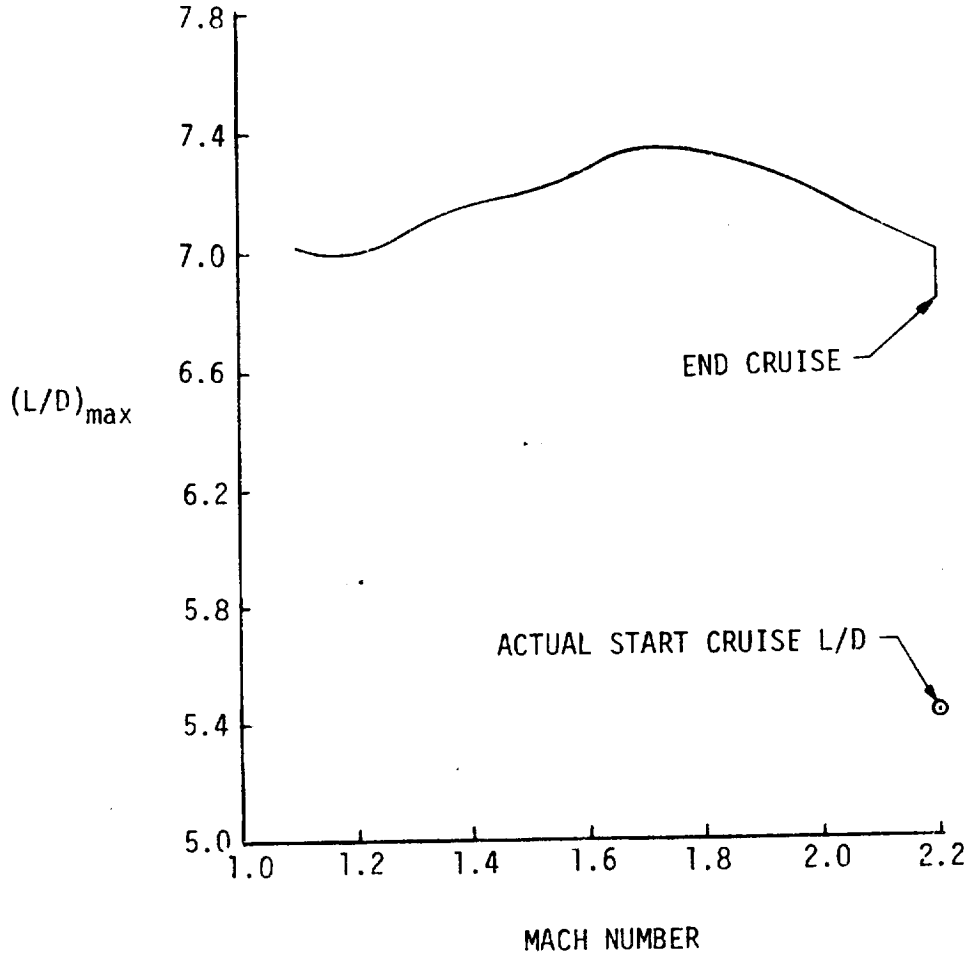

Figure 91. - SEXJET III maximum L/D performance.

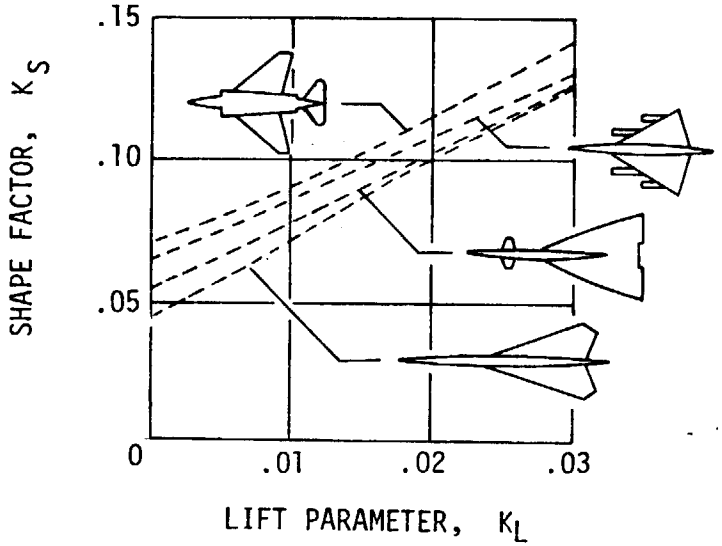

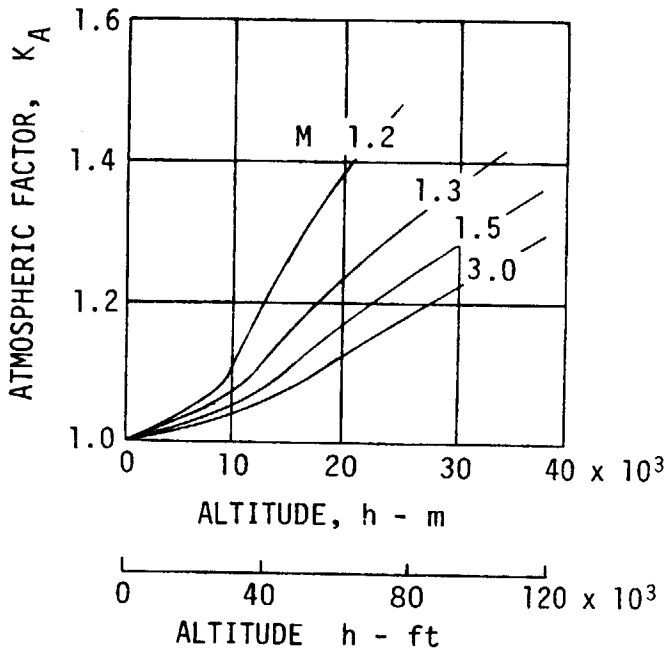

(1) ENTER LIFT PARAMETER

$$K_L = \frac{\beta W}{\alpha P_h M^2 \ell^2}$$

SELECT SHAPE FACTOR, K_S

(2) ENTER ALTITUDE, h, AND MACH NUMBER, M
READ ATMOSPHERIC FACTOR, K_A

(3) CALCULATE OVER PRESSURE

$$\Delta P = 1.9\beta^{.25} \; K_S \; K_A \sqrt{P_h \; P_g} \; / \; (h/\ell)^{.75}$$

Figure 92. - "First cut" sonic boom estimation procedure.

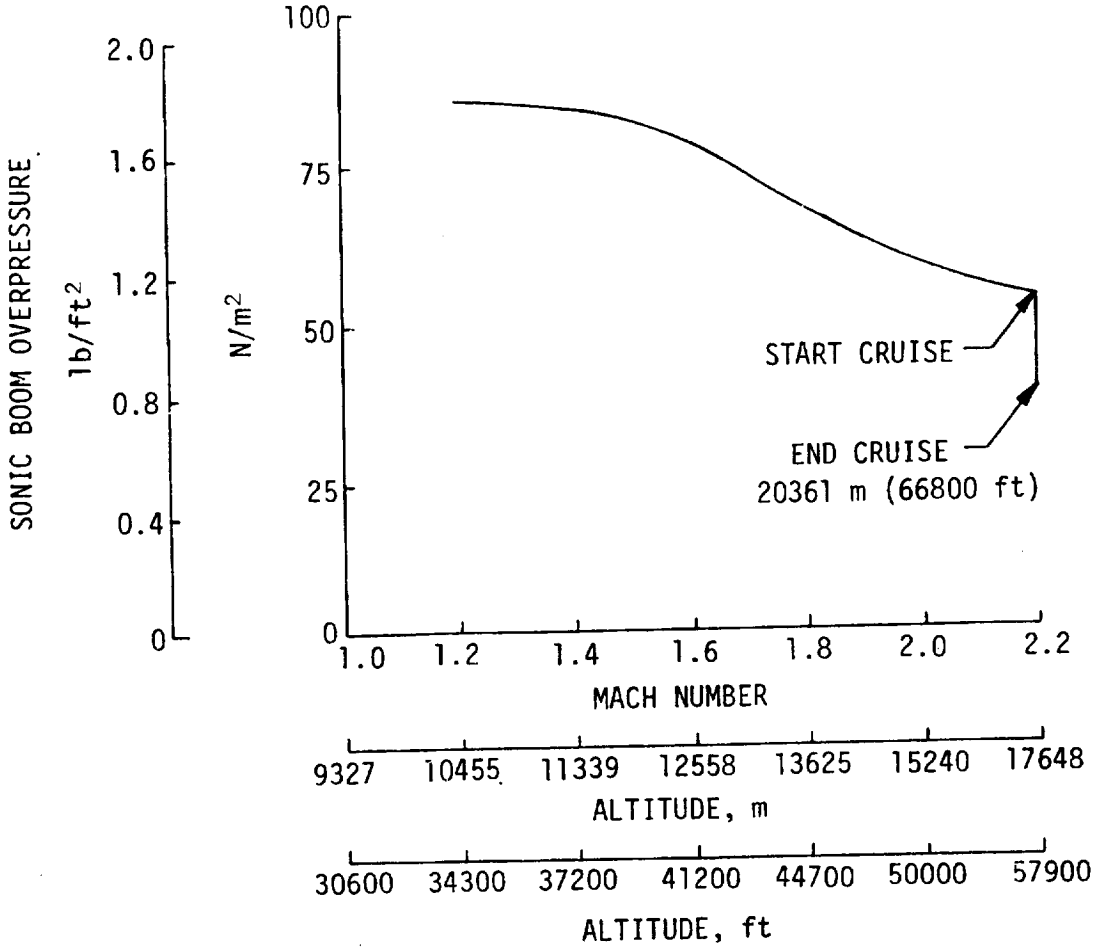

Figure 93. - "First cut" sonic boom estimates for the SSXJET.

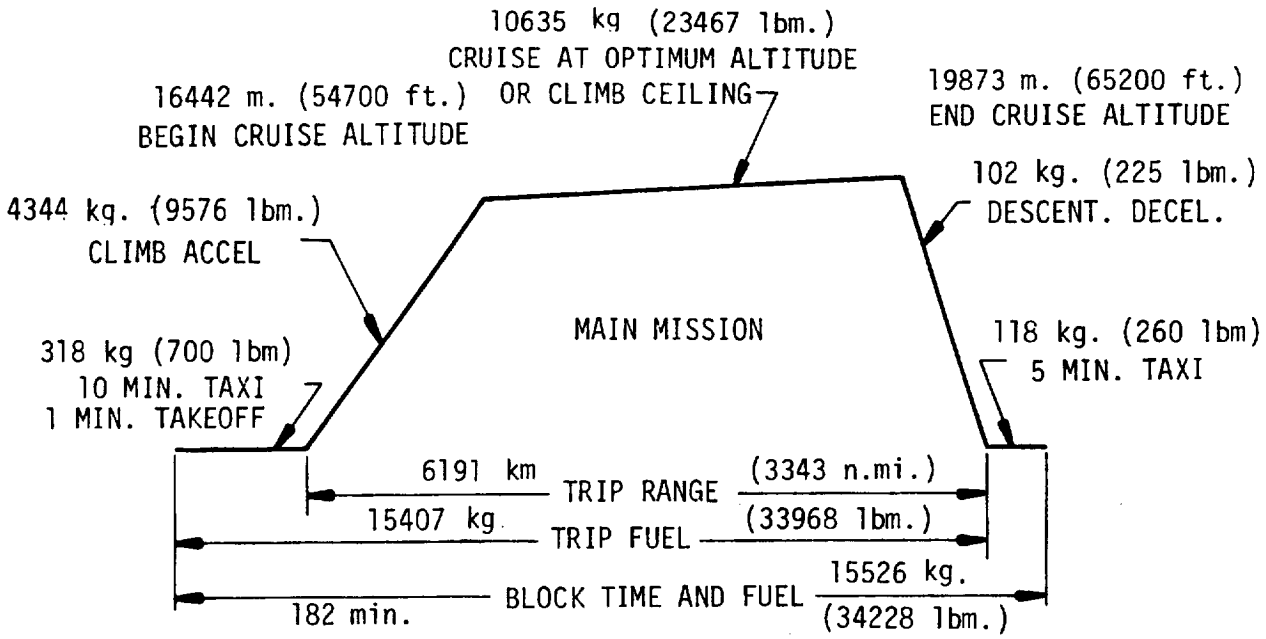

NOTE: C.A.B. RANGE = TRIP RANGE MINUS TRAFFIC ALLOWANCE
AS SPECIFIED FOR SUPERSONIC AIRCRAFT.

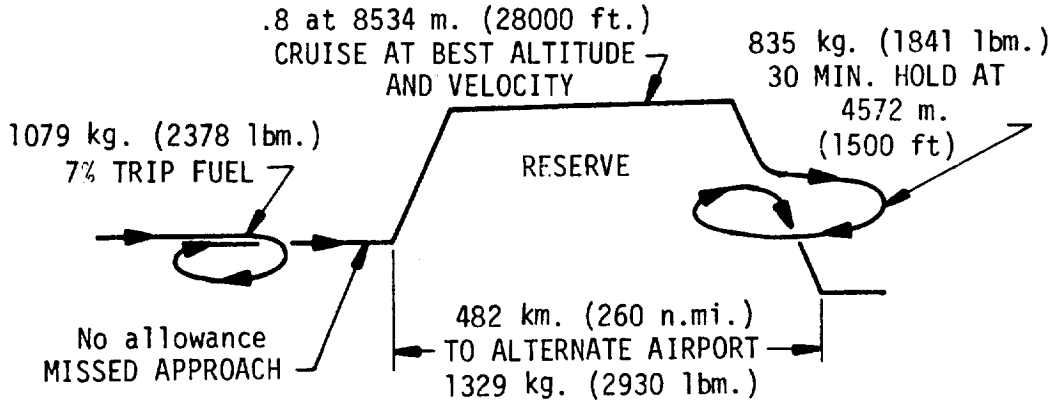

Figure 94. - SSXJET Mission profile

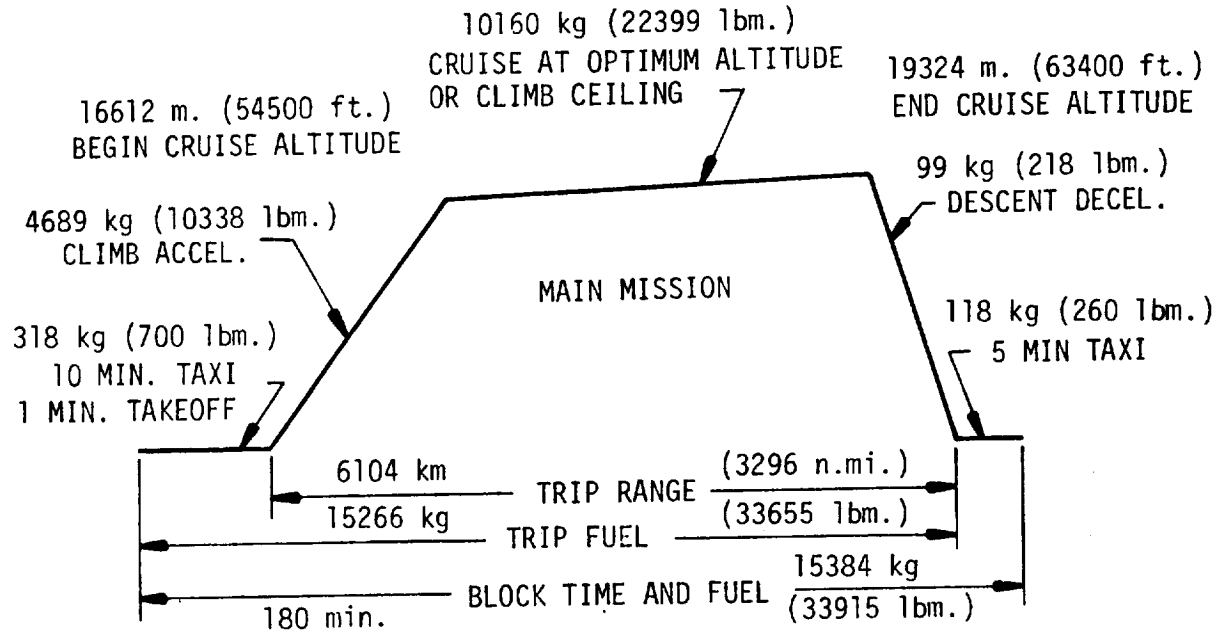

NOTE: C.A.B. = TRIP RANGE MINUS TRAFFIC ALLOWANCE
AS SPECIFIED FOR SUPERSONIC AIRCRAFT

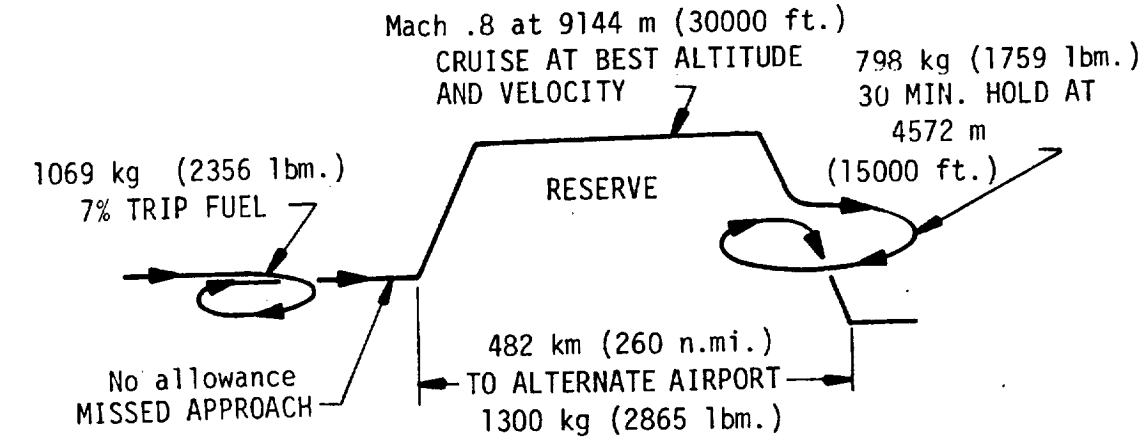

Figure 95. - SSXJET I Mission profile

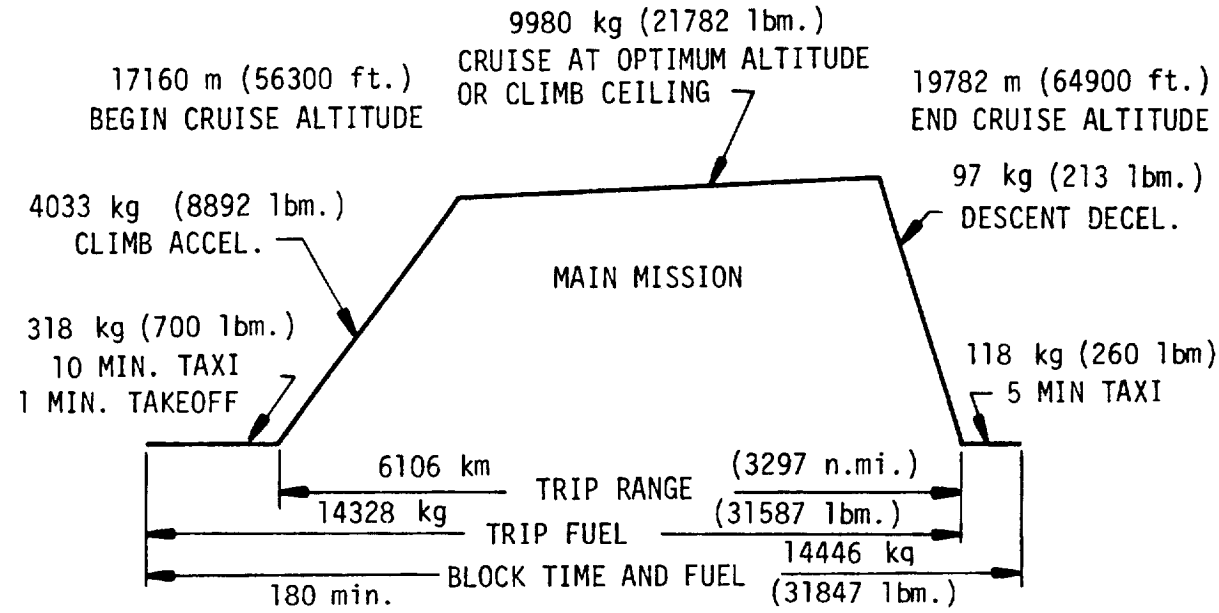

NOTE: C.A.B. = TRIP RANGE MINUS TRAFFIC ALLOWANCE
AS SPECIFIED FOR SUPERSONIC AIRCRAFT

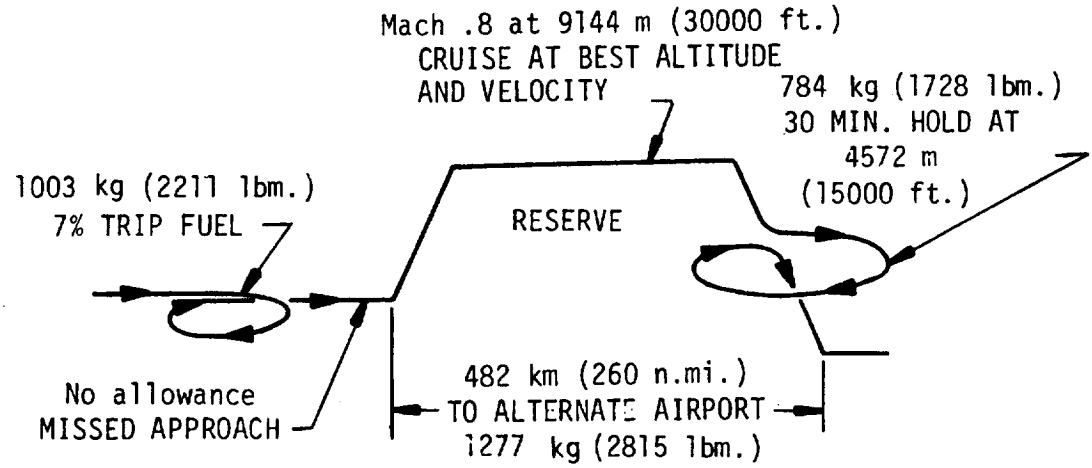

Figure 96. - SSXJET II Mission profile

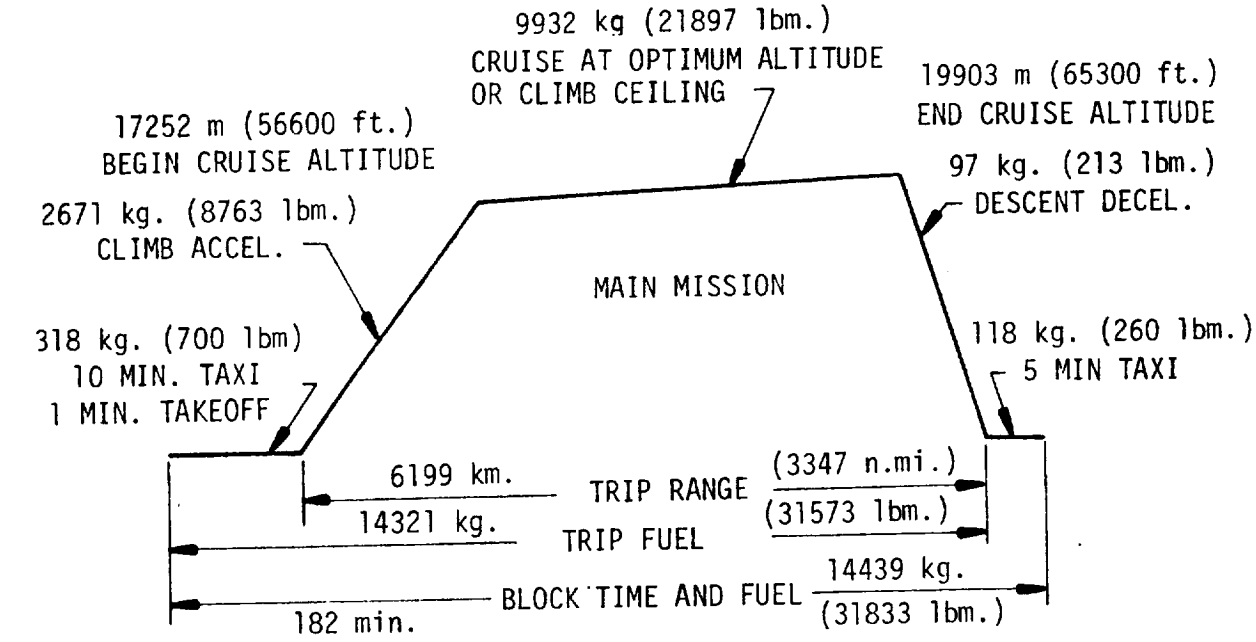

NOTE: C.A.B. = TRIP RANGE MINUS TRAFFIC ALLOWANCE
AS SPECIFIED FOR SUPERSONIC AIRCRAFT

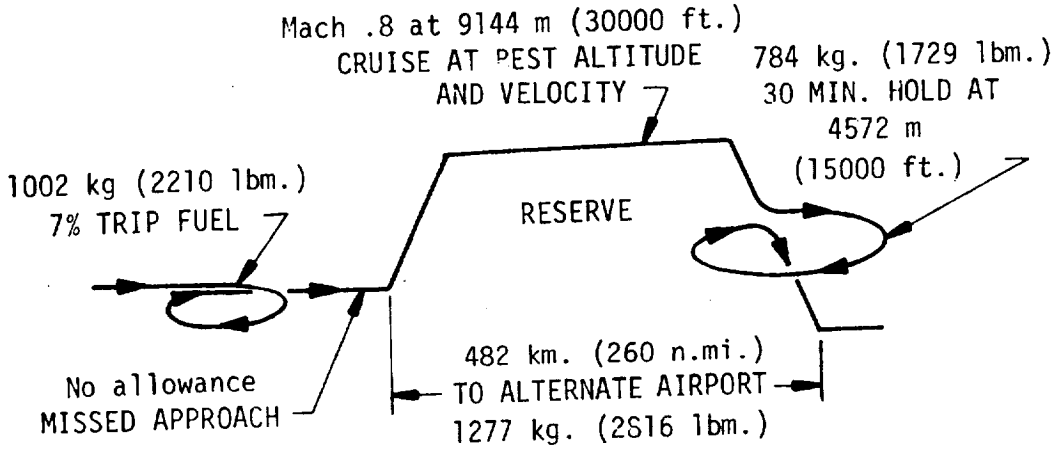

Figure 97. - SSXJET II Tandem mission profile

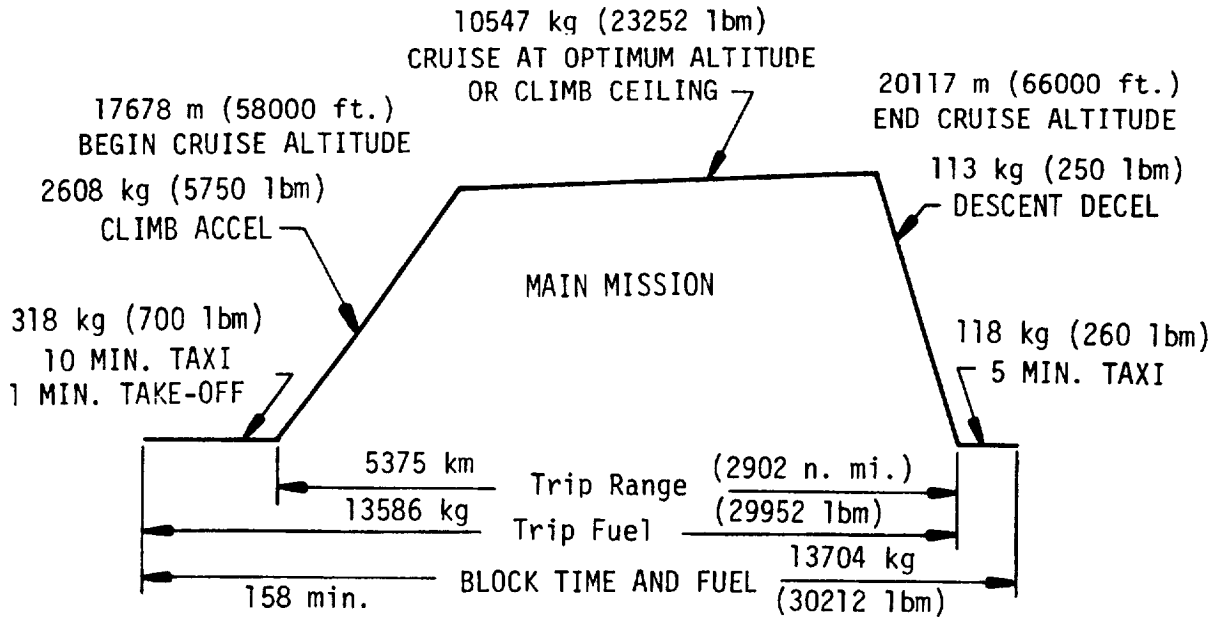

NOTE: C.A.B. RANGE = TRIP RANGE MINUS TRAFFIC ALLOWANCE
AS SPECIFIED FOR SUPERSONIC AIRCRAFT

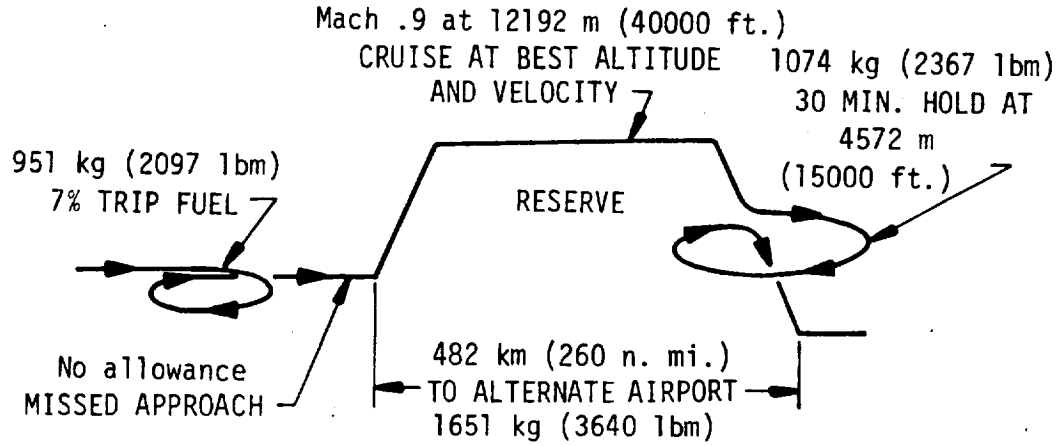

Figure 98. - SSXJET III Mission Profile

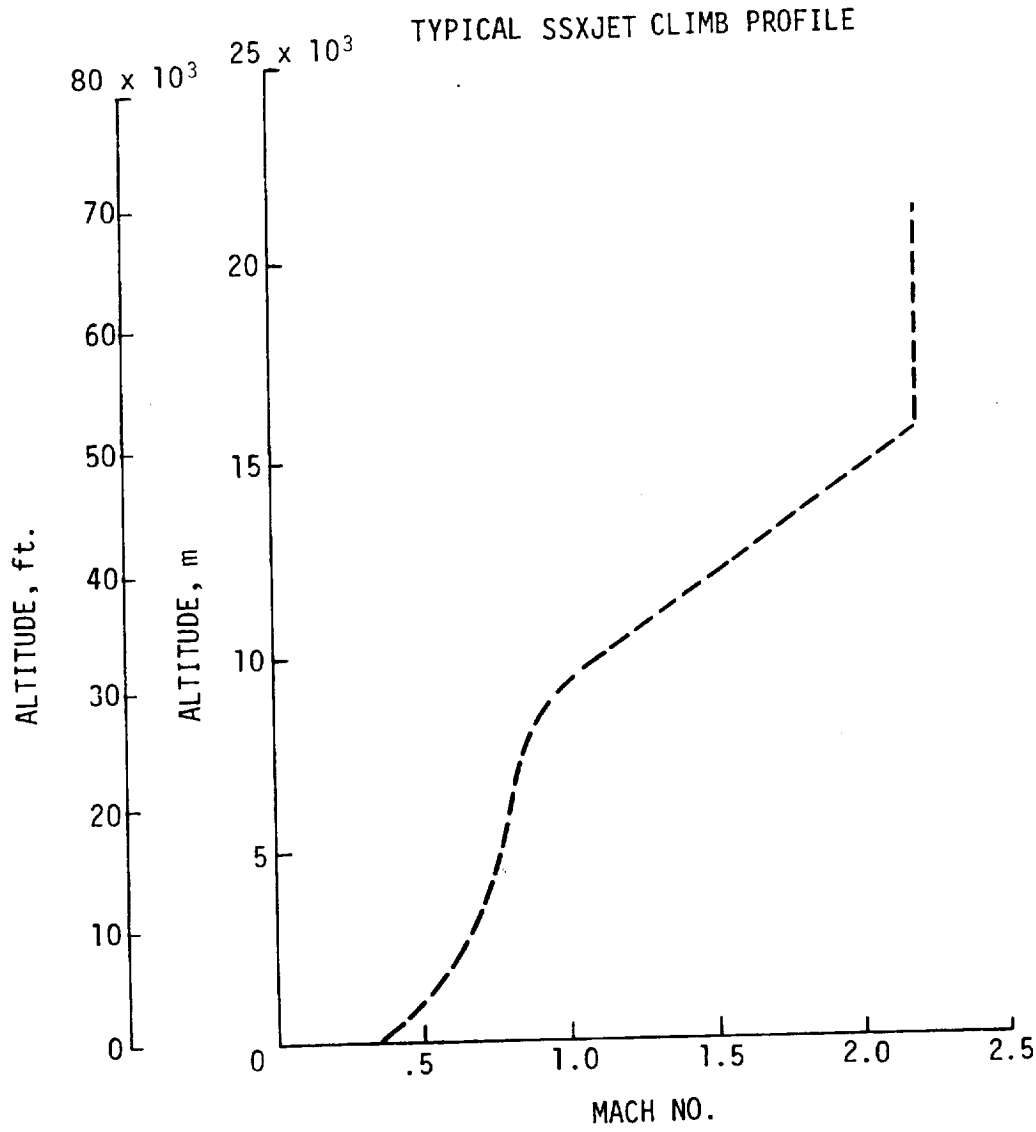

Figure 99. - Mach-altitude climb schedule

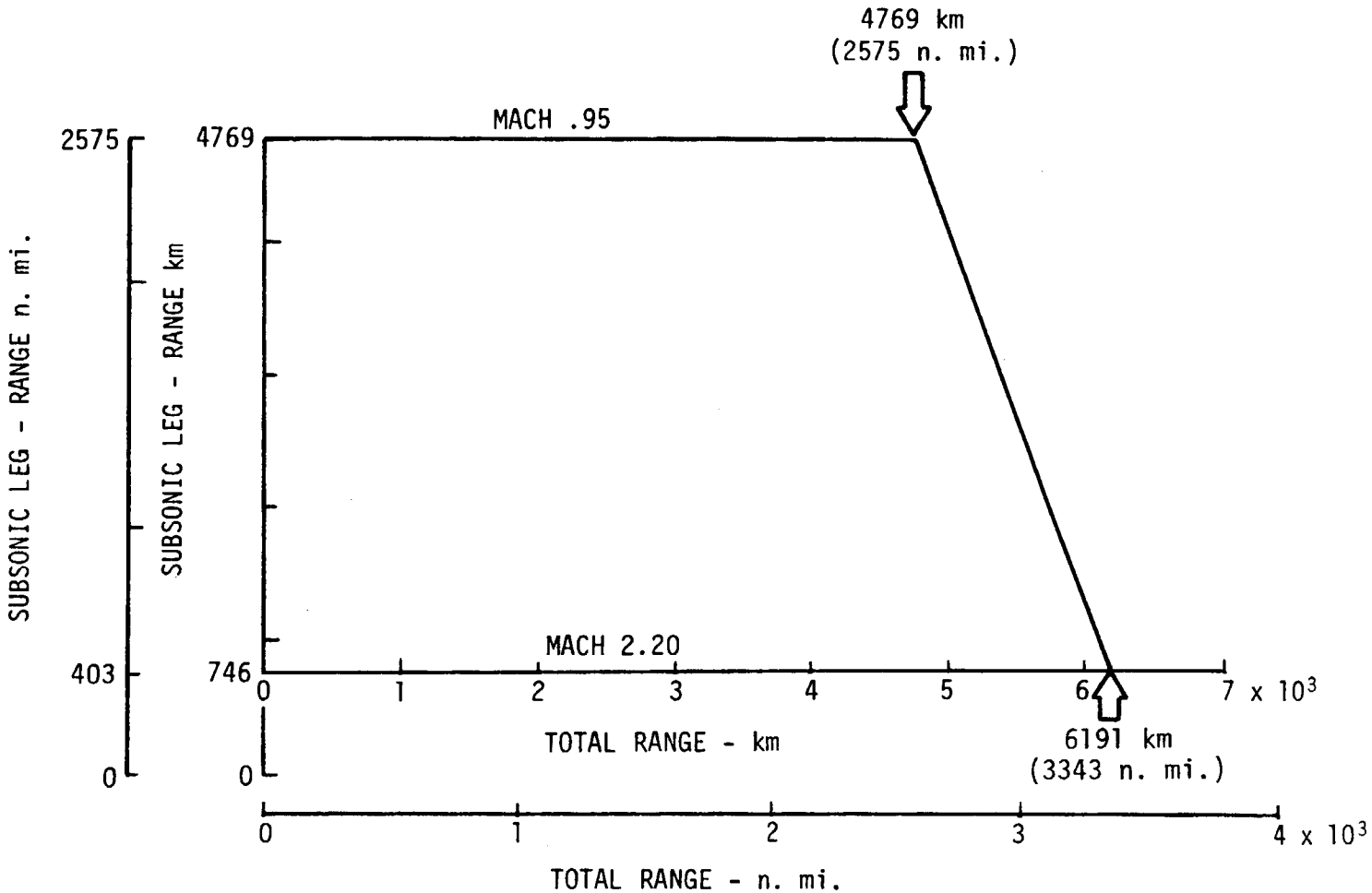

Figure 100. - Effect of subsonic cruise on range

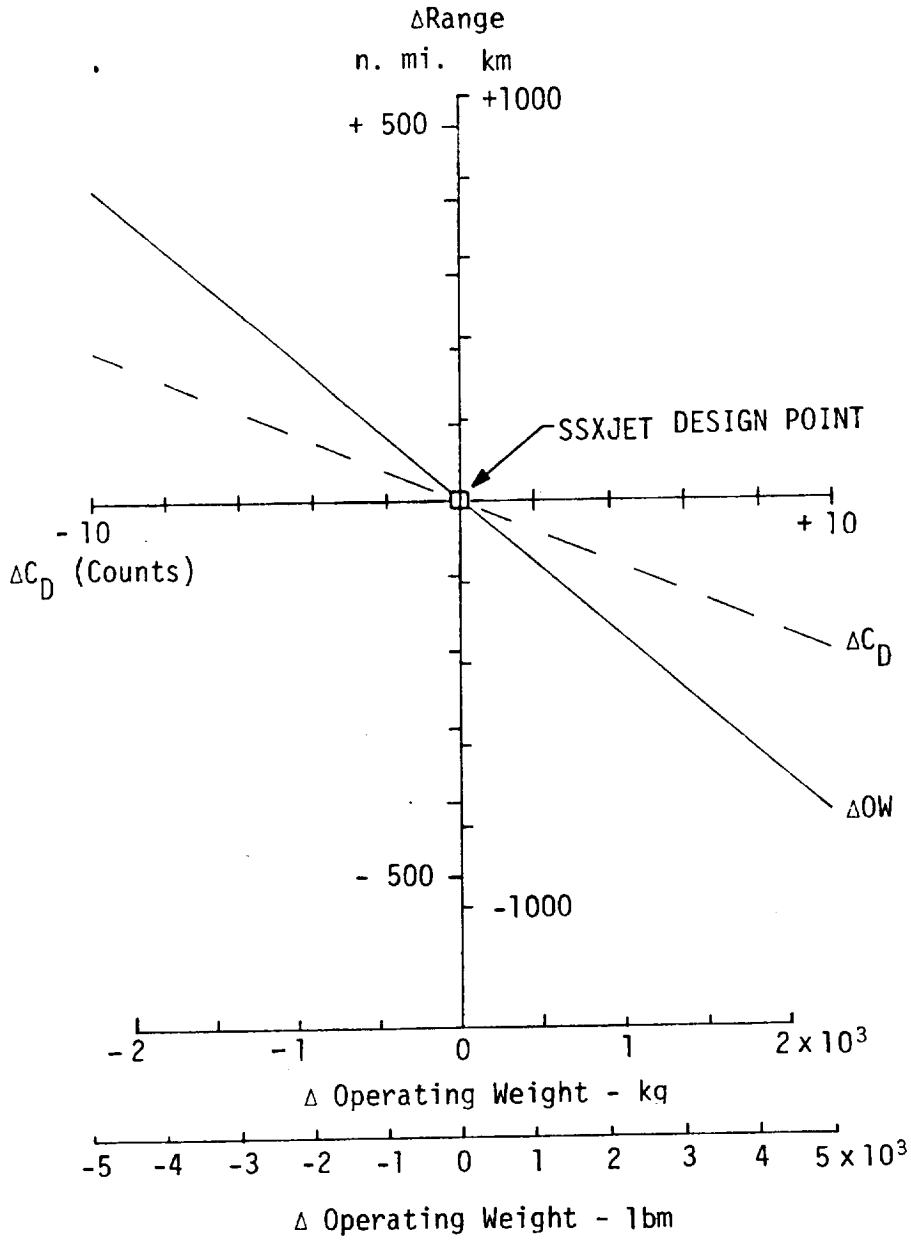

Figure 101. - Range versus weight and drag reduction

STD. +8°C DAY

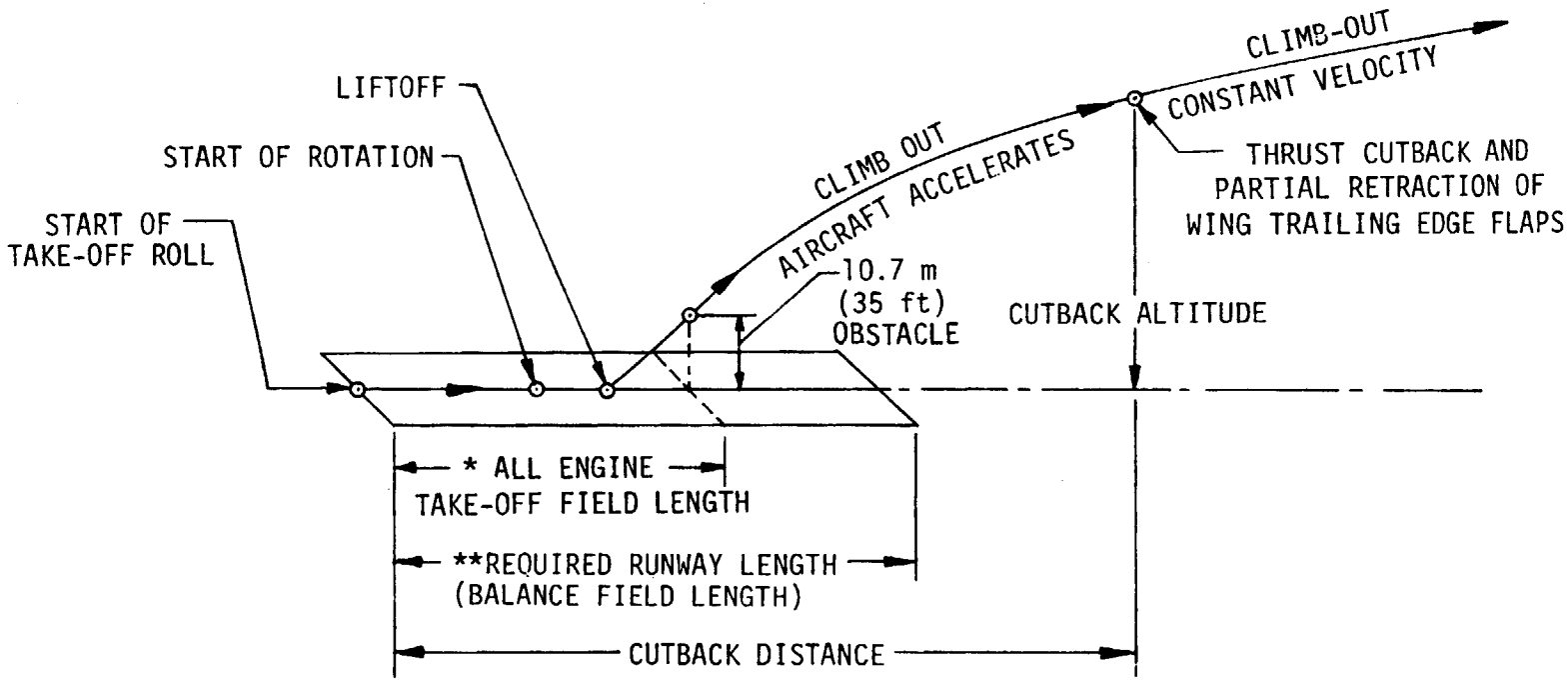

*ALL ENGINE TAKE-OFF FIELD LENGTH = 1723 m (5652 ft)
**BALANCE FIELD LENGTH = 1981 m (6500 ft)

Figure 102. - Typical take-off profile for SSXJET and SSXJET III.

TAKE-OFF

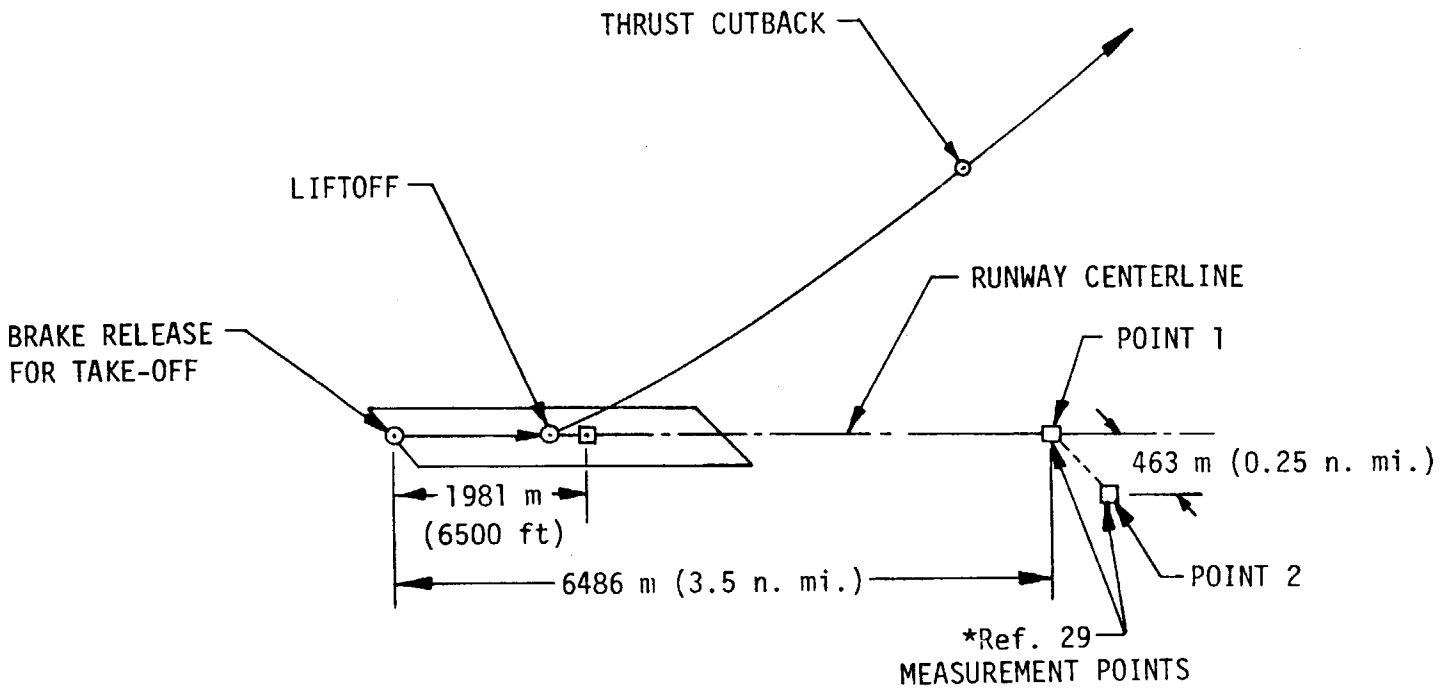

*NOTE: SIDELINE NOISE IS MEASURED WHERE
NOISE LEVEL AFTER LIFTOFF IS GREATEST.

Figure 103. - Noise measurement location for take-off.

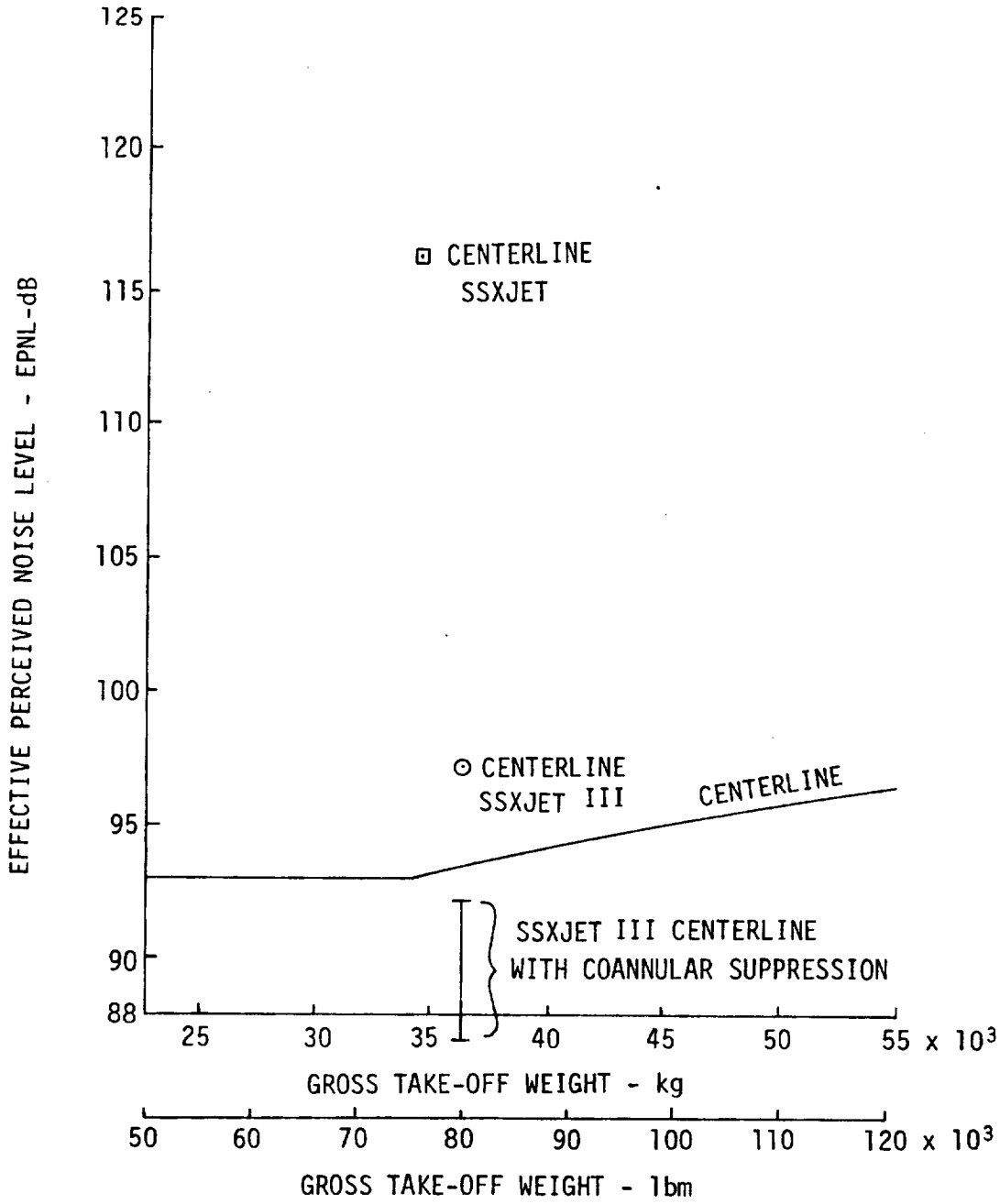

Figure 104. - Variation of maximum allowable EPNL with gross take-off weight per 1969 version of FAR 36 (Ref. 29) at centerline measurement station.

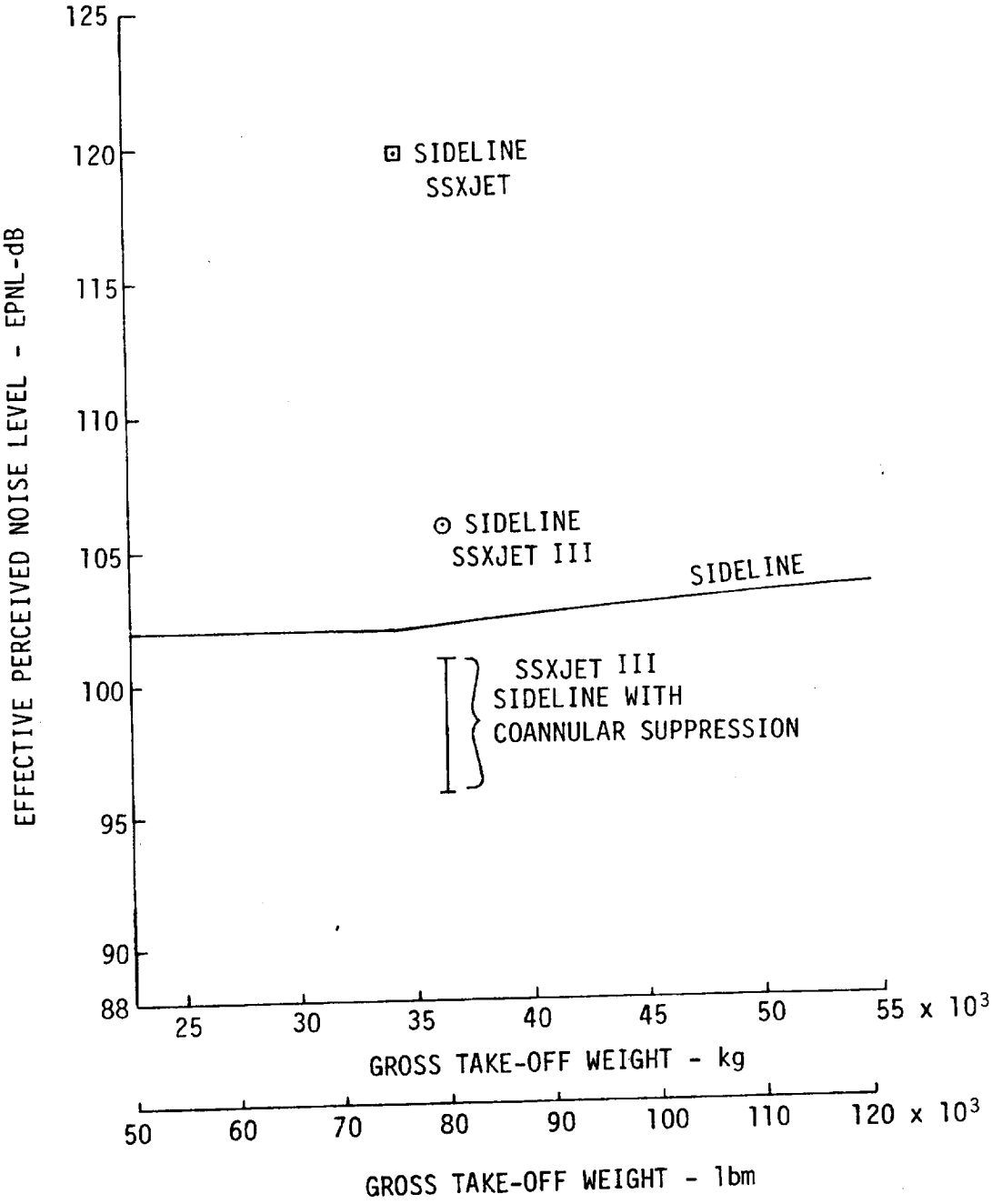

Figure 105. - Variation of maximum allowable EPNL with gross take-off weight per 1969 version of FAR 36 (Ref. 29) at sideline measurement station.

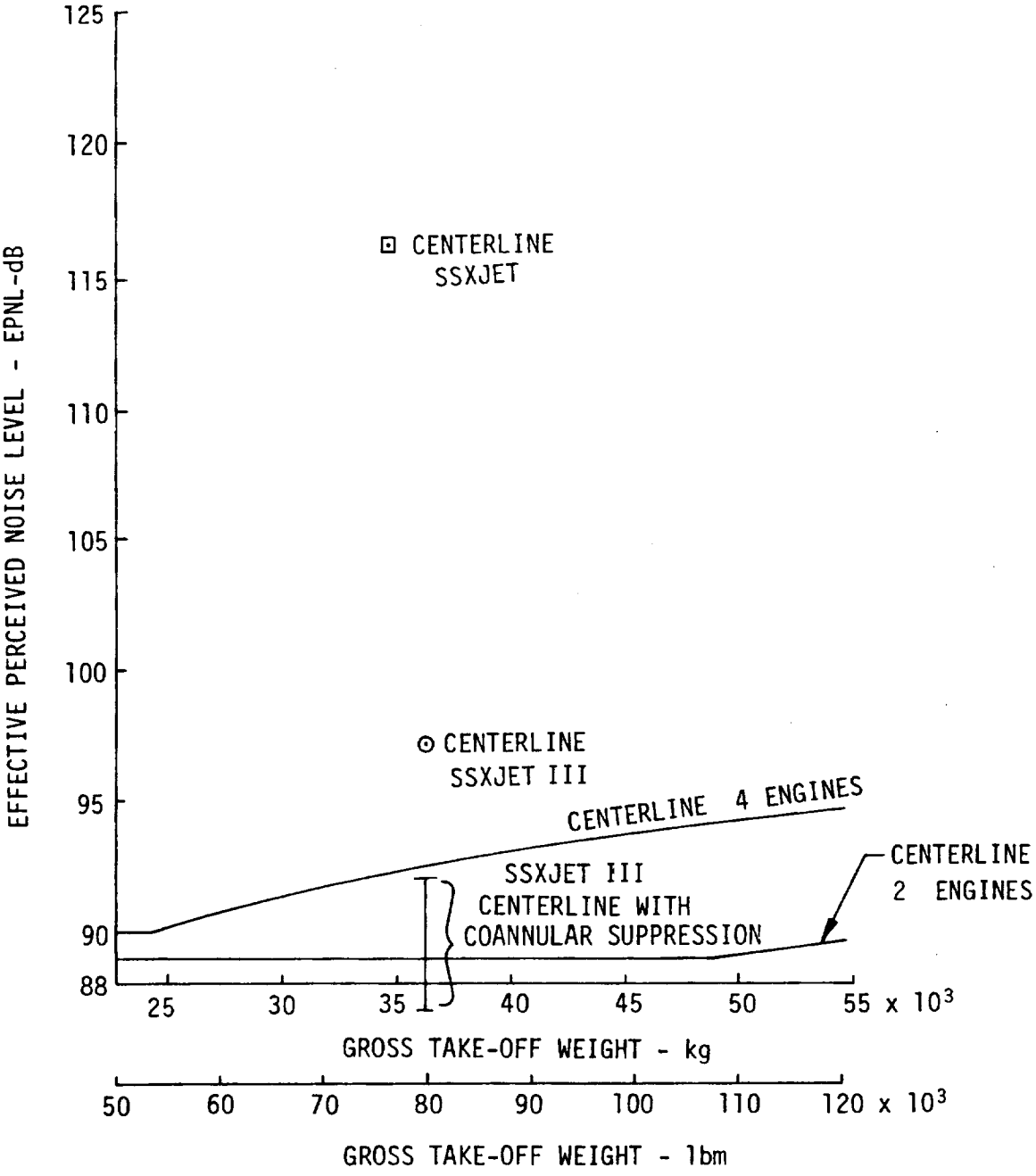

Figure 106. - Variation of maximum allowable EPNL with gross take-off weight per 1977 version of FAR 36 (Ref. 29) at centerline measurement station.

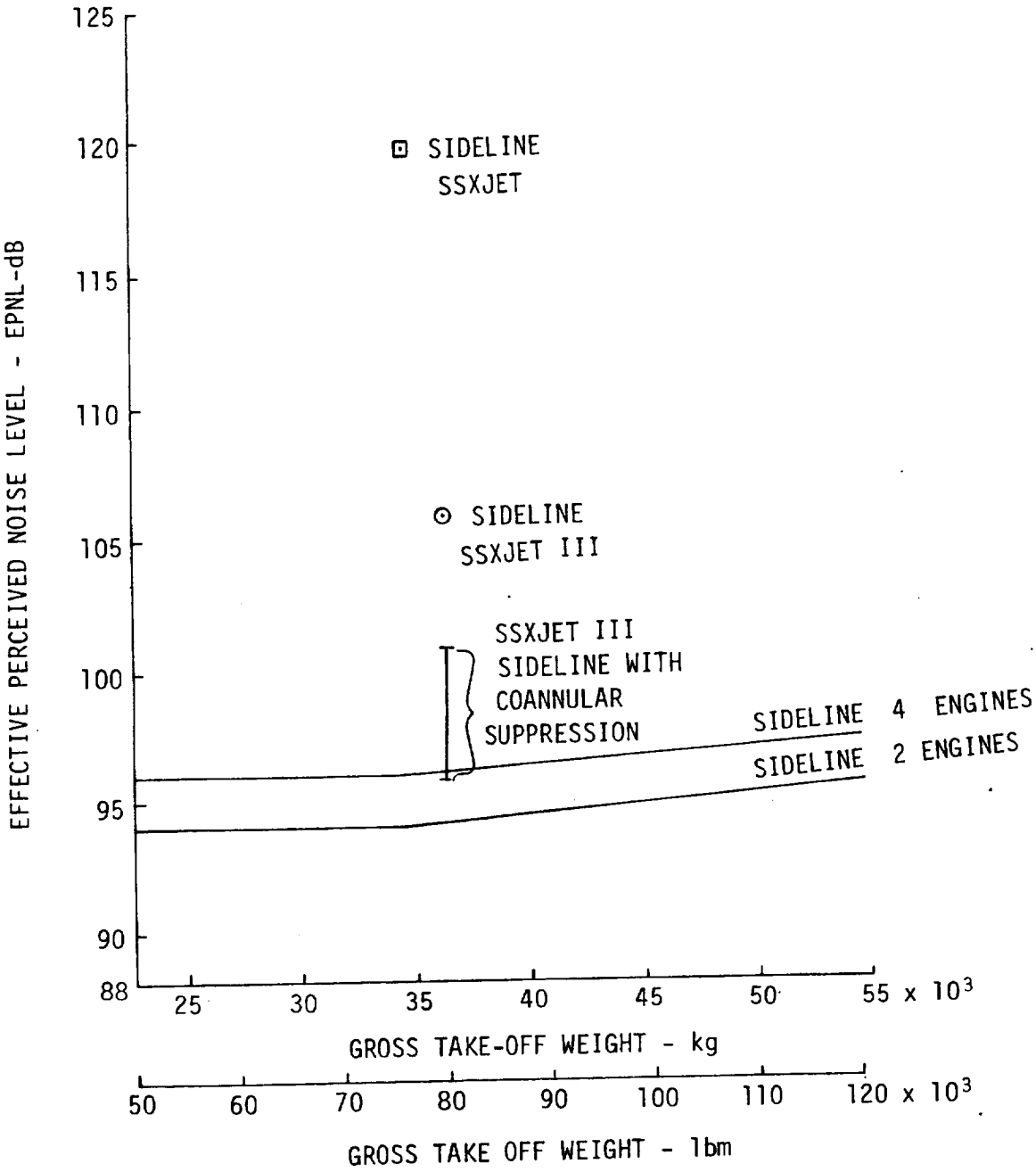

Figure 107. - Variation of maximum allowable EPNL with gross take-off weight per 1977 version of FAR 36 (Ref. 29) at sideline measurement station.

STD. +10°C DAY

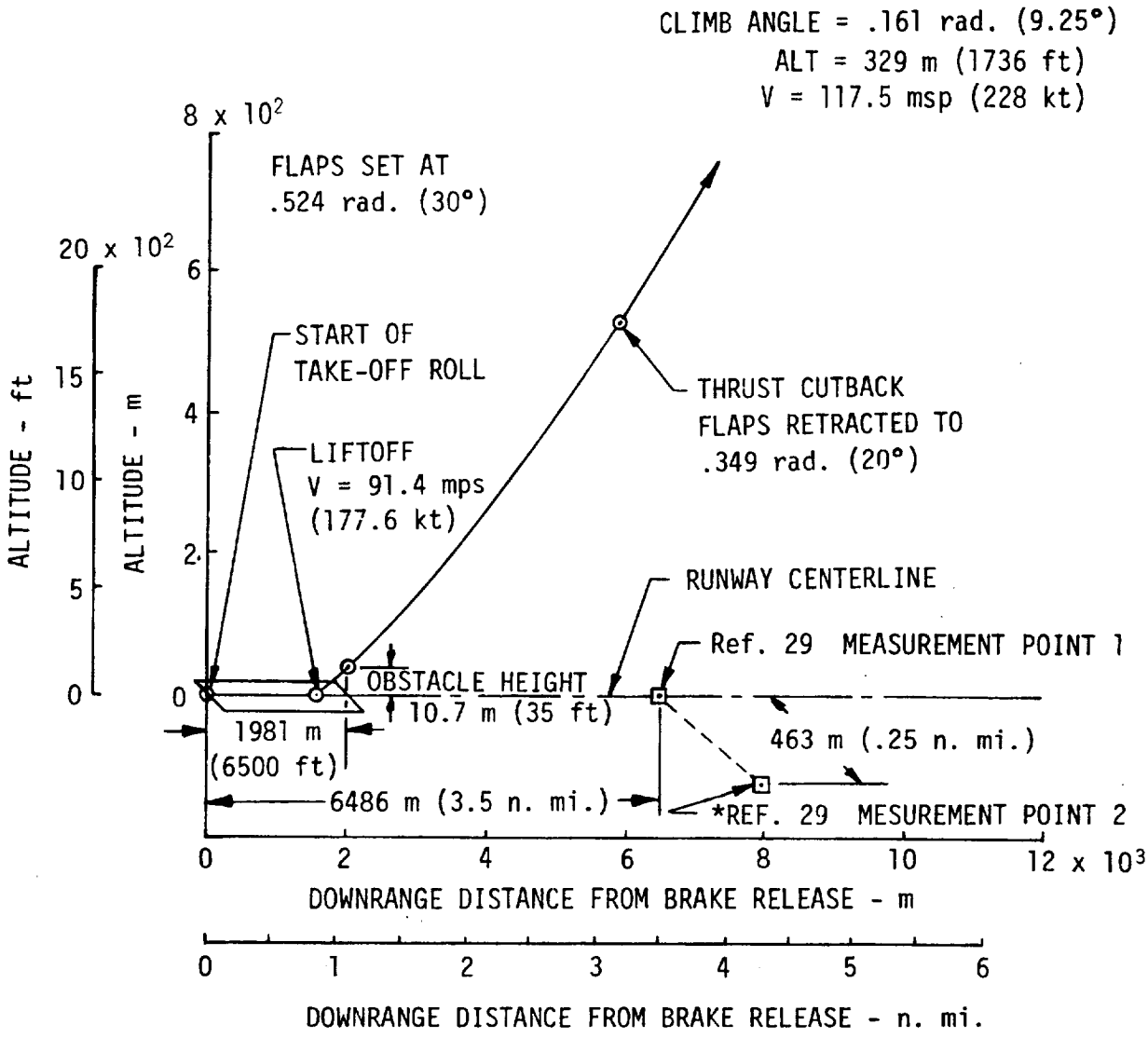

*SIDELINE NOISE IS MEASURED WHERE NOISE LEVEL AFTER TAKE-OFF IS GREATEST

Figure 108. - Take-off profile for noise evaluation of SSXJET

STD. +10°C DAY

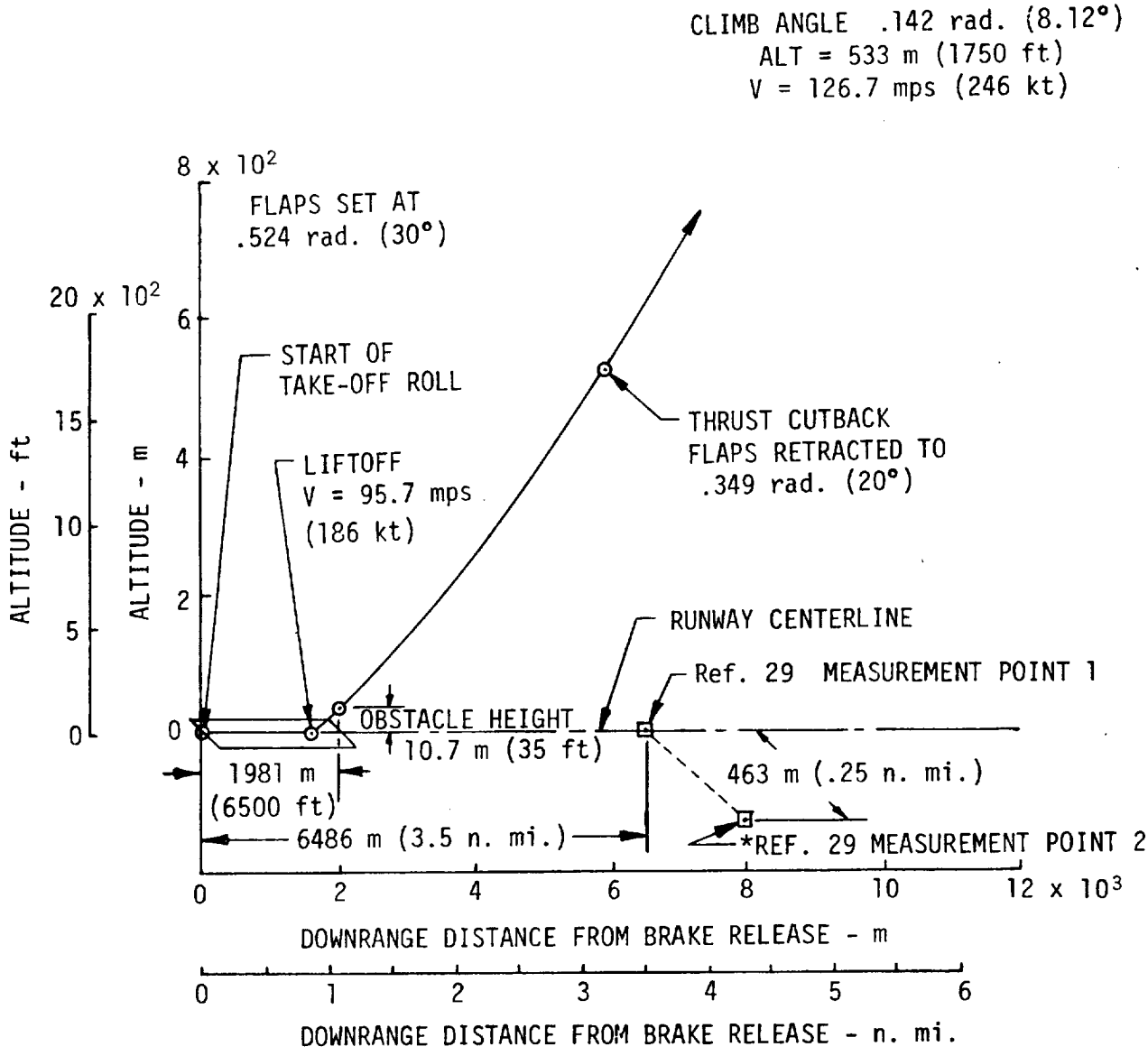

*SIDELINE NOISE IS MEASURED WHERE NOISE LEVEL AFTER TAKE-OFF IS GREATEST

Figure 109. - Take-off profile for noise evaluation of SSXJET III.

1. Report No. NASA TM 74055	2. Government Accession No.	3. Recipient's Catalog No.
4. Title and Subtitle A PRELIMINARY STUDY OF THE PERFORMANCE AND CHARACTERISTICS OF A SUPERSONIC EXECUTIVE AIRCRAFT		5. Report Date September 1977
		6. Performing Organization Code 31.100
7. Author(s) Vincent R. Mascitti		8. Performing Organization Report No.
		10. Work Unit No.
9. Performing Organization Name and Address NASA Langley Research Center Hampton, Virginia		11. Contract or Grant No.
		13. Type of Report and Period Covered Technical Memorandum
12. Sponsoring Agency Name and Address National Aeronautics and Space Administration Washington, DC 20546		14. Sponsoring Agency Code

15. Supplementary Notes Acknowledgment of analytic effort is as follows: Configuration Development-E. E. Swanson and R. A. DeCosta; Stability and Control-G. L. Martin; Aerodynamics-K. B. Walkley; Mass Characteristics and Mission Analysis-G. J. Espil; Propulsion-W. A. Lovell and Takeoff Performance and Noise-J. E. Russell(Vought Corporation, Hampton)

16. Abstract

A preliminary design study has been conducted to determine the impact of advanced supersonic technologies on the performance and characteristics of a supersonic executive aircraft. Four configurations with different engine locations and wing/body blending were studied with an advanced non-afterburning turbojet engine. One configuration incorporated an advanced General Electric variable cycle engine and two-dimensional inlet with internal ducting. An M 2.2 design Douglas scaled arrow-wing was used throughout this study with Learjet 35 accommodations (eight passengers).

All four configurations with turbojet engines meet the performance goals of 5926 km (3200 n.mi.) range, 1981 meters (6500 feet) takeoff field length, and 77 meters per second (150 knots) approach speed. The noise levels of turbojet configurations studied are excessive. However, a turbojet with mechanical suppressor was not studied. The variable cycle engine configuration is deficient in range by 555 km (300 n.mi.) but nearly meets subsonic noise rules (FAR 36 1977 edition), if coannular noise relief is assumed. All configurations are in the 33566 to 36287 kg (74,000 to 80,000 lbm) takeoff gross weight class when incorporating current titanium manufacturing technology.

17. Key Words (Suggested by Author(s))	18. Distribution Statement
Supersonic Cruise SCAR Aircraft Design General Aviation	Unclassified - Unlimited

19. Security Classif. (of this report)	20. Security Classif. (of this page)	21. No. of Pages	22. Price*
Unclassified	Unclassified	191	$7.50

* For sale by the National Technical Information Service, Springfield, Virginia 22161